Polish Academy of Sciences

Institute of Fundamental Technological Research

Archives of Mechanics

Archiwum Mechaniki Stosowanej

volume 48 issue 6

Polish Scientific Publishers PWN

Warszawa 1996

ARCHIVES OF MECHANICS IS DEVOTED TO
Theory of elasticity and plasticity • Theory of nonclassical continua • Physics of continuous media • Mechanics of discrete media • Nonlinear mechanics • Rheology • Fluid gas-mechanics • Rarefied gas • Thermodynamics

---

Printed in Poland, Editorial Office: Świętokrzyska 21,
00-049 Warszawa (Poland)

Arkuszy wydawniczych 11,5. Arkuszy drukarskich 10
Papier offset. kl. III 70 g. B1. Odddano do składania we wrześniu 1996 r.
Druk ukończono w listopadzie 1996 r.
Skład i łamanie: "MAT-TEX"
Druk i oprawa: Drukarnia Braci Grodzickich, Żabieniec ul. Przelotowa 7

Arch. Mech., 48, 6, pp. 959–972, Warszawa 1996

Scattering of oblique waves by a thin vertical wall with a submerged gap

P. DAS, S. BANERJEA and B.N. MANDAL (CALCUTTA)

THIS PAPER is concerned with scattering of an obliquely incident train of surface water waves by a thin vertical wall with a submerged gap. Utilizing Havelock's expansion of water wave potential, two integral equations, one involving the horizontal component of velocity across the gap and the other involving the difference of velocity potential across the wall, are obtained. The quantities of physical interest, namely the reflection and transmission coefficients, are related to the solutions of these integral equations. For the case of normal incidence of the wave train these integral equations have exact solutions. These exact solutions provide one-term Galerkin approximations to the solutions of the corresponding oblique incidence integral equations. Identifying the reflection and transmission coefficients as some inner products involving the solutions of these integral equations and exploiting the properties of self-adjointness and positive semi-definiteness of the integral operators defining the integral equations, the one-term approximations result in some lower and upper bounds for the reflection and transmission coefficients. Numerical evaluation of these bounds for any angle of incidence and any wave number reveals that they are very close to each other, and as such they produce good approximations to the exact values of the quantities of physical interest. For the special case of normal incidence this method produces numerical results which are in good agreement with the results available in the literature obtained by other methods.

1. Introduction

WATER WAVE scattering problems involving fixed plane vertical barriers are being studied in the literature, assuming linear theory, over the last fifty years by employing various mathematical techniques. Since a thin barrier models a breakwater which shelters a port from the rough sea, study of its effect on surface water waves is of some physical importance. PORTER [1] considered the problem of water wave diffraction by a thin vertical wall with a submerged gap for the case of normal incidence of the wave train, and used a complex variable technique as well as an integral equation procedure based on Green's integral theorem to solve it in closed form. A number of researchers also studied the narrow gap problem assuming the gap width to be very small compared to the depth of submergence of its midpoint below the free surface. TUCK [2] used the method of matched asymptotic expansion to obtain the transmission coefficient approximately. PACKHAM and WILLIAMS [3] used an integral equation formulation based on a suitable use of Green's integral theorem for uniform finite depth of water, wherein the integral equation was solved approximately by exploiting the concept of narrowness of the gap, and then the transmission coefficient was obtained approximately. MANDAL [4] also considered the narrow gap problem for

deep water by an integral equation formulation based on Havelock's expansion of water wave potential and used the idea of PACKHAM and WILLIAMS [3] to solve it approximately, and also obtained the transmission coefficient approximately.

For oblique incidence of the wave train, the narrow gap problem was considered by LIU and WU [5] who utilized TUCK'S [2] idea of matched asymptotic expansion to obtain the transmission coefficient apparently for low wave numbers, since approximation of Helmholtz's equation by Laplace equation for obtaining the near-field solution is not valid for large values of the wave number. MANDAL and KUNDU [6] used Havelock's expansion of water wave potential satisfying Helmholtz's equation to obtain an integral equation across the gap, which was then solved by assuming the gap to be narrow and the transmission coefficient was determined approximately.

MANDAL and DOLAI [7] recently used the idea of EVANS and MORRIS [8] to obtain very accurate lower and upper bounds for the reflection and transmission coefficients in oblique wave diffraction problems, involving four basic configurations of a thin vertical barrier present in water of uniform finite depth.

In the present paper the problem of oblique water wave diffraction by a thin vertical wall with a submerged gap (not necessarily narrow) is studied by utilizing the idea of EVANS and MORRIS [8]. The reflection and transmission coefficients are obtained in terms of two integrals involving the unknown horizontal component of velocity across the gap, and difference of velocity potential across the wall, respectively. These unknown functions satisfy some integral equations which have exact solutions for the case of normal incidence. Following EVANS and MORRIS [8], these known exact solutions for normally incident waves are utilized as one-term Galerkin approximations to the solutions of these two integral equations. The reflection and transmission coefficients are identified with some inner products involving the solutions of these integral equations. Exploiting the properties of self-adjointness and positive semi-definiteness of the integral operators defining the integral equations, the one-term Galerkin approximations produce upper and lower bounds for the reflection and transmission coefficients for any angle of incidence and any wave number. It is analytically verified that for the normal incidence case, the upper and lower bounds coincide. The bounds involve a number of integrals which are evaluated numerically by standard techniques. The numerical results reveal that the two bounds for any angle of incidence and any wave number are very close, and as such they produce very good approximations to the exact values of the reflection and transmission coefficients. In our numerical scheme, if the angle of incidence is taken to be zero (for the case of normal incidence of the wave train), the numerical values of the two bounds coincide by more than four decimal places. This verifies the correctness of the numerical scheme. Also, for the normal incidence case, the numerical results obtained by the present method are in good agreement with the graphical results obtained by PORTER [1] and TUCK [2].

2. Formulation of the problem

We choose a rectangular Cartesian coordinate system in which the y-axis is taken vertically downwards into the fluid, $y = 0$ is the undisturbed free surface. A train of progressive surface waves represented by the velocity potential

$$\psi_0(x, y, z, t) = \mathrm{Re}\{\exp(-Ky + i\mu x + i\nu z - i\sigma t)\},$$

where $\mu = K\cos\alpha$, $\nu = K\sin\alpha$, $K = \sigma^2/g$, and g is the gravity and σ is the circular freequency, is assumed to be obliquely incident (from negative infinity) on a fixed thin plane vertical wall at an angle α to the normal to the wall. The wall occupies the position $x = 0$ and has a gap which is represented by $x = 0$, $y \in S$, $S = (a, b)$. The geometry of the problem allows the z-dependence to be eliminated by assuming the velocity potential to be of the form

$$\psi(x, y, z, t) = \mathrm{Re}\{\phi(x, y)\exp(i\nu z - i\sigma t)\}$$

throughout. Then $\phi(x, y)$ satisfies the boundary value problem described by

$$(\nabla^2 - \nu^2)\phi = 0 \qquad \text{for} \quad y \geq 0, \tag{2.1}$$

$$K\phi + \phi_y = 0 \qquad \text{on} \quad y = 0, \tag{2.2}$$

$$\phi_x = 0, \qquad y = 0, \qquad y \in \overline{S} = (0, \infty) - S, \tag{2.3}$$

$$r^{1/2}\nabla\phi \qquad \text{is bounded as} \quad r \to 0, \tag{2.4}$$

where r is the distance from a submerged end of the wall,

$$\nabla\phi \to 0 \quad \text{as} \quad y \to \infty, \tag{2.5}$$

and

$$\phi(x, y) \sim \begin{cases} Te^{-Ky + i\mu x} & \text{as} \quad x \to \infty, \\ e^{-Ky + i\mu x} + Re^{-Ky - i\mu x} & \text{as} \quad x \to -\infty, \end{cases} \tag{2.6}$$

where R and T are the (complex) reflection and transmission coefficients, respectively, to be obtained.

3. Method of solution

By Havelock's expansion of water wave potential, a suitable representation for $\phi(x, y)$ satisfying (2.1), (2.2), (2.5) and (2.6) is given by

$$\phi(x, y) = \begin{cases} Te^{-Ky + i\mu x} + \displaystyle\int_0^\infty A(k)L(k, y)e^{-(\nu^2 + k^2)^{1/2}x}\, dk & \text{for} \quad x > 0, \\ e^{-Ky + i\mu x} + Re^{-Ky - i\mu x} + \displaystyle\int_0^\infty B(k)L(k, y)e^{(\nu^2 + k^2)^{1/2}x}\, dk & \\ & \text{for} \quad x < 0, \end{cases} \tag{3.1}$$

with $L(k, y) = k\cos ky - K\sin ky$.

Let us define

$$f(y) = \phi_x(0, y), \qquad 0 < y < \infty, \tag{3.2}$$

and

$$g(y) = \phi(+0, y) - \phi(-0, y), \qquad 0 < y < \infty, \tag{3.3}$$

then

$$f(y) = 0 \qquad \text{for} \quad y \in \overline{S}, \tag{3.4}$$

and

$$g(y) = 0 \qquad \text{for} \quad y \in S. \tag{3.5}$$

The constants T, R and the functions $A(k), B(k)$ are related to $f(y)$ and $g(y)$ by

$$T = 1 - R = -\frac{2iK}{\mu} \int_S f(y) e^{-Ky}\, dy, \tag{3.6}$$

$$A(k) = -B(k) = -\frac{2}{\pi} \frac{1}{(\nu^2 + k^2)^{1/2}(k^2 + K^2)} \int_S f(y) L(k, y)\, dy, \tag{3.7}$$

$$R = -K \int_{\overline{S}} g(y) e^{-Ky}\, dy, \tag{3.8}$$

$$A(k) = \frac{1}{\pi} \frac{1}{k^2 + K^2} \int_{\overline{S}} g(y) L(k, y)\, dy. \tag{3.9}$$

Using (2.3) in (3.1) along with (3.9) we obtain an integral equation for $g(y)$ in the form

$$\int_{\overline{S}} g(u) M(y, u)\, du = \pi i \mu (1 - R) e^{-Ky} \qquad \text{for} \quad y \in \overline{S}, \tag{3.10}$$

where

$$M(y, u) = \operatorname*{Lt}_{\varepsilon \to 0} \int_0^\infty \frac{(k^2 + \nu^2)^{1/2}}{k^2 + K^2} L(k, y) L(k, u) e^{-\varepsilon k}\, dk, \tag{3.11}$$

so that $M(y, u) = M(u, y)$ and the exponential term is being introduced to ensure the convergence of the integral.

Again, use of (3.5) in (3.1) along with (3.7) produces an integral equation for $f(y)$

$$\int_S f(u)N(y,u)\,du = -\frac{\pi}{2}R\,e^{-Ky} \qquad \text{for} \quad y \in S, \tag{3.12}$$

where

$$N(y,u) = \int_0^\infty \frac{L(k,y)L(k,u)}{(\nu^2+k^2)^{1/2}(k^2+K^2)}\,dk, \tag{3.13}$$

so that $N(y,u) = N(u,y)$.

If we let

$$F(y) = -\frac{2}{\pi R}f(y) \qquad \text{for} \quad y \in S, \tag{3.14}$$

$$G(y) = \frac{1}{\pi i\mu(1-R)}g(y) \qquad \text{for} \quad y \in \overline{S}, \tag{3.15}$$

then $G(y)$ and $F(y)$ satisfy the integral equations

$$\int_{\overline{S}} G(u)M(y,u)\,du = e^{-Ky} \qquad \text{for} \quad y \in \overline{S}, \tag{3.16}$$

and

$$\int_S F(u)N(y,u)\,du = e^{-Ky} \qquad \text{for} \quad y \in S. \tag{3.17}$$

It may be noted that the functions $G(u)$ and $F(u)$ in (3.16) and (3.17), respectively, are real.

The relations (3.6) and (3.8) can be written as

$$\int_S F(y)e^{-Ky}\,dy = C, \tag{3.18}$$

and

$$\int_{\overline{S}} G(y)e^{-Ky}\,dy = \frac{1}{\pi^2K^2C}, \tag{3.19}$$

where

$$C = \frac{1-R}{i\pi R\sec\alpha}. \tag{3.20}$$

It is very important to note that C is real.

4. Upper and lower bounds for C

As in EVANS and MORRIS [8], we define an inner product

$$\langle f, g\rangle = \int_{\overline{S}} f(y)g(y)\,dy. \tag{4.1}$$

Then obviously $\langle f, g\rangle = \langle g, f\rangle$ and $\langle f, g + h\rangle = \langle f, g\rangle + \langle f, h\rangle$. Also, let us define the operator

$$(\mathcal{M}f)(y) = \langle M(y, u), f(u)\rangle. \tag{4.2}$$

Since

$$M(y, u) = M(u, y) \qquad \text{and} \qquad (\mathcal{M}(f_1 + f_2))(y) = (\mathcal{M}f_1)(y) + (\mathcal{M}f_2)(y),$$

we find

$$\langle \mathcal{M}f, g\rangle = \langle f, \mathcal{M}g\rangle$$

and

$$\langle \mathcal{M}f, f\rangle \geq 0 \qquad \text{for all} \quad f(y).$$

Following EVANS and MORRIS [8], for the solution of (3.16) we choose a one-term approximation as

$$G(y) \approx a_1 g_1(y), \tag{4.3}$$

where a_1 is a constant and $g_1(y)$ is to be chosen suitably. Then

$$a_1 = \frac{\langle g_1(y), e^{-Ky}\rangle}{\langle g_1(y), (\mathcal{M}g_1)(y)\rangle}. \tag{4.4}$$

Hence from (3.19)

$$\begin{aligned} \frac{1}{\pi^2 K^2 C} &= \langle G(y), e^{-Ky}\rangle \\ &\geq \langle a_1 g_1(y), e^{-Ky}\rangle, \end{aligned}$$

by utilizing the properties of self-adjointness and positive semi-definiteness of the operator (cf. EVANS and MORRIS [8]).

Thus we get an upper bound for C as

$$C \leq A_0, \tag{4.5}$$

where

$$A_0 = \frac{\operatorname*{Lt}_{\varepsilon\to 0} \int_0^\infty \frac{(\nu^2 + k^2)^{1/2} e^{-\varepsilon k}}{k^2 + K^2} \left[\int_{\bar{S}} g_1(y) L(k, y)\, dy \right]^2 dk}{\pi^2 K^2 \left[\int_{\bar{S}} g_1(y) e^{-Ky}\, dy \right]^2}. \tag{4.6}$$

Again, let us define another inner product

$$\{f, g\} = \int_S f(y) g(y)\, dy \tag{4.7}$$

and another operator

$$(\mathcal{N} f)(y) = \{N(y, u), f(u)\}. \tag{4.8}$$

Then it is obvious that the inner product $\{f, g\}$ is symmetric, linear, and also the operator $\mathcal{N}$ is linear, self-adjoint and positive semi-definite.

Choosing a one-term approximation to $F(y)$ as

$$F(y) \approx b_1 f_1(y), \tag{4.9}$$

where b_1 is a constant and $f_1(y)$ is to be chosen suitably, we find that

$$b_1 = \frac{\{f_1(y), e^{-Ky}\}}{\{f_1(y), (\mathcal{N} f_1)(y)\}}. \tag{4.10}$$

Thus, by using (3.18) and the same argument as before, we find a lower bound for C as

$$C \geq B_0, \tag{4.11}$$

where

$$B_0 = \frac{\left[\int_S f_1(y) e^{-Ky}\, dy \right]^2}{\int_0^\infty \frac{1}{(\nu^2 + k^2)^{1/2}(k^2 + K^2)} \left[\int_{\bar{S}} f_1(y) L(k, y)\, dy \right]^2 dk}. \tag{4.12}$$

Hence for the unknown real constant C, which involves R, we find

$$B_0 \leq C \leq A_0, \tag{4.13}$$

where A_0 and B_0 are given by (4.6) and (4.12), respectively. Thus the upper and lower bounds for $|R|$ and $|T|$ are obtained as

$$R_1 \leq |R| \leq R_2, \qquad T_1 \leq |T| \leq T_2, \tag{4.14}$$

where

$$R_1 = \frac{\cos\alpha}{(\cos^2\alpha + \pi^2 A_0^2)^{1/2}}, \qquad R_2 = \frac{\cos\alpha}{(\cos^2\alpha + \pi^2 B_0^2)^{1/2}}, \tag{4.15}$$

$$T_1 = \frac{\pi B_0}{(\cos^2\alpha + \pi^2 A_0^2)^{1/2}}, \qquad T_2 = \frac{\pi A_0}{(\cos^2\alpha + \pi^2 B_0^2)^{1/2}}. \tag{4.16}$$

5. Functions $g_1(y)$ and $f_1(y)$

The functions $g_1(y)$ and $f_1(y)$ are chosen as the explicit solutions of the appropriate integral equations associated with the problem of submerged gap in deep water for the case of normal incidence of the wave train. These are given by (cf. PORTER [1], MANDAL and DOLAI [7]).

$$g_1(y) = A_1 \chi(y) \qquad (A_1 \neq 0) \tag{5.1}$$

and

$$f_1(y) = B_1 \lambda'(y) \qquad (B_1 \neq 0), \tag{5.2}$$

where

$$\chi(y) = \begin{cases} -e^{-Ky} \displaystyle\int_a^y \frac{te^{Kt}}{S_1(t)} \left[\delta - \frac{2}{\pi} H(a,b,t)\right] dt & \text{for} \quad 0 < y < a, \\ e^{-Ky} \displaystyle\int_b^y \frac{te^{Kt}}{S_3(t)} \left[\delta - \frac{2}{\pi} H(a,b,t)\right] dt & \text{for} \quad y > b \end{cases} \tag{5.3}$$

and

$$\lambda(y) = e^{-Ky} \int_b^y \frac{te^{Kt}}{S_2(t)} \left[\delta - \frac{2}{\pi} H(a,b,t)\right] dt \qquad \text{for} \quad a < y < b \tag{5.4}$$

with

$$\delta = \frac{\dfrac{2}{\pi} \displaystyle\int_a^b \frac{te^{Kt}}{S_2(t)} H(a,b,t)\, dt + \frac{e^{Ka}}{K}}{\displaystyle\int_a^b \frac{te^{Kt}}{S_2(t)} dt},$$

$$H(a,b,t) = \int_0^a \frac{S_1(s)}{s^2 - t^2} ds$$

and

$$S_1(t) = \left\{(a^2 - t^2)(b^2 - t^2)\right\}^{1/2},$$
$$S_2(t) = \left\{(t^2 - a^2)(b^2 - t^2)\right\}^{1/2},$$
$$S_3(t) = \left\{(t^2 - a^2)(t^2 - b^2)\right\}^{1/2}.$$

Substituting these in the expressions (4.6) and (4.12), A_0 and B_0 are obtained as

$$A_0 = \frac{\int_0^\infty \frac{(\nu^2 + k^2)^{1/2}}{k^2 + K^2}\left[-\frac{\sin ka}{k} + \int_a^b \frac{y\cos ky}{S_2(y)}\left\{\delta - \frac{2}{\pi}H(a,b,y)\right\}dy\right]^2 dk}{\frac{1}{4}\pi^2 I^2} \tag{5.5}$$

and

$$B_0 = \frac{\frac{1}{4}J^2}{\int_0^\infty \frac{k^2}{(\nu^2+k^2)^{1/2}(k^2+K^2)}\left[-\frac{\sin ka}{k} + \int_a^b \frac{y\cos ky}{S_2(y)}\left\{\delta - \frac{2}{\pi}H(a,b,y)\right\}dy\right]^2 dk}, \tag{5.6}$$

where

$$I = \delta\{\alpha_1(K) - \alpha_3(K)\} - \frac{2}{\pi}\{\alpha_1(K,H) - \alpha_3(K,H)\},$$
$$J = \delta\alpha_2(K) - \frac{2}{\pi}\alpha_2(K,H) + \frac{e^{-Ka}}{K}$$

with

$$\alpha_i(K) = \int_{\Gamma_i} \frac{ye^{-Ky}}{S_i(y)}dy, \qquad i = 1,2,3$$

and

$$\alpha_i(K,H) = \int_{\Gamma_i} \frac{yH(a,b,y)e^{-Ky}}{S_i(y)}dy, \qquad i = 1,2,3,$$

where the curve Γ_1 is the interval $(-a,a)$, Γ_2 is (a,b) and Γ_3 is (b,∞).

For the case of normal incidence, the numerator of the expression (5.5) and the denominator of the expression (5.6) are identical and equal to

$$\int_0^\infty \frac{k}{k^2 + K^2}\left[-\frac{\sin ka}{k} + \int_a^b \frac{y\cos ky}{S_2(y)}\left\{\delta - \frac{2}{\pi}H(a,b,y)\right\}dy\right]^2 dk. \tag{5.7}$$

Integrating

$$\frac{ze^{ikz}}{\{(z^2-a^2)(z^2-b^2)\}^{1/2}} \qquad (k>0)$$

in the complex z-plane along the contour consisting of the arc of the quarter circle of large radius and centre at the origin, the positive imaginary axis, and a line along the positive real axis cut from 0 to a and b to ∞, the line running slightly above the cuts, we get

$$-\int_0^a \frac{x\sin kx}{S_1(x)}dx + \int_b^\infty \frac{x\sin kx}{S_3(x)}dx = \int_a^b \frac{x\cos kx}{S_2(x)}dx \qquad (k>0).$$

Again, integrating

$$\frac{ze^{ikz}}{\{(z^2-a^2)(z^2-b^2)\}^{1/2}(z^2-v^2)} \qquad (k>0, \quad 0<v<a)$$

along the same contour together with an indentation above the pole at $z = v$ $(0 < v < a)$ on the positive real axis, we obtain

$$-\int_0^a \frac{x\sin kx}{(v^2-x^2)S_1(x)}dx + \int_b^\infty \frac{x\sin kx}{(v^2-x^2)S_3(x)}dx - \frac{\pi}{2}\frac{\cos kv}{S_1(v)}$$
$$= \int_a^b \frac{x\cos kx}{(v^2-x^2)S_2(x)}dx \qquad (k>0, \quad 0<v<a).$$

Using the above two identities suitably in the expression (5.7), interchanging the order of integration and utilizing the result (GRADSTEYN and RYZHIK [9]), pp. 415)

$$\int_0^\infty \frac{k\cos ky\sin ku}{k^2+K^2}dk = \begin{cases} \frac{\pi}{2}e^{-Ku}\cosh Ky, & 0<y<u, \\ -\frac{\pi}{2}e^{-Ky}\sinh Ku, & 0<u<y, \end{cases}$$

we obtain after some calculations that the expression (5.7) is equal to $-(\pi/4)JI$.

Hence for $\alpha = 0$, we have

$$A_0 = B_0 = -\frac{J}{\pi I}$$

thereby giving an exact value of C for $\alpha = 0$, so that in this case $R = iI/(J+iI)$, which was earlier obtained by PORTER [1].

6. Numerical results

The expressions (5.5) and (5.6) of A_0 and B_0, respectively, and hence the lower and upper bounds for $|R|$ and $|T|$ are evaluated numerically for a number of values of the non-dimensional parameters Kb, a/b and the angle of incidence α. The various single integrals appearing in these expressions are evaluated by using the Gauss quadrature formula appropriately. For the repeated integrals, the inner integrals are evaluated by using the Gauss quadrature formula while the outer integrals over $(0, \infty)$ are split into those over $(0, 1)$ and $(1, \infty)$. The integrals over $(0, 1)$ are computed by using the Gauss quadrature formula. The integrals over $(1, \infty)$ are evaluated by Simpson's rule over $(1, X)$ $(X \gg 1)$, where X increases till the values of the integrals correct to some desired decimal places are obtained. A representative set of values of the lower and upper bounds R_1 and R_2 of $|R|$ for various values of the parameters is displayed in Tables 1 to 3. Table 1 gives the bounds of $|R|$ for various values of the wave number Kb, the angle of incidence α and for $a/b = 0.05$. Tables 2 and 3 give the same for $a/b = 0.1$ and 0.5, respectively.

Table 1. Lower and upper bounds for the reflection coefficient $|R|$ for $a/b = 0.05$.

	$\alpha = 0°$	$\alpha = 30°$		$\alpha = 60°$		$\alpha = 85°$	
Kb	$R_1 = R_2$	R_1	R_2	R_1	R_2	R_1	R_2
0.05	0.7065	0.6256	0.6376	0.3899	0.4062	0.0712	0.0783
0.4	0.3250	0.2412	0.2580	0.1181	0.1376	0.0194	0.0233
1.2	0.0787	0.0492	0.0565	0.0215	0.0282	0.0034	0.0047
2.0	0.0316	0.0214	0.0245	0.0100	0.0132	0.0016	0.0023
3.0	0.0382	0.0320	0.0326	0.0178	0.0186	0.0030	0.0032
4.0	0.0657	0.0564	0.0565	0.0321	0.0323	0.0056	0.0056

Table 2. Lower and upper bounds for the reflection coefficient $|R|$ for $a/b = 0.1$.

	$\alpha = 0°$	$\alpha = 30°$		$\alpha = 60°$		$\alpha = 85°$	
Kb	$R_1 = R_2$	R_1	R_2	R_1	R_2	R_1	R_2
0.05	0.7072	0.6264	0.6384	0.3907	0.4070	0.0714	0.0785
0.4	0.3284	0.2444	0.2612	0.1200	0.1397	0.0197	0.0237
1.2	0.0963	0.0640	0.0722	0.0292	0.0374	0.0047	0.0063
2.0	0.0806	0.0636	0.0671	0.0335	0.0377	0.0056	0.0065
3.0	0.1545	0.1324	0.1327	0.0751	0.0756	0.0130	0.0131
4.0	0.2802	0.2411	0.2414	0.1378	0.1386	0.0239	0.0241

It is observed from the Tables 1 – 3 that in most cases the bounds are very close to each other so that their mean value provides a very good approximation to the actual value of $|R|$. It may be noticed that the difference between the bounds

Table 3. Lower and upper bounds for the reflection coefficient $|R|$ for $a/b = 0.5$.

	$\alpha = 0°$	$\alpha = 30°$		$\alpha = 60°$		$\alpha = 85°$	
Kb	$R_1 = R_2$	R_1	R_2	R_1	R_2	R_1	R_2
0.05	0.7251	0.6473	0.6586	0.4106	0.4266	0.0758	0.0831
0.4	0.4343	0.3456	0.3624	0.1824	0.2060	0.0308	0.0059
1.2	0.6502	0.5870	0.5891	0.3752	0.3793	0.0693	0.0705
2.0	0.9466	0.9230	0.9245	0.7861	0.7953	0.2094	0.2175
3.0	0.9960	0.9931	0.9936	0.9725	0.9771	0.5661	0.6106
4.0	0.9996	0.9993	0.9993	0.9967	0.9975	0.8949	0.9206

increases with the increase of the angle of incidence, but not significantly. For fixed Kb and a/b, from each table it is further observed that $|R|$ decreases with the increase of the angle of incidence. For fixed a/b and α, $|R|$ first decreases with the increase of Kb until a minimum is reached, and then it increases to unity asymptotically for further increase in Kb. This behaviour of $|R|$ is expected physically since for small Kb, the wavelength of the incident field is large compared to the width of the gap, so that there occurs a small energy transmission through the gap giving rise to large reflection coefficient. However as Kb increases, the wavelength of the incident field and the width of the gap become comparable, resulting in an increase of energy transmission through the gap. As Kb further increases, wavelength of the incident field further decreases and the waves are then confined within a thin layer below the free surface and as such, the wave energy is almost totally reflected by the part of the wall above the gap. The presence of the gap is hardly felt by these short waves and in the limit $|R| \to 1$ as $Kb \to \infty$. Thus $|R|$ has a minimum for some moderate value of Kb. For the normal incidence case, qualitatively similar behaviour of $|R|$ is noticed in the figure presented by PORTER [1]. It may be noted that for the complementary problem of submerged plate, the reflection coefficient exhibits the opposite behaviour (cf. EVANS [10]).

The results obtained from our numerical scheme for normal incidence have been compared with PORTER'S [1] results. PORTER [1] used the non-dimensional parameters μ and k which are given here by

$$\mu = \frac{2(b-a)}{b+a}, \qquad k = \frac{K(a+b)}{2}.$$

For $\mu = 0.1$ and 1.5 with $k = 0.5$, 2.0 we obtain from our results the following numerical values of $|R|$ (taken as the mean of the two bounds).

k \ μ	0.1	1.5
0.5	0.8080	0.1609
2.0	0.9995	0.4368

These coincide with the results estimated from the graphical result of PORTER [1].

Again, for a narrow gap, the results obtained from the present numerical scheme for normal incidence are also compared with TUCK'S [2] numerical results obtained by utilizing the method of matched asymptotic expansion. The dimensionless parameters used in TUCK'S [2] analysis are $2c/h$ and h/λ (where $2c$ is the width of the gap, h is the depth of the mid-point of the gap and λ is the wavelength) which are given here by

$$\frac{2c}{h} = \frac{2(b-a)}{b+a} \qquad \text{and} \qquad \frac{h}{\lambda} = \frac{K(a+b)}{4\pi}.$$

For $2c/h = 0.05, 0.15, 0.4$ and $h/\lambda = 0.05$ we obtain here $|T|^2 = 1 - |R|^2$ as 0.3972, 0.5459 and 0.7202, respectively.

For $2c/h = 0.4$ and $h/\lambda = 0.1$, the corresponding value of $|T|^2$ as obtained here is 0.5982. As before, for $|R|$ we have taken the mean of its two bounds. These values of $|T|^2$ coincide with the results estimated from the graph of $|T|^2$ against h/λ given by TUCK [2].

Acknowledgments

This work is partially supported by the National Board for Higher Mathematics through a research award to PD, the Department of Science and Technology through a research project to SB under young scientist scheme, and the Council of Scientific and Industrial Research through a research project to BNM.

References

1. D. PORTER, *The transmission of surface waves through a gap in a vertical barrier*, Proc. Camb. Phil. Soc., **71**, 411–422, 1972.

2. E.O. TUCK, *Transmission of water waves through small apertures*, J. Fluid Mech., **49**, 65–75, 1971.

3. B.A. PACKHAM and W.E. WILLIAMS, *A note on the transmission of water waves through small apertures*, J. Inst. Math. Applic., **10**, 176–184, 1972.

4. B.N. MANDAL, *A note on the diffraction of water waves by a vertical wall with a gap*, Arch. Mech., **39**, 269–273, 1987.

5. P.L.-F. LIU and J. WU, *Transmission of oblique waves through submerged apertures*, Appl. Ocean Res., **8**, 144–150, 1986.

6. B.N. MANDAL and P.K. KUNDU, *A note on the transmission of oblique waves through small apertures*, Computers Math. Applic., **21**, 17–22, 1991.

7. B.N. MANDAL and D.P. DOLAI, *Oblique water wave diffraction by thin vertical barriers in water of uniform finite depth*, Appl. Ocean Res., **16**, 195–203, 1994.

8. D.V. EVANS and C.A.N. MORRIS, *The effect of a fixed vertical barrier on oblique incident surface waves in deep water*, J. Inst. Math. Applic., **9**, 198–204, 1972.

9. I.S. GRADSTEYN and I.M. RYZHIK, *Table of integrals, series and products*, Academic Press, New York 1980.

10. D.V. EVANS, *Diffraction of water waves by a submerged vertical plate*, J. Fluid Mech., **40**, 433–451, 1970.

PHYSICS AND APPLIED MATHEMATICS UNIT
INDIAN STATISTICAL INSTITUTE, CALCUTTA
and
DEPARTMENT OF MATHEMATICS
JADAVPUR UNIVERSITY, CALCUTTA, INDIA.

Received February 21, 1996.

Arch. Mech., 48, 6, pp. 973–984, Warszawa 1996

Some existence result for a Stokes flow between two arbitrarily closed curves

M. KOHR (CLUJ – NAPOCA)

THE PROBLEM of determining the slow viscous flow of a fluid between two arbitrarily closed curves is formulated as a system of Fredholm integral equations of the second kind, addying a pair of singularities located outside of the flow region. We show that the integral equations proposed here have a unique continuous solution, when the two closed curves are Lyapunov curves and the fluid velocity is continuous on these curves.

1. Mathematical formulation

WE CONSIDER the creeping flow of an incompressible viscous fluid between two arbitrary closed Lyapunov curves (i.e. they have a continuously varying normal vector) denoted by C^1 and C^2, and supposed to be on the upper half plane $\mathbb{R}^2_+ = \{(x_1, x_2) \in \mathbb{R}^2 : x_2 \geq 0\}$. Also, we suppose that the Reynolds number of the flow is very small. Under this condition, the governing equations for the velocity $\mathbf{u}(u_1, u_2)$ and pressure p can be reduced to the Stokes equations:

$$\begin{aligned} \Delta \mathbf{u}(x) &= \nabla p(x), \qquad x \in \Omega, \\ \nabla \cdot \mathbf{u}(x) &= 0, \qquad x \in \Omega, \end{aligned} \tag{1.1}$$

where the symbols ∇ and Δ mean the gradient operator and the Laplace operator, respectively. Here $x(x_1, x_2) \in \Omega$ and Ω is the two-dimensional bounded domain with the boundaries C^1 and C^2, respectively, such that C^1 is located inside of the domain bounded by C^2.

The fluid velocity $\mathbf{u}$ must satisfy the following boundary conditions on the curves C^1 and C^2:

$$\begin{aligned} \mathbf{u}(x) &= \mathbf{f}_1(x), \qquad \text{for} \quad x \in \Omega, \\ \mathbf{u}(x) &= \mathbf{f}_2(x), \qquad \text{for} \quad x \in \Omega, \end{aligned} \tag{1.2}$$

where the boundary velocities $\mathbf{f}_1$ and $\mathbf{f}_2$ are supposed to be smooth vector functions.

Using the continuity equation $(1.1)_2$, we deduce the following relation:

$$\int_{C^1 \cup C^2} u_j(x) n_j(x)\, ds_x = 0,$$

hence, a necessary condition for our problem to have a solution in Ω is that

$$\int_{C^1} f_{1j}(x)n_j(x)\,ds_x = \int_{C^2} f_{2j}(x)n_j(x)\,ds_x. \tag{1.3}$$

Here $\mathbf{n}(n_1, n_2)$ is the unit outward normal vector at points of C^1 and C^2.

By applying the Green identity for a smooth and solenoidal vector $\mathbf{v}(v_1, v_2)$ and a scalar function q, we obtain:

$$\int_\Omega \left(\Delta v_j - \frac{\partial q}{\partial x_j}\right) u_j\,dx + \frac{1}{2}\int_\Omega \left(\frac{\partial u_j}{\partial x_i} + \frac{\partial u_i}{\partial x_j}\right)\left(\frac{\partial v_j}{\partial x_i} + \frac{\partial v_i}{\partial x_j}\right) dx = \int_{C^1} T_{ij}(\mathbf{v})u_i n_j\,ds - \int_{C^2} T_{ij}(\mathbf{v})u_i n_j\,ds, \tag{1.4}$$

where

$$T_{ij}(\mathbf{v}) = -q\delta_{ij} + \frac{\partial v_i}{\partial x_j} + \frac{\partial v_j}{\partial x_i}, \qquad i, j \in \{1, 2\}, \tag{1.5}$$

are the components of the stress tensor, corresponding to the flow $(\mathbf{v}, q)$.

The formula (1.4) applied to $\mathbf{u} = \mathbf{v}$ and $p = q$, gives the following equality:

$$\frac{1}{2}\int_\Omega \left(\frac{\partial u_i}{\partial x_j} + \frac{\partial u_j}{\partial x_i}\right)^2 dx = \int_{C^1} T_{ij}(\mathbf{u})u_i n_j\,ds - \int_{C^2} T_{ij}(\mathbf{u})u_i n_j\,ds. \tag{1.6}$$

If we suppose that our problem has two solutions $\mathbf{u}_1$ and $\mathbf{u}_2$, then the vector $\mathbf{u} = \mathbf{u}_1 - \mathbf{u}_2$ satisfies homogeneous boundary conditions on C^1 and C^2, and the formula (1.6) gives:

$$\frac{\partial u_i}{\partial x_j}(x) + \frac{\partial u_j}{\partial x_i}(x) = 0, \qquad x \in \Omega, \quad i, j \in \{1, 2\}. \tag{1.7}$$

This system has three linearly independent solutions:

$$\mathbf{u}^1(x) = (1, 0), \qquad \mathbf{u}^2(x) = (0, 1), \qquad \mathbf{u}^3(x) = (x_2, -x_1), \qquad x \in \Omega. \tag{1.8}$$

Hence, we conclude that the fluid motion compatible with homogeneous boundary conditions on C^1 and C^2 is given by the null solution $\mathbf{u} = \mathbf{0}$.

In the following we consider the components of stress tensor $\tilde{\Pi}$ corresponding to the Stokes equations (see [1] and [8]):

$$T_{ijk}(x, y) = -q_j(x, y)\delta_{ik} + \frac{\partial q_{ij}}{\partial x_k}(x, y) + \frac{\partial q_{kj}}{\partial x_i}(x, y), \tag{1.9}_1$$

where q_{ij} and q_j are components of Green tensor G and pressure vector $\mathbf{q}$, respectively. G and $\mathbf{q}$ satisfy the following equations and conditions:

$$(1.9)_{2-5}\qquad \begin{aligned} \Delta_x q_{ij}(x,y) - \frac{\partial q_j}{\partial x_i}(x,y) &= -4\pi\delta_{ij}\delta(x-y), \qquad \text{for} \quad x_2 > 0,\\ \frac{\partial}{\partial x_i} q_{ij}(x,y) &= 0, \qquad \text{for} \quad x_2 > 0,\\ q_{ij}(x,y) &= 0, \qquad \text{for} \quad x_2 = 0,\\ q_{ij}(x,y) \to 0, \qquad q_i(x,y) &\to 0, \qquad \text{as} \quad |x| \to \infty, \end{aligned}$$

where δ is Dirac's distribution.

From [8] it results that the Green tensor G can be written as:

$$(1.9)_6\quad G(x,y) = G^{ST}(x-y) - G^{ST}(x-y^{im}) + 2y_2^2 G^D(x-y^{im}) - 2y_2 G^{SD}(x-y^{im}),$$

where $y^{im} = (y_1, -y_2)$ is the image of the pole y with respect to the boundary $y_2 = 0$, the Green tensor G^{ST} has the components (see [8]):

$$(1.9)_7\qquad q_{ij}^{ST}(x) = -\ln|x|\delta_{ij} + \frac{x_i x_j}{|x|^2}.$$

The matrices which correspond to the tensors G^D and G^{SD} are given by

$$(1.9)_{8-9}\qquad \begin{aligned} q_{ij}^D(x) &= \pm\left(\frac{\delta_{ij}}{|x|^2} - 2\frac{x_i x_j}{|x|^4}\right),\\ q_{ij}^{SD}(x) &= x_2 q_{ij}^D(x) \pm \frac{\delta_{j2}x_i - \delta_{i2}x_j}{|x|^2}, \end{aligned}$$

where the plus sign applies for $j = 1$, in the $0x_1$ direction, and the minus sign for $j = 2$, and in the $0x_2$ direction.

The pressure tensor $\mathcal{P}$, with components Π_{ij}, is associated with the tensor $\tilde{\Pi}$. Precisely, we have

$$(1.10)_1\qquad \Pi_{ij}(x,y) = -P(x,y)\delta_{ij} + \frac{\partial q_i}{\partial y_j}(x,y) + \frac{\partial q_j}{\partial y_i}(x,y),$$

where

$$(1.10)_2\qquad -\frac{\partial P}{\partial x_i}(x,y) + \Delta_x q_i(y,x) = 0, \qquad \text{for} \quad x \neq y, \quad x \in \mathbb{R}^2_+$$

and

$$(1.10)_3\qquad \frac{\partial q_i}{\partial x_i}(y,x) = 0, \qquad x \in \mathbb{R}^2_+, \qquad x \neq y.$$

The pressure vector $\mathbf{q}$ can be written as (see [8]):

$$\mathbf{q}(x,y) = \mathbf{q}^{ST}(x-y) - \mathbf{q}^{ST}(x-y^{im}) - 2y_2\mathbf{q}^{SD}(x-y^{im}), \tag{1.10}_4$$

where

$$q_i^{ST}(x) = \frac{2x_i}{|x|^2}, \qquad \mathbf{q}^{SD}(x) = -\frac{2}{|x|^4}(2x_1x_2,\ x_1^2 - x_2^2). \tag{1.10}_5$$

With the above notations, we consider the following relations:

$$\begin{aligned} K_{ij}(x,y) &= T_{jik}(y,x)n_k(y), \\ K_i(x,y) &= \Pi_{ij}(x,y)n_j(y), \end{aligned} \tag{1.11}$$

where $y(y_1,y_2) \in C^1 \cup C^2$.

We determine the solution $(\mathbf{u}, p)$ of the Stokes problem (1.1), (1.2) in terms of the following double-layer potentials:

$$\begin{aligned} u_j(x) &= \int\limits_{C^1\cup C^2} K_{jl}(x,y)\phi_l(y)\,ds_y, \qquad x \in \Omega, \quad j \in \{1,2\}, \\ p(x) &= \int\limits_{C^1\cup C^2} K_j(x,y)\phi_j(y)\,ds_y, \qquad x \in \Omega. \end{aligned} \tag{1.12}$$

From the boundary conditions (1.2) we obtain a Fredholm integral system of the second kind for the unknown density $\boldsymbol{\phi}(\phi_1,\phi_2)$:

$$\begin{aligned} -2\pi\phi_j(x) + \int\limits_{C^1\cup C^2} K_{jl}(x,y)\phi_l(y)\,ds_y &= f_{1j}(x), \qquad x \in C^1, \\ 2\pi\phi_j(x) + \int\limits_{C^1\cup C^2} K_{jl}(x,y)\phi_l(y)\,ds_y &= f_{2j}(x), \qquad x \in C^2. \end{aligned} \tag{1.13}$$

We used here the following jump relations of the double layer potentials:

$$\lim_{x'\to x\in C} \int\limits_C \phi_j(y)K_{ij}(x',y)\,ds_y = \pm 2\pi\phi_i(x) + \int\limits_C \phi_j(y)K_{ij}(x,y)\,ds_y \tag{1.13'}$$

where C is a closed Lyapunov curve, the sign + corresponds to the internal side of C, and the sign − to the external side.

The above integrals, which appear in (1.13), are considered as the principal values in the Cauchy means.

The system (1.13) has a solution if and only if the non-homogeneous term $\mathbf{f} : C^1 \cup C^2 \to \mathbb{R}^2$, $\mathbf{f}(x) = \mathbf{f}_i(x)$, for $x \in C^i$, $i \in \{1,2\}$, is orthogonal to the

solutions of the corresponding adjoint homogeneous system. We used here the second Fredholm alternative for Fredholm's type integral equations (see [3, 4]).

Let us consider the homogeneous system of (1.13):

$$
\begin{aligned}
&-2\pi\phi_j^0(x) + \int\limits_{C^1\cup C^2} K_{jl}(x,y)\phi_l^0(y)\,ds_y = 0, \qquad x \in C^1,\\
&2\pi\phi_j^0(x) + \int\limits_{C^1\cup C^2} K_{jl}(x,y)\phi_l^0(y)\,ds_y = 0, \qquad x \in C^2.
\end{aligned} \tag{1.14}
$$

Also, the homogeneous adjoint system of (1.13) has the form:

$$
\begin{aligned}
&-2\pi\tau_j(x) + \int\limits_{C^1\cup C^2} K_{lj}(y,x)\tau_l(y)\,ds_y = 0, \qquad x \in C^1,\\
&2\pi\tau_j(x) + \int\limits_{C^1\cup C^2} K_{lj}(y,x)\tau_l(y)\,ds_y = 0, \qquad x \in C^2.
\end{aligned} \tag{1.15}
$$

From the first Fredholm's alternative (see [3, 4]) it results that the vector solutions of the system (1.14) and (1.15), respectively, form two vector spaces of same finite dimension d.

If we use the following properties of the stress tensor:

$$
\begin{aligned}
&\frac{\partial T_{ijk}}{\partial x_i}(x,y) = \frac{\partial T_{kji}}{\partial x_i}(x,y) = -4\pi\delta_{kj}\delta(x-y),\\
&\frac{\partial}{\partial x_k}\left[\varepsilon_{ilm}x_l T_{mjk}(x,y)\right] = -4\pi\varepsilon_{ilj}x_l\delta(x-y),
\end{aligned} \tag{1.16}
$$

where δ is the Dirac distribution, and using the divergence theorem in a bounded domain $D \subset \mathbb{R}^2$, having the boundary C, we obtain the next properties:

$$
\begin{aligned}
&\int\limits_C T_{ijk}(y,x)n_k(y)\,ds_y = \begin{cases} 2\pi\delta_{ij}, & \text{for } x \in C,\\ 0, & \text{for } x \notin D\cup C,\end{cases}\\
&\int\limits_C \varepsilon_{ijk}y_j T_{klm}(y,x)n_m(y)\,ds_y = \begin{cases} 2\pi\varepsilon_{ijl}x_l, & \text{for } x \in C,\\ 0, & \text{for } x \notin D\cup C,\end{cases}
\end{aligned} \tag{1.17}
$$

where the components T_{ijk} are given by $(1.9)_1$, the unit normal vector $\mathbf{n}$ is directed inside of D, and the symbol ε_{ijk} means:

$$
\varepsilon_{ijk} = \begin{cases} 1, & \text{for an old permutation of numbers 1, 2, 3,}\\ -1, & \text{for an eden permutation of numbers 1, 2, 3.}\end{cases}
$$

By applying the properties (1.13), (1.17) we deduce that the functions $\mathbf{u}^i$, $i \in \{1,2,3\}$, given by (1.8), are solutions of the following equations:

$$(1.18) \qquad -2\pi u_j^i(x) + \int_{C^1} K_{jl}(x,y) u_l^i(y)\, ds_y = 0, \quad x \in C^1, \quad i \in \{1,2,3\}, \quad j \in \{1,2\}$$

and

$$(1.19) \qquad \int_{C^1} K_{jl}(x,y) u_l^i(y)\, ds_y = 0, \quad x \in C^2, \quad i \in \{1,2,3\}.$$

Let the vector functions $\boldsymbol{\phi}_i^0 : C^1 \cup C^2 \to \mathbb{R}^2$, $i \in \{1,2,3\}$, be given by

$$\boldsymbol{\phi}_i^0(x) = \begin{cases} \mathbf{u}^i(x), & x \in C^1, \\ 0, & x \in C^2. \end{cases}$$

From (1.18) and (1.19), we deduce that these functions are three linearly independent solutions of homogeneous system (1.14). Hence, we conclude that $d \geq 3$. In the next we shall prove that $d = 3$. For this aim we consider the single-layer potentials

$$(1.20) \qquad V_i^0(x) = \int_{C^1 \cup C^2} q_{ij}(x,y) \tau_j(y)\, ds_y, \qquad i \in \{1,2\}$$

with their corresponding pressure

$$(1.20') \qquad P^0(x) = \int_{C^1 \cup C^2} q_j(x,y) \tau_j(y)\, ds_y$$

where $\boldsymbol{\tau}$ is a possible solution of the adjoint system (1.15), q_{ij} and q_j are given by $(1.9)_{6-9}$ and $(1.10)_{4,5}$, respectively.

From $(1.9)_{2,3}$ it results that the potentials (1.20), (1.20′) determine a Stokes flow in Ω.

Since the potentials (1.20) and (1.20′) are continuous on C^1 and C^2, it follows that (1.20) can be considered as a continuous velocity field at every point $x \in \mathbb{R}^2_+$. On the other hand, the vector tension, of (1.20) and (1.20′), has a jump in points of C^1 and C^2. It is easily seen that the limiting value of the vector tension, when $x \in \Omega^2 = \mathbb{R}^2_+ \setminus (\Omega^1 \cup \overline{\Omega})$ tends to a point $x \in C^2$, is given by the left-hand side of Eqs. $(1.15)_2$. The limiting value of the vector tension, when $x' \in \Omega^1$ (the domain bounded by the curve C^1) tends to a point $x \in C^1$, is given by the left-hand side of Eqs. $(1.15)_1$.

We can see that, for $x \in \Omega^1$, the potentials (1.20) and (1.20′) represent a Stokes flow with zero vector tension in points of C^1. As in (1.6), we deduce that:

$$(1.21) \qquad V_j^0(x) = u_j^i(x), \qquad \text{for} \quad x \in \Omega^1, \quad j \in \{1,2\}, \quad i \in \{1,2,3\},$$

where the functions $\mathbf{u}^i$, $i \in \{1,2,3\}$ are given in (1.8) (or a linear combination of these functions).

In the same way, the potentials (1.20) and (1.20′), for all $x \in \Omega^2$, represent a Stokes flow in Ω^2 with zero vector tension on C^2, with zero velocity on the boundary $x_2 = 0$, and the asymptotic form at infinity:

$$\mathbf{V}^0(x) = O(1), \qquad \text{as} \quad |x| \to \infty.$$

In the above statement we consider the boundary $x_2 = 0$ as a rigid wall, bounding a Stokes flow in Ω^2.

By using the Green's formula in Ω^2, it results that

$$\mathbf{V}^0(x) = \mathbf{0}, \qquad \text{for all} \quad x \in \Omega^2. \tag{1.22}$$

The previous arguments show that the potentials (1.20), (1.20′) represent a Stokes flow in Ω with the following boundary conditions on C^1 and C^2:

$$\begin{aligned} &V_j^0(x) = u_j^i(x), \qquad x \in C^1, \quad j \in \{1,2\}, \quad i \in \{1,2,3\}, \\ &V_j^0(x) = 0, \qquad\quad x \in C^2, \quad j \in \{1,2\}. \end{aligned} \tag{1.23}$$

The above conditions determine the following Fredholm integral system of the first kind for the unknown function $\boldsymbol{\tau}$:

$$\begin{aligned} &\int\limits_{C^1 \cup C^2} q_{ij}(x,y)\tau_j(y)\,ds_y = u_i^k(x), \quad x \in C^1, \quad i \in \{1,2\}, \quad k \in \{1,2,3\}, \\ &\int\limits_{C^1 \cup C^2} q_{ij}(x,y)\tau_j(y)\,ds_y = 0, \qquad\qquad x \in C^2, \quad i \in \{1,2\}. \end{aligned} \tag{1.24}$$

Using the Fredholm's alternative (see [3, 4]), we prove that the system (1.24) has a unique solution, for each $k \in \{1,2,3\}$. In fact we show that the corresponding homogeneous system (1.24) has only a trivial solution.

For this aim, let us consider the following system:

$$\begin{aligned} &\int\limits_{C^1 \cup C^2} q_{ij}(x,y)\tau_j^0(y)\,ds_y = 0, \qquad x \in C^1, \quad i \in \{1,2\}, \\ &\int\limits_{C^1 \cup C^2} q_{ij}(x,y)\tau_j^0(y)\,ds_y = 0, \qquad x \in C^2, \quad i \in \{1,2\}. \end{aligned} \tag{1.25}$$

If we consider the single-layer potentials (1.20) and (1.20′) with density given by any possible continuous solution $\boldsymbol{\tau}^0$ of (1.25), then we conclude that the Stokes velocity $\mathbf{V}^0 = \mathbf{V}^0(\boldsymbol{\tau}^0)$ vanishes identically on C^1 and C^2. From the uniqueness result of the solution corresponding to the boundary-value problem (1.1), (1.2), we conclude that $\mathbf{V}^0 = \mathbf{V}^0(\boldsymbol{\tau}^0)$ must be equal to zero in Ω.

On the other hand, from the continuity property of single-layer potentials $V_j^0 = V_j^0(\boldsymbol{\tau}^0)$, $j \in \{1,2\}$, in each point of upper halfplane $\mathbb{R}^2_+$, it results that

$V_j^0 = V_j^0(\boldsymbol{\tau})(x) = 0$, for all $x \in \Omega^2$. Therefore, $T_{ij}(\mathbf{V}^0(\boldsymbol{\tau}^0)(x)) = 0$, for all $x \in \Omega^2$, and in particular we obtain

$$\lim_{\substack{x' \to x \in C^2 \\ x' \in \Omega^2}} T_{ij}(\mathbf{V}^0(\boldsymbol{\tau}^0)(x'))n_j(x') = -2\pi\tau_i^0(x) - \int_{C^1 \cup C^2} K_{ji}(y,x)\tau_j^0(y)\,ds_y = 0. \tag{1.26}$$

Also, we have

$$\lim_{\substack{x' \to x \in C^2 \\ x' \in \Omega}} T_{ij}(\mathbf{V}^0(\boldsymbol{\tau}^0)(x'))n_j(x') = 2\pi\tau_i^0(x) - \int_{C^1 \cup C^2} K_{ji}(y,x)\tau_j^0(y)\,ds_y = 0. \tag{1.27}$$

From (1.26) and (1.27) we obtain that $\boldsymbol{\tau}^0(x) = 0$, for $x \in C^2$. Analogously, we can prove that $\boldsymbol{\tau}^0(x) = 0$, for $x \in C^1$. Hence, the only solution of the homogeneous system (1.25) is the trivial solution, and also the system (1.24) (with k fixed) has a unique continuous solution. Because the system (1.24) has three linearly independent non-homogeneous terms $\mathbf{u}^1$, $\mathbf{u}^2$, $\mathbf{u}^3$, it is easily shown that the corresponding solutions, denoted by $\boldsymbol{\tau}^1$, $\boldsymbol{\tau}^2$, $\boldsymbol{\tau}^3$, are linearly independent. For this aim, let us consider the real numbers γ_1, γ_2, γ_3, such that

$$\sum_{i=1}^{3} \gamma_i \boldsymbol{\tau}^i(x) = 0, \qquad x \in C^1 \cup C^2.$$

Using (1.24) and the above equality, we obtain:

$$0 = \int_{C^1 \cup C^2} \left\{ q_{lj}(x,y) \sum_{i=1}^{3} \gamma_i \tau_j^i(y) \right\} ds_y = \sum_{i=1}^{3} \gamma_i u_l^i(x), \qquad x \in C^1, \quad l \in \{1,2\}.$$

By applying the linearly independent property of the functions $\mathbf{u}^1$, $\mathbf{u}^2$, $\mathbf{u}^3$, we deduce that $\gamma_1 = \gamma_2 = \gamma_3 = 0$, hence the functions $\boldsymbol{\tau}^1$, $\boldsymbol{\tau}^2$, $\boldsymbol{\tau}^3$, are linearly independent.

On the other hand, each solution $\boldsymbol{\tau}$ of the adjoint system (1.15) is also a solution of system (1.24). Hence, the system (1.15) has at most three linearly independent solutions, which shows that $d \leq 3$. Now we conclude that $d = 3$ and that the system (1.15) has the same solutions as the system (1.24).

By following the second Fredholm alternative (see [3, 4]), it results that a necessary and sufficient condition for the solvability of system (1.13), can be written as:

$$\int_{C^1} f_{1j}(x)\tau_j^i(x)\,ds_x + \int_{C^2} f_{2j}(x)\tau_j^i(x)\,ds_x = 0, \qquad i \in \{1,2,3\}, \tag{1.28}$$

where $\boldsymbol{\tau}^1$, $\boldsymbol{\tau}^2$, $\boldsymbol{\tau}^3$, are linearly independent solutions of system (1.24).

Finally, we can formulate the following result:

THEOREM. *The Stokes problem* (1.1), (1.2) *with the boundary condition* (1.3), *has a unique solution* $(\mathbf{u}, p)$ *on the bounded domain* Ω, *if and only if the functions* $\mathbf{f}_1$ *and* $\mathbf{f}_2$ *satisfy the conditions* (1.28).

The above condition (1.28) is restrictive. Then we consider a modified form for the flow $(\mathbf{u}, p)$.

2. Another form of solution

Using the singularity method, we determine the flow $(\mathbf{u}, p)$ as a sum of a double-layer potential plus some singularities located in a point x_c from the domain Ω^1:

$$
\begin{aligned}
u_j(x) &= \int_{C^1 \cup C^2} K_{jl}(x,y)\phi_l(y)\,ds_y + \alpha_i q_{ji}(x,x_c) \\
&\quad + w_l \varepsilon_{lmi} \frac{\partial q_{ji}}{\partial y_m}(x,x_c), \qquad j \in \{1,2\}, \\
p(x) &= \int_{C^1 \cup C^2} K_j(x,y)\phi_j(y)\,ds_y + \alpha_i q_i(x,x_c) \\
&\quad + \varepsilon_{lmj} \frac{\partial q_j}{\partial y_m}(x,x_c) w_l, \qquad x \in \Omega.
\end{aligned} \tag{2.1}
$$

We choose the constants α_i, $w_3 \in \mathbb{R}$ in the following manner:

$$
\begin{aligned}
\alpha_j &= \int_{C^1 \cup C^2} \phi_l(y) u_l^j(y)\,ds_y, \qquad j \in \{1,2\}, \\
w_3 = \alpha_3 &= \int_{C^1 \cup C^2} \phi_l(y) u_l^3(y)\,ds_y,
\end{aligned} \tag{2.2}
$$

where the functions $\mathbf{u}^1$, $\mathbf{u}^2$, $\mathbf{u}^3$ are given in (1.8).

By applying the boundary conditions (1.2), we obtain the following Fredholm integral system of second kind, with the unknown function $\boldsymbol{\phi}$:

$$
\begin{aligned}
&-2\pi\phi_j(x) + \int_{C^1 \cup C^2} K_{jl}(x,y)\phi_l(y)\,ds_y + \alpha_i q_{ji}(x,x_c) \\
&\quad + w_l \varepsilon_{lmi} \frac{\partial q_{ji}}{\partial y_m}(x) = f_{1j}(x), \qquad x \in C^1, \\
&2\pi\phi_j(x) + \int_{C^1 \cup C^2} K_{jl}(x,y)\phi_l(y)\,ds_y + \alpha_i q_{ji}(x,x_c) \\
&\quad + \varepsilon_{lmi} \frac{\partial q_{ji}}{\partial y_m}(x,x_c) w_l = f_{2j}(x), \qquad x \in C^2.
\end{aligned} \tag{2.3}
$$

According to Fredholm's alternative (see [3, 4]), in order to prove the existence and uniqueness result of solution of system (2.3), it is sufficient to show that the following homogeneous system (2.47) has only the trivial solution:

$$
\begin{aligned}
&-2\pi\phi_j^0(x) + \int_{C^1\cup C^2} K_{jl}(x,y)\phi_l^0(y)\,ds_y + \alpha_i^0 q_{ji}(x,x_c) \\
&\qquad + w_l^0 \varepsilon_{lmi}\frac{\partial q_{ji}}{\partial y_m} = 0, \qquad x \in C^1, \\
&2\pi\phi_j^0(x) + \int_{C^1\cup C^2} K_{jl}(x,y)\phi_l^0(y)\,ds_y + \alpha_i^0 q_{ji}(x,x_c) \\
&\qquad + w_l^0 \varepsilon_{lmi}\frac{\partial q_{ji}}{\partial y_m}(x,x_c) = 0, \qquad x \in C^2,
\end{aligned}
\tag{2.4}
$$

where

$$
\alpha_j^0 = \int_{C^1\cup C^2} \phi_l^0(y) u_l^j(y)\,ds_y, \qquad j \in \{1,2,3\} \tag{2.5}
$$

and $w_3^0 = \alpha_3^0$.

From (1.13′) and (2.4) it results that the vectors $\mathbf{v}^1$ and $\mathbf{v}^2$, given by:

$$
\begin{aligned}
v_j^1(x) &= \int_{C^1\cup C^2} K_{jl}(x,y)\phi_l^0(y)\,ds_y\,, \\
v_j^2(x) &= \left\{\alpha_i^0 q_{ji}(x,x_c) + w_l^0 \varepsilon_{lmi}\frac{\partial q_{ji}}{\partial y_m}(x,x_c)\right\}, \quad j \in \{1,2\}
\end{aligned}
\tag{2.6}
$$

can be considered as Stokes velocity flows in Ω, which are equal on C^1 and C^2. From the uniqueness result of solution corresponding to the Stokes problem (1.1), (1.2) we deduce that $\mathbf{v}^1 = \mathbf{v}^2$ in Ω. It is easy to show that $\mathbf{v}^1$ gives zero total force on C^1 or C^2 (when the tension vector is considered in points of C^1 and C^2 as limiting values), and $\mathbf{v}^2$ gives a non-zero total force on C^1 or C^2, equal to $\pm 4\pi\boldsymbol{\alpha}^0$, where $\boldsymbol{\alpha}^0 = (\alpha_1^0, \alpha_2^0)$. Hence, we obtain

$$
\alpha_1^0 = \alpha_2^0 = 0. \tag{2.7}
$$

On the other hand, $\mathbf{v}^1$ yields zero total torque on C^1 or C^2, and $\mathbf{v}^2$ yields a non-zero torque on C^1 or C^2. Precisely, this torque is equal to $\pm 8\pi\alpha_3^0\mathbf{k}$, where $\mathbf{k}$ is the unit vector of the $0x_3$ axis, orthogonal to the $0x_1x_2$ plane. We conclude that

$$
\alpha_3^0 = w_3^0 = 0. \tag{2.8}
$$

From (2.7) and (2.8) it results that the system (2.4) is reduced to the system (1.14), which has three linearly independent solutions:

$$\phi_i^0(x) = \begin{cases} \mathbf{u}^i(x), & x \in C^1, \\ 0 & x \in C^2, \end{cases} \qquad i \in \{1,2,3\}.$$

Then, any solution of system (2.4) can be written as follows:

$$\phi^0(x) = \sum_{i=1}^{3} \beta_i \phi_i^0(x), \qquad x \in C^1 \cup C^2, \tag{2.9}$$

where β_1, β_2, β_3 are some real constants.

Using (2.7), (2.8) and (2.9) we obtain the following linear algebraic system with unknows β_i, $i \in \{1,2,3\}$:

$$\sum_{i=1}^{3} \beta_i \int_{C^1} u_l^i(y) u_l^j(y)\, ds_y = 0, \qquad j \in \{1,2,3\}. \tag{2.10}$$

Using the form of functions $\mathbf{u}^i$, $i \in \{1,2,3\}$ we infer that the corresponding determinant of system (2.10) is non-zero. Hence, $\beta_1 = \beta_2 = \beta_3 = 0$, which shows that the only solution of system (2.4) is the null solution. It results that the Fredholm integral system (2.3) has a unique continuous solution. With this argument we have proved the existence and uniqueness of solution corresponding to the Stokes problem (1.1)–(1.2).

REMARK. An analogous problem for the creeping flow of an incompressible viscous fluid between two arbitrary closed surfaces, was studied recently by H. POWER and G. MIRANDA (see [7]). Using the theory of single layer potentials, T.M. FISCHER, G.C. HSIAO, W.L. WENDLAND studied the slow viscous flows past obstacles in a half-plane (see [2]). Using the theory of double layer potentials, H. POWER and G. MIRANDA solved the problem of a three-dimensional Stokes flow past a rigid obstacle (see [5]).

The same method as that used in [5], was applied by H. Power to solve the problem of a Stokes flow past n bodies ($n \geq 1$) of arbitrary shapes (see [6]). A complete double-layer method was given by N.P. THIEN, D. TULLOCK and S. KIM in [9], to solve the problem of a Stokes flow past obstacles in a half-space.

References

1. L. DRAGOŞ, *Principles of continuous mechanics media* [in Romanian], Tehnică, Bucharest 1983.
2. T.M. FISCHER, G.C. HISAO and W.L. WENDLAND, *On two-dimensional slow viscous flows past obstacles in a half-plane*, Proc. of the Royal Soc. Edinburgh, **104A**, 205–215, 1986.
3. V. MIKHAILOV, *Equations aux derivées partielles*, Ed. Mir, Moscow 1980.

4. N.I. MUSKHELISHVILI, *Singular integral equations*, P. Nordhoff, Gröningen, the Netherlands 1953.
5. H. POWER and G. MIRANDA, *Second kind integral equations formulation of Stokes flows past a particle of arbitrary shape*, SIAM J. Math., **47**, 4, 689–698, 1987.
6. H. POWER, *Second kind integral equation solution of Stokes flows past n bodies of arbitrary shapes*, [in:] Boundary Element Techniques, C. BREBBIA [Ed.], IX, Springer-Verlag, 1985.
7. H. POWER and G. MIRANDA, *Integral equation for the creeping flow of an incompressible viscous fluid between two arbitrarily closed surfaces, and a possible mathematical model for the brain fluid dynamics*, J. Math. Anal. Appl., 137, 1989.
8. C. POZRIKIDIS, *Boundary integral and singularity methods for the linearized viscous flow*, Cambridge Univ. Press, 1992.
9. N.P. THIEN, D. TULLOCK and S. KIM, *Completed double layer in half-space: a boundary element method*, Comput. Mech., 9, 121–135, 1992.

"BABEŞ-BOLYAI" UNIVERSITY OF CLUJ-NAPOCA
FACULTY OF MATHEMATICS, CLUJ-NAPOCA, ROMANIA.

Received February 26, 1996.

Arch. Mech., 48, 6, pp. 985–1010, Warszawa 1996

Thermoelastic materials with heat flux evolution equation

GH. GR. CIOBANU (IAŞI)

THE RESULTS obtained in this paper refer to the class of materials for which *specific free energy* ψ, the *specific entropy* η, and *the first Piola–Kirchhoff stress tensor* $\mathbf{S}$ are, respectively, determined through the *constitutive functionals* $\overline{\psi}$, $\overline{\eta}$, and $\overline{S}$ which are defined in their common domain consisting of quadruples $(\mathbf{F}, \theta, \mathbf{G}, \mathbf{Q})$, called *states* of the material, and where $\mathbf{F}$ is the *deformation gradient*, θ is the *absolute temperature*, $\mathbf{G}$ is the *material gradient* of the temperature, and $\mathbf{Q}$ is the *referential heat flux*. The heat flux $\mathbf{Q}$ behaves as a "*hidden variable*" or an "*internal variable*" [1] and its evolution in time is described by a differential equation $\dot{\mathbf{Q}} = \mathbf{H}(\mathbf{F}, \theta, \mathbf{G}; \mathbf{Q})$, where $\mathbf{H}$ is a constitutive functional of the material. Such materials will be called *thermoelastic materials with heat flux evolution equation*. To a certain extent, this class of materials may be considered as a limit case of thermomechanical materials with internal state variables examined by COLEMAN and GURTIN [1]. It is for this reason that this fundamental work of modern continuum thermodynamics inspired much of the results in this paper. On the other hand, the above heat flux evolution equation is generalizing Cattaneo's heat conduction equation [2] for isotropic materials. So this theory is convenient for predicting thermal waves propagating at finite speed.

Introduction

THE BASIC FUNCTIONAL and conceptual underpinnings of the classical continuum thermodynamics are briefly presented in Sec. 1.

The axiomatic definition of thermoelastic materials with heat flux evolution equation and their constitutive equations are given in Sec. 2.

The general form of constitutive functionals $\overline{\psi}$, $\overline{\eta}$, and $\overline{S}$ in the assumption that the *heat evolution functional* $\mathbf{H}$ is linear in $\mathbf{G}$ and $\mathbf{Q}$, i.e. in the Cattaneo's case, is presented in Sec. 3.

The notions of *equilibrium state* (E.S.), *isothermal E.S.* and its *domain of attraction* for a given material point are introduced in Sec. 4. We point out that our definition of E.S. includes the usual one as a special case, but it is not confined to it. A state $(\boldsymbol{\lambda}_0, \mathbf{G}_0; \mathbf{Q}_0)$, $\boldsymbol{\lambda}_0 = (\mathbf{F}_0, \theta_0)$ is an E.S. if

$$\mathbf{G}_0 \cdot \mathbf{Q}_0 = 0, \qquad \mathbf{H}(\boldsymbol{\lambda}_0, \mathbf{G}_0; \mathbf{Q}_0) = \mathbf{0}.$$

The strictly E.S., i.e. a state $(\boldsymbol{\lambda}_0, \mathbf{0}; \mathbf{Q}_0)$ which satisfies the condition

$$\mathbf{H}(\boldsymbol{\lambda}_0, \mathbf{0}; \mathbf{Q}_0) = \mathbf{0},$$

coincides with what is usually understood by an E.S. It is showed that the free energy function has a local minimum at an asymptotically stable isothermal E.S. and that if a strictly isothermal E.S. is a strict local minimum for the free energy function then this E.S. is Lyapunov stable. Results regarding asymptotic and Lyapunov stability of a strict isothermal E.S. for *strictly dissipative materials* are also obtained.

A theorem of *consistency with thermostatics* [3] on the set of asymptotically isothermal E.S. is proved in Sec. 5.

The specific entropy is taken as an independent variable in Sec. 6. In this case the implications of the Cattaneo's equation on constitutive functionals are derived and conditions of asymptotic and Lyapunov stability of an *isentropic* E.S. at constant strain for a material point are obtained.

In Sec. 7 the specific internal energy is taken as an independent variable and results regarding the asymptotic and Lyapunov stability of an *isoenergetic* E.S., similar to the results in Sec. 4 and Sec. 6, are established. Some links between asymptotic and Lyapunov stability of isothermal, isentropic, and isoenergetic E.S. are rendered evident, and the restrictions the Cattaneo heat flux evolution equation imposes upon constitutive functionals are pointed out.

Finally, we mention that some of the problems here discussed have been approached by the author in [10].

1. General formulae

1.1. The basic functional framework

Let $\mathbf{E}$ be the three-dimensional Euclidean point space, $\mathbf{V}$ the translation space of $\mathbf{E}$, and Lin the space of linear transformations of $\mathbf{V}$. We denote by $\mathcal{V}$ the set of triplets

$$\Lambda = (\mathbf{A}, a, \mathbf{a}) \in \mathrm{Lin} \times \mathbb{R} \times \mathbf{V}. \tag{1.1}$$

$\mathcal{V}$ is a 13-dimensional Euclidean space with respect to the linear operation

$$\alpha(\mathbf{A}, a, \mathbf{a}) + \beta(\mathbf{B}, b, \mathbf{b}) = (\alpha\mathbf{A} + \beta\mathbf{B},\ \alpha a + \beta b,\ \alpha\mathbf{a} + \beta\mathbf{b}) \tag{1.2}$$

for every $(\mathbf{A}, a, \mathbf{a}), (\mathbf{B}, b, \mathbf{b}) \in \mathcal{V}$, $\alpha, \beta \in \mathbb{R}$, and the inner product

$$(\mathbf{A}, a, \mathbf{a}) \cdot (\mathbf{B}, b, \mathbf{b}) = \mathbf{A} \cdot \mathbf{B} + ab + \mathbf{a} \cdot \mathbf{b}, \tag{1.3}$$

where $\mathbf{A} \cdot \mathbf{B} = \mathrm{tr}(AB^T)$ and $\mathbf{a} \cdot \mathbf{b}$ are the inner product in Lin and $\mathbf{V}$, respectively. The corresponding Euclidean norm in $\mathcal{V}$ is given by

$$(\mathbf{A}, a, \mathbf{a}) \mapsto |(\mathbf{A}, a, \mathbf{a})| = (\mathbf{A} \cdot \mathbf{A} + a^2 + \mathbf{a} \cdot \mathbf{a})^{1/2} \geq 0, \qquad (\mathbf{A}, a, \mathbf{a} \in \mathcal{V}). \tag{1.4}$$

Also, the notation $\boldsymbol{\lambda} = (\mathbf{A}, a) \in \mathrm{Lin} \times \mathbb{R}$ will be used, so that

$$\Lambda = (\mathbf{A}, a, \mathbf{a}) = (\boldsymbol{\lambda}, \mathbf{a}). \tag{1.5}$$

We denote by $\mathcal{V}^+$ the subset of $\mathcal{V}$ defined by

$$\mathcal{V}^+ = \mathrm{Lin}^+ \times \mathbb{R}^+ \times \mathbf{V}, \tag{1.6}$$

where $\mathrm{Lin}^+ = \{\mathbf{A} \in \mathrm{Lin} \,/\, \det A > 0\}$ and $\mathbb{R}^+ = (0, \infty)$.

Of course, $\mathcal{V}$ is a Banach space with respect to the Euclidean norm (1.4) and $\mathcal{V}^+$ is an open set in $\mathcal{V}$.

1.2. Classical continuum thermodynamics

A body [3], or a *continuous medium*, $\mathcal{B}$ is identified with the region [5] $\mathbf{B} \subset \mathbf{E}$ it occupies in a fixed reference configuration κ, and the material element, or particle $X \in \mathcal{B}$ is identified with its position $\mathbf{X} \in \mathbf{B}$. It is assumed that a *referential mass density* $\varrho_\kappa : \mathbf{B} \to (0, \infty)$ of $\mathcal{B}$ in the reference configuration is given such that the mass of the subpart $\mathbf{P}$ of B is

$$m(\mathbf{P}) = \int_P \varrho_\kappa \, dm.$$

Along with $\mathcal{B}$ and its referential mass distribution, the *process class* $\mathbb{P}(\mathcal{B})$ ([4, 5]) is given characterizing the material comprising $\mathcal{B}$. The elements $\pi \in \mathbb{P}(\mathcal{B})$ are called *processes* and they are ordered 8-tuples of mappings on $\mathbf{B} \times \mathbb{R}$.

$$\pi = (\chi, \theta, \varepsilon, \eta, \mathbf{S}, \mathbf{Q}, \mathbf{b}, r), \tag{1.7}$$

where, during the process π, at particle $\mathbf{X}$, and time t, $\mathbf{x} = \chi(\mathbf{X}, t) \in \mathbf{E}$ is the *motion*, $\theta = \theta(\mathbf{X}, t) \in \mathbb{R}^+$ is the *absolute temperature*, $\varepsilon = \varepsilon(\mathbf{X}, t) \in \mathbb{R}$ is the *specific internal energy* per unit mass, $\eta = \eta(\mathbf{X}, t) \in \mathbb{R}$ is the *specific entropy per unit mass*, $\mathbf{S} = \mathbf{S}(\mathbf{X}, t) \in \mathrm{Lin}$ is the *first Piola–Kirchhoff stress tensor*, $\mathbf{Q} = \mathbf{Q}(\mathbf{X}, t) \in \mathbf{V}$ is the *referential heat flux*, $\mathbf{b} = \mathbf{b}(\mathbf{X}, t) \in \mathbf{V}$ is the *specific body force* per unit mass, and $r = r(\mathbf{X}, t) \in \mathbb{R}$ is the *radiant heating* per unit mass.

DEFINITION 1.1. *A process $\pi \in \mathbb{P}(\mathcal{B})$ is said to be admissible if its components mappings are satisfying sufficiently smooth conditions and the laws of balance of linear momentum, balance of moment of momentum, balance of energy, and imbalance of entropy* [3].

The *deformation gradient*

$$\mathbf{F} = \mathbf{F}(\mathbf{X}, t) = \mathrm{Grad}\,\chi(\mathbf{X}, t), \tag{1.8}$$

where Grad denotes the gradient with respect to $\mathbf{X}$, is assumed to be in Lin^+, i.e. $J = \det F > 0$. The velocity $\mathbf{v}$ of particle $\mathbf{X}$ at time t is determined by the material time derivate of motion

$$\mathbf{v} = \mathbf{v}(\mathbf{X}, t) = \dot{\chi}(\mathbf{X}, t). \tag{1.9}$$

The *mass conservation law* requires

$$\varrho = J \varrho_\kappa, \tag{1.10}$$

where $\varrho = \varrho(\mathbf{X}, t)$ is the mass density at particle $\mathbf{X}$ at time t.

For any admissible process $\pi \in \mathbb{P}(\mathcal{B})$ the laws of balance of linear momentum, balance of moment of momentum, balance of energy, and imbalance of entropy are equivalent to the local referential equations [3]:

$$\varrho_\kappa \dot{v} = \operatorname{Div} \mathbf{S} + \varrho_\kappa \mathbf{b}, \tag{1.11}$$

$$\mathbf{F}\mathbf{S}^T = \mathbf{S}\mathbf{F}^T, \tag{1.12}$$

$$\varrho_\kappa \dot{\varepsilon} = \mathbf{S} \cdot \dot{\mathbf{F}} - \operatorname{Div} \mathbf{Q} + \varrho_\kappa r, \tag{1.13}$$

$$\varrho_\kappa \dot{\eta} \geq \varrho_\kappa (r/\theta) - \operatorname{Div} (\mathbf{Q}/\theta), \tag{1.14}$$

where Div denotes the divergence operator with respect to $\mathbf{X}$.

By using the *specific free energy* $\psi = \psi(\mathbf{X}, t)$ per unit mass defined by

$$\psi = \varepsilon - \theta\eta \tag{1.15}$$

and taking into account the energy balance equation (1.13), it results that the *Clausius–Duhem inequality* (1.14) takes the form

$$\varrho_\kappa \left(\dot{\psi} + \eta \dot{\theta} \right) - \mathbf{S} \cdot \dot{\mathbf{F}} + \mathbf{Q} \cdot (\mathbf{G}/\theta) \leq 0, \tag{1.16}$$

where $\mathbf{G} = \mathbf{G}(\mathbf{X}, t) = \operatorname{Grad} \theta(\mathbf{X}, t)$ is the *temperature gradient* with respect to the reference configuration κ. The inequality (1.16) is called the *Reduced Dissipation Inequality* [3]. If $\gamma = \gamma(\mathbf{X}, t)$ denotes the *specific rate of entropy production* [1] of particle $\mathbf{X}$ at time t

$$\varrho_\kappa \gamma = \varrho_\kappa \dot{\eta} - [\varrho_\kappa (r/\theta) - \operatorname{Div} (\mathbf{Q}/\theta)], \tag{1.17}$$

then the Clausius-Duhem inequality (1.14) asserts that

$$\gamma \geq 0. \tag{1.18}$$

From the energy balance equation (1.13) it follows that for any admissible process $\pi \in \mathbb{P}(\mathcal{B})$ we may write (1.17) in the form

$$\gamma = \dot{\eta} - \dot{\varepsilon}/\theta + (1/\varrho_\kappa \theta)\mathbf{S} \cdot \dot{\mathbf{F}} - (1/\varrho_\kappa \theta^2)\mathbf{Q} \cdot \mathbf{G} \tag{1.19}$$

and, since $\psi = \dot{\varepsilon} - \theta \dot{\eta} - \dot{\theta} \eta$, from where we get

$$\theta\gamma = -\dot{\psi} - \eta \dot{\theta} + (1/\varrho_\kappa)\mathbf{S} \cdot \dot{\mathbf{F}} - (1/\varrho_\kappa \theta)\mathbf{Q} \cdot \mathbf{G}. \tag{1.20}$$

The following implications hold:

$$\dot{\theta} = 0, \quad \dot{\mathbf{F}} = 0, \quad \text{and} \quad \mathbf{Q} \cdot \mathbf{G} = 0 \Rightarrow \dot{\psi} \leq 0, \tag{1.21}$$

$$\dot{\eta} = 0, \quad \dot{\mathbf{F}} = 0, \quad \text{and} \quad \mathbf{Q} \cdot \mathbf{G} = 0 \Rightarrow \dot{\varepsilon} \leq 0, \tag{1.22}$$

$$\dot{\varepsilon} = 0, \quad \dot{\mathbf{F}} = 0, \quad \text{and} \quad \mathbf{Q} \cdot \mathbf{G} = 0 \Rightarrow \dot{\eta} \leq 0. \tag{1.23}$$

2. Thermoelastic materials with heat flux evolution

The theory studied in this paper assumes that the material comprising the body undergoes only admissible processes, in the sense of Definition 1.1, and that the specific free energy $\psi(\mathbf{X}, t)$, the specific entropy $\eta(\mathbf{X}, t)$, the first Piola–Kirchhoff stress tensor $\mathbf{S}(\mathbf{X}, t)$, and the specific time rate of the heat flux $\dot{\mathbf{Q}}$ of a particle $\mathbf{X}$ and at time t are determined by the *state functions corresponding to the admissible processes* $\pi \in \mathbb{P}(\mathcal{B})$

$$(2.1) \qquad (\mathbf{\Lambda}; \mathbf{Q}) \equiv (\mathbf{F}, \theta, \mathbf{G}; \mathbf{Q}) : \mathbf{B} \times \mathbb{R} \to \mathrm{Lin}^+ \times \mathbb{R}^+ \times \mathbf{V} \times \mathbf{V} = \mathcal{V}^+ \times \mathbf{V}$$

through the *constitutive functionals* of the material

$$(2.2) \qquad \psi(t) = \overline{\psi}(\mathbf{\Lambda}(t); \mathbf{Q}(t)),$$

$$(2.3) \qquad \eta(t) = \overline{\eta}(\mathbf{\Lambda}(t); \mathbf{Q}(t)),$$

$$(2.4) \qquad \mathbf{S}(t) = \overline{\mathbf{S}}(\mathbf{\Lambda}(t); \mathbf{Q}(t)),$$

$$(2.5) \qquad \dot{\mathbf{Q}}(t) = \mathbf{H}(\mathbf{\Lambda}(t); \mathbf{Q}(t)).$$

The variable $\mathbf{X} \in \mathbf{B}$ is understood to enter both sides of (2.2)–(2.5), but it is not written there because all the subsequent considerations refer to one particular material point $X \in \mathcal{B}$.

We now make the following *constitutive assumptions* defining the material under consideration. These assumptions refer to the common domain of the constitutive functionals $\overline{\psi}$, $\overline{\eta}$, $\overline{\mathbf{S}}$, $\mathbf{H}$ and their smoothness properties.

A 1. The constitutive functionals $\overline{\psi}$, $\overline{\eta}$, $\overline{\mathbf{S}}$, and $\mathbf{H}$ have for their domain of definition the set $\mathcal{D} \times \mathbf{V}$, where $\mathcal{D} \subset \mathcal{V}^+$ is an open and connected set satisfying the condition

$$(2.6) \qquad (\mathbf{A}, a, \mathbf{a}) \in \mathcal{D} \Rightarrow (\mathbf{A}, a, \mathbf{0}) \in \mathcal{D}.$$

A 2. The free energy functional $\overline{\psi}$ is continuous differentiable on $\mathcal{D} \times \mathbf{V}$, i.e. for every $\mathbf{\Lambda} = (\boldsymbol{\lambda}, \mathbf{G}) \in \mathcal{D}$, $\boldsymbol{\lambda} = (\mathbf{F}, \theta)$, and $\mathbf{Q} \in \mathbf{V}$ we have

$$(2.7) \qquad \overline{\psi}(\mathbf{\Lambda} + \mathbf{\Gamma}; \mathbf{Q} + \mathbf{u}) = \overline{\psi}(\mathbf{\Lambda}; \mathbf{Q}) + \partial_{\mathbf{\Lambda}} \overline{\psi}(\mathbf{\Lambda}; \mathbf{Q}) \cdot \mathbf{\Gamma} + \partial_{\mathbf{Q}} \overline{\psi} \mathbf{\Lambda}; \mathbf{Q}) \cdot \mathbf{u} + o(|\mathbf{\Gamma}| + |\mathbf{u}|),$$

for any $\mathbf{\Gamma} = (\mathbf{A}, a, \mathbf{a}) \in \mathcal{V}$, and $\mathbf{u} \in \mathbf{V}$, with $(\mathbf{\Lambda} + \mathbf{\Gamma}; \mathbf{Q} + \mathbf{u}) \in \mathcal{D} \times \mathbf{V}$.

Moreover, the *partial derivative of* $\overline{\psi}$ with respect to $\mathbf{\Lambda}$

$$(2.8) \qquad \partial_{\mathbf{\Lambda}} \overline{\psi} = (\partial_{\boldsymbol{\lambda}} \overline{\psi}, \partial_{\mathbf{G}} \overline{\psi}) : \mathcal{D} \times \mathbf{V} \to \mathcal{V}, \qquad \partial_{\boldsymbol{\lambda}} \overline{\psi} = (\partial_{\mathbf{F}} \overline{\psi}, \partial_{\theta} \overline{\psi}),$$

and the *partial derivative* of $\overline{\psi}$ *with respect to* $\mathbf{Q}$

$$(2.9) \qquad \partial_{\mathbf{Q}} \overline{\psi} : \mathcal{D} \times \mathbf{V} \to \mathbf{V},$$

are continuous applications on $\mathcal{D} \times \mathbf{V}$.

A 3. The mappings $\overline{\eta}$, $\overline{\mathbf{S}}$ and $\mathbf{H}$ are continuous on $\mathcal{D} \times \mathbf{V}$.

A 4. The *heat evolution function* $\mathbf{H}$ is locally Lipschitzian, with respect to $\mathbf{Q}$, on $\mathcal{D} \times \mathbf{V}$ for *any fixed mapping*

$$\mathbf{\Lambda} : \mathbf{B} \times \mathbb{R} \to \mathcal{D}.$$

REMARK 2.1. From the assumption A 1 it results that if $(\mathbf{A}, a, \mathbf{a}) \in \mathcal{D}$, then for every $\mathbf{a} \in \mathbf{V}\backslash\{\mathbf{0}\}$ there exists $\delta > 0$ such that $(\mathbf{A}, a, \alpha\mathbf{a}) \in \mathcal{D}$ as soon as $|\alpha| < \delta$.

REMARK 2.2. Suppose we are giving an initial time t_0, an *initial heat flux distribution* on $\mathcal{B}$,

$$\mathbf{X} \mapsto \mathbf{Q}_0 = \mathbf{Q}_0(\mathbf{X}) \in \mathbf{V}, \qquad \mathbf{X} \in \mathbf{B},$$

a smooth motion $\mathbf{x} = \boldsymbol{\chi}(\mathbf{X}, t)$, and a smooth temperature field $\theta = \theta(\mathbf{X}, t)$ such that

$$\mathbf{\Lambda}(t) = (\mathbf{F}(X, t),\ \theta(\mathbf{X}, t),\ \mathbf{G}(\mathbf{X}, t)) \in \mathcal{D}, \qquad t \in \mathbf{I},$$

where $I \subset \mathbb{R}$ is an interval containing t_0. Assumption A 4 guarantees the existence and the uniqueness [6, 7] of the solution

$$\dot{\mathbf{Q}} = \mathbf{H}(\mathbf{\Lambda}(t); \mathbf{Q}). \tag{2.10}$$

With $(\mathbf{\Lambda}(t); \mathbf{Q}(t)) \in \mathcal{D} \times \mathbf{V}$, $t \in (t_0 - \delta, t_0 + \delta)$, determined in this manner, from (1.15), (2.2)–(2.4), we obtain $\psi(t) = \psi(\mathbf{X}, t)$, $\eta(t) = \eta(\mathbf{X}, t)$, $\varepsilon(t) = \varepsilon(\mathbf{X}, t) = \psi(t) + \theta(t)\eta(t)$, $\mathbf{S}(t) = \mathbf{S}(\mathbf{X}, t)$ and, from (1.11), (1.13), we get the specific body force $\mathbf{b}(\mathbf{X}, t)$ and the radiant heating $r(\mathbf{X}, t)$.

Thus to each sufficiently smooth choice of $\mathbf{Q}_0$, χ, and θ there corresponds a unique process

$$\pi^* = (\chi, \theta, \varepsilon, \eta, \mathbf{S}, \mathbf{Q}, \mathbf{b}, r) \in \mathbb{P}(\mathcal{B}), \quad \text{on} \quad (t_0 - \delta, t_0 + \delta). \tag{2.11}$$

REMARK 2.3. For every state $(\boldsymbol{\lambda}_0; \mathbf{Q}_0) = (\mathbf{F}_0, \theta_0, \mathbf{G}_0, \mathbf{Q}_0) \in \mathcal{D} \times \mathbf{V}$, given at the material point $X \in \mathcal{B}$ occupying the place $\mathbf{X} \in \mathbf{B}$, for every $t_0 \in \mathbb{R}$, and for arbitrarily chosen $\Gamma = (\mathbf{A}, a, \mathbf{a}) \in \mathcal{V}$ there exists an admissible process $\pi \in \mathbb{P}(\mathcal{B})$ such that the states

$$(\mathbf{\Lambda}(\mathbf{X}, t);\ \mathbf{Q}(\mathbf{X}, t)) = (\mathbf{F}(\mathbf{X}, t), \theta(\mathbf{X}, t), \mathbf{G}(\mathbf{X}, t); \mathbf{Q}(\mathbf{X}, t))$$

corresponding to the process π satisfy the conditions

$$(\mathbf{\Lambda}(\mathbf{X}, t_0); \mathbf{Q}(\mathbf{X}, t_)) = (\mathbf{\Lambda}_0; \mathbf{Q}_0), \qquad \dot{\mathbf{\Lambda}}\,(\mathbf{X}, t_0) = \Gamma. \tag{2.12}$$

The proof of the statements in this Remark may be found in [1, 4, 5].

DEFINITION 2.1. *The constitutive equations* (2.2)–(2.5) *are said to be* ***compatible with the Second Law of Thermodynamics*** *if for every choice of sufficiently smooth initial heat flux distribution* $\mathbf{Q}_0$, *motion* $\boldsymbol{\chi}$, *and temperature field* θ, *the process*

$\pi^* \in \mathbb{P}(\mathcal{B})$ is an admissible process i.e. the constitutive functionals $\overline{\psi}$, $\overline{\eta}$, $\overline{\mathbf{S}}$, and $\mathbf{H}$ satisfy the dissipation inequality (1.16) *at each time t and for all material points $X \in \mathcal{B}$.*

The content of this definition is referred to as the *Principle of Thermomechanically Compatible Determinism* [3].

Using the line of arguments in [1, 4, 5] and the results of the Remark 2.3 the following theorem can be proved (cf. [8]).

THEOREM 2.1. *If the functions $\overline{\psi}$, $\overline{\eta}$, $\overline{\mathbf{S}}$, and $\mathbf{H}$ obey the assumptions* **A** 1 – **A** 4 *then the constitutive equations* (2.2) – (2.4) *are compatible with the second law of thermodynamics if and only if for any smooth motion, temperature field, and initial heat flux distribution, the following conditions hold:*

1) *the free energy function $\overline{\psi}$ is independent of* $\mathbf{G}$, *i.e.*

$$\psi(t) = \hat{\psi}(\boldsymbol{\lambda}(t); \mathbf{Q}(t)), \qquad \boldsymbol{\lambda}(t) = (\mathbf{F}(t), \theta(t)); \tag{2.13}$$

2) *the functions $\overline{\eta}$ and $\overline{\mathbf{S}}$ are independent of* $\mathbf{G}$, *i.e.*

$$\eta(t) = \hat{\eta}(\boldsymbol{\lambda}(t); \mathbf{Q}(t)), \qquad \mathbf{S}(t) = \hat{\mathbf{S}}(\boldsymbol{\lambda}(t); \mathbf{Q}(t)), \tag{2.14}$$

and the functionals $\hat{\eta}$ and $\hat{\mathbf{S}}$ are determined by the function $\hat{\psi}$ through the relations

$$\hat{\eta} = -\partial_\theta \hat{\psi} \qquad \hat{\mathbf{S}} = \varrho_\kappa \partial_{\mathbf{F}} \hat{\psi}; \tag{2.15}$$

3) *the* ***Dissipation Inequality*** *is satisfied*

$$\varrho_\kappa \theta(t) \partial_{\mathbf{Q}} \hat{\psi}(\boldsymbol{\lambda}(t); \mathbf{Q}(t)) \cdot \mathbf{H}(\boldsymbol{\Lambda}(t); \mathbf{Q}(t)) + \mathbf{Q}(t) \cdot \mathbf{G}(t) \leq 0. \tag{2.16}$$

REMARK 2.4. Following [1], the quantity

$$\sigma = \hat{\sigma}(\boldsymbol{\Lambda}; \mathbf{Q}) = -(1/\theta) \partial_{\mathbf{Q}} \hat{\psi}(\boldsymbol{\lambda}; \mathbf{Q}) \cdot \mathbf{H}(\boldsymbol{\Lambda}; \mathbf{Q}) \tag{2.17}$$

is referred to as the *internal dissipation*.

If we denote by $\hat{\sigma}_0$ the restriction of $\hat{\sigma}$ to the set

$$\Delta = \{(\boldsymbol{\Lambda}; \mathbf{Q}) \equiv (\mathbf{F}, \theta, \mathbf{G}; \mathbf{Q}) \in \mathcal{D} \times \mathbf{V} / \mathbf{Q} \cdot \mathbf{G} = 0\}, \tag{2.18}$$

then from (2.16) we get the inequality

$$\sigma_0 = \hat{\sigma}_0(\boldsymbol{\lambda}, \mathbf{G}; \mathbf{Q}) \geq 0, \tag{2.19}$$

which is called *internal dissipation inequality*. In virtue of (2.6) we remark that $\delta \neq 0$ and that

$$\hat{\sigma}_0(\boldsymbol{\lambda}, \mathbf{0}; \mathbf{Q}) = -(1/\theta) \partial_{\mathbf{Q}} \hat{\psi}(\boldsymbol{\lambda}; \mathbf{Q}) \cdot \mathbf{H}(\boldsymbol{\Lambda}, \mathbf{0}; \mathbf{Q}) \geq 0. \tag{2.20}$$

Because of (2.15) we have

$$\dot{\psi} = \partial_{\mathbf{F}}\hat{\psi}(\boldsymbol{\lambda};\mathbf{Q})\cdot\dot{\mathbf{F}} + \partial_{\theta}\hat{\psi}(\boldsymbol{\lambda};\mathbf{Q})\dot{\theta} + \partial_{\mathbf{Q}}\hat{\psi}(\boldsymbol{\lambda};\mathbf{Q})\cdot\mathbf{H}(\boldsymbol{\Lambda};\mathbf{Q}) = \mathbf{S}\cdot\mathbf{F} - \eta\dot{\theta} - \theta\sigma \tag{2.21}$$

so that

$$\dot{\boldsymbol{\lambda}} = (\dot{\mathbf{F}}, \dot{\theta}) = \mathbf{0} \Rightarrow \sigma = -(1/\theta)\dot{\psi}. \tag{2.22}$$

Since, as it results from (1.15) and $(2.21)_2$,

$$\dot{\varepsilon} = \mathbf{S}\cdot\dot{\mathbf{F}} - \theta\dot{\eta} - \theta\sigma, \tag{2.23}$$

we obtain the following implications

$$\dot{\mathbf{F}} = 0, \qquad \dot{\eta} = 0 \quad \Rightarrow \quad \sigma = -(\dot{\varepsilon}/\theta), \tag{2.24}$$

$$\dot{\mathbf{F}} = 0, \qquad \dot{\eta} = 0 \quad \Rightarrow \quad \sigma = \dot{\eta}. \tag{2.25}$$

In the present theory σ plays the part it did in [1].

REMARK 2.5. The Dissipation Inequality (2.16) imposes a severe limitation on the free energy functional $\hat{\psi}$ and on the heat evolution functional $\mathbf{H}$. The restriction of this limitation to the set Δ (see (2.18)) takes the form

$$\partial_{\mathbf{Q}}\hat{\psi}(\boldsymbol{\lambda};\mathbf{Q})\cdot\mathbf{H}(\boldsymbol{\Lambda};\mathbf{Q}) \leq 0, \qquad (\boldsymbol{\lambda},\mathbf{G};\mathbf{Q}) \in \mathcal{D}\times\mathbf{V}. \tag{2.26}$$

In particular, we have

$$\partial_{\mathbf{Q}}\hat{\psi}(\boldsymbol{\lambda};\mathbf{Q})\cdot\mathbf{H}(\boldsymbol{\Lambda},\mathbf{0};\mathbf{Q}) \leq 0, \qquad (\boldsymbol{\lambda},\mathbf{0};\mathbf{Q}) \in \mathcal{D}\times\mathbf{V}. \tag{2.27}$$

3. Materials with Cattaneo heat flux equation

In this section we suppose that the heat flux evolution functional is linear in $\mathbf{Q}$ and $\mathbf{G}$, i.e.

$$\begin{aligned} &\mathbf{H}(\boldsymbol{\Lambda};\mathbf{Q}) = \mathbf{M}(\boldsymbol{\lambda})\mathbf{Q} + \mathbf{N}(\boldsymbol{\lambda})\mathbf{G}, \\ &(\boldsymbol{\Lambda};\mathbf{Q}) = (\boldsymbol{\lambda},\mathbf{G};\mathbf{Q}) \in \mathcal{D}\times\mathbf{V}, \qquad \boldsymbol{\lambda} = (\mathbf{F},\theta), \end{aligned} \tag{3.1}$$

where the second order tensor functions

$$\boldsymbol{\lambda} \to \mathbf{M}(\boldsymbol{\lambda}), \qquad \mathbf{N}(\boldsymbol{\lambda}) \in \mathrm{Lin}, \qquad (\boldsymbol{\lambda},\mathbf{G};Q) \in \mathcal{D}\times\mathbf{V} \tag{3.2}$$

are nonsingular, and we derive the implication of this assumption on the constitutive functionals $\hat{\psi}$, $\hat{\eta}$, $\hat{\mathbf{S}}$, and

$$\hat{\varepsilon} = \hat{\psi} + \theta\hat{\eta}. \tag{3.3}$$

Inserting (3.1) into (2.16) we conclude that the tensor functions (3.2) must satisfy the inequality

$$\varrho_\kappa \left[\mathbf{M}^T(\boldsymbol{\lambda})\partial_{\mathbf{Q}}\hat{\psi}(\boldsymbol{\lambda};\mathbf{Q})\right]\cdot\mathbf{Q} + \left[\varrho_\kappa \mathbf{N}^T(\boldsymbol{\lambda})\partial_{\mathbf{Q}}\hat{\psi}(\boldsymbol{\lambda};\mathbf{Q}) + (1/\theta)\mathbf{Q}\right]\cdot\mathbf{G} \leq 0 \tag{3.4}$$

for every $(\boldsymbol{\lambda}, \mathbf{G}; \mathbf{Q}) \in \mathcal{D} \times \mathbf{V}$.

THEOREM 3.1. *The inequality* (3.4) *holds on* $\mathcal{D} \times \mathbf{V}$ *if and only if the relations*

$$\left[\mathbf{M}^T(\boldsymbol{\lambda})\partial_{\mathbf{Q}}\hat{\psi}(\boldsymbol{\lambda};\mathbf{Q})\right]\cdot\mathbf{Q} \leq 0, \tag{3.5}$$

$$\varrho_\kappa \mathbf{N}^T(\boldsymbol{\lambda})\partial_{\mathbf{Q}}\hat{\psi}(\boldsymbol{\lambda};\mathbf{Q}) = -(1/\theta)\mathbf{Q} \tag{3.6}$$

are satisfied on $\mathcal{D} \times \mathbf{V}$.

P r o o f. If $\mathbf{Q}, \mathbf{G} \in \mathbf{V}$ are arbitrary, as they are supposed to be in [8], the theorem is rather evident. But this is not the case because $(\boldsymbol{\lambda}, \mathbf{G}; \mathbf{Q}) \in \mathcal{D} \times \mathbf{V}$, and the domain $\mathcal{D}$ is *a priori* given. It is obvious that (3.5) and (3.6) are sufficient for (3.4). On the other hand, (3.4) and (3.6) imply (3.5). So it remains to prove that (3.4) implies (3.6). To prove this implication we will prove its contrapositive assertion. The relation (3.6) does not hold on $\mathcal{D} \times \mathbf{V}$ if there exists $\boldsymbol{\lambda}_0 = (\mathbf{F}_0, \theta_0) \in \mathrm{Lin}^+ \times \mathbb{R}$ and $\mathbf{G} \in \mathbf{V}$ with $(\boldsymbol{\lambda}_0, \mathbf{G}) \in \mathcal{D}$ such that $\varrho_\kappa \mathbf{N}^T(\boldsymbol{\lambda}_0)\partial_{\mathbf{Q}}\hat{\psi}(\boldsymbol{\lambda}_0; \mathbf{0}) = \mathbf{u} \neq \mathbf{0}$.

From the assumption A 1 and from Remark 2.1 it results that there exists $\alpha_0 > 0$ such that $(\boldsymbol{\lambda}_0, \mathbf{G}_0) \in \mathcal{D}$ where $\mathbf{G}_0 = \alpha_0 \mathbf{u}$. For the point $(\boldsymbol{\lambda}_0, \mathbf{G}_0; \mathbf{0}) \in \mathcal{D} \times \mathbf{V}$ the left-hand side of (3.4) becomes $\alpha_0 \mathbf{u}\cdot\mathbf{u} > 0$ and this contradicts (3.4). The theorem is proved.

REMARK 3.1. For any $(\boldsymbol{\lambda}, G) = (\mathbf{F}, \theta, \mathbf{G}) \in \mathcal{D}$ the mapping

$$\theta \mathbf{N}^T(\boldsymbol{\lambda})\partial_{\mathbf{Q}}\psi(\lambda;\cdot) \,:\, \mathbf{V} \to \mathbf{V} \tag{3.7}$$

is an invertible linear transformation on $\mathbf{V}$, namely a similarity transformation of coefficient $k = 1/\varrho_\kappa$.

REMARK 3.2. Let us introduce the notations

$$\mathbf{T} = -\mathbf{M}^{-1}, \qquad \mathbf{Z} = -\mathbf{N}^{-1}, \qquad \mathbf{K} = \mathbf{T}\mathbf{Z}^{-1}. \tag{3.8}$$

With these notations, from (3.1) and (2.5), we obtain

$$\mathbf{T}(\boldsymbol{\lambda})\dot{\mathbf{Q}} + \mathbf{Q} = -\mathbf{K}(\boldsymbol{\lambda})\mathbf{G}, \qquad (\boldsymbol{\lambda}, \mathbf{G}; \mathbf{Q}) \in \mathcal{D} \times \mathbf{V}, \tag{3.9}$$

where the tensor functions $\boldsymbol{\lambda} \to \mathbf{T}(\lambda), \mathbf{K}(\lambda) \in \mathrm{Lin}$ are nonsingular.

Equation (3.9) is the *Cattaneo heat flux evolution equation*.

Supposing that $\hat{\psi}$ is twice continuously differentiable on $\mathcal{D} \times \mathbf{V}$ it results that $\mathbf{Z}$, and therefore $\mathbf{N}$, is symmetric and it is given by

$$\mathbf{Z} = -\mathbf{N}^{-1} = \varrho_\kappa \theta \partial_{\mathbf{Q}^2}\hat{\psi}(\boldsymbol{\lambda}; \mathbf{Q}). \tag{3.10}$$

On the other hand, in view of (3.8) and (3.6), from (3.5) it follows

$$\mathbf{Q}\cdot\mathbf{K}^{-1}(\boldsymbol{\lambda})\mathbf{Q}\geq 0, \tag{3.11}$$

which shows that $\mathbf{K}$ is positive definite because $\mathbf{Q}\in\mathbf{V}$ is arbitrary and $\mathbf{K}$ is invertible.

The internal dissipation (2.17) is now given by

$$\sigma=\hat{\sigma}(\Lambda;\mathbf{Q})=(1/\varrho_\kappa\theta^2)\left[\mathbf{Q}\cdot\mathbf{K}^{-1}\mathbf{Q}+\mathbf{Q}\cdot\mathbf{G}\right], \tag{3.12}$$

and (3.11) is a consequence of the internal dissipation inequality which now becomes

$$\sigma_0=\hat{\sigma}_0(\Lambda;\mathbf{Q})=(1/\varrho_\kappa\theta^2)\mathbf{Q}\cdot\mathbf{K}^{-1}(\boldsymbol{\lambda})\mathbf{Q}\geq 0. \tag{3.13}$$

Taking into account that $\mathbf{N}^T=\mathbf{N}=-\mathbf{Z}^{-1}$, from (3.6) we obtain (see [9] and [8])

$$\varrho_\kappa\hat{\psi}(\boldsymbol{\lambda};\mathbf{Q})=\varrho_\kappa\hat{\psi}_0(\boldsymbol{\lambda})+(1/2\theta)\mathbf{Q}\cdot\mathbf{Z}(\boldsymbol{\lambda})\mathbf{Q}. \tag{3.14}$$

From this relation, (2.15), and (1.15) we get

$$\varrho_\kappa\hat{\varepsilon}(\boldsymbol{\lambda};\mathbf{Q})=\varrho_\kappa\hat{\varepsilon}_0(\boldsymbol{\lambda})+\mathbf{Q}\cdot\mathbf{A}(\boldsymbol{\lambda})\mathbf{Q}, \tag{3.15}$$

$$\varrho_\kappa\hat{\eta}(\boldsymbol{\lambda};\mathbf{Q})=\varrho_\kappa\hat{\eta}_0(\boldsymbol{\lambda})+\mathbf{Q}\cdot\mathbf{B}(\boldsymbol{\lambda})\mathbf{Q}, \tag{3.16}$$

$$\hat{\mathbf{S}}(\Lambda;\mathbf{Q})=\hat{\mathbf{S}}_0(\boldsymbol{\lambda})+\mathbf{Q}\cdot\mathbf{P}(\boldsymbol{\lambda})\mathbf{Q}, \tag{3.17}$$

where

$$\hat{\eta}_0=-\partial_\theta\hat{\psi}_0,\qquad \hat{\varepsilon}_0=\hat{\psi}_0-\theta\partial_\theta\hat{\psi}_0=\hat{\psi}_0+\theta\hat{\eta}_0,\qquad \hat{\mathbf{S}}_0=\varrho_x\partial_{\mathbf{F}}\hat{\psi}_0 \tag{3.18}$$

and

$$\begin{aligned}&\mathbf{A}=-(1/2\theta^2)\partial_\theta\left[(1/\theta^2)\mathbf{Z}\right],\qquad \mathbf{B}=-(1/2\theta)\partial_\theta\left[(1/\theta)\mathbf{Z}\right],\\ &\mathbf{P}=(1/2\theta)\partial_{\mathbf{F}}\mathbf{Z}.\end{aligned} \tag{3.19}$$

REMARK 3.3. When the heat flux evolution functional $\mathbf{H}$ is of the form (3.1), the observations in Remark 2.5 are more specific. From (3.10) it results that for every $(\boldsymbol{\lambda},\mathbf{G})\in\mathcal{D}$ the mapping

$$\hat{\psi}(\boldsymbol{\lambda};\cdot)\ :\ \mathbf{V}\to\mathbb{R} \tag{3.20}$$

is a nonsingular quadratic form having the matrix $-(1/\varrho_\kappa\theta)\mathbf{N}^{-1}(\boldsymbol{\lambda})=(1/\varrho_\kappa\theta)\mathbf{Z}$.

So the nonsingular tensor $\mathbf{N}(\boldsymbol{\lambda})$ in (3.10) is completely determined by the free energy functional $\hat{\psi}$. The invertible tensor $\mathbf{M}(\boldsymbol{\lambda})$ in (3.10) depends on $\hat{\psi}$ through the relation $\mathbf{M}(\boldsymbol{\lambda})=\mathbf{N}(\boldsymbol{\lambda})\mathbf{K}^{-1}(\boldsymbol{\lambda})$ where $\mathbf{K}(\boldsymbol{\lambda})$ is a arbitrary positive definite second order tensor.

4. Stability of isothermal equilibrium states (E.S.)

Throughout this and the following section we suppose that the heat flux evolution functional $\mathbf{H}$ is continuously differentiable on $\mathcal{D} \times \mathbf{V}$ and that the second order tensors $\partial_{\mathbf{G}}\mathbf{H}(\boldsymbol{\lambda}, \mathbf{G}; \mathbf{Q})$ and $\partial_{\mathbf{Q}}\mathbf{H}(\boldsymbol{\lambda}, \mathbf{G}; \mathbf{Q})$ are nonsingular on $\mathcal{D} \times \mathbf{V}$.

With these conditions, the equation

$$\mathbf{H}(\boldsymbol{\lambda}, \mathbf{G}; \mathbf{Q}) = 0 \tag{4.1}$$

defines the implicit functions

$$\mathbf{Q} = \hat{\mathbf{Q}}(\boldsymbol{\lambda}, \mathbf{G}), \qquad \mathbf{H}(\boldsymbol{\lambda}, \mathbf{G}; \hat{\mathbf{Q}}(\boldsymbol{\lambda}, \mathbf{G})) = \mathbf{0}; \qquad \mathbf{Q}_0 = \hat{\mathbf{Q}}(\boldsymbol{\lambda}_0, \mathbf{G}_0) \tag{4.2}$$

and

$$\mathbf{G} = \hat{\mathbf{G}}(\boldsymbol{\lambda}; \mathbf{Q}), \qquad \mathbf{H}(\boldsymbol{\lambda}, \hat{\mathbf{G}}(\boldsymbol{\lambda}; \mathbf{Q}); \mathbf{Q}) = \mathbf{0}; \qquad \mathbf{G}_0 = \hat{\mathbf{G}}(\boldsymbol{\lambda}_0; \mathbf{Q}_0) \tag{4.3}$$

in a neighbourhood $U \subset \mathcal{D} \times \mathbf{V}$ of a solution $(\boldsymbol{\lambda}_0, \mathbf{G}_0; \mathbf{Q}_0)$ of the equation (4.1).

The functions $(4.2)_1$ and $(4.3)_1$ are satisfying the indentities

$$\hat{\mathbf{Q}}(\boldsymbol{\lambda}, \hat{\mathbf{G}}(\boldsymbol{\lambda}; \mathbf{Q})) = \mathbf{Q}, \qquad \hat{\mathbf{G}}(\boldsymbol{\lambda}; \hat{\mathbf{Q}}(\boldsymbol{\lambda}, \mathbf{G})) = \mathbf{G} \tag{4.4}$$

on U and are differentiable in certain neighbourhoods of $(\boldsymbol{\lambda}_0, \mathbf{G}_0)$ and $(\boldsymbol{\lambda}_0, \mathbf{Q}_0)$, respectively.

All the following considerations refer to an arbitrary fixed material point $X \in \mathcal{B}$ having the position $\mathbf{X} \in \mathbf{B}$ in the configuration κ.

DEFINITION 4.1. *The state* $(\boldsymbol{\lambda}_0, \mathbf{G}_0; \mathbf{Q}_0) \in \mathcal{D} \times \mathbf{V}$, $\boldsymbol{\lambda}_0 = (\mathbf{F}_0, \theta_0)$, *is called an* ***isothermal E.S. at constant strain*** $\mathbf{F}_0$ *for the material point* $X \in \mathcal{B}$ *if it is a solution of* Eq. (4.1) *and if* $\mathbf{G}_0 \cdot \mathbf{Q}_0 = 0$. *The state* $(\boldsymbol{\lambda}_0, \mathbf{0}; \mathbf{Q}_0) \in \mathcal{D} \times \mathbf{V}$, $\boldsymbol{\lambda}_0 = (\mathbf{F}_0, \theta_0)$ *is called a* ***strictly isothermal E.S. at constant strain*** $\mathbf{F}_0$ *for the material point* $X \in \mathcal{B}$ *if it verifies* Eq. (4.1).

With these definitions, the following theorem can be proved (see [8]).

THEOREM 4.1. *If the functional* $\mathbf{H}$ *satisfies the above conditions, then*:

1) *every state* $(\boldsymbol{\lambda}, \mathbf{0}; \mathbf{0}) \in \mathcal{D} \times \mathbf{V}$ *is a strictly E.S.*;

2) *the second order tensor*

$$[\partial_{\mathbf{Q}}\mathbf{H}(\boldsymbol{\lambda}, \mathbf{0}; \mathbf{0})]^{-1}\, \partial_{\mathbf{G}}\mathbf{H}(\boldsymbol{\lambda}, \mathbf{0}; \mathbf{0}) \tag{4.5}$$

is positive definite.

We denote by $\mathcal{E} \subset \mathcal{D} \times \mathbf{V}$ the set of isothermal E.S. and by $\mathcal{E}_0 \subset \mathcal{E}$ the subset of strictly isothermal E.S. at constant strain for a material point $X \in \mathcal{B}$.

REMARK 4.1. The preceding theorem shows that $\mathcal{E}_0$ and therefore $\mathcal{E}$ are nonvoid sets. Moreover, for every *a priori* given $\boldsymbol{\lambda}_0 = (\mathbf{F}_0, \theta_0) \in \mathrm{Lin}^+ \times \mathbb{R}^+$ at $X \in \mathcal{B}$ the nonvoid set

$$\Sigma(\boldsymbol{\lambda}_0) = \{(\boldsymbol{\lambda}_0, \mathbf{G}; \mathbf{Q}) \in \mathcal{D} \times \mathbf{V} \mid \mathbf{G} \cdot \mathbf{Q} = 0,\ \mathbf{H}(\boldsymbol{\lambda}_0, \mathbf{G}; \mathbf{Q}) = \mathbf{0}\} \subset \mathcal{E} \tag{4.6}$$

is a 2-dimensional manifold in the 6-dimensional space of tuples $(\mathbf{G};\mathbf{Q})$ and $(\mathbf{0};\mathbf{0}) \in \Sigma(\lambda_0)$. From (4.1)–(4.4) it results that for every $(\mathbf{G}_0;\mathbf{Q}_0) \in \Sigma(\lambda_0)$ there exists a neighbourhood $U(\mathbf{G}_0;\mathbf{Q}_0)$ such that

$$
\begin{aligned}
(4.7)\qquad U(\mathbf{G},\mathbf{Q}_0)\cap\Sigma(\lambda_0) &= \left\{(\lambda_0,\mathbf{G};\mathbf{Q})\in\mathcal{D}\times\mathbf{V}\,|\,\mathbf{G}=\hat{\mathbf{G}}(\lambda_0;\mathbf{Q}),\,\mathbf{Q}\cdot\hat{\mathbf{G}}(\lambda_0;\mathbf{Q})=0\right\}\\
&= \left\{(\lambda_0,\mathbf{G};\mathbf{Q})\in\mathcal{D}\times\mathbf{V}\,|\,\mathbf{Q}=\hat{\mathbf{Q}}(\lambda_0;\mathbf{G}),\;\mathbf{G}\cdot\hat{\mathbf{Q}}(\lambda_0;\mathbf{G})=0\right\}\\
&= \left\{(\lambda_0,\mathbf{G};\mathbf{Q})\in\mathcal{D}\times\mathbf{V}\,|\,\mathbf{G}=\hat{\mathbf{G}}(\lambda_0;\mathbf{Q}),\;\mathbf{Q}=\hat{\mathbf{Q}}(\lambda_0;\mathbf{G}),\;\hat{\mathbf{G}}(\lambda_0;\mathbf{Q})\cdot\hat{\mathbf{Q}}(\lambda_0;\mathbf{G})=0\right\}.
\end{aligned}
$$

REMARK 4.2. The only isothermal E.S. at constant strain for a material point $X \in \mathcal{B}$ of the thermoelastic materials with Cattaneo's heat flux evolution equation (3.9) is the strictly E.S. $(\lambda_0, \mathbf{0}; \mathbf{0})$.

DEFINITION 4.2 *If $(\lambda_0, \mathbf{G}_0; \mathbf{Q}_0) \in \mathcal{E}$, then the set $D(\lambda_0, \mathbf{G}_0; \mathbf{Q}_0) \subset \mathbf{V}$ of vectors $\mathbf{Q}^* \in \mathbf{V}$ for which the solution $\mathbf{Q} = \mathbf{Q}(t)$ of the Cauchy problem*

$$
(4.8)\qquad \dot{\mathbf{Q}} = \mathbf{H}(\lambda_0, \mathbf{G}_0; \mathbf{Q}), \qquad \mathbf{Q}(0) = \mathbf{Q}^*,
$$

exists on $[0, \infty)$ and satisfies the condition

$$
(4.9)\qquad \lim_{t\to\infty} \mathbf{Q}(t) = \mathbf{Q}_0,
$$

*is called the **domain of attraction** of the E.S. $(\lambda_0, \mathbf{G}_0; \mathbf{Q}_0)$ at constant strain and temperature.*

*If $\mathbf{Q}_0 \in D(\lambda_0, \mathbf{G}_0; \mathbf{Q}_0)$ is an interior point, then $(\lambda_0, \mathbf{G}_0; \mathbf{Q}_0) \in \mathcal{E}$ is said to be an **asymptotically stable** E.S.*

The E.S. $(\lambda_0, \mathbf{G}_0; \mathbf{Q}_0) \in \mathcal{E}$ *is called **Lyapunov stable** if for each $\varepsilon > 0$ there exists $\delta = \delta(\varepsilon) > 0$ such that every solution $\mathbf{Q} = \mathbf{Q}(t)$ of* Eq. $(4.8)_1$ *satisfies*

$$
(4.10)\qquad |\mathbf{Q}(t) - \mathbf{Q}_0| < \varepsilon, \qquad t \geq 0,
$$

whenever

$$
(4.11)\qquad |\mathbf{Q}(0) - \mathbf{Q}| < \delta.
$$

REMARK 4.3. For every $\mathbf{Q}^* \in D(\lambda_0, \mathbf{G}_0; \mathbf{Q}_0)$ and every $\mathbf{X} \in \mathbf{B}$ there exists at least one process $\pi^* \in \mathbb{P}(\mathcal{B})$ such that

$$
(4.12)\qquad \begin{aligned} \mathbf{Q}(\mathbf{X},0) = \mathbf{Q}^*, \qquad \mathbf{F}(\mathbf{X},t) = \mathbf{F}_0\,, \qquad \theta(\mathbf{X},t) = \theta_0,\\ \mathbf{G}(\mathbf{X},t)\cdot\mathbf{Q}(\mathbf{X},t) = 0, \qquad t \geq 0. \end{aligned}
$$

Indeed, using the Remark 2.1 it results that the process $\pi^* \in \mathbb{P}(\mathcal{B})$ defined by the motion

$$
(4.13)\qquad \mathbf{x} = \mathbf{X}(\mathbf{Y},t) = \mathbf{X} + \mathbf{F}_0[\mathbf{Y} - \mathbf{X}], \qquad (\mathbf{Y},t) \in \mathbf{B}\times[0,\infty),
$$

and by the temperature field

$$\theta = \theta(\mathbf{Y}, t) = \theta_0 + \mathbf{g}(t) \cdot [\mathbf{Y} - \mathbf{X}], \qquad (\mathbf{Y}, t) \in \mathbf{B} \times [0, \infty), \tag{4.14}$$

where $t \to \mathbf{g}(t) \in \mathbf{V}$, $t \in [0, \infty)$, is a differentiable application satisfying the condition $\mathbf{g}(t) \cdot \mathbf{Q}(t) = 0$, $t \geq 0$, and $\mathbf{Q}(t) = \mathbf{Q}(\mathbf{X}, t)$, the solution of the Cauchy problem (4.8), satisfies (4.12). For the process here defined we have $\dot{\mathbf{F}}(\mathbf{x}, t) = 0$ and $\dot{\theta}(\mathbf{x}, t) = 0$.

THEOREM 4.2.

1) *If* $(\boldsymbol{\lambda}_0, \mathbf{G}_0; \mathbf{Q}_0) \in \mathcal{E}$, $\boldsymbol{\lambda}_0 = (\mathbf{F}_0, \theta_0)$, *then*

$$\hat{\psi}(\boldsymbol{\lambda}_0; \mathbf{Q}^*) \geq \hat{\psi}(\boldsymbol{\lambda}_0; \mathbf{Q}_0), \qquad \mathbf{Q} \in D(\boldsymbol{\lambda}_0, \mathbf{G}_0; \mathbf{Q}_0); \tag{4.15}$$

2) *if* $(\boldsymbol{\lambda}_0, \mathbf{G}_0; \mathbf{Q}_0) \in \mathcal{E}$ *is asymptotically stable then the preceding inequality holds in a neighbourhood* $U(\mathbf{Q}_0)$ *of* $\mathbf{Q}_0$, $U(\mathbf{Q}_0) \subset D(\boldsymbol{\lambda}_0, \mathbf{G}_0; \mathbf{Q}_0)$ *and, consequently, there exists* $\nu_0 \in \mathbb{R}$ *such that*

$$\partial_{\mathbf{Q}} \hat{\psi}(\boldsymbol{\lambda}_0; \mathbf{Q}_0) = \nu_0 \mathbf{G}_0; \tag{4.16}$$

3) *if* $(\boldsymbol{\lambda}_0, 0; \mathbf{Q}_0) \in \mathcal{E}_0$ *and there exists a neighbourhood* $U(\mathbf{Q}_0)$ *of* $\mathbf{Q}_0$ *such that*

$$\hat{\psi}(\boldsymbol{\lambda}_0; \mathbf{Q}) > \hat{\psi}(\boldsymbol{\lambda}_0; \mathbf{Q}_0), \qquad \mathbf{Q} \neq \mathbf{Q}_0 \in U(\mathbf{Q}_0) \cap D(\boldsymbol{\lambda}_0, \mathbf{G}_0; \mathbf{Q}_0), \tag{4.17}$$

then $(\boldsymbol{\lambda}_0, \mathbf{0}; \mathbf{Q}_0)$ *is Lyapunov stable.*

Proof.

1. From (1.21) it results that for processes π^* constructed as in Remark 4.3 we have $\dot{\hat{\psi}}(t) \leq 0$ on $[0, \infty)$, and consequently

$$\hat{\psi}(\boldsymbol{\lambda}_0; \mathbf{Q}(t)) = \hat{\psi}(t) \leq \hat{\psi}(0) = \hat{\psi}(\boldsymbol{\lambda}_0; \mathbf{Q}(0)) = \hat{\psi}(\boldsymbol{\lambda}_0; \mathbf{Q}^*), \qquad t \geq 0.$$

If we make here $t \to \infty$, and take into account that $\lim_{t \to \infty} \mathbf{Q}(t) = \mathbf{Q}_0$ because $\mathbf{Q}^* \in D(\boldsymbol{\lambda}_0, \mathbf{G}_0; \mathbf{Q}_0)$, we obtain (4.15).

2. In our hypotheses the differentiable function $\hat{\psi}(\boldsymbol{\lambda}_0, \cdot)$ attains its minimum at $\mathbf{Q}_0$ on the set $U(\mathbf{G}_0, \mathbf{Q}_0) \cap \Sigma(\boldsymbol{\lambda}_0)$, as described in $(4.7)_1$. This means that $\mathbf{Q}_0$ is a point of local conditional minimum under the side condition $\mathbf{Q} \cdot \mathbf{G}(\boldsymbol{\lambda}_0; \mathbf{Q}) = 0$. Therefore there exists $\nu_0 \in \mathbb{R}$ such that

$$\text{(a)} \qquad \partial_{\mathbf{Q}} \hat{\psi}(\boldsymbol{\lambda}_0; \mathbf{Q}_0) = \nu_0 \left[\hat{\mathbf{G}}(\boldsymbol{\lambda}_0; \mathbf{Q}_0) + \mathbf{Q}_0 \partial_{\mathbf{Q}} \hat{\mathbf{G}}(\boldsymbol{\lambda}_0; \mathbf{Q}_0) \right].$$

On the other hand, differentiating the relation $\hat{\mathbf{Q}}(\boldsymbol{\lambda}_0; \mathbf{G}) \cdot \hat{\mathbf{G}}(\boldsymbol{\lambda}_0; \mathbf{Q}) = 0$ (see $(4.7)_3$) with respect to $\mathbf{Q}$ at the point $\mathbf{Q}_0$ and taking into account $(4.2)_3$ we obtain

$$\text{(b)} \qquad \mathbf{Q}_0 \partial_{\mathbf{Q}} \hat{\mathbf{G}}(\boldsymbol{\lambda}_0; \mathbf{Q}_0) = 0.$$

From (a) and (b) we get (4.16).

3. From (2.20) we have

$$\partial_{\mathbf{Q}}\widehat{\psi}(\boldsymbol{\lambda}_0;\mathbf{Q})\cdot\mathbf{H}(\boldsymbol{\lambda}_0,\mathbf{0};\mathbf{Q}_0)\le 0,\qquad \mathbf{Q}\in\mathbf{V}.$$

This condition together with (4.17) shows that the function

$$\widehat{\psi}(\boldsymbol{\lambda};\cdot):\mathbf{V}\to\mathbb{R}$$

can serve as a Lyapunov function [6, 7] for the autonomous differential system

$$\dot{\mathbf{Q}}=\mathbf{H}(\boldsymbol{\lambda}_0,\mathbf{0};\mathbf{Q}_0) \tag{4.18}$$

and therefore $(\boldsymbol{\lambda}_0,\mathbf{0};\mathbf{Q}_0)\in\mathcal{E}_0$ is asymptotically stable.

Concluding this theorem we note that if $(\boldsymbol{\lambda}_0,\mathbf{0};\mathbf{Q}_0)\in\mathcal{E}_0$ is asymptotically stable then

$$\partial_{\mathbf{Q}}\widehat{\psi}(\boldsymbol{\lambda}_0;\mathbf{Q}_0)=\mathbf{0}. \tag{4.16'}$$

DEFINITION 4.3. *Let* $\boldsymbol{\lambda}^0=(\mathbf{F}^0,\theta^0)\in \mathrm{Lin}^+\times\mathbb{R}^+$ *be given at the material point* $X\in\mathcal{B}$. *The vectorial equation*

$$\partial_{\mathbf{Q}}\widehat{\psi}(\boldsymbol{\lambda}^0;\mathbf{Q})=\nu\mathbf{G} \tag{4.19}$$

is referred to as the ***equation of isothermal internal equilibrium*** *at constant temperature* θ^0 *and constant strain* $\mathbf{F}^0$ *for the material point* $X\in\mathcal{B}$.

REMARK 4.4. The unknowns in (4.19) are the triplets $(\mathbf{G},\mathbf{Q},\nu)\in\mathbf{V}\times\mathbf{V}\times\mathbb{R}$. The part 1 of the preceding theorem shows that if $(\boldsymbol{\lambda}^0,\mathbf{G}_0;\mathbf{Q}_0)$ is an asymptotically stable E.S. then there exists $\nu_0\in\mathbb{R}$ such that $(\mathbf{G}_0,\mathbf{Q}_0,\nu_0)$ satisfies (4.19), i.e. is a solution of the system

$$\mathbf{G}\cdot\mathbf{Q}=0,\qquad \mathbf{H}(\boldsymbol{\lambda}^0,G;\mathbf{Q})=\mathbf{0},\qquad \partial_{\mathbf{Q}}\widehat{\psi}(\boldsymbol{\lambda}^0;Q)=\nu\mathbf{G}. \tag{4.20}$$

DEFINITION 4.4. *The thermoelastic material under consideration is called* ***strictly dissipative*** [1] *if*

$$\dot{\boldsymbol{\lambda}}=(\dot{\mathbf{F}},\dot{\boldsymbol{\theta}})=\mathbf{0},\qquad \mathbf{G}\cdot\mathbf{Q}=0,\qquad \dot{\mathbf{Q}}\neq\mathbf{0}\ \Rightarrow\ \gamma>0, \tag{4.21}$$

where γ *is the specific rate of production of entropy defined by* (1.20).

REMARK 4.5. From (1.20) and (2.16) it follows that the considered material is strictly dissipative if and only if

$$\mathbf{G}_0\cdot\mathbf{Q}=0\ \text{ and }\ (\boldsymbol{\lambda}_0,\mathbf{G}_0;\mathbf{Q})\notin\mathcal{E}\ \Rightarrow\ \partial_{\mathbf{Q}}\widehat{\psi}(\boldsymbol{\lambda}_0;\mathbf{Q})\cdot\mathbf{H}(\boldsymbol{\lambda}_0,\mathbf{G}_0;\mathbf{Q})<0. \tag{4.22}$$

Using the same line of arguments which leads us to the part 1 of the preceding theorem we can prove the

THEOREM 4.3. *If* $(\boldsymbol{\lambda}_0, \mathbf{G}_0; \mathbf{Q}_0) \in \mathcal{E}$ *is asymptotically stable and if there exists* $U(\mathbf{Q}_0) \subset D(\boldsymbol{\lambda}_0, \mathbf{G}_0; \mathbf{Q}_0)$, *a neighbourhood* $\mathbf{Q}_0$, *such that the inequality in* (4.22) *holds on* $U(\mathbf{Q}_0)\backslash\{\mathbf{Q}_0\}$, *then*

$$\widehat{\psi}(\boldsymbol{\lambda}_0, \mathbf{Q}) > \widehat{\psi}(\boldsymbol{\lambda}_0, \mathbf{Q}_0), \qquad \mathbf{Q}_0 \neq \mathbf{Q} \in U(\mathbf{Q}_0). \tag{4.23}$$

THEOREM 4.4. *If* $(\boldsymbol{\lambda}_0, \mathbf{0}; \mathbf{Q}_0) \in \mathcal{E}_0$ *and*

$$\partial_{\mathbf{Q}} \widehat{\psi}(\boldsymbol{\lambda}_0; \mathbf{Q}) \cdot \mathbf{H}(\boldsymbol{\lambda}_0, \mathbf{0}; \mathbf{Q}) < 0, \qquad \mathbf{Q}_0 \neq \mathbf{Q} \in U(\mathbf{Q}_0), \tag{4.24}$$

where $U(\mathbf{Q}_0)$ *is a neighbourhood of* $\mathbf{Q}_0$, *then:*

1) $(\boldsymbol{\lambda}_0, \mathbf{0}; \mathbf{Q}_0)$ *is asymptotically stable if and only if* (4.23) *holds;*

2) *if* $(\boldsymbol{\lambda}_0, \mathbf{0}; \mathbf{Q}_0)$ *is asymptotically stable then it is Lyapunov stable.*

P r o o f. The necessary part of 1 is a result of the preceding theorem. The sufficiency of 1 follows from Lyapunov's theorem on asymptotic stability since in this case the function $\widehat{\psi}(\boldsymbol{\lambda}_0; \cdot)$ is a Lyapunov function [6, 7] for the autonomous differential system (4.18). The part 2 of the theorem is a consequence of the preceding theorem and of the Lyapunov's stability theorem [6, 7].

REMARK 4.6. If the material is strictly dissipative and $(\boldsymbol{\lambda}_0, \mathbf{0}; \mathbf{Q}_0) \in \mathcal{E}_0$ is asymptotically stable, the inequality (4.23) holds and $(\boldsymbol{\lambda}_0, \mathbf{0}; \mathbf{Q}_0) \in \mathcal{E}_0$ is Lyapunov stable.

REMARK 4.7. The only E.S. $(\boldsymbol{\lambda}_0, \mathbf{0}; \mathbf{0}) \in \mathcal{E}_0$ (see Remark 4.2) of a thermoelastic material obeying the Cattaneo's heat flux evolution equation (3.9) is asymptotically stable if and only if the characteristic roots of $\mathbf{T}^{-1}(\boldsymbol{\lambda}_0)$ have positive real parts [6, 7].

5. Consistency with thermostatics

In this section we assume that for each $\boldsymbol{\lambda}_0 = (\mathbf{F}_0, \theta_0) \in \mathrm{Lin}^+ \times \mathbb{R}^+$ there exists a unique pair $(\mathbf{G}_0, \mathbf{Q}_0) \in \mathbf{V} \times \mathbf{V}$ such that $(\boldsymbol{\lambda}_0, \mathbf{G}_0; \mathbf{Q}_0) \in \mathcal{E}$. Using $(4.2)_3$ we denote

$$\mathcal{D}_0 = \{(\boldsymbol{\lambda}_0, \mathbf{G}_0) \in \mathcal{D} \; (\boldsymbol{\lambda}_0, \mathbf{G}_0; \mathbf{Q}_0) = (\boldsymbol{\lambda}_0, \mathbf{G}_0; \widehat{\mathbf{Q}}(\boldsymbol{\lambda}_0; \mathbf{G}_0)) \in \mathcal{E}\}. \tag{5.1}$$

The set $\mathcal{D}_0 \subset \mathcal{D}$ is referred to as the *equilibrium part* of $\mathcal{D}$ and is supposed to be a subdomain of $\mathcal{D}$.

On $\mathcal{D}_0$ we define the *equilibrium response functions* $\overline{\psi}_0$, $\overline{\eta}_0$, and $\overline{\mathbf{S}}_0$ giving the *equilibrium free energy* ψ_0, the *equilibrium entropy* η_0, and the *equilibrium first Piola–Kirchhoff stress tensor* $\mathbf{S}_0$ through *equilibrium constitutive equations*.

$$\psi_0 = \overline{\psi}_0(\boldsymbol{\lambda}_0; \mathbf{G}_0) \equiv \widehat{\psi}(\boldsymbol{\lambda}_0; \widehat{Q}(\boldsymbol{\lambda}_0; \mathbf{G}_0)), \tag{5.2}$$

$$\eta_0 = \overline{\eta}_0(\boldsymbol{\lambda}_0; \mathbf{G}_0) \equiv \widehat{\eta}(\boldsymbol{\lambda}_0; \widehat{Q}(\boldsymbol{\lambda}_0; \mathbf{G}_0)) = -\partial_\theta \widehat{\psi}(\boldsymbol{\lambda}_0; \widehat{\mathbf{Q}}(\boldsymbol{\lambda}_0, \mathbf{G}_0)), \tag{5.3}$$

$$\mathbf{S}_0 = \overline{\mathbf{S}}_0(\boldsymbol{\lambda}_0; \mathbf{G}_0) \equiv \widehat{\mathbf{S}}(\boldsymbol{\lambda}_0; \widehat{\mathbf{Q}}(\boldsymbol{\lambda}_0; \mathbf{G}_0)) = \partial_{\mathbf{F}} \widehat{\psi}(\boldsymbol{\lambda}_0; \widehat{\mathbf{Q}}(\boldsymbol{\lambda}_0, \mathbf{G}_0)). \tag{5.4}$$

REMARK 5.1. If $(\boldsymbol{\lambda}_0, \mathbf{G}_0) \in \mathcal{D}_0$ is asymptotically stable, i.e. $(\boldsymbol{\lambda}_0, \mathbf{G}_0; \hat{\mathbf{Q}}(\boldsymbol{\lambda}_0; \mathbf{G}_0)) \in \mathcal{E}$ is asymptotically stable, then

$$\partial_{\mathbf{G}} \overline{\psi}_0(\boldsymbol{\lambda}_0; \mathbf{G}_0) = \mathbf{0}, \tag{5.5}$$

$$\partial_\theta \overline{\psi}_0(\boldsymbol{\lambda}_0; \mathbf{G}_0) = \partial_\theta \hat{\psi}(\boldsymbol{\lambda}_0; \mathbf{G}_0), \tag{5.6}$$

$$\partial_{\mathbf{F}} \overline{\psi}_0(\boldsymbol{\lambda}_0; \mathbf{G}_0) = \partial_{\mathbf{F}} \hat{\psi}(\boldsymbol{\lambda}_0; \mathbf{G}_0). \tag{5.7}$$

Indeed from $(4.7)_2$ and (5.2) it results that in a neighbourhood of $(\boldsymbol{\lambda}_0, \mathbf{G}_0; \mathbf{Q}_0)$ we have

$$\overline{\psi}_0(\boldsymbol{\lambda}; \mathbf{G}) \equiv \hat{\psi}(\boldsymbol{\lambda}; \mathbf{Q}(\boldsymbol{\lambda}, \mathbf{G})), \qquad \mathbf{Q} = \hat{\mathbf{Q}}(\lambda, \mathbf{G}), \qquad \mathbf{G} \cdot \hat{\mathbf{Q}}(\boldsymbol{\lambda}; \mathbf{G}) = 0. \tag{5.8}$$

Applying the chain rules with respect to $\mathbf{G}$, θ and $\mathbf{F}$ for $(5.8)_1$ we obtain

$$\partial_{\mathbf{G}} \overline{\psi}_0(\boldsymbol{\lambda}; \mathbf{G}) \equiv \partial_Q \hat{\psi}(\boldsymbol{\lambda}; \hat{\mathbf{Q}}(\boldsymbol{\lambda}; \mathbf{G})) \partial_{\mathbf{G}} \hat{\mathbf{Q}}(\lambda; G), \tag{5.9}$$

$$\partial_\theta \overline{\psi}_0(\boldsymbol{\lambda}; \mathbf{G}) \equiv \partial_\theta \hat{\psi}(\boldsymbol{\lambda}; \hat{\mathbf{Q}}(\boldsymbol{\lambda}; \mathbf{G})) + \partial_{\mathbf{Q}} \hat{\psi}(\boldsymbol{\lambda}; \hat{\mathbf{Q}}(\boldsymbol{\lambda}; \mathbf{G})) \partial_\theta \hat{\mathbf{Q}}(\boldsymbol{\lambda}; \mathbf{G}), \tag{5.10}$$

$$\partial_{\mathbf{F}} \overline{\psi}_0(\boldsymbol{\lambda}_0; \mathbf{G}) \equiv \partial_{\mathbf{F}} \hat{\psi}(\boldsymbol{\lambda}; \hat{\mathbf{Q}}(\boldsymbol{\lambda}; \mathbf{G})) + \partial_{\mathbf{Q}} \hat{\psi}(\boldsymbol{\lambda}; \hat{\mathbf{Q}}(\boldsymbol{\lambda}; \mathbf{G})) \partial_{\mathbf{F}} \hat{\mathbf{Q}}(\boldsymbol{\lambda}; \mathbf{G}). \tag{5.11}$$

If $(\boldsymbol{\lambda}_0, \mathbf{G}_0) \in \mathcal{D}_0$, is asymptotically stable then in view of Theorem 4.2, there exists $\nu_0 \in \mathbb{R}$ such that (a) $\partial_{\mathbf{Q}} \hat{\psi}(\boldsymbol{\lambda}_0; \mathbf{Q}_0) = \nu_0 \mathbf{G}_0$, and therefore we have (b) $\partial_{\mathbf{G}} \overline{\psi}_0(\boldsymbol{\lambda}_0; \mathbf{G}_0) = \nu_0 \mathbf{G}_0 \partial_{\mathbf{G}} \hat{\mathbf{Q}}(\boldsymbol{\lambda}_0, \mathbf{G}_0)$. Differentiating $\hat{\mathbf{Q}}(\boldsymbol{\lambda}; \mathbf{G}) \cdot \hat{\mathbf{G}}(\boldsymbol{\lambda}; \mathbf{Q}) = 0$ with respect to $\mathbf{G}$ in the point $(\boldsymbol{\lambda}_0, \mathbf{G}_0) \in \mathcal{D}_0$ and taking into account $(4.2)_3$ we have $\mathbf{G}_0 \partial_{\mathbf{G}} \hat{\mathbf{Q}}(\boldsymbol{\lambda}_0; \mathbf{G}_0) = \mathbf{0}$ which, together with (5.9) and (b), implies (5.5). Differentiating $(5.8)_3$ with respect to θ and $\mathbf{F}$ in the point $(\boldsymbol{\lambda}_0, \mathbf{G}_0) \in \mathcal{D}_0$ we obtain (c) $\mathbf{G}_0 \partial_\theta \hat{\mathbf{Q}}(\boldsymbol{\lambda}_0; \mathbf{G}_0) = 0$ and (d) $\mathbf{G}_0 \partial_{\mathbf{F}} \hat{\mathbf{Q}}(\boldsymbol{\lambda}_0; \mathbf{G}_0) = \mathbf{0}$. If we evaluate (5.10), (5.11) in $(\boldsymbol{\lambda}_0, \mathbf{G}_0) \in \mathcal{D}_0$ we obtain (5.6) and (5.7) in virtue of (b), (c) and (d).

Thus we obtain the following *theorem of consistency with thermostatics* ([1, 3]).

THEOREM 5.1. *If the set $\mathcal{D}_0^* \subset \mathcal{D}_0$ of asymptotically stable pairs $(\boldsymbol{\lambda}^*, \mathbf{G}^*)$, $\boldsymbol{\lambda}^* = (F^*, \theta^*)$ is an open and connected set then:*

1) *the equilibrium function of free energy is independent of $\mathbf{G}^*$, i.e.*

$$\psi_0 = \hat{\psi}_0(\boldsymbol{\lambda}^*); \tag{5.12}$$

2) *the equilibrium functions of entropy and of the stress tensor are independent of $\mathbf{G}^*$, i.e.*

$$\eta_0 = \hat{\eta}_0(\boldsymbol{\lambda}^*), \qquad \mathbf{S}_0 = \hat{\mathbf{S}}_0(\boldsymbol{\lambda}^*), \tag{5.13}$$

and they are determined by the function $\hat{\psi}_0$ through the relations

$$\hat{\eta}_= - \partial_{\theta^*} \hat{\psi}_0, \qquad \hat{\mathbf{S}}_0 = \partial_{\mathbf{F}^*} \hat{\psi}_0. \tag{5.14}$$

REMARK 5.2. Of course we have

$$\mathbf{G}^* \cdot \hat{\mathbf{Q}}(\boldsymbol{\lambda}^*; \mathbf{G}^*) = 0, \qquad (\boldsymbol{\lambda}^*, \mathbf{G}^*) \in \mathcal{D}_0^* . \tag{5.15}$$

Writing the first order Taylor's formula of $\hat{\mathbf{Q}}$ in the point $(\boldsymbol{\lambda}^*, \mathbf{0}) \in \mathcal{D}_0^*$ we obtain

$$\hat{\mathbf{Q}}(\boldsymbol{\lambda}^*; \mathbf{G}^*) = \mathbf{K}_0(\boldsymbol{\lambda}^*)\mathbf{G}^* + o(|\mathbf{G}^*|), \tag{5.16}$$

where

$$\mathbf{K}_0(\boldsymbol{\lambda}^*) = \left[\partial_{\mathbf{G}^*} \hat{\mathbf{Q}}(\boldsymbol{\lambda}^*; \mathbf{0})\right]^T , \tag{5.17}$$

because (5.15) implies $\hat{\mathbf{Q}}(\boldsymbol{\lambda}^*; \mathbf{0}) = \mathbf{0}$ [4].

The relation (5.16) shows that at an asymptotically E.S. the Fourier law holds within an error of order $o(|\mathbf{G}^*|)$ ([4, 5, 1]).

6. Entropy as an independent variable

The quantity

$$c = \partial_\theta \hat{\varepsilon}(\boldsymbol{\lambda}; \mathbf{Q}), \tag{6.1}$$

is called the *heat capacity* of the body. In virtue of (3.3) and $(2.15)_1$

$$c = \theta \partial_\theta \hat{\eta}(\boldsymbol{\lambda}; \mathbf{Q}). \tag{6.2}$$

In what follows we suppose $c > 0$ [1] on $\mathcal{D} \times \mathbf{V}$. This hypothesis implies that the function

$$(\boldsymbol{\lambda}; \mathbf{Q}) \to \hat{\eta}(\boldsymbol{\lambda}; \mathbf{Q}) \in \mathbb{R}, \qquad (\boldsymbol{\lambda}, \mathbf{G}; \mathbf{Q}) \in \mathcal{D} \times \mathbf{V}, \qquad \boldsymbol{\lambda} = (\mathbf{F}, \theta), \tag{6.3}$$

is smoothly invertible with respect to θ on $\mathcal{D} \times \mathbf{V}$. Consequently the constitutive functionals of the thermoelastic material may be written as follows

$$\varepsilon = \tilde{\varepsilon}(\tilde{\boldsymbol{\lambda}}; \mathbf{Q}), \tag{6.4}$$

$$\theta = \tilde{\theta}(\tilde{\boldsymbol{\lambda}}; \mathbf{Q}), \tag{6.5}$$

$$\mathbf{S} = \tilde{\mathbf{S}}(\tilde{\boldsymbol{\lambda}}; \mathbf{Q}), \tag{6.6}$$

$$\dot{\mathbf{Q}} = \tilde{\mathbf{H}}(\tilde{\boldsymbol{\lambda}}, \mathbf{G}; \mathbf{Q}), \qquad (\tilde{\boldsymbol{\lambda}}, \mathbf{G}; \mathbf{Q}) \in \tilde{\mathcal{D}} \times \mathbf{V}, \qquad \tilde{\boldsymbol{\lambda}} = (\mathbf{F}, \eta), \tag{6.7}$$

where the function $\tilde{\theta}(\mathbf{F}, \cdot\,; \mathbf{Q})$ is the inverse of the function $\hat{\eta}(\mathbf{F}, \cdot\,; \mathbf{Q})$ defined in (6.3), $\tilde{\mathcal{D}} \subset \mathrm{Lin}^+ \times \mathbb{R} \times \mathbf{V}$ is a domain completely determined by the domain $\mathcal{D}$, and

$$\tilde{\varepsilon}(\tilde{\boldsymbol{\lambda}}; \mathbf{Q}) = \hat{\varepsilon}(\mathbf{F}, \tilde{\theta}(\tilde{\boldsymbol{\lambda}}; \mathbf{Q}); \mathbf{Q}) = \hat{\psi}(\mathbf{F}, \tilde{\theta}(\tilde{\boldsymbol{\lambda}}; \mathbf{Q}); \mathbf{Q}) + \eta \tilde{\theta}(\tilde{\boldsymbol{\lambda}}; \mathbf{Q}), \tag{6.8}$$

$$\tilde{\mathbf{S}}(\tilde{\boldsymbol{\lambda}}; \mathbf{Q}) = \hat{\mathbf{S}}(\mathbf{F}\tilde{\theta}(\tilde{\boldsymbol{\lambda}}; \mathbf{Q}); \mathbf{Q}), \tag{6.9}$$

$$\tilde{\mathbf{H}}(\tilde{\boldsymbol{\lambda}}, \mathbf{G}; \mathbf{Q}) = H(\mathbf{F}, \tilde{\theta}(\tilde{\boldsymbol{\lambda}}; \mathbf{Q}), \mathbf{G}; \mathbf{Q}). \tag{6.10}$$

Applying the chain rule to (6.8) with respect to η and $\mathbf{F}$ and taking into account the entropy relation $(2.15)_1$, we obtain

$$\tilde{\theta} = \partial_\eta \tilde{\varepsilon}, \qquad \tilde{\mathbf{S}} = \varrho_\kappa \partial_{\mathbf{F}} \tilde{\varepsilon} \tag{6.11}$$

which means that the temperature functional $\tilde{\theta}$ and the stress tensor functional $\tilde{\mathbf{S}}$ are determined by the internal energy functional $\tilde{\varepsilon}$.

The chain rule with respect to $\mathbf{Q}$ applied to (6.8) and the entropy relation $(2.15)_1$ leads to

$$\partial_{\mathbf{Q}} \tilde{\varepsilon}(\tilde{\boldsymbol{\lambda}}; \mathbf{Q}) = \partial_{\mathbf{Q}} \hat{\psi}(\mathbf{F}, \tilde{\theta}(\tilde{\boldsymbol{\lambda}}; \mathbf{Q}), \mathbf{G}; \mathbf{Q}), \tag{6.12}$$

so that the Dissipation Inequality (2.16) becomes

$$\varrho_\kappa \partial_\eta \tilde{\varepsilon}(\tilde{\boldsymbol{\lambda}}; \mathbf{Q}) \partial_{\mathbf{Q}} \tilde{\varepsilon}(\tilde{\boldsymbol{\lambda}}; \mathbf{Q}) \cdot \tilde{\mathbf{H}}(\tilde{\boldsymbol{\lambda}}, \mathbf{G}; \mathbf{Q}) + \mathbf{G}\mathbf{Q} \leq 0. \tag{6.13}$$

Therefore

$$\mathbf{Q} \cdot \mathbf{G} = 0 \;\Rightarrow\; \partial_{\mathbf{Q}} \tilde{\varepsilon}(\tilde{\boldsymbol{\lambda}}; \mathbf{Q}) \cdot \tilde{\mathbf{H}}(\tilde{\boldsymbol{\lambda}}, \mathbf{G}; \mathbf{Q}) \leq 0, \tag{6.14}$$

and, in particular, we have

$$\partial_{\mathbf{Q}} \tilde{\varepsilon}(\tilde{\boldsymbol{\lambda}}; \mathbf{Q}) \cdot \tilde{\mathbf{H}}(\tilde{\boldsymbol{\lambda}}, \mathbf{0}; \mathbf{Q}) \leq 0. \tag{6.15}$$

The counterpart of theorem 3.1 is the

THEOREM 6.1. *If $\tilde{\varepsilon}$ is twice continuously differentiable and the heat flux evolution equation* (6.7) *has the Cattaneo's form*

$$\tilde{\mathbf{T}}(\tilde{\boldsymbol{\lambda}})\, \dot{\mathbf{Q}} + \mathbf{Q} = -\tilde{\mathbf{K}}(\tilde{\boldsymbol{\lambda}})\mathbf{G}, \qquad \tilde{\boldsymbol{\lambda}} = (\mathbf{F}, \eta), \tag{6.16}$$

where the second order tensors $\tilde{\mathbf{T}}$ and $\tilde{\mathbf{K}}$ are nonsingular, then the dissipation inequality (6.13) *holds if and only if on $\mathcal{D} \times \mathbf{V}$:*

1) *$\tilde{\mathbf{K}}(\tilde{\boldsymbol{\lambda}})$ is positive definite and*

2) *the second order tensor function*

$$\tilde{\boldsymbol{\lambda}} \to \tilde{\mathbf{Z}}(\tilde{\boldsymbol{\lambda}}) \equiv \left[\tilde{\mathbf{K}}(\tilde{\boldsymbol{\lambda}})\right]^{-1} \tilde{\mathbf{T}}(\tilde{\boldsymbol{\lambda}}) \in \mathrm{Lin}, \qquad \tilde{\boldsymbol{\lambda}} = (\mathbf{F}, \eta), \tag{6.17}$$

is given by

$$\tilde{\mathbf{Z}} = \varrho_\kappa \left[\partial^2_{\eta \mathbf{Q}} \tilde{\varepsilon}) \otimes (\partial_{\mathbf{Q}} \tilde{\varepsilon}) + \partial_\eta \tilde{\varepsilon} \partial^2_{Q} \tilde{\varepsilon}\right]. \tag{6.18}$$

P r o o f. As in the proof of Theorem 3.1, we conclude that the inequality obtained by inserting (6.16) into (6.13) holds if and only if we have

$$\left[(\tilde{\mathbf{T}}^{-1}(\boldsymbol{\lambda}))^T \partial_{\mathbf{Q}} \tilde{\varepsilon}(\tilde{\boldsymbol{\lambda}}; \mathbf{Q})\right] \cdot \mathbf{Q} \geq 0, \tag{6.19}$$

$$\varrho_\kappa \partial_\eta \tilde{\varepsilon}(\tilde{\boldsymbol{\lambda}}; \mathbf{Q})(\tilde{\mathbf{Z}}^{-1}(\boldsymbol{\lambda}))^T \partial_{\mathbf{Q}} \tilde{\varepsilon}(\tilde{\boldsymbol{\lambda}}; \mathbf{Q}) = \mathbf{Q}. \tag{6.20}$$

Using the *temperature relation* $(6.11)_1$ we write (6.20) in the form

$$\varrho_\kappa \partial_\eta \tilde{\varepsilon}(\tilde{\boldsymbol{\lambda}}; \mathbf{Q}) \partial_{\mathbf{Q}} \tilde{\varepsilon}(\tilde{\boldsymbol{\lambda}}; \mathbf{Q}) = \tilde{\mathbf{Z}}^T(\tilde{\boldsymbol{\lambda}})\mathbf{Q}. \tag{6.20'}$$

Differentiating this relation with respect to $\mathbf{Q}$ we get (6.18). From (6.20') and (6.19) it results

$$\mathbf{Q} \cdot \tilde{\mathbf{K}}^{-1}(\tilde{\boldsymbol{\lambda}})\mathbf{Q} \geq 0, \qquad \mathbf{Q} \in \mathbf{V}, \tag{6.21}$$

which means that $\mathbf{K}^{-1}$, and therefore $\tilde{\mathbf{K}}$ is positive definite.

REMARK 6.1. We have to note that in this case it is difficult to derive relations similar to the relations (3.14) – (3.19). On the other hand, the $\tilde{\mathbf{Z}}$ is not symmetric.

DEFINITION 6.1. *The state* $(\tilde{\boldsymbol{\lambda}}_0, \mathbf{G}_0; \mathbf{Q}_0) \in \tilde{\mathcal{D}} \times \mathbf{V}$, $\tilde{\boldsymbol{\lambda}}_0 = (\mathbf{F}_0, \eta_0)$ *is called an* ***isentropic E.S. at constant strain*** $\mathbf{F}_0$ *for the material point* $X \in \mathcal{B}$ *if*

$$\mathbf{G}_0 \cdot \mathbf{Q}_0 = 0, \qquad \tilde{\mathbf{H}}(\tilde{\boldsymbol{\lambda}}_0, \mathbf{G}_0; \mathbf{Q}_0) = \mathbf{0}. \tag{6.22}$$

The state $(\tilde{\boldsymbol{\lambda}}_0, \mathbf{0}; \mathbf{Q}_0) \in \tilde{\mathcal{D}} \times \mathbf{V}$, $\tilde{\boldsymbol{\lambda}}_0 = (\mathbf{F}_0, \eta_0)$, *is a* ***strictly isentropic E.S. at constant strain*** $\mathbf{F}_0$ *for the material point* $X \in \mathcal{B}$ *if*

$$\tilde{\mathbf{H}}(\tilde{\boldsymbol{\lambda}}_0, \mathbf{0}; \mathbf{Q}_0) = \mathbf{0}. \tag{6.23}$$

We will denote by $\tilde{\mathcal{E}}$ *the set of isentropic E.S. and by* $\tilde{\mathcal{E}}_0 \subset \tilde{\mathcal{E}}$ *the* ***subset of strictly isentropic*** *E.S. for a given material point* $X \in \mathcal{B}$.

REMARK 6.2. From (6.10) it follows that if $(\boldsymbol{\lambda}_0, \mathbf{G}_0; \mathbf{Q}_0) \in \mathcal{D} \times \mathbf{V}$ and $(\tilde{\boldsymbol{\lambda}}_0, \mathbf{G}_0; \mathbf{Q}_0) \in \tilde{\mathcal{D}} \times \mathbf{V}$ are two states related by $\theta_0 = \tilde{\theta}(\tilde{\boldsymbol{\lambda}}; \mathbf{Q}_0)$, then

$$(\boldsymbol{\lambda}, \mathbf{G}_0; \mathbf{Q}_0) \in \mathcal{E} \Leftrightarrow (\tilde{\boldsymbol{\lambda}}_0, \mathbf{G}_0; \mathbf{Q}_0) \in \tilde{\mathcal{E}}. \tag{6.24}$$

DEFINITION 6.2. *If* $(\tilde{\boldsymbol{\lambda}}_0, \mathbf{G}_0; \mathbf{Q}_0) \in \tilde{\mathcal{E}}$, *then the set* $\tilde{D}(\boldsymbol{\lambda}_0, \mathbf{G}_0; \mathbf{Q}_0) \subset \mathbf{V}$ *of points* $\mathbf{Q}^* \in \mathbf{V}$ *for which the solution* $\mathbf{Q} = \mathbf{Q}(t)$ *of the Cauchy problem*

$$\dot{\mathbf{Q}} = \tilde{\mathbf{H}}(\tilde{\boldsymbol{\lambda}}_0, \mathbf{G}_0; \mathbf{Q}), \qquad \mathbf{Q}(0) = \mathbf{Q}^*, \tag{6.25}$$

exists in $[0, \infty)$ *and satisfies the condition*

$$\lim_{t \to \infty} \mathbf{Q}(t) = Q_0, \tag{6.26}$$

will be referred to as the ***domain of attraction*** *of the E.S.* $(\tilde{\boldsymbol{\lambda}}_0, \mathbf{G}_0; \mathbf{Q}_0)$ *at constant strain and entropy* $\tilde{\boldsymbol{\lambda}}_0 = (\mathbf{F}_0, \eta_0)$.

The isentropic E.S. $(\tilde{\boldsymbol{\lambda}}_0, \mathbf{G}_0; \mathbf{Q}_0)$ is said to be *asymptotically stable* if $\mathbf{Q}_0 \in \tilde{D}$ $(\tilde{\boldsymbol{\lambda}}_0, \mathbf{G}_0; \mathbf{Q}_0)$ is an interior point.

The isentropic E.S. $(\tilde{\boldsymbol{\lambda}}_0, \mathbf{G}_0; \mathbf{Q}_0)$ will be called *Lyapunov stable* if for every $\varepsilon > 0$ there exists a $\delta = (\varepsilon) > 0$ such that every solution $\mathbf{Q} = \mathbf{Q}(t)$ of the differential equation $(6.25)_1$ satisfies the condition $|\mathbf{Q}(t) - \mathbf{Q}_0| < \varepsilon$ on $[0, \infty)$ whenever $|\mathbf{Q}(0) - \mathbf{Q}_0| < \delta$.

Similar results to those of theorem 4.2 are given by the

THEOREM 6.2.

1) *If* $(\tilde{\boldsymbol{\lambda}}_0, \mathbf{G}_0; \mathbf{Q}_0) \in \tilde{\mathcal{E}}$, $\tilde{\boldsymbol{\lambda}}_0 = (\mathbf{F}_0, \eta_0)$, *then*

$$\tilde{\varepsilon}(\tilde{\boldsymbol{\lambda}}_0; \mathbf{Q}^*) \geq \tilde{\varepsilon}(\tilde{\boldsymbol{\lambda}}_0; \mathbf{Q}_0), \qquad \mathbf{Q}^* \in \tilde{D}(\tilde{\boldsymbol{\lambda}}_0, \mathbf{G}_0; \mathbf{Q}_0); \tag{6.27}$$

2) *if* $(\tilde{\boldsymbol{\lambda}}_0; \mathbf{G}_0; \mathbf{Q}_0) \in \tilde{\mathcal{E}}$ *is asymptotically stable then the preceding inequality holds in a neighbourhood* $U(\mathbf{Q}_0) \subset \tilde{D}(\tilde{\boldsymbol{\lambda}}_0, \mathbf{G}_0; \mathbf{Q}_0)$ *of* $\mathbf{Q}_0$ *and there exists* $\tilde{\nu}_0 \in \mathbb{R}$ *such that*

$$\partial_{\mathbf{Q}} \tilde{\varepsilon}(\tilde{\boldsymbol{\lambda}}_0, \mathbf{Q}_0) = \tilde{\nu}_0 \mathbf{G}_0 ; \tag{6.28}$$

3) *if* $(\tilde{\boldsymbol{\lambda}}_0, \mathbf{0}; \mathbf{Q}_0) \in \tilde{\mathcal{E}}_0$ *and if there exists a neighbourhood* $U(\mathbf{Q}_0)$ *of* $\mathbf{Q}_0$ *such that*

$$\tilde{\varepsilon}(\tilde{\boldsymbol{\lambda}}_0; \mathbf{Q}) > \tilde{\varepsilon}(\tilde{\boldsymbol{\lambda}}_0; \mathbf{Q}_0), \qquad \mathbf{Q}_0 \neq \mathbf{Q} \in U(\mathbf{Q}_0) \cap \tilde{D}(\tilde{\boldsymbol{\lambda}}_0, \mathbf{G}_0; \mathbf{Q}_0), \tag{6.29}$$

then $(\tilde{\boldsymbol{\lambda}}_0, \mathbf{0}; \mathbf{Q}_0)$ *is Lyapunov stable E.S.*

REMARK 6.3. From (6.10), (6.12) and Remark 4.5 it results that the material is strictly dissipative if and only if

$$\mathbf{G}_0 \cdot \mathbf{Q} = 0 \quad \text{and} \quad (\tilde{\boldsymbol{\lambda}}_0, \mathbf{G}_0; \mathbf{Q}) \notin \tilde{\mathcal{E}} \Rightarrow \partial_{\mathbf{Q}} \tilde{\varepsilon}(\tilde{\boldsymbol{\lambda}}_0; \mathbf{Q}) \cdot \tilde{\mathbf{H}}(\tilde{\boldsymbol{\lambda}}_0; \mathbf{G}_0; \mathbf{Q}_0) < 0. \tag{6.30}$$

Thus we obtain the following two theorems which are counterparts of Theorems 4.3 and 4.4.

THEOREM 6.3. *If* $(\tilde{\boldsymbol{\lambda}}_0, \mathbf{G}_0; \mathbf{Q}_0) \in \tilde{\mathcal{E}}$ *is asymptotically stable and if there exists a neighbourhood* $U(\mathbf{Q}_0) \subset \tilde{D}(\tilde{\boldsymbol{\lambda}}_0, \mathbf{G}_0; \mathbf{Q}_0)$ *of* $\mathbf{Q}_0$ *such that the inequality in* (6.30) *holds on* $U(\mathbf{Q}_0) \backslash \{\mathbf{Q}_0\}$ *then*

$$\tilde{\varepsilon}(\tilde{\boldsymbol{\lambda}}_0; \mathbf{Q}) > \tilde{\varepsilon}(\tilde{\boldsymbol{\lambda}}_0; \mathbf{Q}_0), \qquad \mathbf{Q}_0 \neq \mathbf{Q} \in U(\mathbf{Q}_0). \tag{6.31}$$

THEOREM 6.4. *If* $(\tilde{\boldsymbol{\lambda}}_0; \mathbf{0}; \mathbf{Q}_0) \in \tilde{\mathcal{E}}_0$ *and*

$$\partial_{\mathbf{Q}} \tilde{\varepsilon}(\tilde{\boldsymbol{\lambda}}_0; \mathbf{Q}) \cdot \tilde{\mathbf{H}}(\tilde{\boldsymbol{\lambda}}_0; \mathbf{0}; \mathbf{Q}) < 0, \qquad \mathbf{Q}_0 \neq \mathbf{Q} \in U(\mathbf{Q}_0), \tag{6.32}$$

where $U(\mathbf{Q}_0)$ *is a neighbourhood of* $\mathbf{Q}_0$ *then:*

1) $(\tilde{\boldsymbol{\lambda}}_0, \mathbf{0}; \mathbf{Q}_0)$ *is asymptotically stable if and only if* (6.31) *holds and*

2) *if* $(\tilde{\boldsymbol{\lambda}}_0, \mathbf{0}; \mathbf{Q}_0)$ *is asymptotically stable then it is Lyapunov stable.*

REMARK 6.4. From theorems 6.3 and 6.4 we conclude that if the material is strictly dissipative and $(\tilde{\boldsymbol{\lambda}}_0, \mathbf{0}; \mathbf{Q}_0) \in \tilde{\mathcal{E}}_0$ is asymptotically stable, then (6.31) holds and $(\boldsymbol{\lambda}_0, \mathbf{0}; \mathbf{Q}_0)$ is Lyapunov stable.

7. Internal energy as an independent variable

Because $\theta > 0$, the temperature relation $(6.11)_1$

$$\theta = \partial_\eta \tilde{\varepsilon}(\tilde{\lambda}; \mathbf{Q}), \qquad \tilde{\lambda} = (\mathbf{F}, \eta), \tag{7.1}$$

implies that the function $\eta \to \varepsilon = \tilde{\varepsilon}(\mathbf{F}, \eta; \mathbf{Q}) \in \mathbb{R}$, $\eta \in \mathbb{R}$, is smoothly invertible for any fixed $\mathbf{F}$ and $\mathbf{Q}$. Denoting by $\varepsilon \to \eta = \check{\eta}(\mathbf{F}, \varepsilon; \mathbf{Q}) \in \mathbb{R}$, $\varepsilon \in \mathbb{R}$ the inverse of the function $\tilde{\varepsilon}(\mathbf{F}, \cdot\,; \mathbf{Q})$ and substituting it into (6.5) – (6.7) we obtain the following constitutive equations of the thermoelastic material

$$\eta = \check{\eta}(\check{\lambda}; \mathbf{Q}), \tag{7.2}$$

$$\theta = \check{\theta}(\check{\lambda}; \mathbf{Q}), \tag{7.3}$$

$$\mathbf{S} = \check{\mathbf{S}}(\check{\lambda}; \mathbf{Q}), \tag{7.4}$$

$$\dot{\mathbf{Q}} = \check{\mathbf{H}}(\check{\lambda}, \mathbf{G}; \mathbf{Q}), \qquad (\check{\lambda}, \mathbf{G}; \mathbf{Q}) \in \check{\mathcal{D}} \times \mathbf{V}, \qquad \check{\lambda} = (\mathbf{F}, \eta), \tag{7.5}$$

where $\check{\mathcal{D}} \subset \mathrm{Lin}^+ \times \mathbb{R} \times \mathbf{V}$ is a domain completely determined by the domain $\tilde{\mathcal{D}}$ and therefore by the domain $\mathcal{D}$, and

$$\check{\theta}(\check{\lambda}; \mathbf{Q}) = \tilde{\theta}(\mathbf{F}, \check{\eta}(\check{\lambda}; \mathbf{Q}); \mathbf{Q}), \tag{7.6}$$

$$\check{\mathbf{S}}(\check{\lambda}; \mathbf{Q}) = \tilde{\mathbf{S}}(\mathbf{F}, \check{\eta}(\check{\lambda}; \mathbf{Q}); \mathbf{Q}), \tag{7.7}$$

$$\check{\mathbf{H}}(\check{\lambda}; \mathbf{Q}) = \tilde{\mathbf{H}}(\mathbf{F}, \check{\eta}(\check{\lambda}; \mathbf{Q}); \mathbf{Q}). \tag{7.8}$$

Applying the chain rules with respect to ε, $\mathbf{F}$, and $\mathbf{Q}$ to the identity

$$\varepsilon = \tilde{\varepsilon}(\mathbf{F}, \check{\eta}(\check{\lambda}; \mathbf{Q}); \mathbf{Q}), \qquad \check{\lambda} = (\mathbf{F}, \varepsilon), \tag{7.9}$$

and taking into account the temperature relation $(6.11)_1$, we obtain

$$\check{\theta} = (\partial_\varepsilon \check{\eta})^{-1}, \qquad \check{\mathbf{S}} = -\varrho_\kappa \check{\theta} \partial_{\mathbf{F}} \check{\eta} = -\varrho_\kappa (\partial_\varepsilon \check{\eta})^{-1} \partial_{\mathbf{F}} \check{\eta} \tag{7.10}$$

which means that the temperature functional $\check{\theta}$ and the stress tensor functional are determined by the entropy functional $\check{\eta}$.

Differentiating (7.9) with respect to $\mathbf{Q}$ and using (7.1) we get

$$\partial_{\mathbf{Q}} \tilde{\varepsilon}(\tilde{\lambda}; \mathbf{Q}) = -\theta \partial_{\mathbf{Q}} \check{\eta}(\check{\lambda}; \mathbf{Q}). \tag{7.11}$$

Thus the Dissipation Inequality (6.13) becomes

$$\varrho_\kappa \left[\partial_\varepsilon \check{\eta}(\check{\lambda}; \mathbf{Q})\right]^{-2} \partial_{\mathbf{Q}} \check{\eta}(\check{\lambda}; \mathbf{Q}) \cdot \check{\mathbf{H}}(\check{\lambda}, \mathbf{G}; \mathbf{Q}) - \mathbf{G} \cdot \mathbf{Q} \geq 0. \tag{7.12}$$

From here we have the implication

$$\mathbf{Q}\cdot\mathbf{G}=0 \;\Rightarrow\; \partial_{\mathbf{Q}}\check{\eta}(\check{\boldsymbol{\lambda}};\mathbf{Q})\cdot\check{\mathbf{H}}(\check{\boldsymbol{\lambda}},\mathbf{G};\mathbf{Q})\geq 0, \tag{7.13}$$

and in particular we get

$$\partial_{\mathbf{Q}}(\check{\eta};\mathbf{Q})\cdot\check{\mathbf{H}}(\boldsymbol{\lambda},\mathbf{0};\mathbf{Q})\geq 0. \tag{7.14}$$

DEFINITION 7.1. *The state* $(\check{\boldsymbol{\lambda}}_0,\mathbf{G}_0;\mathbf{Q}_0)\in\check{\mathcal{D}}\times\mathbf{V}$, $\check{\boldsymbol{\lambda}}_0=(\mathbf{F}_0,\varepsilon_0)$, *is called an* ***isoenergetic*** *E.S. at constant strain* $\mathbf{F}_0$ *for the material point* $X\in\mathcal{B}$ *if*

$$\check{\mathbf{H}}(\check{\boldsymbol{\lambda}}_0,\mathbf{G}_0;\mathbf{Q}_0)=\mathbf{0},\qquad \mathbf{G}_0\cdot\mathbf{Q}_0=\mathbf{0}. \tag{7.15}$$

The state $(\check{\boldsymbol{\lambda}},\mathbf{0};\mathbf{Q}_0)\in\check{\mathcal{D}}\times\mathbf{V}$ is a *strictly isoenergetic* E.S. at *constant strain* $\mathbf{F}_0$ for the material point $X\in\mathcal{B}$ if

$$\check{\mathbf{H}}(\check{\boldsymbol{\lambda}},\mathbf{0};\mathbf{Q}_0)=\mathbf{0}. \tag{7.16}$$

We will note by $\check{\mathcal{E}}$ the *set of isoenergetic* E.S. and by $\check{\mathcal{E}}_0\subset\check{\mathcal{E}}$ the *subset of strictly isoenergetic* E. S. of the material point $X\in\mathcal{B}$.

REMARK 7.1. From (7.8) it follows that if $(\tilde{\boldsymbol{\lambda}}_0,\mathbf{G}_0,\mathbf{Q}_0)\in\tilde{\mathcal{D}}\times\mathbf{V}$, $\tilde{\boldsymbol{\lambda}}_0=(\mathbf{F}_0,\eta_0)$, and $(\check{\boldsymbol{\lambda}},\mathbf{G}_0;\mathbf{Q}_0)\in\check{\mathcal{D}}\times\mathbf{V}$, $\check{\boldsymbol{\lambda}}_0=(\mathbf{F}_0,\varepsilon_0)$ are two states related by $\eta_0=\check{\eta}(\check{\boldsymbol{\lambda}};\mathbf{Q}_0)$ then

$$(\tilde{\boldsymbol{\lambda}},\mathbf{G}_0;\mathbf{Q}_0)\in\tilde{\mathcal{E}}\;\Leftrightarrow\;(\check{\boldsymbol{\lambda}},\mathbf{G}_0;\mathbf{Q}_0)\in\check{\mathcal{E}}. \tag{7.17}$$

DEFINITION 7.2. *If* $(\check{\boldsymbol{\lambda}}_0,\mathbf{G}_0;\mathbf{Q}_0)\in\check{\mathcal{E}}$ *then the set* $\check{D}(\check{\boldsymbol{\lambda}}_0,\mathbf{G}_0;\mathbf{Q}_0)\subset\mathbf{V}$ *of vectors* $\mathbf{Q}^*\in\mathbf{V}$ *for which the solution* $\mathbf{Q}=\mathbf{Q}(t)$ *of the Cauchy problem*

$$\dot{\mathbf{Q}}=\hat{\mathbf{H}}(\check{\boldsymbol{\lambda}}_0,\mathbf{G}_0;\mathbf{Q}),\qquad \mathbf{Q}(0)=\mathbf{Q}^* \tag{7.18}$$

is defined on $[0,\infty)$ *and satisfies the condition*

$$\lim_{t\to\infty}\mathbf{Q}(t)=\mathbf{Q}_0\,, \tag{7.19}$$

is called the ***domain of attraction*** *of the E.S.* $(\check{\boldsymbol{\lambda}}_0,\mathbf{G}_0;\mathbf{Q}_0)$.

The isoenergetic E.S. $(\check{\boldsymbol{\lambda}}_0,\mathbf{G}_0;\mathbf{Q}_0)$ is said to be *asymptotically stable* if $\mathbf{Q}_0$ is an interior point of the set $\check{D}(\check{\boldsymbol{\lambda}},\mathbf{G}_0;\mathbf{Q}_0)$.

The isoenergetic E.S. $(\check{\boldsymbol{\lambda}},\mathbf{G}_0;\mathbf{Q}_0)$ will be referred to as Lyapunov stable if for each $\varepsilon>0$ there exists a $\delta=\delta(\varepsilon)>0$ such that every solution $\mathbf{Q}=\mathbf{Q}(t)$ of the differential system $(7.18)_1$ with $|\mathbf{Q}(0)-\mathbf{Q}_0|<\delta$ satisfies $|\mathbf{Q}(t)-\mathbf{Q}_0<\varepsilon$ for all $t\geq 0$.

The following three theorems are counterparts of theorems (4.2)–(4.4) and (6.2)–(6.4).

THEOREM 7.1.
1) *If* $(\check{\boldsymbol{\lambda}}_0, \mathbf{G}_0; \mathbf{Q}_0) \in \check{\mathcal{E}}$, $\check{\boldsymbol{\lambda}}_0 = (\mathbf{F}_0, \varepsilon_0)$, *then*

$$\check{\eta}(\check{\boldsymbol{\lambda}}_0; \mathbf{Q}) \leq \check{\eta}(\check{\boldsymbol{\lambda}}_0; \mathbf{Q}_0), \qquad \mathbf{Q} \in \check{D}(\check{\boldsymbol{\lambda}}_0, \mathbf{G}_0; \mathbf{Q}_0); \tag{7.20}$$

2) *if* $(\check{\boldsymbol{\lambda}}_0, \mathbf{G}_0; \mathbf{Q}_0) \in \check{\mathcal{E}}$ *is asymptotically stable then the preceding inequality holds in a neighbourhood* $U(\mathbf{Q}_0) \subset \check{D}(\check{\boldsymbol{\lambda}}_0, \mathbf{G}_0; \mathbf{Q}_0)$ *of the point* $\mathbf{Q}_0$ *and there exists* $\check{\nu}_0 \in \mathbb{R}$ *such that*

$$\partial_{\mathbf{Q}} \check{\eta}(\check{\boldsymbol{\lambda}}_0; \mathbf{Q}_0) = \check{\nu}_0 \mathbf{G}_0 ; \tag{7.21}$$

3) *if* $(\check{\boldsymbol{\lambda}}_0, \mathbf{0}; \mathbf{Q}_0) \in \check{\mathcal{E}}_0$ *and for a neighbourhood* $U(\mathbf{Q}_0)$ *of* $\mathbf{Q}_0$ *we have*

$$\check{\eta}(\check{\boldsymbol{\lambda}}_0; \mathbf{Q}) < \check{\eta}(\check{\boldsymbol{\lambda}}_0; \mathbf{Q}_0), \qquad \mathbf{Q}_0 \neq \mathbf{Q} \in U(\mathbf{Q}_0) \subset \check{D}(\check{\boldsymbol{\lambda}}_0, \mathbf{G}_0; \mathbf{Q}_0), \tag{7.22}$$

then $(\check{\boldsymbol{\lambda}}_0, \mathbf{0}; \mathbf{Q}_0)$ *is Lyapunov stable.*

REMARK 7.2. From (7.8), (7.11), and (6.30) we come to the conclusion that the thermoelastic material is strictly dissipative if and only if

$$\mathbf{G}_0 \cdot \mathbf{Q} = 0 \quad \text{and} \quad (\check{\boldsymbol{\lambda}}_0, \mathbf{G}_0; \mathbf{Q}) \notin \check{\mathcal{E}} \;\Rightarrow\; \partial_{\mathbf{Q}} \check{\eta}(\check{\boldsymbol{\lambda}}_0; \mathbf{Q}) \cdot \check{\mathbf{H}}(\check{\boldsymbol{\lambda}}_0, \mathbf{G}_0; \mathbf{Q}) > 0. \tag{7.23}$$

THEOREM 7.2. *If* $(\check{\boldsymbol{\lambda}}_0, \mathbf{G}_0; \mathbf{Q}_0) \in \check{\mathcal{E}}$ *is asymptotically stable and there exists a neighbourhood* $U(\mathbf{Q}_0)$ *of* $\mathbf{Q}_0$, $U(\mathbf{Q}_0) \subset \check{D}(\check{\boldsymbol{\lambda}}_0, \mathbf{G}_0; \mathbf{Q}_0)$, *such that the inequality in* (7.22) *holds on* $U(\mathbf{Q}_0) \backslash \{\mathbf{Q}_0\}$, *then*

$$\check{\eta}(\check{\boldsymbol{\lambda}}_0; \mathbf{Q}) < \check{\eta}(\check{\boldsymbol{\lambda}}_0; \mathbf{Q}_0), \qquad \mathbf{Q}_0 \neq \mathbf{Q} \in U(\mathbf{Q}_0). \tag{7.24}$$

THEOREM 7.3. *If* $(\check{\boldsymbol{\lambda}}_0, \mathbf{0}; \mathbf{Q}_0) \in \check{\mathcal{E}}_0$ *and*

$$\partial_{\mathbf{Q}} \check{\eta}(\check{\boldsymbol{\lambda}}_0; \mathbf{Q}) \cdot \check{\mathbf{H}}(\check{\boldsymbol{\lambda}}_0, \mathbf{0}; \mathbf{Q}) > 0, \qquad \mathbf{Q}_0 \neq \mathbf{Q} \in U(\mathbf{Q}_0), \tag{7.25}$$

$U(\mathbf{Q}_0)$ *being a neighbourhood of* $\mathbf{Q}_0$, *then*

1) $(\check{\boldsymbol{\lambda}}_0, \mathbf{0}; \mathbf{Q}_0)$ *is asymptotically stable if and only if* (7.24) *holds and*

2) *if* $(\check{\boldsymbol{\lambda}}_0, \mathbf{0}; \mathbf{Q}_0)$ *is asymptotically stable then it is Lyapunov stable.*

REMARK 7.3. In virtue of Theorems 7.1 and 7.2 it results that if the thermoelastic material is strictly dissipative and $(\check{\boldsymbol{\lambda}}_0, \mathbf{0}; \mathbf{Q}_0) \in \check{\mathcal{E}}_0$ is asymptotically stable, then the inequality (7.24) holds and $(\check{\boldsymbol{\lambda}}_0, \mathbf{0}; \mathbf{Q}_0)$ is a Lyapunov stable E.S.

Now, by using arguments similar to those in Sec. 9 of [1] we prove the following theorem giving some relations between isothermal, isentropic and isoenergetic asymptotic stability of an E.S.

THEOREM 7.4. *Let* $(\boldsymbol{\lambda}_0, \mathbf{0}; \mathbf{Q}_0) \in \mathcal{E}_0$, $\boldsymbol{\lambda}_0 = (\mathbf{F}_0, \theta_0)$, *be a strictly isothermal E.S. at constant strain* $\mathbf{F}_0$ *for the material point* $X \in \mathcal{B}$, *and let us suppose that*

$$\eta_0 = \hat{\eta}_0(\boldsymbol{\lambda}_0; \mathbf{Q}_0); \qquad \varepsilon_0 = \tilde{\varepsilon}(\tilde{\lambda}_0; \mathbf{Q}_0), \qquad \tilde{\lambda}_0 = (\mathbf{F}_0, \eta_0); \tag{7.26}$$

1) *if the inequalities* (4.24) *and* (6.32) *hold, then the asymptotic stability of* $(\boldsymbol{\lambda}_0, \mathbf{0}; \mathbf{Q}_0)$ *entails the asymptotic stability of* $(\tilde{\lambda}_0, \mathbf{0}; \mathbf{Q}_0) \in \tilde{\mathcal{E}}_0$;

2) *if the inequalities* (6.32) *and* (7.25) *hold, then* $(\tilde{\boldsymbol{\lambda}}_0, \mathbf{0}; \mathbf{Q}_0) \in \tilde{\mathcal{E}}_0$ *is asymptotically stable if and only if* $(\check{\boldsymbol{\lambda}}_0, \mathbf{0}; \mathbf{Q}_0) \in \check{\mathcal{E}}_0$, $\check{\boldsymbol{\lambda}}_0 = (\mathbf{F}_0, \varepsilon_0)$ *is asymptotically stable.*

P r o o f.

1. Making use of the assumption

$$c = \partial_\theta \hat{\varepsilon}(\boldsymbol{\lambda}; \mathbf{Q}) = \theta \partial_\theta \hat{\eta}(\tilde{\lambda}; \mathbf{Q}) > 0$$

from $(2.15)_1$ we obtain

$$\partial_\theta^2 \hat{\psi}(\boldsymbol{\lambda}; \mathbf{Q}) < 0, \tag{7.27}$$

due to the hypothesis that $\hat{\psi}$ is twice continuous differentiable.

Writing the second order Taylor's formula with respect to the variable θ and using again $(2.15)_1$ we have

$$\hat{\psi}(\mathbf{F}, \theta, \mathbf{Q}) - \hat{\psi}(\mathbf{F}, \theta'; \mathbf{Q}) + (\theta - \theta')\hat{\eta}(\mathbf{F}, \theta'; \mathbf{Q}) = 1/2(\theta - \theta')^2 \partial_\theta^2 \hat{\psi}(\mathbf{F}, \theta_*, \mathbf{Q}),$$

where $\theta_* = \theta_*(\mathbf{F}, \theta, \theta', \mathbf{Q}) \in (\theta, \theta')$, and in view of (8.27) we get

$$\text{(a)} \qquad \hat{\psi}(\mathbf{F}, \theta'; \mathbf{Q}) \geq \hat{\psi}(\mathbf{F}, \theta; \mathbf{Q}) + (\theta - \theta')\hat{\eta}(\mathbf{F}, \theta'; \mathbf{Q}).$$

From (6.5), (6.8), and $(7.26)_1$ we get

$$\text{(b)} \qquad \tilde{\varepsilon}(\tilde{\boldsymbol{\lambda}}_0; \mathbf{Q}) - \tilde{\varepsilon}(\tilde{\boldsymbol{\lambda}}_0; \mathbf{Q}_0) = \left[\hat{\psi}(\mathbf{F}_0, \tilde{\theta}(\tilde{\boldsymbol{\lambda}}_0; \mathbf{Q}); \mathbf{Q}) - \hat{\psi}(\boldsymbol{\lambda}_0; \mathbf{Q}_0)\right] + \left[\tilde{\theta}(\boldsymbol{\lambda}_0; \mathbf{Q}) - \theta_0\right] \eta_0 .$$

Because $\tilde{\theta}(\mathbf{F}, \cdot; \mathbf{Q})$ is the inverse of $\hat{\eta}(\mathbf{F}, \cdot; \mathbf{Q})$ we have $\hat{\eta}(\mathbf{F}, \tilde{\theta}(\tilde{\boldsymbol{\lambda}}_0; \mathbf{Q}); \mathbf{Q}) = \eta_0$ and, in view of (a) and (b), we obtain

$$\tilde{\varepsilon}(\tilde{\boldsymbol{\lambda}}_0; \mathbf{Q}) - \varepsilon_0 = \tilde{\varepsilon}(\tilde{\boldsymbol{\lambda}}_0; \mathbf{Q}) - \tilde{\varepsilon}(\tilde{\boldsymbol{\lambda}}_0; \mathbf{Q}_0) \geq \hat{\psi}(\boldsymbol{\lambda}_0; \mathbf{Q}) - \hat{\psi}(\boldsymbol{\lambda}_0; \mathbf{Q}_0). \tag{7.28}$$

Our hypotheses, Theorem 4.3, and (7.28) imply that if $(\boldsymbol{\lambda}_0, \mathbf{0}; \mathbf{Q}_0) \subset \mathcal{E}_0$ is asymptotically stable then it holds (6.27). Now by Theorem (6.4) we have that $(\tilde{\boldsymbol{\lambda}}_0, \mathbf{0}; \mathbf{Q}_0) \in \tilde{\mathcal{E}}_0$ is asymptotically stable. The conclusion 2 of the same Theorem 6.4 shows that $(\boldsymbol{\lambda}_0, \mathbf{0}; \mathbf{Q}_0) \in \mathcal{E}_0$ is even Lyapunov stable.

2. From $(7.10)_1$ it follows that the function $\check{\eta}(\mathbf{F}, \cdot; \mathbf{Q})$, which is inverse of $\tilde{\varepsilon}(\mathbf{F}, \cdot; \mathbf{Q})$, is a strictly increasing function and therefore we have

$$\varepsilon_0 < \tilde{\varepsilon}(\tilde{\boldsymbol{\lambda}}_0; \mathbf{Q}) \Leftrightarrow \eta_0 = \check{\eta}(\check{\boldsymbol{\lambda}}_0; \mathbf{Q}) < \check{\eta}(\mathbf{F}_0, \tilde{\varepsilon}(\tilde{\boldsymbol{\lambda}}_0; \mathbf{Q}); \mathbf{Q}). \tag{7.29}$$

Now, the desired result is an immediate consequence of the Conclusion 1 of the Theorem (6.4), of the equivalence (7.29), and of the Conclusion 1 of the Theorem 7.3.

REMARK 7.4. Combining this result with the point 2 of Theorems 6.4 and 7.3 it follows that if $(\lambda_0, \mathbf{0}; \mathbf{Q}_0)$ is an isentropic (resp. isoenergetic) asymptotically stable E.S., then it is an isoenergetic (resp. isentropic) Lyapunov stable E.S.

The counterpart of Theorems (3.1) and (6.1) is the following

THEOREM 7.5. *If the functional $\check{\eta}$ is twice continuously differentiable and the heat flux evolution equation* (7.5) *is of the Cattaneo kind*

$$\check{\mathbf{T}}(\check{\lambda})\,\dot{\mathbf{Q}} + \mathbf{Q} = -\check{\mathbf{K}}(\check{\lambda})\mathbf{G}, \tag{7.30}$$

where the second order tensor functions $\check{\mathbf{T}}$ and $\check{\mathbf{K}}$ are invertible, then the Dissipation Inequality (7.12) is satisfied if and only if on $\check{\mathcal{D}} \times \mathbf{V}$

1. $\mathbf{K}(\check{\lambda})$ *is positive definite and*
2. *The second order tensor function*

$$\check{\lambda} \to \check{\mathbf{Z}}(\check{\lambda}) = \left[\check{\mathbf{K}}(\check{\lambda})\right]^{-1} \check{\mathbf{T}}(\check{\lambda}) \in \mathrm{Lin}, \qquad \check{\lambda} = (\mathbf{F}, \varepsilon), \tag{7.31}$$

is given by

$$\check{\mathbf{Z}} = \varrho_\kappa \left[\partial_\varepsilon \check{\eta} \partial_{\mathbf{Q}}^2 \check{\eta} - 2\partial_{\varepsilon\mathbf{Q}} \check{\eta} \otimes \partial_{\mathbf{Q}} \check{\eta}\right] (\partial_\varepsilon \check{\eta})^{-3}. \tag{7.32}$$

The proof of the theorem follows by using the same line of arguments as in the proof of Theorem (6.1).

References

1. B.D. COLEMAN and M.E. GURTIN, *Thermodynamics with internal state variables*, J. Chem. Phys., **47**, 597–613, 1967.
2. C. CATTANEO, *Sulla conduzione del calore*, Atti. Sem. Mat. Fis. Univ. Modena, **3**, 83–101, 1948.
3. C.A. TRUESDELL, *A first course in rational continuum mechanics*, The Johns Hopkins University, Baltimore, Md. 1973.
4. B.D. COLEMAN and W. NOLL, *The thermodynamics of elastic materials with heat conduction and viscosity*, Arch. Rational Mech. Anal., **13**, 167–178, 1963.
5. B.D. COLEMAN and V.J. MIZEL, *Thermodynamics and departures from Fourier's law of heat conduction*, Arch. Rational Mech. Anal., **13**, 245–261, 1963.
6. V. BARBU, *Ecuaţii diferentiale* [in Romanian], Editura Junimea, Iaşi 1985.
7. C. CORDUNEANU, *Principles of differential and integral equations*, Chelsea Publishing Company, The Bronx, New York 1977.
8. T.S. ÖNCÜ and T.B. MOODIE, *On constitutive relations for second sound in elastic solids*, Arch. Rational Mech. Anal., **121**, 87–99, 1992.

9. B.D. COLEMAN, M. FABRIZIO and D.R. OWEN, *On the thermodynamics of second sound in dielectric crystals*, Arch. Rational Mech. Anal., **80**, 135–158, 1982.

10. GH. GR. CIOBANU, *Some results of the thermoelasticity theory with heat flux evolution equation*, Rev. Roum. Math. Pures Appl., **40**, 301–324, 1995.

SEMINARUL MATEMATIC "AL. MYLLER",
UNIVERSITATEA "AL. I. CUZA", IAȘI, ROMANIA.

Received March 13, 1996; *new version June* 10, 1996.

Arch. Mech., 48, 6, pp. 1011–1024, Warszawa 1996

Analysis of stress distribution in a thin rectangular plate by the method of caustics

J. WANG, R. C. BATRA (BLACKSBURG) and K. ISOGIMI (TSU)

We discuss some characteristics of caustics in a rectangular plate loaded by distributed in-plane loads on a part of two opposite edges with the other two edges kept traction-free. It is assumed that plane state of stress prevails in the plate. The theoretical developments are valid for an arbitrary location of the reflective plane within the plate. A good agreement is found between the computed and observed caustics. A simple inverse problem of determining the intensity of the distributed load from the size of caustics is also investigated.

1. Introduction

The method of caustics was first proposed by Manogg [1] and has been employed by Theocaris [2, 3] and Kalthoff [4] to ascertain stresses at singular points. The method is widely used in fracture mechanics to determine stress intensity factors under Modes I, II and III loading [5]. Here we apply this method to another kind of singular problem, namely, distributed load acting on a part of the width of a plate; this is a simplified model of loads acting on a cutting tool. The deformations and stresses will be singular at points where the distributed load jumps from zero to a finite value or vice-versa. Here we consider a thin plate subjected to in-plane distributed loads at two opposite edges with the other two edges traction-free and assume that a plane stress state prevails in the plate. We use the method of caustics to transform the stress singularity to an optical singularity and determine the stress distribution at singular points. It is assumed that the intensity of the distributed load is such that the linear elasticity theory can be used to describe deformations of the plate. The work is motivated by the desire to ascertain stresses induced in a cutting tool; however no machining problem is studied herein.

2. Analytical developments of caustics

Referring to Fig. 1, consider parallel rays impinging upon the plane surface of a transparent, homogeneous, and both mechanically and optically isotropic rectangular plate subjected to in-plane distributed loads on two opposite edges. The direction of the light reflected from a point on the incident surface will depend upon its deformations. This light when projected on a screen, will form caustics whose patterns will depend upon the state of stress at points on the incident surface. If the location of the plane from which the incident light is

reflected can be varied, then the state of stress at points within the body can also be ascertained by the method of caustics.

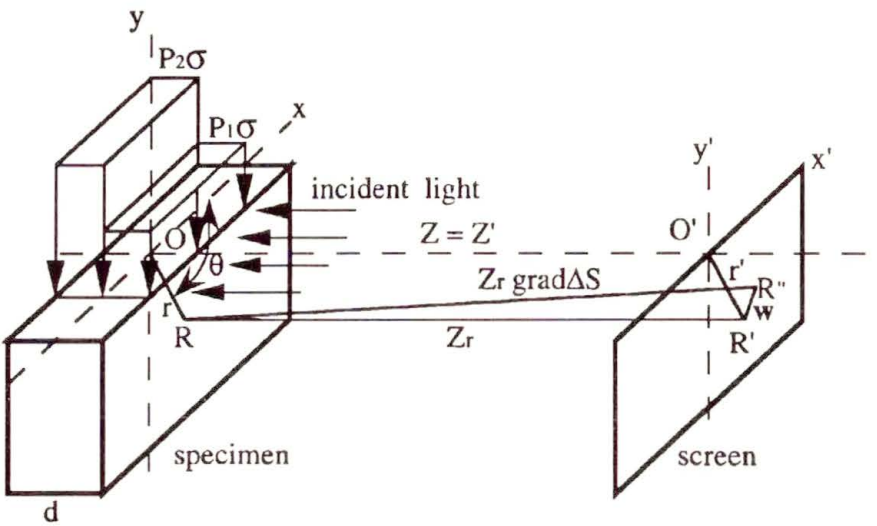

FIG. 1. A schematic sketch of the problem studied.

2.1. Optical path difference

We assume that the distributed load on the edge of a plate can be approximated by a series of step loads as shown in Fig. 2. Herein we assume the distributed load to be such that points on the central plane of the plate do not move laterally. Also with the plate divided into several layers with thickness of each layer equaling the thickness of the edge over which the load intensity is constant, we presume that a plane state of stress exists within each layer. Let the plate be divided into n layers of thicknesses $d_1, d_2, \ldots, d_N$ and in-plane loads acting on their edges equal $P_1\sigma, P_2\sigma, \ldots, P_N\sigma$, respectively. Under the action of these loads, the thickness d_i and refractive index n_i of the i-th layer $(1 \leq i \leq N)$ will change by Δd_i and Δn_i, respectively. We designate by subscripts c and m the central surface of the plate and the plane from which light is reflected.

A lateral displacement of a material point in the direction of increasing optical path is taken as positive. Thus under a compressive edge load, the lateral displacement of the front surface of the plate is $-\Delta d_f$ and that of the rear surface equals $+\Delta d_r$. Of course, as assumed above, the lateral displacement of the central surface is zero.

As shown in Fig. 2, we consider a reflective plane located at a distance of kd $(0 \leq k \leq 1)$ from the front surface of the plate. Measuring distances from the deformed position of the front surface, the optical path S_1 to the reflective plane in the unstressed reference configuration is given by

$$S_1 = 2(\Delta d_f + nkd), \tag{2.1}$$

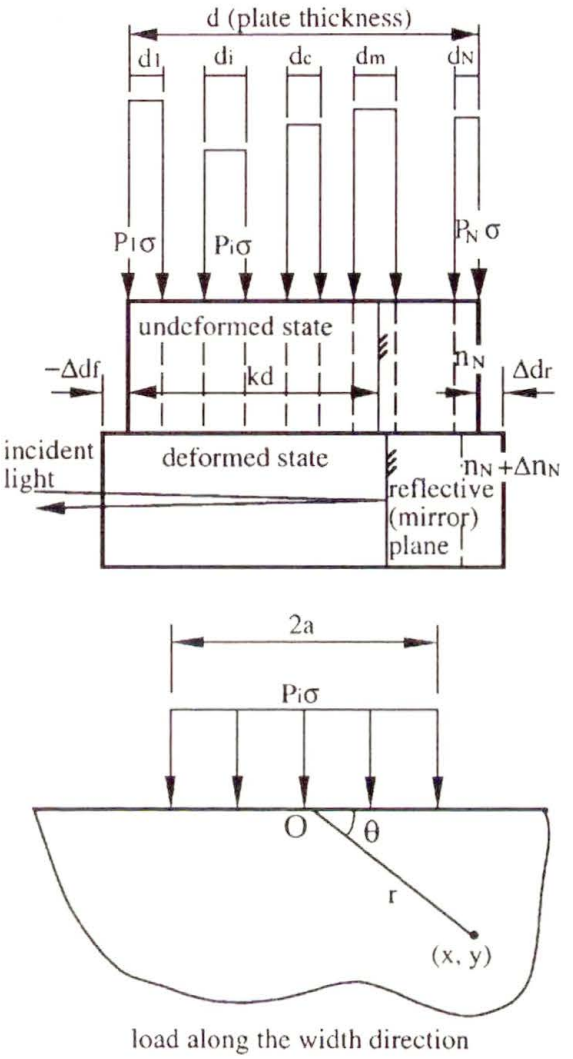

FIG. 2. a) Load distribution along the thickness of the plate; b) load distribution along the width of the plate.

where n is the refractive index of the plate material in the unstressed state and the refractive index of air equals 1. After the load is applied, the optical path will change to S_2 given by

$$S_2 = 2\left[\sum_{i=1}^{m-1}(n+\Delta n_i)(d_i+\Delta d_i) + (n+\Delta n_m)\frac{1}{d_m}\left(kd - \sum_{i=1}^{m-1} d_i\right)(d_m+\Delta d_m)\right]. \tag{2.2}$$

In writing equation (2.2) we have assumed that the reflective plane (or mirror) is located in the m-th layer. Subtracting (2.1) from (2.2) and neglecting terms of second order in Δd and/or Δn, we obtain the following formula for the optical path difference

$$\Delta S = 2\left[\sum_{i=1}^{m-1}(\Delta n_i d_i + n\Delta d_i) + \left(\Delta n_m + \frac{n}{d_m}\Delta d_m\right)\left(kd - \sum_{i=1}^{m-1} d_i\right) - \Delta d_f\right]. \tag{2.3}$$

The variation in the thickness of the i-th layer subjected to in-plane edge loads $P_i\sigma$ can be expressed as

$$\Delta d_i = -\frac{\nu}{E} P_i d_i(\sigma_1 + \sigma_2), \tag{2.4}$$

where E and ν equal, respectively, Young's modulus and Poisson's ratio for the material of the plate, and σ_1 and σ_2 are the principal stresses induced at a point in the plate layer subjected to in-plane surface traction σ (recall that the third principal stress is zero because of the assumption of plane stress). Since the central plane is assumed not to move laterally, therefore, the displacement Δd_f of the front surface is given by

$$\Delta d_f = -\frac{\nu}{E}\left[\sum_{i=1}^{c} P_i d_i - P_c\left(\sum_{i=1}^{c} d_i - \frac{d}{2}\right)\right](\sigma_1 + \sigma_2), \tag{2.5}$$

where it has been assumed that the central plane lies in the c-th layer. For an optically isotropic i-th layer, the change in the refractive index at a point is given by

$$\Delta n_i = AP_i(\sigma_1 + \sigma_2), \tag{2.6}$$

where A is the optical constant for the plate material. Substitution from (2.4), (2.5) and (2.6) into (2.3) results in the following expression for ΔS:

$$\Delta S = K(\sigma_1 + \sigma_2), \tag{2.7}$$

where

$$K = 2\left\{\left(A - n\frac{\nu}{E}\right)\sum_{i=1}^{m-1} P_i d_i + \left(kd - \sum_{i=1}^{m} d_i\right)\left(AP_m - nP_m\frac{\nu}{E}\right) + \frac{\nu}{E}\left[\sum_{i=1}^{c} P_i d_i - P_c\left(\sum_{i=1}^{c} d_i - \frac{d}{2}\right)\right]\right\}. \tag{2.8}$$

2.2. Equation of caustics

Referring to Fig. 1, let R' be the image of R on a plane screen located at a distance Z_r from R when there is no load applied to the plate, and R'' be the image of R when the plate has been deformed by in-plane loads applied at the two opposite edges. The vector $\mathbf{w} = \overrightarrow{R'R''}$ is given by [6]

$$\mathbf{w} = Z_r \operatorname{grad} \Delta S = K Z_r \operatorname{grad} (\sigma_1 + \sigma_2) \tag{2.9}$$

where we have used (2.7).

Let the stress state at an arbitrary point in the plate with two opposite edges subjected to uniform in-plane tractions σ be described by the complex-valued function $\phi(z)$ of the complex variable $z = x + iy$. Then

$$4 \operatorname{Re} (\phi(z)) = \sigma_1 + \sigma_2, \tag{2.10}$$

where $\operatorname{Re}(\phi(z))$ denotes the real part of ϕ. In the complex variable notation, Eq. (2.9) becomes

$$w = 4 K Z_r \overline{\phi}'(z), \tag{2.11}$$

where $\overline{\phi}$ denotes the complex conjugate of ϕ. Assuming that the origin O of the rectangular Cartesian coordinate system is located on the top surface of the undeformed plate and the applied tractions are distributed symmetrically about it, O' is its image on the screen and $\mathbf{r} = \overrightarrow{OR}$, then

$$\mathbf{W} = \overrightarrow{O'R''} = \mathbf{w} + \mathbf{r}. \tag{2.12}$$

However, when the incident light is not a parallel beam but a convergent beam, then Eq. (2.12) is modified to

$$\mathbf{W} = \mathbf{w} + \lambda \mathbf{r}, \tag{2.13}$$

where

$$\lambda = (Z_i - Z_r)/Z_i, \tag{2.14}$$

and Z_i is the distance of the focal point of the light from the reflective plane (cf. Fig. 3). Of course, for a parallel incident beam, $\lambda = 1$.

In the complex plane, Eqs. (2.11) and (2.13) yield

$$W = x' + iy' = \lambda(x + iy) + 4 K Z_r \overline{\phi}'(z) \tag{2.15}$$

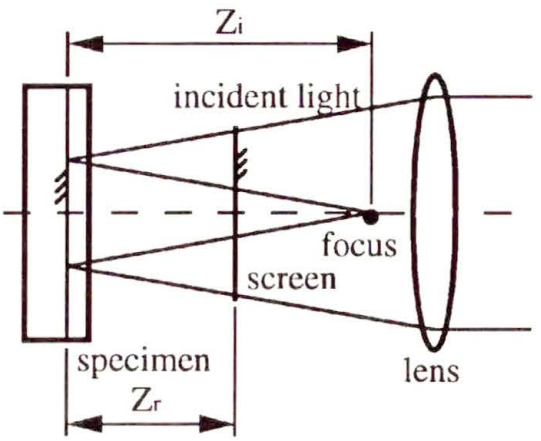

FIG. 3. A schematic sketch of the convergent light beam and illustrations of distances Z_i and Z_r.

and the condition

$$J = \frac{\partial(x', y')}{\partial(x, y)} = 0 \tag{2.16}$$

for the existence of a singular point becomes

$$\left| \frac{4}{\lambda} K Z_r \phi''(z) \right| = 1. \tag{2.17}$$

Thus the caustic curve is obtained from Eqs. (2.17) and (2.15).

For the load distribution depicted in Fig. 2, Eq. (2.17) gives

$$AB = 4arC/\lambda, \tag{2.18}$$

where

$$\begin{aligned} A &= r^2 + a^2 - 2ar\cos\theta, \\ B &= r^2 + a^2 + 2ar\cos\theta, \\ C &= 2\sigma K Z_r/\pi, \end{aligned} \tag{2.19}$$

(r, θ) are the cylindrical polar coordinates of the point (x, y) (e.g. see Fig. 2), and $2a$ is the width of the loaded region. Equation (2.15) describing a caustic curve can be written as

$$\begin{aligned} x' &= \lambda r \left(\cos\theta - \frac{1}{2}\sin 2\theta \right), \\ y' &= \lambda r \left(\sin\theta - \frac{1}{2}\cos 2\theta - \frac{1}{2}\frac{a^2}{r^2} \right). \end{aligned} \tag{2.20}$$

We identify the size of a caustic curve with the maximum horizontal distance, $D = L_{\max}$, between any two points on the curve. For the load applied symmetrically about O, it is reasonable to assume that the caustic curve is symmetrical about O'. Thus if points (r_0, θ_0) and $(r_0, -\theta_0)$ on the caustic curve determine D, then

$$D = L_{\max} = br_0, \tag{2.21}$$

where

$$b = 2\lambda\left(\cos\theta_0 - \frac{1}{2}\sin 2\theta_0\right). \tag{2.22}$$

Equations (2.18) and (2.21) give the following relation between the applied uniform traction σ and the size of a caustic.

$$\sigma = \frac{\pi\lambda}{8KZ_r a}\frac{D}{b}\left[\left(\frac{D}{b} + \frac{b}{D}a^2\right)^2 - 4a^2\cos^2\theta_0\right]. \tag{2.23}$$

Knowing D, nonlinear equations (2.18) and (2.21) can be solved iteratively for r_0 and θ_0, and then σ can be evaluated from Eq. (2.23). Subsequently, the stress distribution at any point in the plate can be ascertained.

3. Experimental method

A schematic sketch of the experimental set-up is shown in Fig. 4. All of the components depicted in the figure, except for the video monitor and recording equipment, are mounted on a vibration-isolated table. A laser light from the

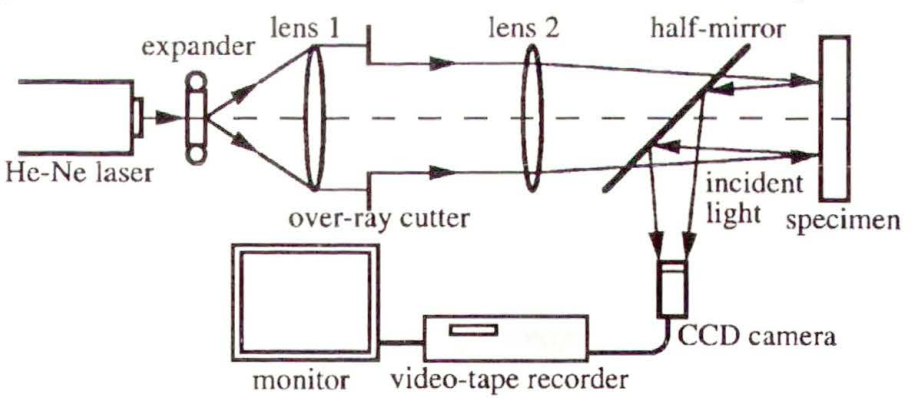

FIG. 4. A layout of the experimental apparatus.

source is expanded by the expander, changed into collimated light by lens 1 and into a convergent beam by lens 2. The region of interest with singular stress distribution in the object is illuminated with the laser light through a half-mirror.

Light falling from the object and the half-mirror is received by a CCD camera, recorded on a video-tape and monitored. The dimension ratio λ, defined by Eq. (2.14), of the convergent light is determined and adjusted by altering the positions of lens 2, the half-mirror and the CCD camera.

The specimen length, width and thickness equal, respectively, 63 mm, 45 mm and 6 mm and it is made of transparent acrylate. The reflective surface of the specimen is formed by vapor depositing a layer of aluminum film on either the front or the rear surface of the plate.

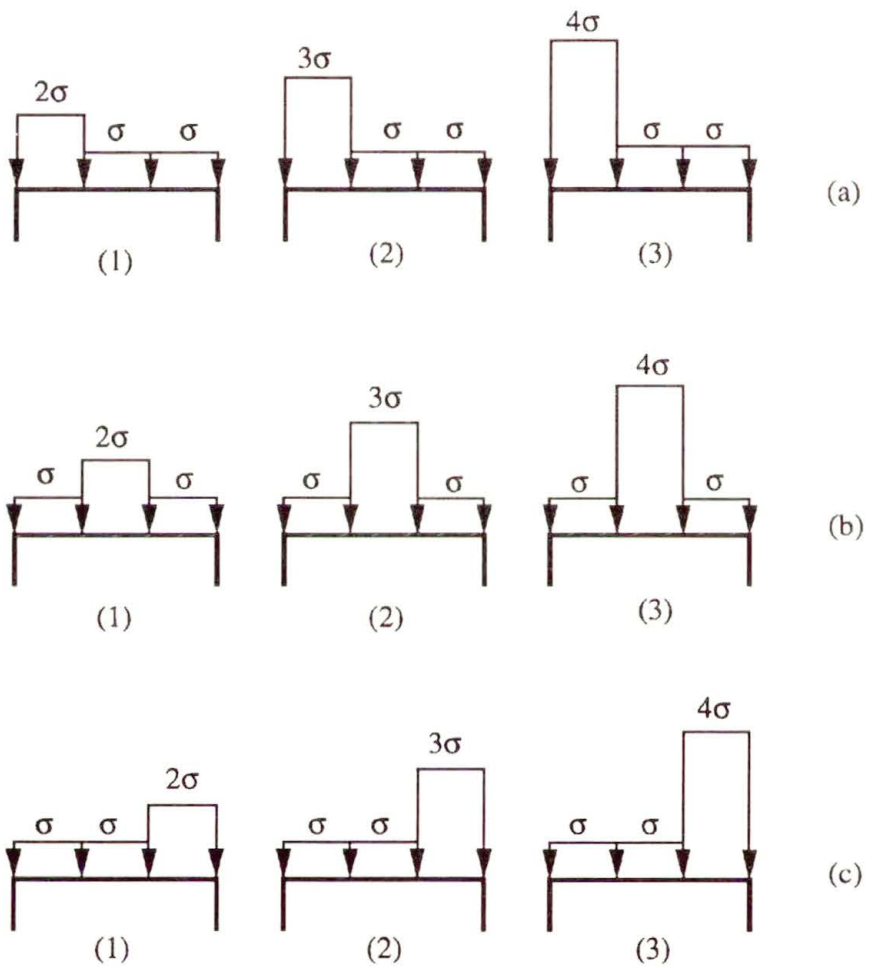

FIG. 5. Different load distributions considered.

Nine different loads described below and shown in Fig. 5 were examined. The plate thickness is divided into three equal parts; on each part the tractions are uniformly distributed and span over the middle 4.5 mm width of the plate.

4. Comparison of experimental and computed results

Figure 6 shows the experimental and computed caustic curves for the three load distributions of group (a) of Fig. 5; the top, middle and bottom figures correspond respectively to load distributions 1, 2 and 3. Unless otherwise noted, the reflective plane is located on the front surface of the plate. The computed results are obtained by assigning following values to the material parameters: $A = -0.55 \times 10^{-18}\,\mathrm{m^2/N}$, $n = 1.491$, $E = 1.6\,\mathrm{GPa}$, $\nu = 0.399$. The experimentally obtained caustic curves are not completely symmetric about the centerline probably because of the slight asymmetry in the externally applied tractions. However, the experimental and computed curves look similar implying that the assumptions made in deriving the equation for a caustic curve are reasonable. In Fig. 7 we have plotted the computed and experimental values of the size of the

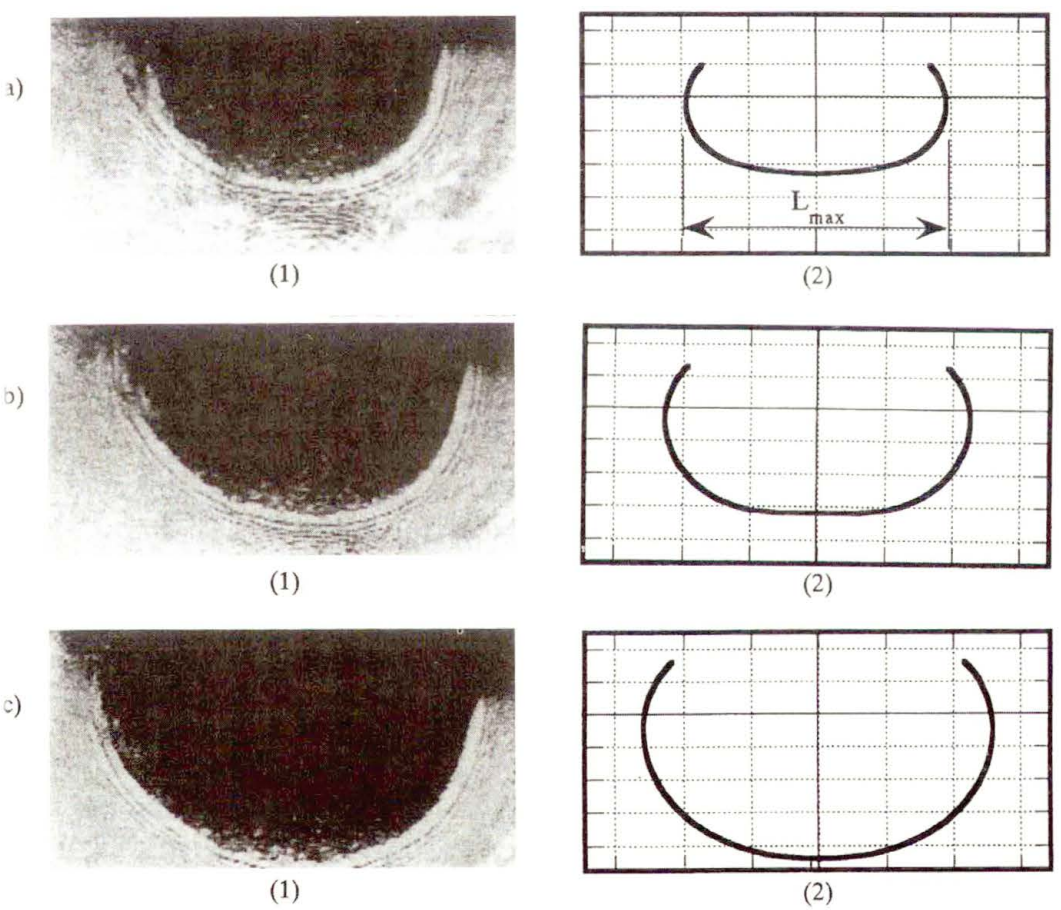

FIG. 6. Experimental (1) and computed (2) caustic curves for the three load distributions of group (a) of Fig. 5 with the reflective plane located on the front surface of the plate.

caustic curves for the load distribution of group (a) versus the maximum traction; it is clear that the two sets of values agree well with each other. The plot of the optical path difference computed from Eq. (2.7) shows that there is an affine relationship between it and the maximum traction.

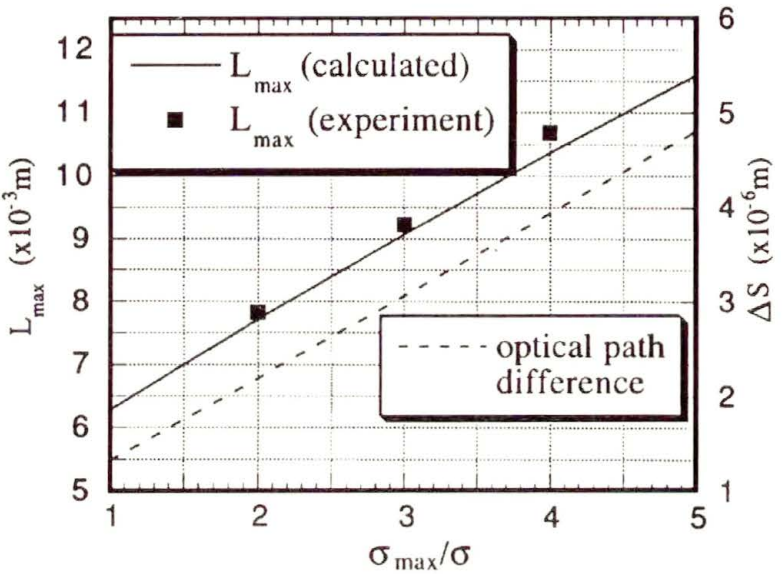

FIG. 7. Dependence of the size of the caustic curve and the computed optical path difference upon the magnitude of the maximum load.

The effect of the location of the maximum traction on the experimental and computed caustic curves is illustrated in Fig. 8 where the two sets of caustics obtained by applying the maximum traction ($= 4\sigma$) on the front layer, middle layer and the rear layer (i.e. loading 3 of groups (a), (b) and (c)) are exhibited. It is clear that the shape of the caustic produced depends strongly upon the location of the maximum traction. The computed and experimental values of the size of the caustic curve versus the location of the position of σ_{max} are compared in Fig. 9; the two sets of values match well with each other. Also shown in Fig. 9 is the dependence of the computed L_{max} upon the location of σ_{max} with the reflective plane located on the rear surface of the specimen. One can conclude from these results that the location of σ_{max} influences strongly the size of the caustic curve only when this location is near the reflective plane. Figure 10 depicts the experimental and computed caustic curves under the third loading condition of group (a) of Fig. 5 and with reflective planes located on the front and back surfaces of the specimen; it is evident that the curves obtained with these two locations of the reflective plane are dramatically different. However, the experimental and computed curves coincide well with each other.

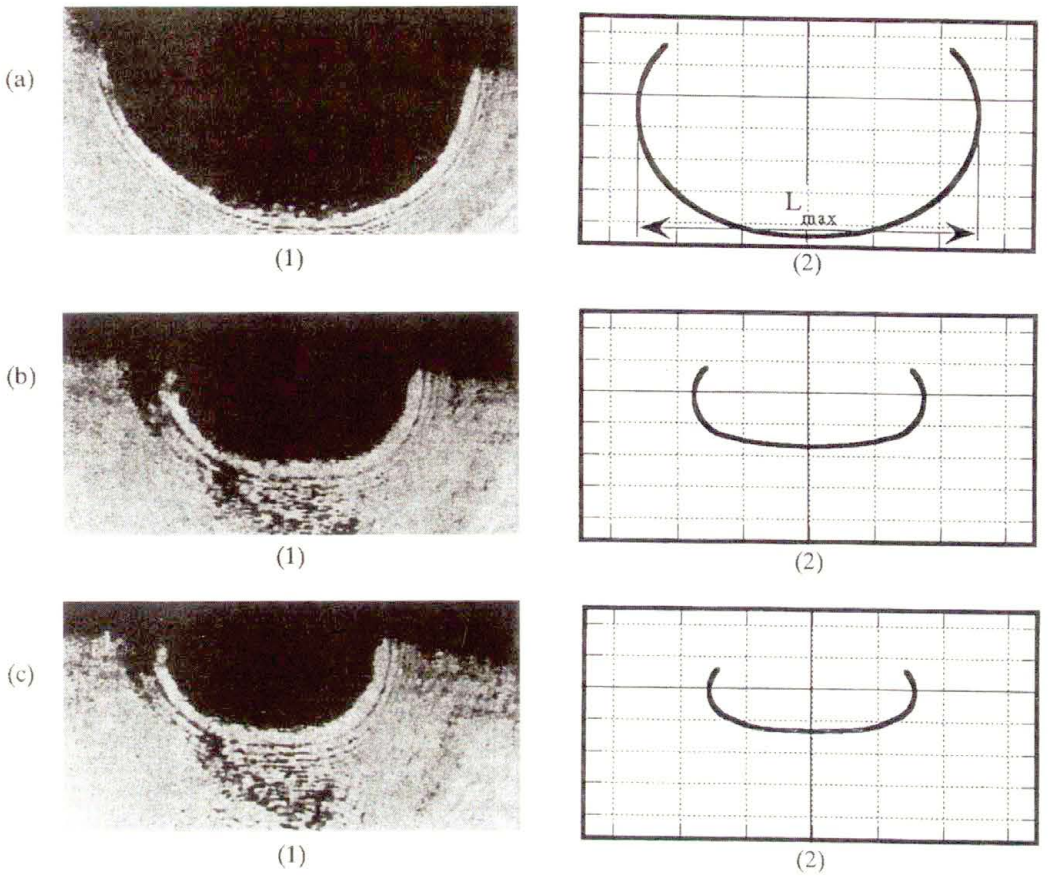

FIG. 8. Experimental and computed caustic curves for different locations ((a) the front layer, (b) the middle layer and (c) the rear layer) of the maximum load 4σ.

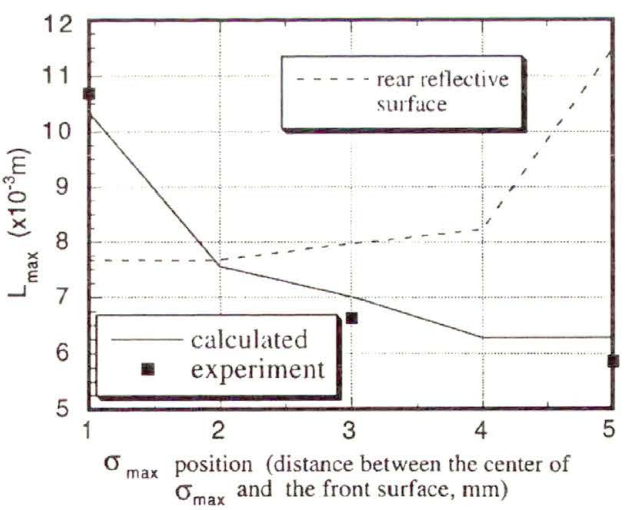

FIG. 9. Dependence of the size of the caustic curve upon the location of the maximum traction for two different positions of the reflective plane.

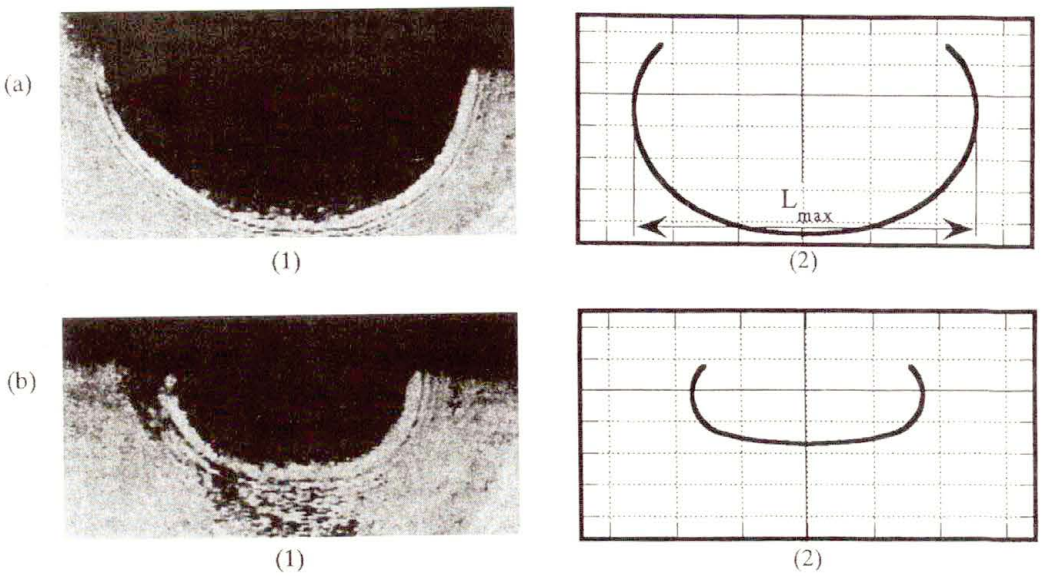

FIG. 10. Experimental and computed caustics for loading 3 (a) of Fig. 5 with (a) reflective plane located on the front surface of the plate, (b) reflective plane located on the rear surface of the plate.

5. A simple inverse problem

In applications one wishes to determine the externally applied load and/or the stress distribution from the knowledge of the shape and dimension of the caustics. However, if the external force pattern is known, its amplitude may be estimated from the dimensions of the caustic curve. We assume the load distribution $a(1)$ of Fig. 5 with the reflective plane located on the front surface of the plate. In Table

Table 1. Comparison of the tractions computed from caustics and the applied tractions.

$P_1 : P_2 : P_3$	2:1:1	3:1:1	4:1:1
D or L_{max} (mm)	7.82	9.22	10.69
Applied traction σ MN/m^2	2.00	2.00	2.00
Computed traction σ_{est} MN/m^2	2.15	2.15	2.26
Difference %	7.5	7.5	13.0

1 we have listed the measured L_{max}, the traction computed from Eq. (2.23), and the traction applied in tests. The maximum difference between the computed and the applied tractions of 13% suggests that the method gives acceptable results.

Figure 11 shows contours of nondimensional principal stresses σ_1 and σ_2 obtained from the experimentally observed caustics. Here p_{est} (MN/m^2) is the intensity of applied tractions estimated from Eq. (2.23) and the size of the caustic curve. These contours show high gradients of stress near the point where the applied traction jumps from zero to a finite value.

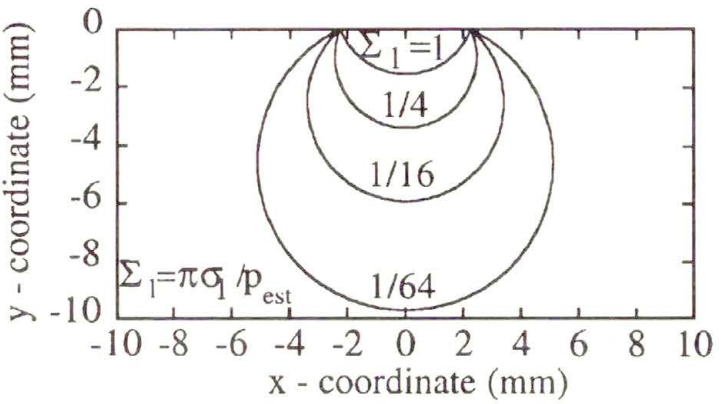

(a)

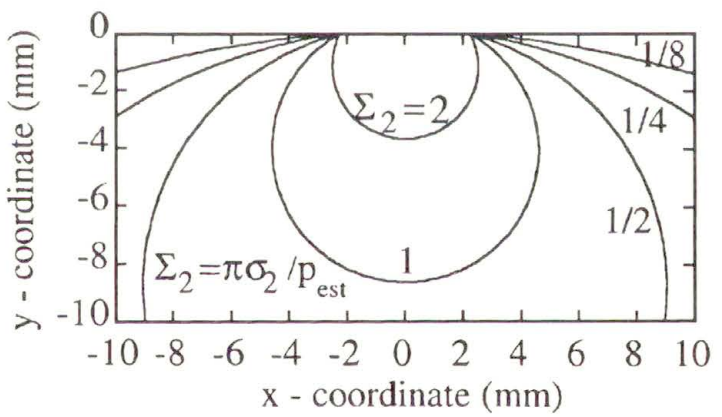

(b)

FIG. 11. Distribution of nondimensional principal stresses.

6. Conclusions

We have studied some basic characteristics of caustics produced in a homogeneous and both optically and mechanically isotropic thin rectangular plate subjected to in-plane loads on two opposite edges, with the other two edges kept traction-free. The applied load is such that points on the central plane of the plate do not undergo any lateral displacement. The effects of different distributions of

the edge loads and the location of the reflective plane upon the caustics produced has been discussed. Computed shapes of caustics and their sizes have been found to compare well with those observed experimentally. The pattern of the caustic curves produced is found to depend strongly upon the location of the reflective plane; the shapes of caustic curves are quite different when the reflective plane abuts on the front or rear surface of the plate. The magnitude of the applied load influences strongly the size of the caustic produced if the reflective plane is located near the point of application of the peak load. An inverse problem of determining the applied tractions from the size of the caustic curve has also been studied.

Acknowledgment

This work was partially supported by the U.S. Office of Naval Research grant N00014-94-1-1211 with Dr. Y. D. S. RAJAPAKSE as the program manager.

References

1. P. MANOGG, *Anwendung der Schattenoptik zur Untersuchung der Zerreissvorgangs von Platten*, Dissertation, Freiburg, Germany 1964.
2. P.S. THEOCARIS, *Stress-singularities at concentrated load*, Exp. Mech., **13**, 511–528, 1973.
3. P.S. THEOCARIS, *Stress-singularities due to uniformly distributed loads along boundaries*, Int. J. Solids Structures, **9**, 655–669, 1973.
4. J.F. KALTHOFF, *Experimental fracture dynamics*, Crack dynamics in metallic materials, Springer-Verlag, New York, 69–253, 1987.
5. A.S. KOBAYASHI, *Handbook on experimental mechanics*, Second revised edition, SEM, New York 1993.
6. M. BORN and E. WOLF, *Principles of optics*, Pergamon Press, Oxford 1959.

DEPARTMENT OF ENGINEERING SCIENCE AND MECHANICS
VIRGINIA POLYTECHNIC INSTITUTE AND STATE UNIVERSITY, BLACKSBURG, VA, USA
and
DEPARTMENT OF MECHANICAL ENGINEERING
MIE UNIVERSITY, TSU, JAPAN.

Received February 27, 1996; *new version July* 18, 1996.

Arch. Mech., 48, 6, pp. 1025–1045, Warszawa 1996

Experimental study of pseudoelastic behaviour of a Cu Zn Al polycrystalline shape memory alloy under tension-torsion proportional and non-proportional loading tests

C. ROGUEDA, C. LEXCELLENT and L. BOCHER (BESANÇON)

SOME TENSION-TORSION loading experiments on thin-walled tubular specimens of a Cu Zn Al polycrystalline shape memory alloy have been performed using a special experimental device. Proportional loading tests allow to verify the normality rule for the pseudoelastic strain rate and enable the experimental validation of the thermodynamical model of pseudoelastic behaviour developed by Raniecki *et al.* Non-proportional loadings show how the pseudoelastic behaviour depends on the chosen loading path. The chosen training path seems to have small effect on the obtained efficiency values which are very high (around 70–80%). A microstructural experimental study must be done to understand the mechanism of formation and reorientation of martensite plates when the stress vector direction changes.

1. Introduction

THE MECHANICAL BEHAVIOUR of shape memory alloys (S.M.A.) is studied, as a rule, through some uniaxial tensile or compressive tests. As a consequence, mechanical models of, e.g., pseudoelastic behaviour, are usually written and also validated only in the case of uniaxial stress. However, it is necessary to understand the S.M.A. behaviour under multiaxial loading since it is the case in most of the industrial constructions. Some tests on mechanical structures have been performed for "complex" loadings: thin rectangular plates loaded in torsion [1], thin rectangular plates loaded in bending by a terminal force [2], springs loaded in tension [2] or in compression [3], ... But these tests were done either in order to study the efficiency of training, or in order to analyse the microstructure evolution.

In [4], B. RANIECKI *et al.* proposed a three-dimensional model of the pseudoelastic behaviour of S.M.A. In order to verify some of those hypotheses, the three-dimensional (3D), or at least two-dimensional (2D) loading tests have to be performed. The simplest two-dimensional loading to apply is a tension-torsion one. Some such experiments on SMA have been reported in [5] but the specimens used were rigid bar specimens (Cu Al Zn Mn) which were associated with an important shear stress gradient in torsion.

Some results of this kind of test on thin tubes are also reported in [6], but these experiments were performed on a Ni Ti polycrystal and the results are still quite qualitative. Moreover, only a few tests were performed.

In this paper, the experimental device and the results of proportional loading tests are discussed. Some non-proportional loading tests are also exposed, to show the importance of the loading sequence. Training of samples during these tests

have been analyzed. Finally, the modelling described in [4] (and applied to proportional loading tests) is used to show a reasonable agreement with experimental data.

2. Material and technique

The tests have been performed on a Cu Zn Al polycrystalline S.M.A. without any additional components (weight composition: Cu 70.17 %, Zn 25.63 %, Al 4.2 %) prepared by the "Tréfimétaux" company. Its characteristic phase transformation temperatures, determined by home electric measurements, are 287 K for M_S, 278 K for M_F (temperature start – and end – of the austenite to martensite phase transformation) and 290 K for A_S, 293 K for A_F (temperature start – and end – of the reverse transformation). The heat treatment is quite standard. Specimens are heated at 1123 K during 15 minutes, quenched in a 393 K oil bath and maintained at this temperature for one hour. The specimens are carried out few days later, in order to make the austenitic phase more stable.

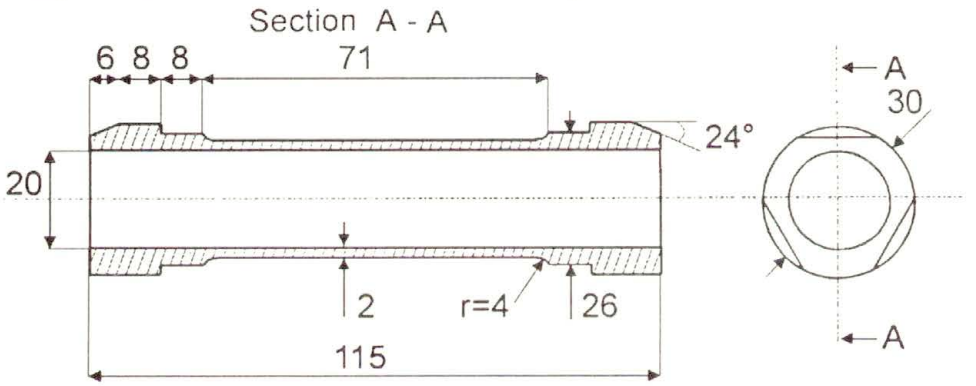

FIG. 1. Sample shape definition.

In order to avoid internal stresses, samples were manufactured by electro-erosion technique from 30 mm diameter rigid bars. Their dimensions (given in Fig. 1) are characteristic for thin tubes condition. During the tension-torsion tests, the stress tensor has the form:

$$\boldsymbol{\sigma} = \begin{pmatrix} 0 & 0 & 0 \\ 0 & 0 & \sigma_{z\theta} \\ 0 & \sigma_{z\theta} & \sigma_{zz} \end{pmatrix}, \tag{2.1}$$

with

$$\sigma_{zz} = F/2\pi Re, \qquad \sigma_{z\theta} = C/2\pi R^2 e, \tag{2.2}$$

F, C, R and e are, respectively, the axial loading force, the torque, the mean radius and thickness of the sample. It must be remembered that in the S.M.A.

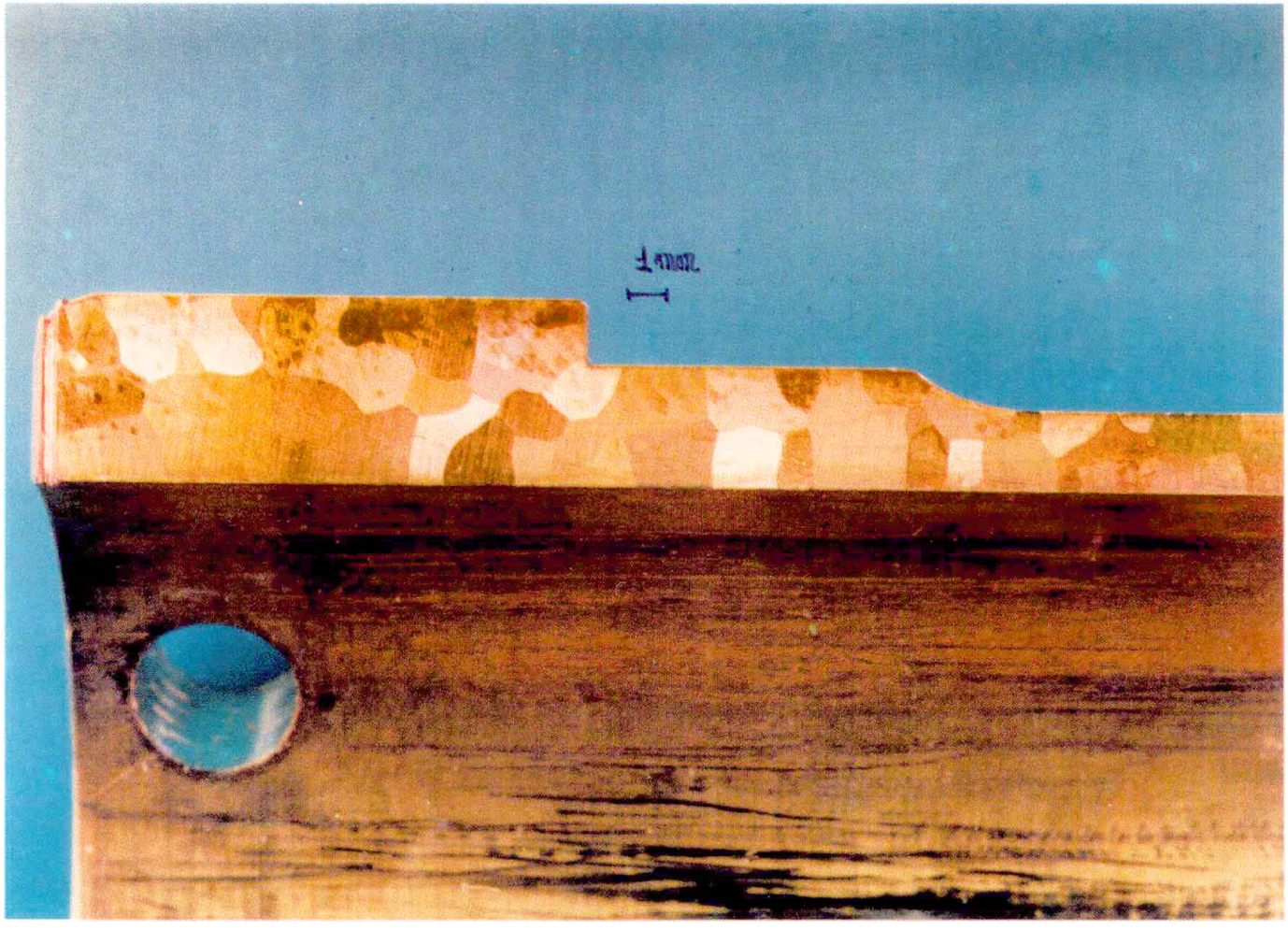

FIG. 2. Photograph of the sample.

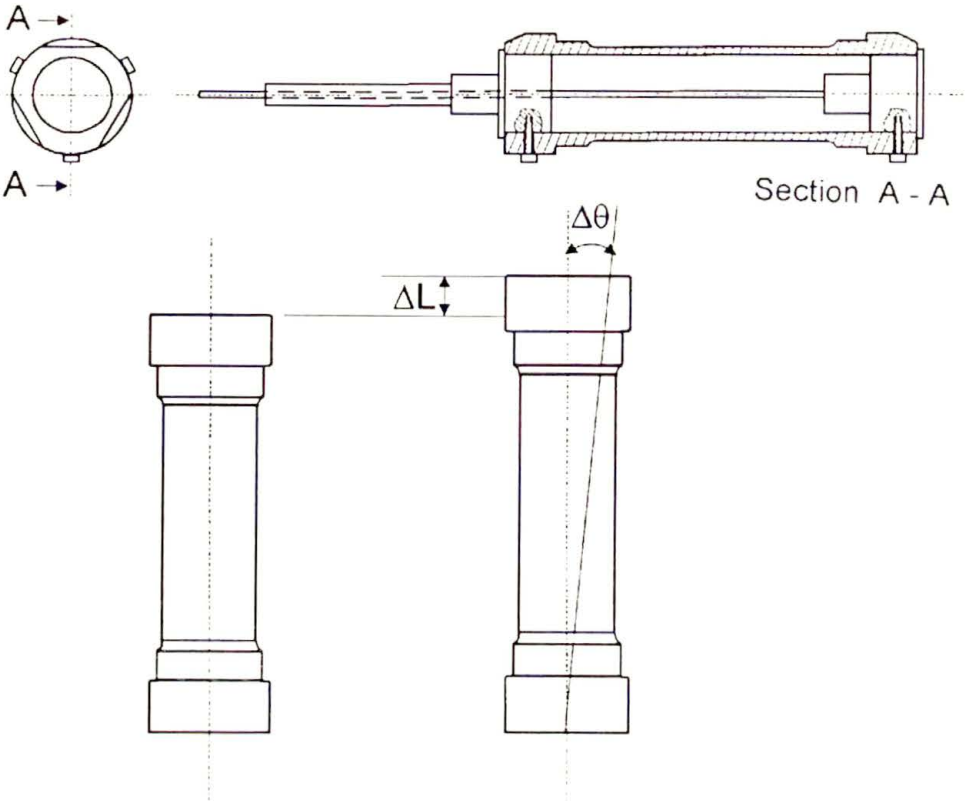

FIG. 3. Strain measurement device.

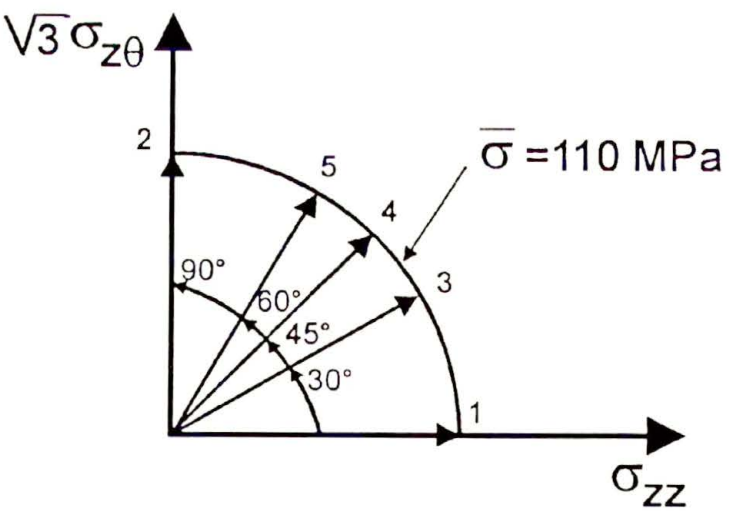

FIG. 4. Repartition of the five proportional loading tests on $\bar{\sigma}_{max}$ = 110 MPa.

case, the thin tube condition must take into account the mean grain size which is about 1 mm (see Fig. 2). Some 1800 grains have been numbered in the measured part.

The sample shape is adapted to a specific mechanical device which takes over the whole loading and ensures the specimen to be properly fixed. Tests were performed on a Schenk 3D test machine (tension, torsion and internal pressure), connected with the H.P. microcomputer. This hydraulic machine has load limits ± 63 kN and ± 1000 Nm. Every test has been performed under a force control.

The temperature was maintained constant at $T = 303$ K ($T > A_F$).

Stresses are calculated from F and C values with the accuracy of ± 3.1 N and ± 0.12 Nm. Axial and torsional strains are obtained from a mechanical differential system illustrated in the Fig. 3. Linear and rotative sensors (L.V.D.T and R.V.D.T) are linked to each stem of this system, in order to separate strain components from each other. They measure axial and angular displacements (ΔL and $\Delta\theta$).

Assuming the strains to be small, axial and torsional strains ε_{zz} and $\varepsilon_{z\theta}$ can be easily calculated from the formulae

$$\varepsilon_{zz} = \Delta L/L, \qquad \varepsilon_{z\theta} = \frac{r\Delta\theta}{2L}. \tag{2.3}$$

Here L is the effective length, estimated by means of a classical extensometer to be equal 69 mm. Displacements are known with the accuracy of $\pm 5 \cdot 10^{-6}$ m for the axial sensor and $\pm 1.22 \cdot 10^{-3}$ rad. for the angular one.

Strain gauges were also tried but it was so difficult to obtain a good adherence between the sample and gauges that this technique has been abandoned. This behaviour is probably due to copper corrosion.

3. Experimental results

3.1. Proportional loading tests

In tension-torsion loading tests, the equivalent stress, in agreement with the von Mises criterion, is defined by

$$\bar{\sigma} = \left(\sigma_{zz}^2 + 3\sigma_{z\theta}^2\right)^{1/2}. \tag{3.1}$$

For each proportional test, the maximum equivalent stress $\bar{\sigma}_{\max}$ is 110 MPa. Hence, each point corresponding to the end of loading belongs to a quarter of circle, the radius of which is $\bar{\sigma}_{\max}$ in the $(\sigma_{zz}, \sqrt{3}\sigma_{z\theta})$-plane representation. The courses of the five tests performed in this quarter of circle is presented in the Fig. 4. As the loading is proportional, axial and torsional stresses are connected with each other by the relation

$$\sigma_{z\theta} = \alpha\sigma_{zz} \qquad (\alpha = C^{te}). \tag{3.2}$$

The value of α, fixed in each test, characterizes the direction of loading and can vary between 0 (pure tensile test) and ∞ (pure torsional test).

The test frequency is 10^{-3} Hz. Loading and unloading periods are similar. The first cycle is repeated 35 times in order to evaluate the possible training of the samples.

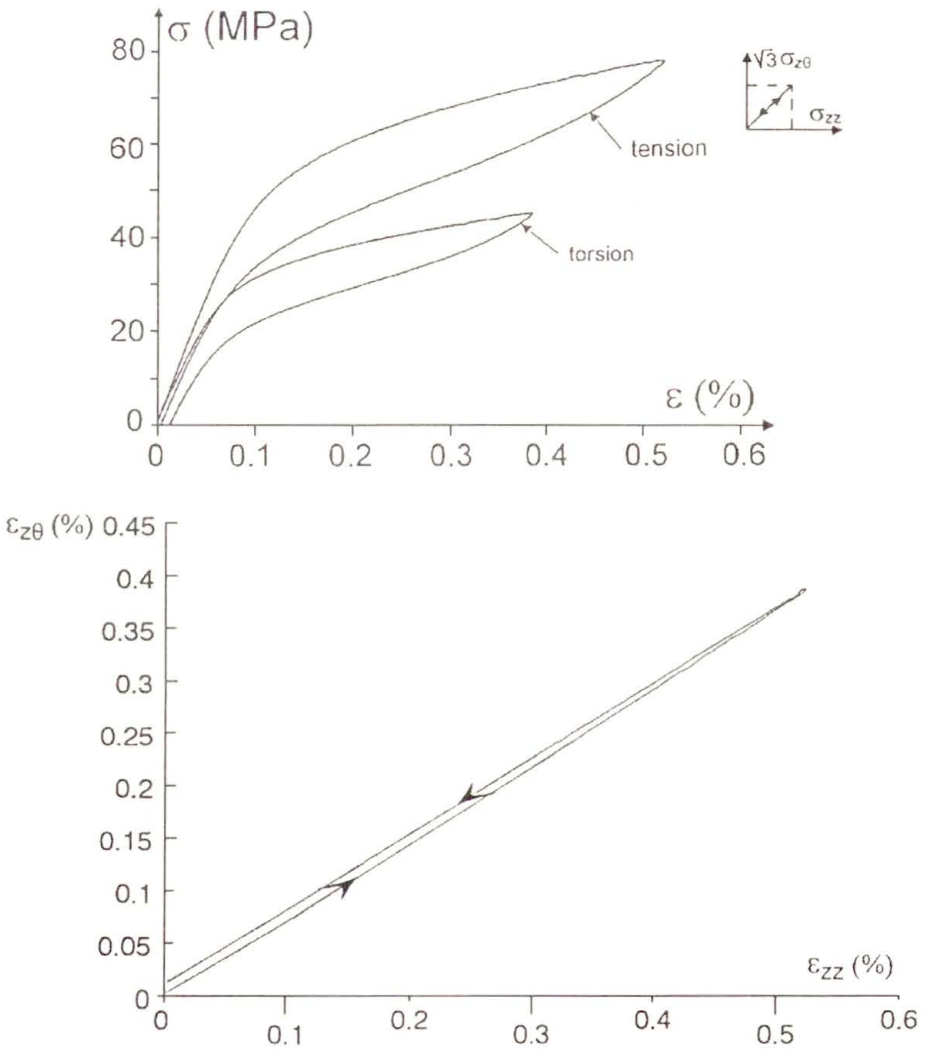

FIG. 5. Tension-torsion proportional loading test (α = 0.577).

The stress-strain curve corresponding to the No. 4 test (α = 0.577) is presented in Fig. 5, as a representative test. In the following parts of this paper, the elastic behaviour, the yield stress of phase transition, the pseudoelastic behaviour and finally the training efficiencies are studied.

3.1.1. Classical elastic behaviour. Elastic strains and stresses are related by the Poisson coefficient ν and the Young modulus E as follows:

$$\begin{aligned} \varepsilon^e_{rr} &= \varepsilon^e_{\theta\theta} = -\frac{\nu}{E}\sigma_{zz}\,, & \varepsilon^e_{zz} &= \frac{1}{E}\sigma_{zz}\,, \\ \varepsilon^e_{z\theta} &= \frac{1+\nu}{E}\sigma_{z\theta}\,, & \varepsilon^e_{r\theta} &= \varepsilon^e_{rz} = 0. \end{aligned} \tag{3.3}$$

E and ν are calculated from the slope of each stress-strain curve. A considerable scatter of E values can be observed. This can be explained by a possible dispersion during heat treatment because the samples are thick, or by a relative non-homogeneity of the alloy. This observation in the elastic domain, where the behaviour is well known, is important to estimate the dispersion of further results.

3.1.2. Yield stress of phase transformation. To characterize the beginning of the direct phase transformation (i.e. austenite to martensite), the usual von Mises yield stress is defined as:

$$\bar{\sigma}^{AM} = \left((\sigma^{AM}_{zz})^2 + 3(\sigma^{AM}_{z\theta})^2\right)^{1/2}, \tag{3.4}$$

where (σ^{AM}_{zz}) and $(\sigma^{AM}_{z\theta})$ are the axial and torsional threshold stresses. They correspond to the linearity loss of the $(\varepsilon_{zz}, \sigma_{zz})$ and $(\varepsilon_{z\theta}, \sigma_{z\theta})$ curves. For each test, the $\bar{\sigma}^{AM}$ value is calculated and $\left((\sigma^{AM}_{zz}), \sqrt{3}(\sigma^{AM}_{z\theta})\right)$ are given on the $(\sigma_{zz}, \sqrt{3}\sigma_{z\theta})$ plane. As it is shown in Fig. 6, $\bar{\sigma}^{AM}$ seems to be rather constant in these tests, and a criterion surface can be defined as $\bar{\sigma}^{AM} = 30.3$ MPa.

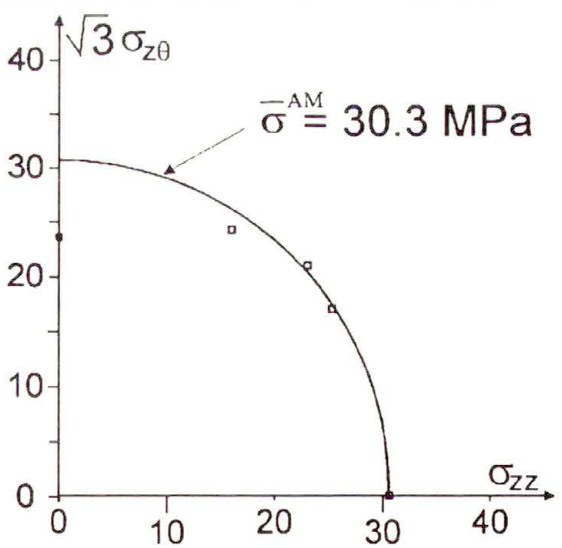

FIG. 6. Yield surface phase transformation: austenite → martensite.

In a tensile test, the critical stress σ^{AM} and the temperature T are linked by the following relation:

$$\sigma^{AM} = b(T - M_S). \tag{3.5}$$

Generalizing this relation for multidimensional loading tests, the constant b is found to be equal to $1.9\,\mathrm{MPaK}^{-1}$ which is a known value for a Cu Zn Al polycrystal. In [7], uniaxial tests with the same alloy were presented and b was estimated to be $2.0\,\mathrm{MPaK}^{-1}$.

3.1.3. Study of pseudoelastic behaviour. First, the total deformation is split into two parts, the elastic and the pseudoelastic deformation:

$$\boldsymbol{\varepsilon} = \boldsymbol{\varepsilon}^{e} + \boldsymbol{\varepsilon}^{pe}. \tag{3.6}$$

For tensile tests, VACHER in [7] has established the proportionality between the pseudoelastic deformation and the volume fraction of martensite, by performing the electrical resistance measurements during mechanical tests.

For a 2D or a 3D proportional loading, as in "plasticity", the existence of a current flow surface ($\bar{\sigma}$ = cte) is postulated. It is homothetic to the initial one ($\bar{\sigma}^{AM}$ = cte); the normality rule, i.e. the pseudoelastic strain rate is perpendicular to this surface.

In a classical way, it follows that

$$\dot{\boldsymbol{\varepsilon}}^{pe} = \dot{\lambda}\frac{\partial f}{\partial \boldsymbol{\sigma}}, \tag{3.7}$$

with

$$f = \bar{\sigma} - \bar{\sigma}^{AM}(T), \qquad \dot{\lambda} = \gamma\,\dot{z}. \tag{3.8}$$

So, the pseudoelastic strain rate is obtained as

$$\dot{\boldsymbol{\varepsilon}}^{pe} = \frac{3}{2}\frac{\operatorname{dev}\boldsymbol{\sigma}}{\bar{\sigma}}\gamma\,\dot{z}, \tag{3.9}$$

where γ is the maximal pseudoelastic strain obtained for a complete phase transformation occurring in a tensile test.

In a tension-torsion proportional loading test, the expressions (3.2) and (3.9) lead to:

$$\begin{aligned}
\dot{\varepsilon}^{pe}_{zz} &= \frac{\sigma_{zz}}{\bar{\sigma}}\gamma\,\dot{z} = \frac{1}{(1+3\alpha^2)^{1/2}}\gamma\,\dot{z},\\
\dot{\varepsilon}^{pe}_{\theta\theta} &= \dot{\varepsilon}^{pe}_{rr} = -\frac{1}{2}\dot{\varepsilon}^{pe}_{zz},\\
\dot{\varepsilon}^{pe}_{z\theta} &= \frac{3}{2}\frac{\sigma_{z\theta}}{\bar{\sigma}}\gamma\,\dot{z} = \frac{3}{2}\frac{\alpha}{(1+3\alpha^2)^{1/2}}\gamma\,\dot{z}.
\end{aligned} \tag{3.10}$$

In this case, the integration yields

$$\boldsymbol{\varepsilon}^{pe} = \frac{3}{2}\frac{\operatorname{dev}\boldsymbol{\sigma}}{\overline{\sigma}}\gamma z. \tag{3.11}$$

It is possible to evaluate $\varepsilon^{pe}_{\theta\theta}/\varepsilon^{pe}_{zz}$ from strain measurements obtained by the gauges. As it is shown in Fig. 7, the experimental value of $\varepsilon^{pe}_{\theta\theta}/\varepsilon^{pe}_{zz}$ is not far from the theoretical value which is -0.5. The small dispersion can result from the position of the gauges.

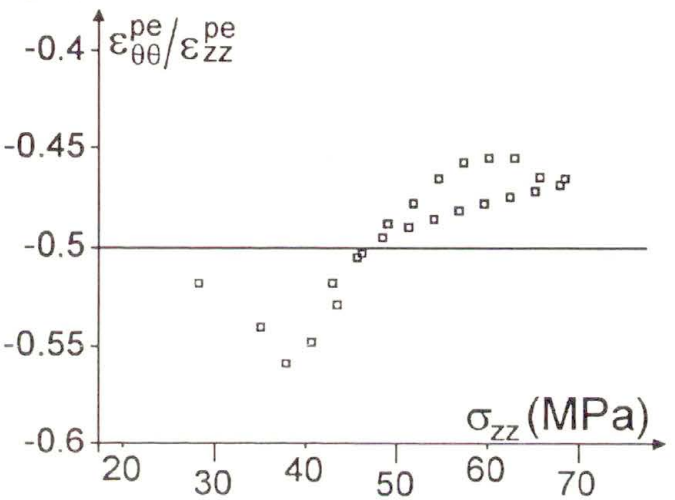

FIG. 7. Ratio $\varepsilon^{pe}_{\theta\theta}/\varepsilon^{pe}_{zz}$ evolution during a tensile-torsion proportional loading.

Validity of the expression (3.11) is verified by studying the evolution of $\varepsilon^{pe}_{z\theta}/\varepsilon^{pe}_{zz}$. Parameter Q is defined as:

$$Q = \frac{\varepsilon^{pe}_{zz}}{\varepsilon^{pe}_{z\theta}}\frac{\sigma_{z\theta}}{\sigma_{zz}}. \tag{3.12}$$

From (3.11) it follows that Q is theoretically constant and equal to 2/3. The evolution of Q with respect to the tensile stress σ_{zz} during the test No. 4 ($\alpha = 0.577$) is presented in the Fig. 8. It can be noticed that even though Q seems to be a constant, its value is slighty higher than the theoretical one. Q values for the three biaxial loading tests are presented in the Tab. 1.

Table 1. Value of Q obtained for each proportional test.

Test	3	4	5
Q	0.72	0.75	0.75

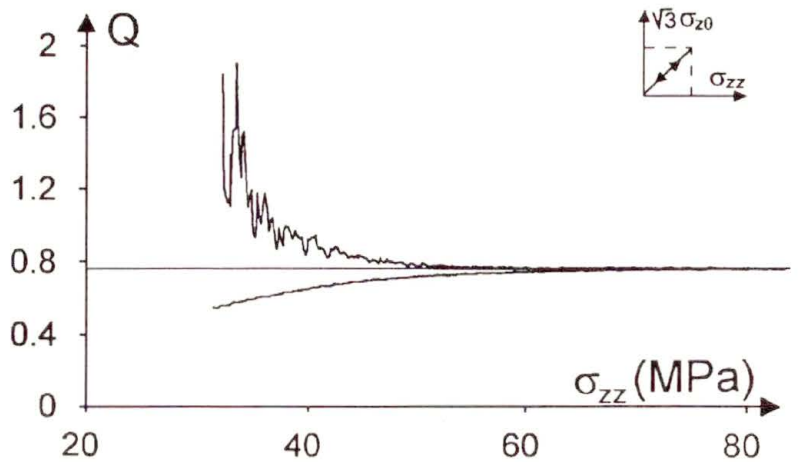

FIG. 8. Experimental evolution of the Q parameter (during the test described in Fig. 5).

The equivalent pseudoelastic strain is defined by:

$$\bar{\varepsilon}^{pe} = \left[(\varepsilon_{zz}^{pe})^2 + \frac{4}{3} (\varepsilon_{z\theta}^{pe})^2 \right]^{1/2}. \tag{3.13}$$

Its maximum value is reached when $\bar{\sigma}$ is maximum ($\bar{\sigma}_{\max} = 110\,\text{MPa}$). The Tab. 2 shows $\bar{\varepsilon}_{\max}^{pe}$ for each test. In a pure tension test, $\varepsilon_{z\theta}^{pe}$ is theoretically null, and in a pure torsional test, ε_{zz}^{pe} is also zero. From the Tab. 2, the material seems to be slightly anisotropic. This can explain why Q is not equal to its theoretical value.

Table 2. Experimental tensile and torsional pseudoelastic strain values.

Test	1	2	3	4	5
ε_{zz}^{PE} (%)	0.339	0.011	0.384	0.369	0.193
$\varepsilon_{z\theta}^{PE}$ (%)	0.025	0.215	0.173	0.277	0.356
$\bar{\varepsilon}^{PE}$ (%)	0.34	0.248	0.433	0.488	0.454

The pseudoelastic strain measurements allow also to determine the pseudoelastic strain rate vector $\dot{\boldsymbol{\varepsilon}}^{pe}$. As the loading is proportional, the following relation holds (expressions (3.9) and (3.11)):

$$\frac{\varepsilon_{z\theta}^{pe}}{\varepsilon_{zz}^{pe}} = \frac{\dot{\varepsilon}_{z\theta}^{pe}}{\dot{\varepsilon}_{zz}^{pe}}. \tag{3.14}$$

Then, it is easy to draw $\dot{\boldsymbol{\varepsilon}}^{pe}$ on the $(\sigma_{zz}, \sqrt{3}\sigma_{z\theta})$ plane, for each test, when the equivalent stress is maximal, as it is shown in the Fig. 9. This figure shows also that

the strain rate vector is perpendicular to the loading surface ($\bar{\sigma}_{max}$ = 110 MPa) what proves the validity of the normality rule. Moreover, it allows to see the expansion of the criterion surface from $\bar{\sigma}^{AM}$ = 30.3 MPa to $\bar{\sigma}_{max}$ = 110 MPa.

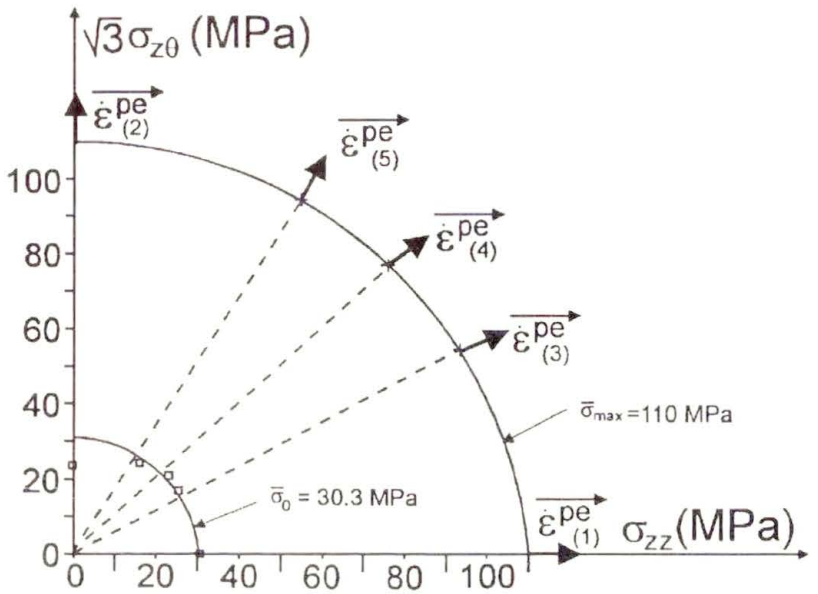

FIG. 9. Experimental validation of the normality rule.

3.1.4. The training process. After N_{max} = 35 loading-unloading cycles (between $\bar{\sigma}$ = 0 and $\bar{\sigma}$ = $\bar{\sigma}_{max}$ = 110 MPa), the training effect is measured. Figure 10 represents the first ten cycles corresponding to the test No. 4. The Fig. 11 shows the training effect in this sample, placed (at a stress-free state) in an oil bath of temperature varying from 232 K to 313 K.

In order to study the training effect, it is necessary to define three training efficiencies: the tension efficiency ($\varrho_{zz} = (\Delta\varepsilon_{zz})_{\sigma=0}/(\varepsilon^{pe}_{zz\,max})_{N=N_{max}}$), the torsion efficiency ($\varrho_{z\theta} = (\Delta\varepsilon_{z\theta})_{\sigma=0}/(\varepsilon^{pe}_{z\theta\,max})_{N=N_{max}}$) and the equivalent efficiency ($\varrho = (\Delta\bar{\varepsilon})_{\sigma=0}/(\bar{\varepsilon}^{pe}_{max})_{N=N_{max}}$).

These efficiencies are measured for the five training tests. These values seem to be much higher (around 75–80%) than the ones obtained under a more complex loading (c.f. for example [1]). In [5], where rigid bars are also loaded in tension and torsion, the first cycle is repeated in order to study the stabilization of stress-induced martensite. Unfortunately, the efficiency values are not presented. Nevertheless, the pseudoelastic loop stabilizes after a few cycles, as in our experiments. Training values lead us to assume that the density of dislocations is quite important since, according to [8], the density of dislocations is a good parameter helping to evaluate the training effect. Until now, no microstructural analysis has been performed to verify the assumption.

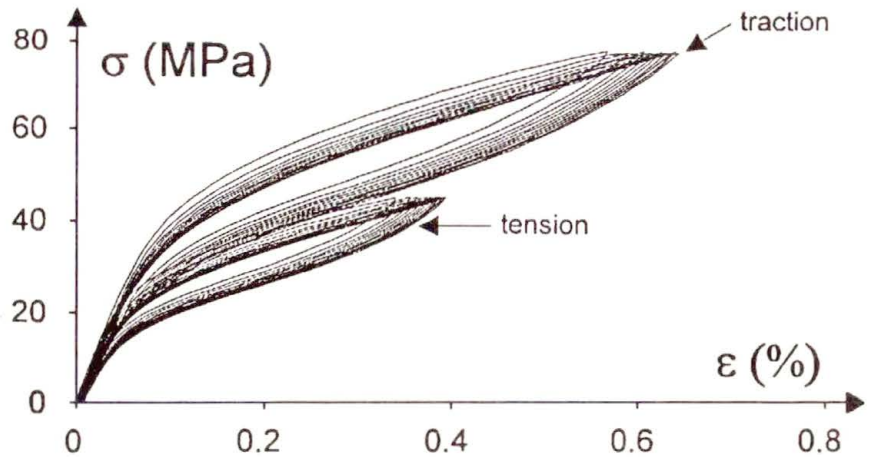

FIG. 10. The first ten half-cycles of a training process (test No. 4, $\alpha = 0.577$).

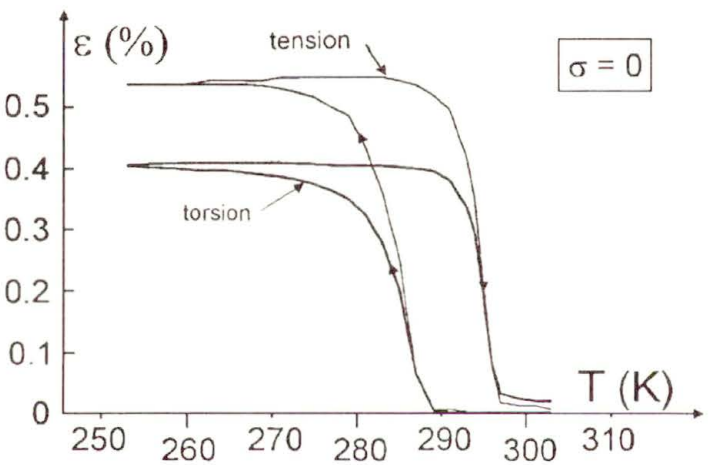

FIG. 11. Two-way shape memory effect measured after training process of Fig. 10.

3.2. Non-proportional tests

Even if the modelling of non-proportional loadings is, in most of cases, not simple, the importance of such tests appears to be in answering the queston: "what is the effect of a rough change of the mechanical loading upon the material behaviour?" Indeed, in every single crystal, the best oriented habit planes are activated (with respect to the maximum shear rule) for a given loading direcion [9]. If the direction of the stress vector is changed by applying torsion upon the tension, other variants ("secondary variants") can be activated and interact vith the primary variants. Here, it is interesting to see what happens macroscopically to a polycrystalline sample.

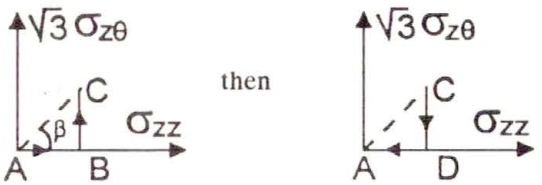

Path of type I

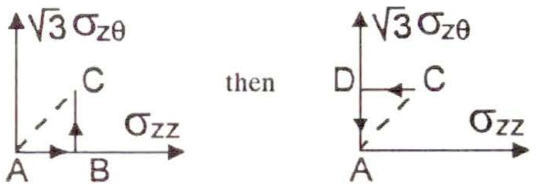

Path of type II

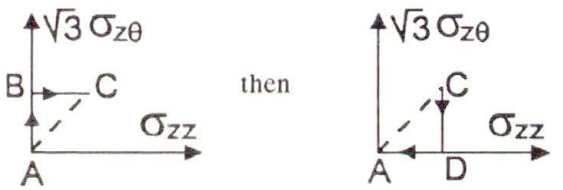

Path of type III

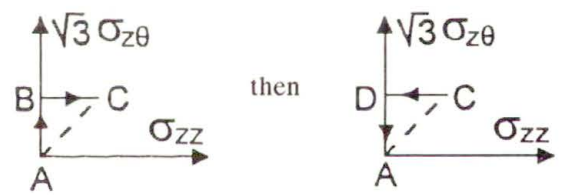

Path of type IV

FIG. 12. Definition of non-proportional paths.

As in the proportional loading tests, the maximum equivalent stress $\bar{\sigma}_{\max}$ is 110 MPa, but it is reached through four different possible paths: I, II, III and IV (see Fig. 12). β is the angle characterizing the test [$\operatorname{tg}\beta = (\sqrt{3}\sigma_{z\theta}^{\max})/\sigma_{zz}^{\max}$]. Its possible values are 30°, 45°, 60° as in the respective tests 3, 4 and 5 with proportional loading.

3.2.1. Pseudoelastic loop of the first cycle. For each path, the tensile $(\sigma_{zz}, \varepsilon_{zz})$ and torsional curves $(\sigma_{z\theta}, \varepsilon_{z\theta})$ are given (Figs. 13 to 16). So, the resulting deformation path $(\varepsilon_{z\theta}, \varepsilon_{zz})$ is known. As it was already observed in the previous part, material

isotropy is not perfect since during the first loading (uniaxial), the small strain is measured along the other axis.

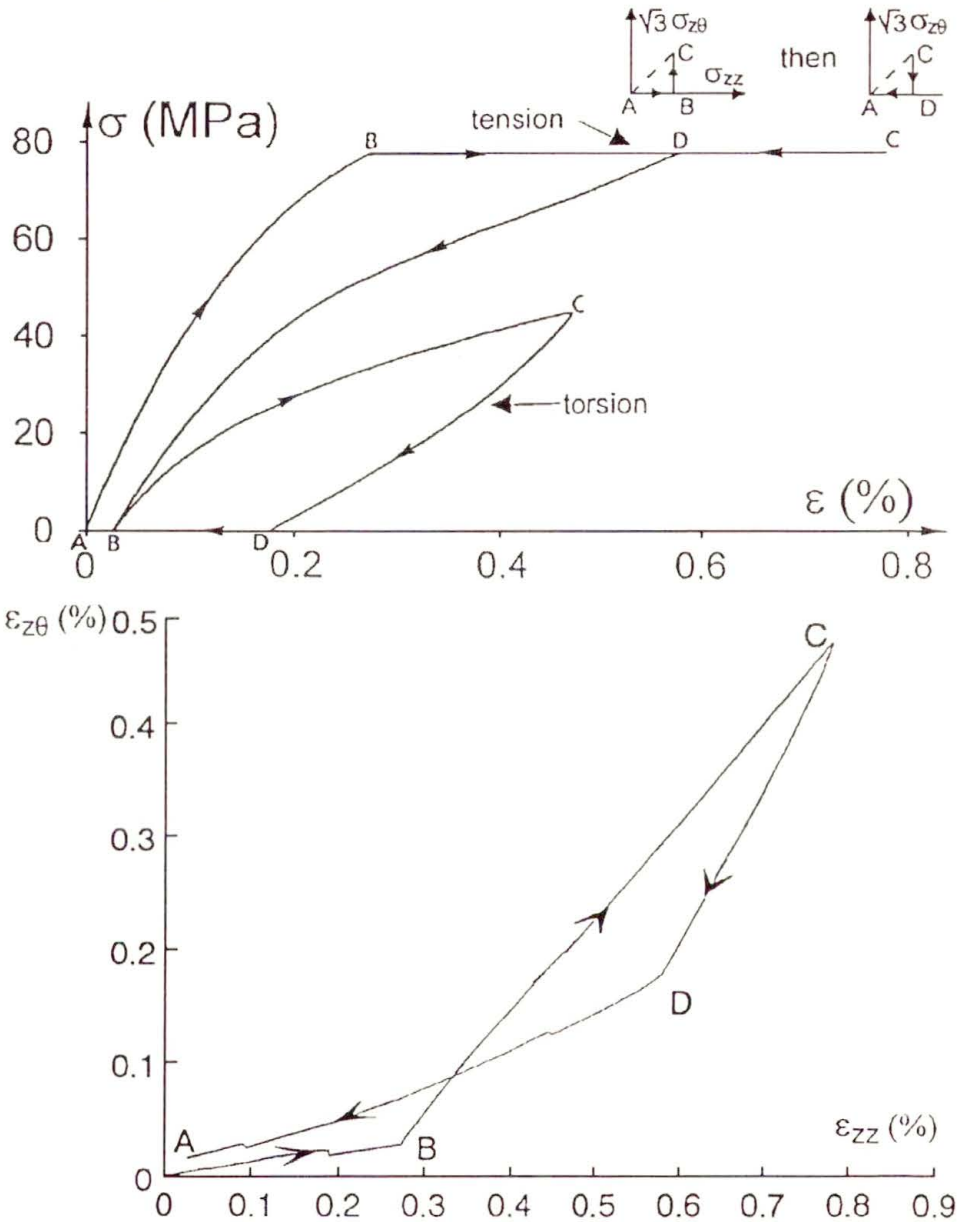

FIG. 13. Tension-torsion non-proportional loading test (path I, $\beta = 45°$).

Maximum equivalent pseudoelastic strain $\bar{\varepsilon}^{pe}_{max}$ is higher than that in the proportional loading tests. This observation confirms the assumption that new habit planes ("secondary" planes) are activated when the mechanical loading direction

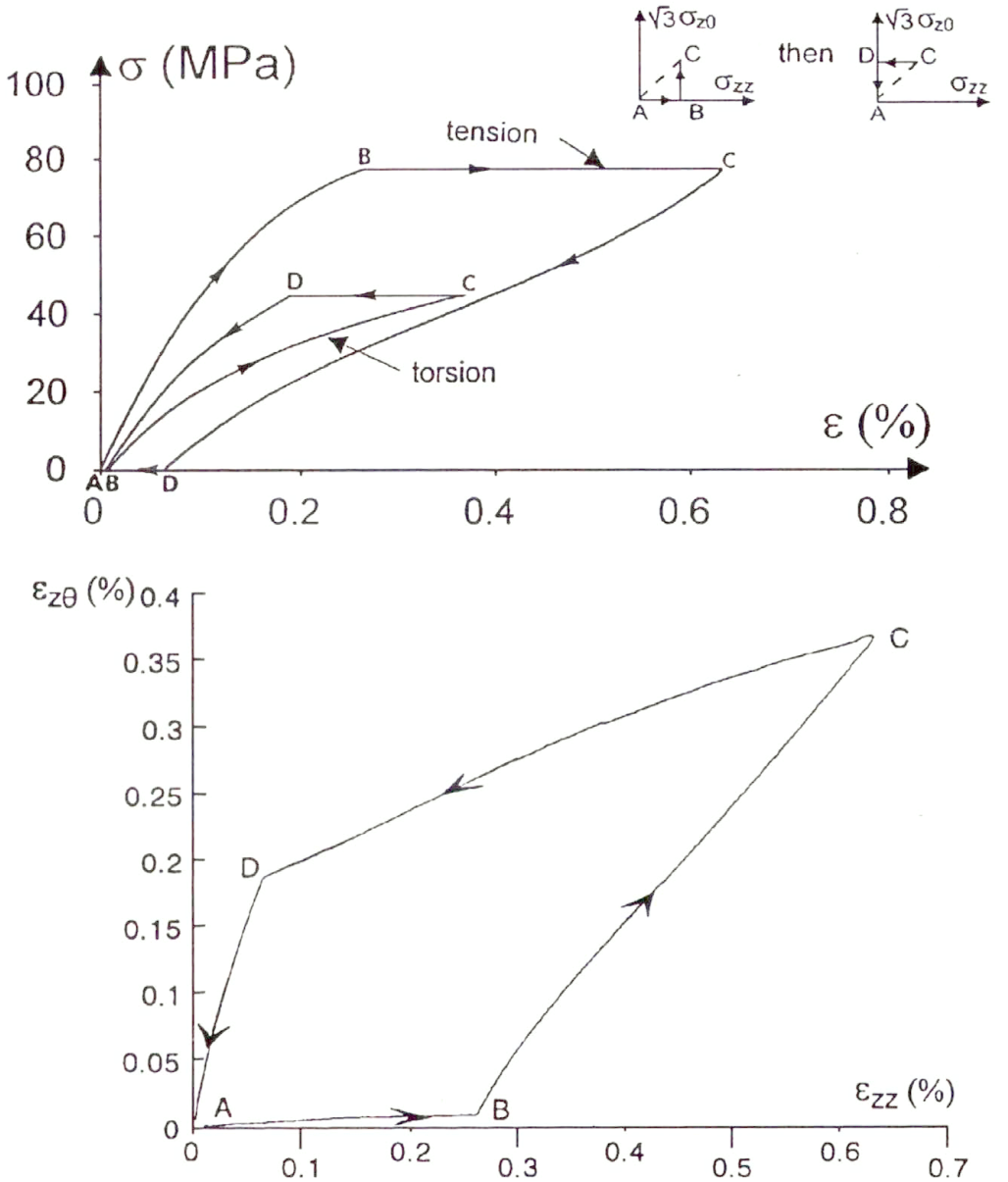

FIG. 14. Tension-torsion non-proportional loading test (path II, $\beta = 45°$).

changes. Moreover, it seems that the hardening induced by interactions between primary and secondary habit planes does not play any important role. Moreover, during the second loading (BC), a reorientation of primary variants may occur with the change of the stress vector orientation. Such variant reorientations are reported in [5].

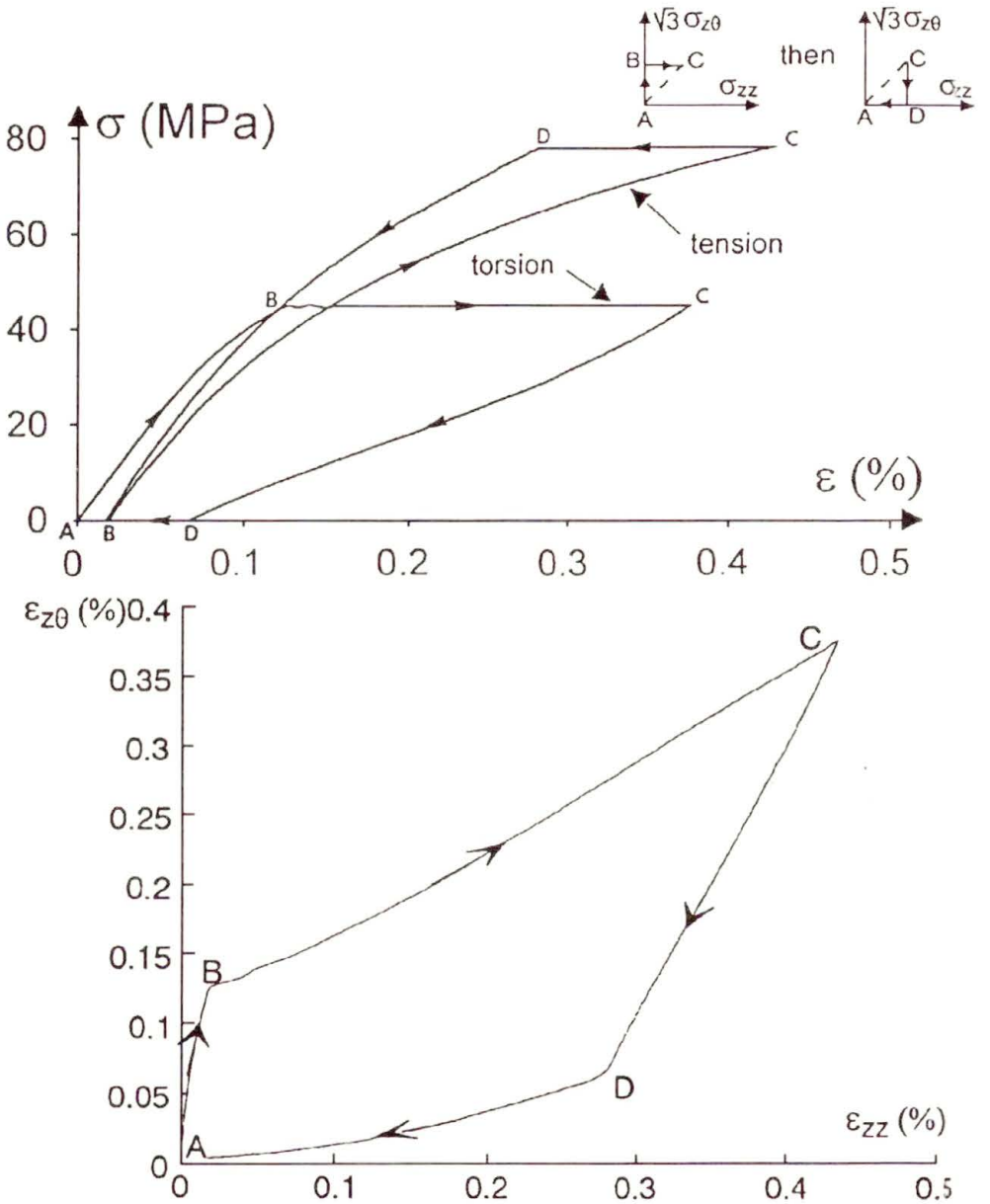

FIG. 15. Tension-torsion non-proportional loading test (path III, $\beta = 45°$).

In fact, during these non-proportional loading tests, observation of the microstructure evolution is necessary to understand the micromechanisms invoved by the stress path. From the phenomenological point of view, the comparson between the shape of the imposed stress path (rectangular in Figs. 14 and 15) and the resulting shape in the deformation path is interesting.

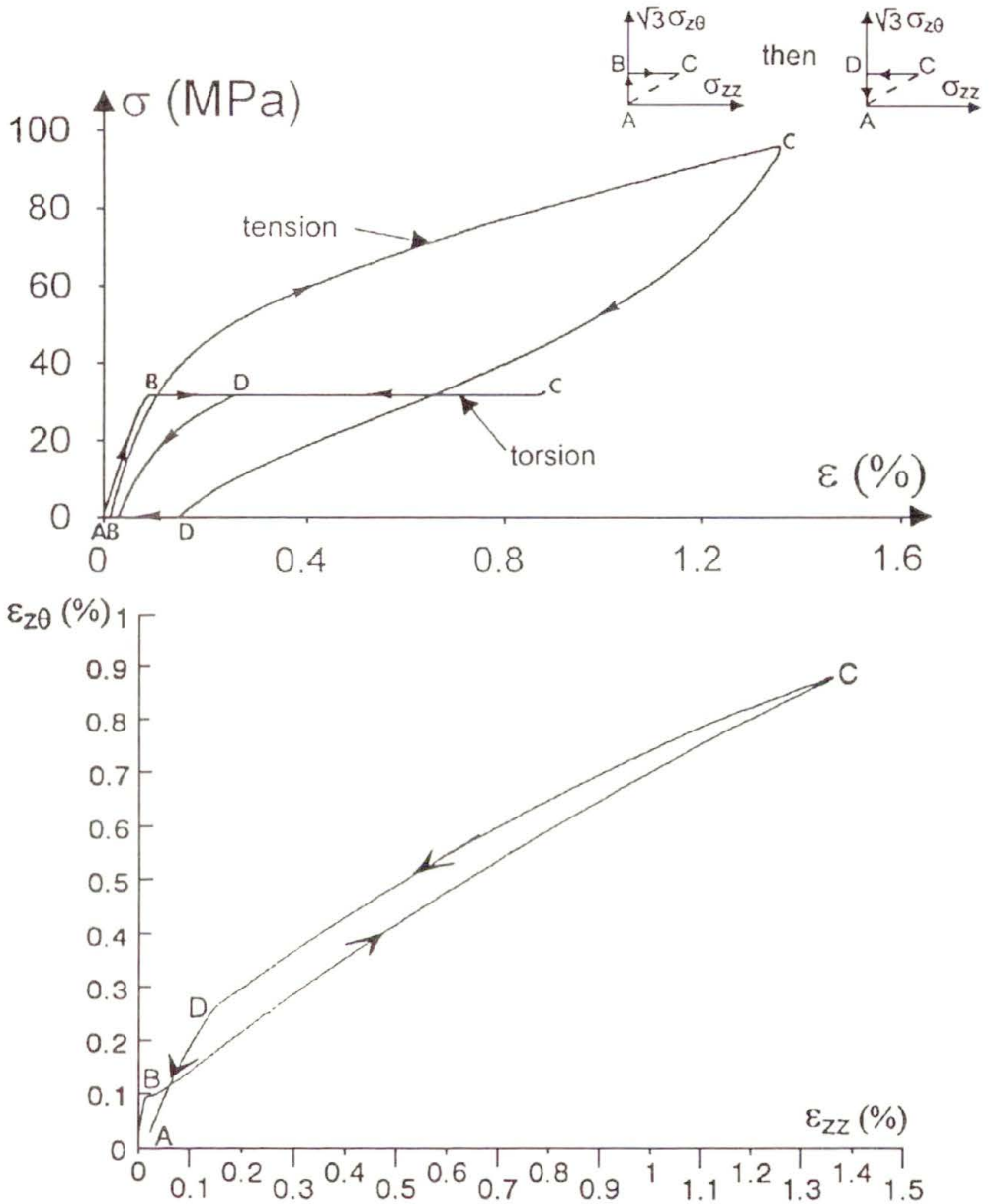

FIG. 16. Tension-torsion non-proportional loading test (path IV, $\beta = 30°$).

3.2.2. The training process. The ten first cycles of a training are presented in Fig. 17. After $N = N_{max} = 35$ cycles, the training effect is measured (Fig. 18). Efficiency definitions are the same as in the previous case.

The global efficiency ϱ lies between 60 and 80 % and its dependence on the chosen path is not clear.

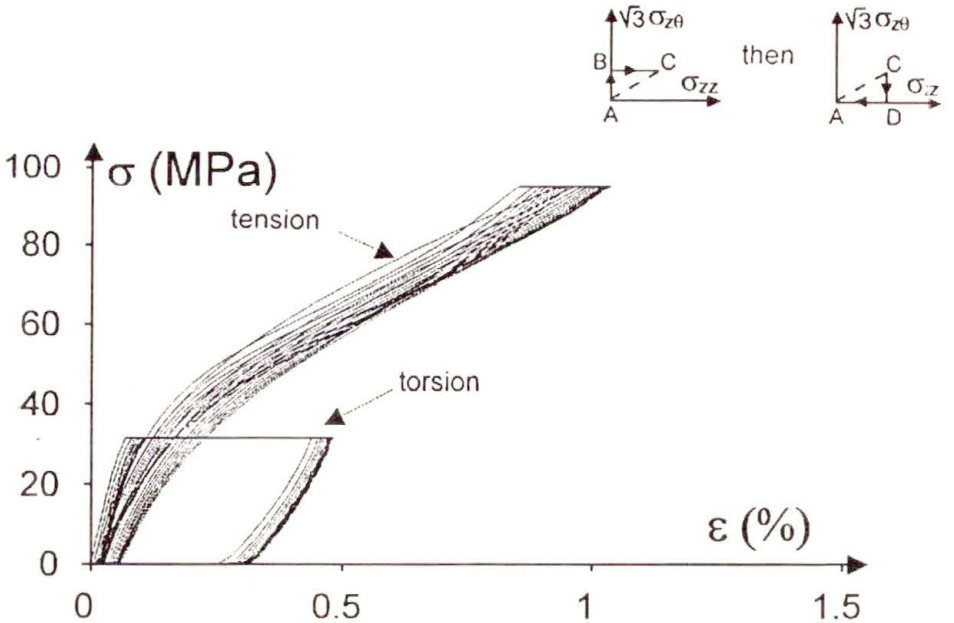

FIG. 17. The first ten half-cycles of a non-proportional loading training process (path III, $\beta = 30°$).

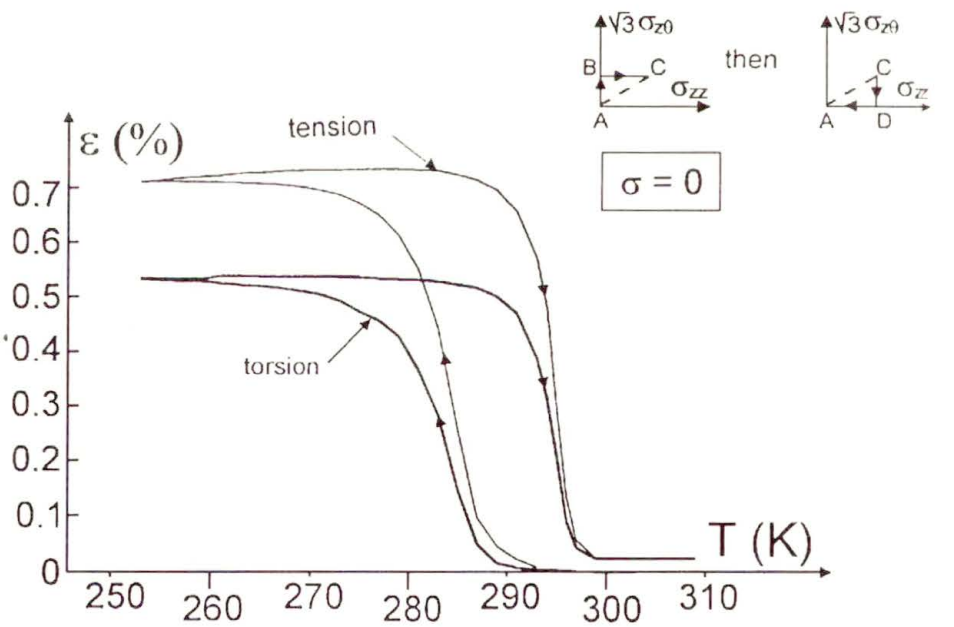

FIG. 18. Two-way shape memory effect measured after training process of Fig. 17.

4. Modelling of a proportional loading test

4.1. General equations

In [4], RANIECKI *et al.* propose to model the pseudoelastic behaviour in two steps. First, the free energy of the two phases system $(A + M)$ is written as

$$\Phi = (1 - z)\Phi_1 + z\Phi_2 + \Delta\Phi. \tag{4.1}$$

Φ_1 and Φ_2 are the specific free energies of the austenite and of the martensite phases, respectively. $\Delta\Phi$ is called the configurational energy and represents the interaction which appears between the two phases, for example produced by incompatibilities between deformations. The main property of this energy is that it disappears if only one phase is present in the material. In agreement with MULLER and XU [10], the simplest expression for $\Delta\Phi$ is:

$$\Delta\Phi = z(1 - z)\Phi_{it}\,, \tag{4.2}$$

where Φ_{it} is the interaction energy $(\Phi_{it}(T) = \overline{u}_0 - T\overline{s}_0)$.

In [4], the free energy expression is obtained in the form (z is the volume fraction of martensite and ϱ the mass density of the material):

$$\Phi(\boldsymbol{\varepsilon}, T, z) = u_0^1 - Ts_0^1 - z\pi_0^f(T) + \frac{1}{2\varrho}(\boldsymbol{\varepsilon} - \boldsymbol{\varepsilon}^{pe})\mathsf{L}(\boldsymbol{\varepsilon} - \boldsymbol{\varepsilon}^{pe}) + c_v\left[(T - T_0) - T\ln\left(\frac{T}{T_0}\right)\right] + \Delta\Phi \tag{4.3}$$

with

$$\begin{aligned} \boldsymbol{\sigma} &= \varrho\frac{\partial\Phi}{\partial\boldsymbol{\varepsilon}} = \mathsf{L}(\boldsymbol{\varepsilon} - \boldsymbol{\varepsilon}^{pe}) = \mathsf{L}\boldsymbol{\varepsilon}^{e}, \\ s &= -\frac{\partial\Phi}{\partial T}\,, \\ \pi_0^f(T) &= (u_0^1 - u_0^2) - T(s_0^1 - s_0^2) = \Delta u - T\Delta s. \end{aligned} \tag{4.4}$$

π_0^f is the thermodynamic force of the martensitic transformation at stress-free state. u_o^α and s_0^α are the specific energy and entropy of the α phase ($\alpha = 1$ for the austenite and $\alpha = 2$ for the martensite).

The thermodynamical force associated to the phase transition under non-zero stress is:

$$\pi^f = -\frac{\partial\Phi}{\partial z} = \pi_0^f(T) + \gamma\overline{\sigma}/\varrho - \Phi_{it}(1 - 2z). \tag{4.5}$$

The Clausius-Duhem inequality ($\pi^f\,dz \geq 0$) is chosen to be the criterion of phase transition [4]:

$$\begin{aligned} &\text{direct transformation} \quad dz > 0 \quad \pi^f \geq 0, \\ &\text{inverse transformation} \quad dz < 0 \quad \pi^f \leq 0, \end{aligned} \tag{4.6}$$

$\pi^f = 0$ represents the absolute equilibrium states of the system. It is unstable if $\Phi_{it} > 0$, what characterizes the martensitic transformations.

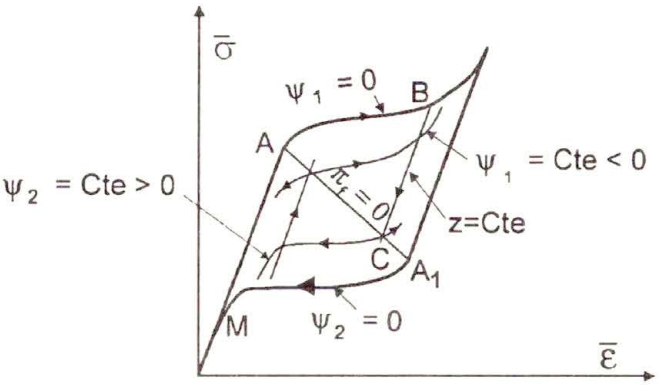

FIG. 19. Description of the external and internal loops in the model of Raniecki et al. [4].

It is then possible to determine the equivalent stress threshold of the martensitic transformation $\overline{\sigma}^{AM}$ (point A in the Fig. 19) and for the reverse transformation $\overline{\sigma}^{MA}$ (point A_1) as:

$$
\begin{aligned}
&\pi^f(\overline{\sigma}^{AM}, z=0, T) = 0 \;\Rightarrow\; \overline{\sigma}^{AM}(T) = \overline{\sigma}^{eq}(z=0) = \varrho\frac{\Phi_{it}(T) - \pi_0^f(T)}{\gamma}, \\
&\pi^f(\overline{\sigma}^{MA}, z=1, T) = 0 \;\Rightarrow\; \overline{\sigma}^{MA}(T) = \overline{\sigma}^{eq}(z=1) = \overline{\sigma}^{AM}(T) - 2\varrho\frac{\Phi_{it}(T)}{\gamma}.
\end{aligned}
\tag{4.7}
$$

The instability of the equilibrium yields the conclusion that there exists no thermodynamical relation which could give the equations of the hysteresis loop. Taking a similar framework as in the plasticity approach, the functions Ψ_1 (for the direct transformation) and Ψ_2 (for the reverse one) are assumed to be constant during the phase transition. $\Psi_1 = 0$ and $\Psi_2 = 0$ are the functions which represent the complete martensitic and reverse transformations (they describe the "external loop"). $\Psi_1 = n$ and $\Psi_2 = m$ (m and n are negative constants) represents the internal loops where the transformation is not total.

$$
\begin{aligned}
\Psi_1(\boldsymbol{\sigma}, T, z) &\equiv \pi^f(\boldsymbol{\sigma}, T, z) - k_1(z), \\
\Psi_2(\boldsymbol{\sigma}, T, z) &\equiv -\pi^f(\boldsymbol{\sigma}, T, z) + k_2(z).
\end{aligned}
\tag{4.8}
$$

The functions $k_1(z)$ and $k_2(z)$ are chosen [4] such that the kinetics of the phase transformation are in agreement with the ones proposed by metallurgists [11]:

$$
\begin{aligned}
k_1(z) &= -(A_1 + B_1 z)\ln(1-z) + C_1 z, \\
k_2(z) &= (A_2 - B_2(1-z))\ln z - C_2(1-z)
\end{aligned}
\tag{4.9}
$$

with

$$
\begin{aligned}
C_1 &= 2\Phi_{it}(M_s), \qquad & C_2 &= 2\Phi_{it}(A_s),\\
a_1A_1 &= \Delta s + \bar{s}_0, \qquad & a_2A_2 &= \Delta s - \bar{s}_0,\\
a_1B_1 &= a_2B_2 = 2\bar{s}_0.
\end{aligned}
\tag{4.10}
$$

4.2. Application to a tension-torsion proportional loading test

The behaviour is elastic as long as the equivalent stress does not reach the critical equivalent stress $\bar{\sigma}^{AM}$ $(z = 0)$:

$$
\bar{\sigma}^{AM} = (\sigma_{zz})^{AM}\sqrt{1 + 3\alpha^2}. \tag{4.11}
$$

Then the pseudoelastic behaviour must be simulated. The volume fraction of martensite is increasing from 0 to z_d, which is the z value obtained just before the unloading. The pseudoelastic flow is represented by $\Psi_1 = 0$. It gives:

$$
\pi_0^f + \gamma\bar{\sigma}/\varrho - \Phi_{it}(1 - 2z) = k_1(z). \tag{4.12}
$$

Since during the whole test tensile and torsion stresses are proportional ($\bar{\sigma} = (\sigma_{zz})\sqrt{1 + 3\alpha^2}$ with $\sigma_{z\theta} = \alpha\sigma_{zz}$), it is possible to determine the stress values from the relations

$$
\begin{aligned}
\sigma_{zz} &= \frac{\varrho}{\gamma(1 + 3\alpha^2)}\left[k_1(z) + \Phi_{it}(1 - 2z) - \pi_0^f\right],\\
\sigma_{z\theta} &= \alpha\sigma_{zz}\,.
\end{aligned}
\tag{4.13}
$$

The corresponding strains follow from (3.6) and (3.11),

$$
\begin{aligned}
\varepsilon_{zz} &= \frac{\sigma_{zz}}{E} + \gamma z,\\
\varepsilon_{z\theta} &= \sigma_{z\theta}\left(\frac{1 + \upsilon}{E} + \frac{3\gamma z}{2\bar{\sigma}}\right).
\end{aligned}
\tag{4.14}
$$

The reverse transformation is represented by the $\Psi_2 = k_2(z_d)$ curve ($k_2(z_d)$ is a negative constant) where z_d is the volumic part of martensite at the end of the loading process. So, during the unloading to the stress σ_1, the stresses are given by

$$
\begin{aligned}
\sigma_{zz} &= \frac{\varrho}{\gamma(1 + 3\alpha^2)}\left[k_2(z) - k_2(z_d) + \Phi_{it}(1 - 2z) - \pi_0^f\right],\\
\sigma_{z\theta} &= \alpha\sigma_{zz}\,.
\end{aligned}
\tag{4.15}
$$

The corresponding strains are still given by Eq. (4.14).

The seven parameters A_1, B_1, C_1, A_2, B_2, C_2 and γ which determine the functions k_1 and the k_2, Φ_{it} and π_0^f are determined from tensile loading tests described in [2] by the following constants.

Δu (Jkg^{-1})	Δs ($Jkg^{-1}K^{-1}$)	$\overline{u}_0$ (Jkg^{-1})	$\overline{s}_0$ ($Jkg^{-1}K^{-1}$)	γ	a_1 (K^{-1})	a_2 (K^{-1})
6 944	23.36	1 495	4.22	0.0416	0.032	0.06

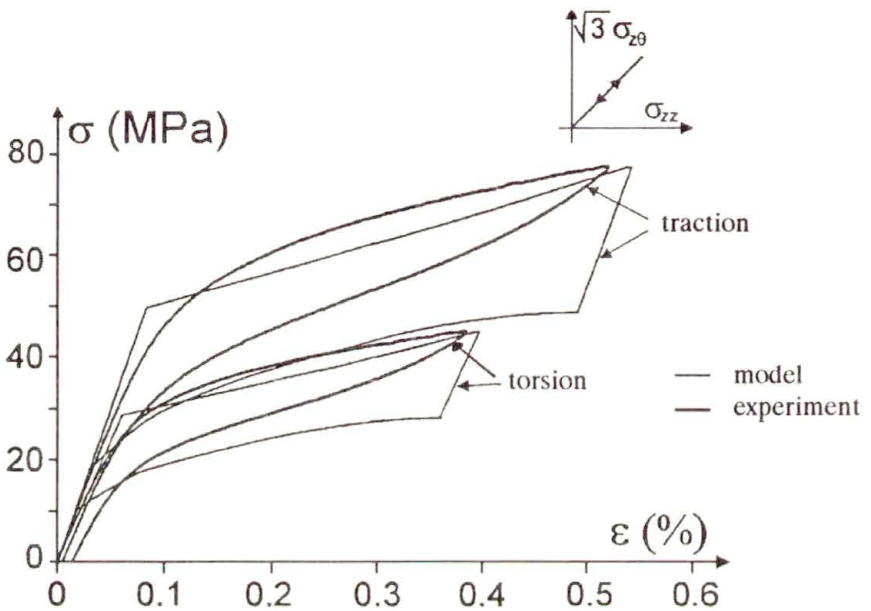

FIG. 20. Experimental and modelled curves concerning the test No. 4.

Modelling of the test No. 4 is presented in the Fig. 20. The form of the theoretical loops are acceptable but some corrections are necessary. The results prove the validity of the 3D model proposed by RANIECKI *et al.* in [4] and the proposed state equations of pseudoelasticity (3.11).

5. Conclusion

Proportional and non-proportional tests have been performed by means of a special experimental device, in order to increase the number of experimental data in the case of complex loading.

Proportional loading tests allows us to verify the normality rule for pseudoelastic strain rate, and hence it enables the experimental verification of the thermodynamical model of pseudoelastic behavior developed by RANIECKI *et al.* in [4]. In the future, other stress-strain curve simulations will be presented.

Non-proportional loading tests brought a lot of informations not easy to interprete. It shows the evidence that the pseudoelastic nonlinear behavior depends on the chosen stress path. The main physical features are the creation of new variants (called "secondary" ones) when the stress direction change, or (and) the reorientation of the first variants under the stress.

Only a microstructural observation will allow us to describe the mechanism of martensite plates displacement and creation by the stress path.

For an isothermal pseudoelastic cycling ($N_{max} = 35$), both proportional and non-proportional training processes are associated with very high efficiency values: this is a very good information for technical applications.

We believe that the analysis of such complex loading processes will help us to understand the S.M.A. pseudoelastic behaviour.

Acknowledgments

We are very grateful to M. G. LAITHIER (CNRS technician) for his precious experimental help.

References

1. L. CONTARDO, *Etude des traitements d'éducation, de la stabilité et de l'origine de l'effet mémoire double sens dans un alliage CuZnAl*, Thèse INSA Lyon, France, No. 88ISAL0048, 1988.
2. C. ROGUEDA, *Modelisation thermodynamique du comportement pseudoélastique des alliages à mémoire de forme*, Thèse Université de Franche-Comté, France, No. 336, 1993.
3. C.M. FRIEND, *The effect of applied stress on the reversible strain in CuZnAl shape memory alloys*, Scripta. Met., 20, 995–998, 1986.
4. B. RANIECKI, C. LEXCELLENT and K. TANAKA, *Thermodynamic models of pseudoelastic behaviour of shape memory alloys*, Arch. Mech., **44**, 3, 261–288, 1992.
5. P. SITTNER, K. HARA and M. TOKUDA, *Pseudoelastic deformation in combined tension and torsion*, [in:] Strength of Materials, OIKAWA *et al.* [Eds.], 319–322, 1994.
6. Z.G. WANG, *Experimental study of mechanical behaviour of Ti Ni shape memory alloys. 2. Multiaxial stress*, Acta Mech. Sinica, [to be published].
7. P. VACHER, *Etude du comportement pseudoélastique d'alliages à mémoire de forme CuZnAl polycristallins*, Thése Université de Franche-Comté, France, No. 215, 1991.
8. R. STALMANS, J.V. HUMBEECK and L. DELAEY, *The two-way memory effect in copper-based shape memory alloy – thermodynamics and mechanisms*, Acta Met. Mater., **40**, 11, 2921–2931, 1992.
9. B.C GOO, *Modélisation micromécanique du comportement thermomécanique d'alliages à mémoire de forme monocristallins et polycristallins*, Thèse Université de Franche-Comté, France, No. 491, 1995.
10. I. MULLER, H. XU, *On the pseudoelastic hysteresis*, Acta. Met. Mat, **39**, 263–271, 1991.
11. D.P. KOISTINEN and R.E. MARBURGER, *A general equation prescribing the extent of the austenite-martensite transformation in pure iron-carbon alloys and plain carbon steels*, Acta. Metall., **7**, 59–70, 1959.

LABORATOIRE DE MÉCANIQUE APPLIQUÉE R. CHALÉAT
UNIVERSITÉ DE FRANCHE-COMTÉ, BESANÇON, FRANCE.

Received February 21, 1996.

Arch. Mech., 48, 6, pp. 1047–1067, Warszawa 1996

Integral equations for disturbance propagation in linearized Vlasov plasmas Numerical results

A. J. TURSKI and J. WÓJCIK (WARSZAWA)

SPACE-TIME responses of linearized Vlasov plasmas on the basis of multiple integral equations are considered. An initial-value problem for Vlasov–Poisson/Ampere equations is reduced to one integral equation and the solution is expressed in terms of a forcing function and its space-time convolution with the resolvent kernel. The forcing function is responsible for the initial disturbance and the resolvent is responsible for the equilibrium velocity distribution. For Maxwellian equilibrium distribution, a closed-form solution of the resolvent kernel equation is still unknown but the equation is eligible for computer calculations. Three types of exact analytical solutions of the space-time resolvent equations are shown to relate them to Maxwellian plasmas. Numerical calculations reveal the nature of the plasma response as a compound of a diffusive transition, being essentially a plasma oscillation mode with plasma frequency, a Gaussian type of amplitude profiles, and also a damped dispersive wave mode. The plasma response appears immediately in the whole space of x and zeros (nodes) travel according to the diffusion law, at least for long times. By use of the resolvent equations, time-reversibility and space-reflexivity can be revealed. The step-density disturbance of electron Maxwellian plasmas appears to be the electric current forcing function, which is proportional to the Maxwellian plasma kernel; hence the resolvent is the plasma response to the step-density disturbance. From inspections of the series representations of Maxwellian resolvent and its Fourier transform, a symmetry property with respect to the transformation is found. It is used for constructing approximate formulae for the resolvent kernels.

1. Introduction

THIS ARTICLE contains a unified treatment of disturbance propagation in linearized Vlasov plasmas, based on the space-time convolution integral equations. Although there already exists a vast literature on the subject, a complete and coherent discussion of space-time plasma response in relation to equilibrium distributions of particles, especially the Maxwellian equilibrium, is still lacking. Most of the papers are dealing with dispersion relations, approximate Fourier transforms of disturbances and asymptotic evolution of time-dependent stationary waves. However, papers dealing with integral equation presentation of wave propagation in linearized plasmas appear rather seldom, see the recently published paper [1].

The problem is of a linear nature but can be considered in relation to nonlinear Langmuir waves and solitary wave excitations, where we need space-time solutions, but under simplified assumptions concerning equilibrium of plasmas and the so-called "far field" approximations, which allow us to reduce the problem to model equations, e.g. NLS, KdV, Boussinesq, see [2]. To be more specific and at the same time, to present the general issue in the simplest way, let us consider the ion-sound solitary waves in Vlasov plasmas. It can be shown [3]

that assuming a delta-Dirac velocity distribution for cold ions, "square distribution" for hot electrons, "far field" dependence of space-time in the form $x - vt$ and nonlinearity of the second order, we arrive at a Boussinesq equation for space-time propagation. The equation can be exactly solved leading to nonlinear oscillations or solitary waves. The seemingly simpler case of linear plasma of hot electrons and cold ions has no exact solution to an initial-value problem for linearized Vlasov–Poisson eqations. In Sec. 3 of the paper, we present the exact solution for the response function, but only for one-component electron plasma with square equilibrium distribution. The solution is a Riemann function for a wave equation with dispersion. The other exact solution in the case of the Lorentz equilibrium distribution of electrons is presented and the solution demonstrates "diffusive transition of oscillations". The space-time response for Maxwellian equilibrium is very important but a closed-form solution is still unknown (e.g., see [4]). The problem is easily analysed by computer calculations. There is another point of a general nature that deserves mentioning, namely, the way in which the disturbance propagation behaves. The question arises whether we are faced with diffusive transition of oscillations or with wave propagation. We shall especially focus on two distinctive features of the disturbance of the Maxwellian equilibrium. The first is that a step-density disturbance response is proportional to the resolvent kernel of our space-time convolution equations, that is a unique property of Maxwellian electron plasmas. The second feature is that the resolvent kernel is invariant with respect to the Fourier transform since the original and its transform are expandable in symmetric Hermite orthogonal series.

The article is organized as follows. In Sec. 2 analytical initial-value and one-point boundary-value problems of linearized Vlasov–Poisson/Ampere equations are reduced to equivalent two-dimensional integral equations to demonstrate the analytical approach to real functions in real space-time as compared with the Fourier-transform techniques. Section 3 is devoted to the main features of the integral equations in relation to plasma responses, dispersion relations and a presentation of exact solutions. Section 4 constitutes the main body of the article and contains a complete description of the Maxwellian plasma response based on orthogonal Hermite series presentations of the response. The computer-calculated characteristics are discussed on the basis of approximate formulae and compared with the exact solution of the "square" equilibrium case. Diffusive transition of resolvent zeros (nodes) is revealed for long time range. The final section contains the general discussion and conclusions.

2. Convolution equations for electric field, potential, current and charge density

We investigate the Vlasov–Ampere/Poisson system of equations for multicom-

ponent plasmas, i.e.

$$\left[\partial_t + u\partial_x + \frac{q_\alpha}{m_\alpha}\mathsf{E}(x,t)\partial_u\right]\mathsf{F}_\alpha(u,x,t) = 0, \qquad \partial/\partial u \equiv \partial_u \qquad \text{(Vlasov)}, \tag{2.1}$$

$$\varepsilon_0\partial_t\mathsf{E} + \sum_\alpha q_\alpha \int_{-\infty}^{\infty} u\mathsf{F}_\alpha\, du = 0, \qquad \partial/\partial x \equiv \partial_x\,, \quad \partial/\partial t \equiv \partial_t \qquad \text{(Ampere)}, \tag{2.2}$$

$$\varepsilon_0\partial_x\mathsf{E} - \sum_\alpha q_\alpha \int_{-\infty}^{\infty} \mathsf{F}_\alpha\, du = 0, \qquad \mathsf{E} = -\partial_x\phi, \qquad \text{(Poisson)}, \tag{2.3}$$

where x, u and t are independent variables of one-dimensional space, velocity and time, respectively. $\mathsf{E} = \mathsf{E}(x,t)$, $\phi = \phi(x,t)$, $\mathsf{F}_\alpha = \mathsf{F}_\alpha(u,x,t)$, q_α and m_α are electric field, potential, velocity distribution, charge and mass of α-particles, respectively. In view of (2.1), equations (2.2) and (2.3) are equivalent if appropriate constrains are applied to initial conditions for F_α. We emphasize that in order to derive the Vlasov equation, one must assume that F_α is analytic in its variables. This assumption of analyticity is reasonable since F_α is a physically measurable quantity, see [5].

Let us assume

$$\mathsf{F}_\alpha(u,x,t) \cong N_0^\alpha \mathsf{F}_{0\alpha}(u) + \mathsf{F}_{1\alpha}(u,x,t), \tag{2.4}$$

where N_0^α, $\mathsf{F}_{0\alpha}(u)$ are the equilibrium particle concentration and velocity distribution for $\mathsf{E} = 0$, and $\mathsf{F}_{1\alpha}$ is of the order E.

Substituting (2.4) into (2.1), we derive the well-known linear equation

$$(\partial_t + u\partial_x)\mathsf{F}_{1\alpha} = -(N_0^\alpha q_\alpha/m_\alpha)\mathsf{E}\partial_u\mathsf{F}_{0\alpha}\,. \tag{2.5}$$

For the initial-value problem

$$\mathsf{F}_{1\alpha}(u,x,0) = g_\alpha(u,x), \qquad g_\alpha(u,x=\pm\infty) = 0 \tag{2.6}$$

$$\text{and} \qquad \mathsf{E}(x,t) = 0 \quad \text{for} \quad t \le 0$$

we write the solution of Eq. (2.5)

$$\mathsf{F}_{1\alpha} = -(N_0^\alpha q_\alpha/m_\alpha)\mathsf{F}'_{0\alpha}(u)\int_0^t \mathsf{E}(x-ut_1, t-t_1)\, dt_1 + g_\alpha(u, x-ut). \tag{2.7}$$

Substituting into (2.2), we have

$$\partial_t\mathsf{E} = \sum_\alpha \omega_\alpha^2 \int_{-\infty}^{\infty} u\mathsf{F}'_{0\alpha}(u)\int_0^t \mathsf{E}(x-ut_1, t-t_1)\, dt_1\, du \tag{2.8}$$

$$-\sum_\alpha (q_\alpha/\varepsilon_0)\int_{-\infty}^{\infty} u g_\alpha(u, x-ut)\, du$$

where $\omega_\alpha^2 \equiv N_0^\alpha q_\alpha^2/\varepsilon_0 m_\alpha$, and changing variables of integration in Eq. (2.8) as follows: $tu = \xi$, $t\,du = d\xi$, then integrating by parts, we obtain

$$\mathsf{E}(x,t) = \int_0^t dt_1 \int_{-\infty}^{\infty} \mathsf{K}(x,\xi)\mathsf{E}(x-\xi, t-t_1)\,d\xi\,dt_1 + G(x,t), \tag{2.9}$$

where

$$G(x,t) = -\sum_\alpha (q_\alpha/\varepsilon_0) \int_0^t \int_{-\infty}^{\infty} u g_\alpha(u, x-ut_1)\,du\,dt_1, \qquad \text{for} \quad t \geq 0,$$

and

$$\mathsf{K}(x,t) = -\sum_\alpha \omega_\alpha^2 \mathsf{F}_{0\alpha}(x/t).$$

More detailed derivation of Eq. (2.9) can be found in [6–8].

It is worth noting that the charge density, electric current and electric potential satisfy the same equations with the same kernel $\mathsf{K}(x,t)$ but with the respective forcing functions.

In the same way, we can derive the following integral equation, see [7].

$$\overline{\mathsf{E}}(x,t) = \int_0^x d\xi \int_{-\infty}^{\infty} \overline{\mathsf{K}}(\xi,t_1)\overline{\mathsf{E}}(x-\xi, t-t_1)\,dt_1 + \overline{G}(x,t) \tag{2.10}$$

for the one-point boundary value-problem

$$\mathsf{F}_{1\alpha}(u,x,t) = \overline{g}_\alpha(u,t) \quad \text{for} \quad x = 0, \qquad \overline{\mathsf{E}}(x,t) = 0 \quad \text{for} \quad x \leq 0,$$

where

$$\overline{\mathsf{K}}(x,t) = -\sum_\alpha \omega_\alpha^2 \left[\mathsf{F}_{0\alpha}\left(\frac{x}{t}\right) - \mathsf{F}_{0\alpha}(0)\right]$$

and

$$\overline{\mathsf{G}}(x,t) = -\sum_\alpha \frac{q_\alpha}{\varepsilon_0} \int_0^x d\xi \int_{-\infty}^{\infty} \overline{g}\left(u, t - \frac{\xi}{u}\right) du.$$

Taking space-Fourier transform of (2.9) one can derive one-dimensional Volterra integral equations for plasma density and plasma in an external electric ield obtained in [1], where complex space-Fourier components are assumed. Similarly, time-Fourier transform of (2.10) leads to the planar case of the forced oscillatons investigated in [1]. We have derived here equations (2.9) and (2.10) analyticully, without use of the Fourier–Laplace transform technique. It guarantees analyticity, existence and uniqueness of the solutions.

The existence and uniqueness of an analytic solution of Eq. (2.5) is determned by $g_\alpha(u,x)$ alone. The fact that we are given an independent function $\overline{g}_\alpha(\iota,t)$ does not contradict this statement since the solution is not necessarily anaytic along the characteristic $x = ut$.

3. Properties of convolution equations in plasma context

Space-time convolution equations (2.9) can be solved by use of resolvent (reciprocal) kernels $\mathsf{R}(x,t)$. We write the solution in the form

$$\mathsf{E}(x,t) = G(x,t) + \int_0^t dt_1 \int_{-\infty}^{\infty} \mathsf{R}(x-\xi, t-t_1) G(\xi, t_1)\, d\xi, \tag{3.1}$$

where $G(x,t)$ is a forcing function and $\mathsf{R}(x,t)$ satisfies the following resolvent equation

$$\mathsf{R}(x,t) = \mathsf{K}(x,t) + \int_0^t dt_1 \int_{-\infty}^{\infty} \mathsf{K}(x-\xi, t-t_1) \mathsf{R}(\xi, t_1)\, d\xi. \tag{3.2}$$

The last equation describes plasma dynamic response $\mathsf{R}(x,t)$ and its functional dependence of the plasma equilibrium state only. We note that for the infinite support $x \in (-\infty, \infty)$ of a kernel $\mathsf{K}(x,t)$, the resolvent $\mathsf{R}(x,t)$ also possesses the infinite support $x \in (-\infty, \infty)$. The physical consequence of the property is that the plasma response to any disturbance, even if with a limited support, appears immediately in the full space $x \in (-\infty, \infty)$. On the ground of Eq. (3.2) we note, that for $\mathsf{K}(x,t) = \mathsf{K}(x,-t)$ it follows that $\mathsf{R}(x,t) = \mathsf{R}(x,-t)$ and for $\mathsf{K}(x,t) = \mathsf{K}(-x,t)$ we have $\mathsf{R}(x,t) = \mathsf{R}(-x,t)$. The property is reversible with respect to $\mathsf{R}(x,t)$ and $\mathsf{K}(x,t)$. It is called time reversibility and space reflexivity.

3.1. Dynamic response of Maxwellian plasmas to step-density disturbances

It is obvious, that the resolvent kernel can be considered as a response to the Dirac-delta disturbances $\delta(t)\delta(x)$ and sometimes the resolvent kernel is misnamed a Green function.

We show that a step-density disturbance of Maxwellian plasma will now become proportional to the kernel $\mathsf{K}(x,t)$ and according to Eqs. (3.1) and (3.2), it leads to plasma response being the resolvent. Considering the electric current forcing disturbance

$$G_J(x,t) \equiv \mathsf{J}_0(x,t) \equiv \sum_\alpha q_\alpha \int_{-\infty}^{\infty} u g_\alpha(u, x-ut)\, du \tag{3.3}$$

for multi-component plasmas, we have the following step-density disturbance

$$\sum_\alpha g_\alpha(u,x) = \sum_\alpha \Delta N_\alpha \mathsf{F}_{0\alpha}(u) H(x), \tag{3.4}$$

where $H(x)$ is the Heaviside unit-step function, and

$$\mathsf{F}_{0\alpha}(u) = a_\alpha \pi^{-1/2} \exp(-u^2 a_\alpha^2), \qquad \alpha = e, i, \tag{3.5}$$

where $\langle u_\alpha^2 \rangle = 1/2a_\alpha^2$.

Roughly speaking, the disturbance can be realized in double- or triple- plasma devices.

According to (3.3), we have

$$\mathsf{J}_0(x,t) = \sum_\alpha q_\alpha \int_{-\infty}^{\infty} u\mathsf{F}_{0\alpha}(u)H(x-ut)\,du$$

and by virtue of

$$(3.6) \qquad u\mathsf{F}_{0\alpha}(u) = -\mathsf{F}'_{0\alpha}(u)/2a_\alpha^2, \qquad \text{since} \qquad \mathsf{F}_\alpha(u) \sim \exp(-a_\alpha^2 u^2)$$

we have

$$\int_{-\infty}^{\infty} u\mathsf{F}_{0\alpha}(u)H(x-ut)\,du = -(1/2a_\alpha^2)\mathsf{F}_{0\alpha}\left(\frac{x}{t}\right)$$

and

$$\mathsf{J}_0(x,t) = -\sum_\alpha A_\alpha \mathsf{F}_{0\alpha}(x/t) \simeq -A_e\mathsf{F}_{0e}(x/t),$$

where $A_\alpha = \Delta N_\alpha q_\alpha/2a_\alpha^2$. Neglecting the ion contribution to the electron plasma oscillations in view of the equation

$$\mathsf{J}(x,t) = \mathsf{J}_0(x,t) + \int_0^t dt_1 \int_{-\infty}^{\infty} \mathsf{R}(x-\xi, t-t_1)\mathsf{J}_0(\xi,t_1)\,d\xi$$

and Eq. (3.2), we have

$$\mathsf{J}(x,t) \simeq (A_e/\omega_e^2)\mathsf{R}(x,t).$$

The dynamic response of electron plasmas to the step-density disturbance is proportional to the resolvent $\mathsf{R}(x,t)$. It takes place uniquely only for Maxwelian plasmas because of relation (3.6). In order to obey linearization assumptions, the step-density ΔN must be small enough in relation to N_0.

3.2. Exact solutions

The advantage of the integral equation treatment of Vlasov plasmas consists in obtaining the solutions separately composed of the forcing function $G(x,t)$ resulting from the initial value disturbance $g(u,t)$, and the resolvent kernel depending only on the plasma equilibrium $\sum_\alpha \mathsf{F}_{0\alpha}(u)$. It opens up new possibilities for computer calculations. One may expect readily available computer program, say for PC, calculating and graphically illustrating resolvents, forcing functions and convolutions of these functions for real time and space. First of all, we review exact and approximate solutions for resolvent kernels and compare them with numerical results.

Assuming the hot electron plasma with the so-called "square" electron equilibrium velocity distribution

$$\mathsf{F}_{0e}(u) = \big[\mathsf{H}(u+\alpha) - \mathsf{H}(u-\alpha)\big]/2\alpha,$$

we have

$$\mathsf{K}(x,t) = -\omega_0^2\big[\mathsf{H}(x+\alpha t) - \mathsf{H}(x-\alpha t)\big]/2\alpha,$$

and the transforms of the kernel are

$$\begin{aligned} \mathsf{K}(k;t) &= -(\omega_0^2/\alpha k)\sin(k\alpha t), \\ \mathsf{K}(k;s) &= -\omega_0^2/(s^2 + k^2\alpha^2). \end{aligned} \tag{3.8}$$

The resolvent kernel can be readily calculated as follows:

$$\begin{aligned} \mathsf{R}(k;t) &= -\frac{\omega_0^2}{(\omega_0^2 + k^2\alpha^2)^{1/2}} \sin\big[(\omega_0^2 + k^2\alpha^2)^{1/2} t\big], \\ \mathsf{R}(k;s) &= -\frac{\omega_0^2}{s^2\omega_0^2 + k^2\alpha^2}, \end{aligned} \tag{3.9}$$

and

$$\mathsf{R}(x,t) = \begin{cases} -(\omega_0^2/2\alpha)\mathsf{J}_0\big[\omega_0(t^2 - x^2/\alpha^2)^{1/2}\big] & \text{for} \quad t^2 \geq x^2/\alpha^2, \\ 0 & \text{elsewhere.} \end{cases} \tag{3.10}$$

The dispersion relation takes the form

$$\mathsf{D}(k;s) \equiv 1 - \mathsf{K}(k;s) = (s^2 + \omega_0^2 + k^2\alpha^2)/(s^2 + k^2\alpha^2) = 0.$$

Substituting $s = -i\omega$ and since $\langle u^2\rangle = \alpha^2/3$, we have the well-known Bohm – Gross dispersion relation, see also [2],

$$\omega^2 \simeq \omega_0^2 + 3\langle u^2\rangle k^2.$$

We note, that $\mathsf{K}(x,t)$ and $\mathsf{R}(x,t)$ are time reversible and x-space reflexive and the resolvent is an undamped dispersive wave, i.e. the Riemann function of the following dispersive wave equation

$$\big(\alpha^2\partial_{xx} - \partial_{tt} + \omega_0^2\big)\mathsf{R}(x,t) = 0. \tag{3.11}$$

The asymptotic expansion of the function is

$$\mathsf{R}(x,t) \simeq -\omega_0(4\pi Dt)^{-1/2}\sin(\omega_0 t + \pi/4), \qquad t \to \infty, \tag{3.12}$$

where $D = 3\langle u^2\rangle/2\omega_0$. It appears that the asymptotic formula is common for all resolvents in cases of equilibrium velocity distributions possessing all moments and the mean-square velocity being $\langle u^2\rangle$. We do not present here the proof of these properties.

The next exact solution known to us is the resolvent for the Lorentz electron plasma. The equilibrium distribution is

$$\mathsf{F}_0(u) = \frac{1}{\pi}\frac{\lambda}{\lambda^2 + u^2}$$

where λ is a positive parameter. The distribution has some unrealistic features, for instance, infinite mean-square velocity, but many authors consider it to be of interest. A generalized Lorentzian distribution (possessing a finite number of moments) is useful for modelling plasma with a high-energy tail that typically occurs in space [9].

We quote results of papers [6, 7] presenting kernels

$$\begin{aligned} \mathsf{K}(x,t) &= -(\omega_0^2/\pi)\,\lambda/(\lambda^2 + u^2)\Big|_{u=x/t}, \\ \mathsf{K}(k;t) &= -\omega_0^2 t\exp(-|k|\lambda t), \end{aligned} \tag{3.13}$$

and resolvents

$$\begin{aligned} \mathsf{R}(x,t) &= -(\omega_0/t)\mathsf{F}_0(x/t)\sin(\omega_0 t), \\ \mathsf{R}(k;t) &= -\omega_0\Big[\exp(-|k|\lambda t)\Big]\sin(\omega_0 t). \end{aligned} \tag{3.14}$$

The resolvent is drastically different from the previous one. It does not exhibit wave propagation and there is no dispersion relation. We observe a rather "diffusive transition" of oscillations. The amplitude $t^{-1}\cdot\mathsf{F}_0(x/t)$ of oscillations does obey the Chapman-Kolmogoroff equation (see Eq. (4.12) and [6]). Wave damping has no meaning, but time reversibility and space reflexivity are preserved.

Let us note that for the kernels

$$\begin{aligned} \mathsf{K}(x,t) &= -\omega_0^2(t/4\pi D)^{1/2}\exp(-x^2/4Dt), \\ \mathsf{R}(x,t) &= -\omega_0(4\pi Dt)^{-1/2}\Big[\exp(-x^2/4Dt)\Big]\sin(\omega_0 t), \end{aligned} \tag{3.15}$$

Equation (3.2) is satisfied. The example exhibits a pure diffusive transition of oscillations. However there is no equilibrium velocity distribution $\mathsf{F}_0(u)$, which could be regained from the kernel (3.15), and there is no time reversibility.

4. Maxwellian plasmas

Maxwellian equilibrium distribution (3.5) is considered to be most appropriate but analytically almost intractable. In this section, Maxwellian plasmas are analysed by means of approximate formulae and computer diagram presentations.

For numerical calculations we introduce dimensionless variables, based on the following characteristic quantities; $\omega_0 = 2\pi f_0$ [1/s]-plasma frequency, $\langle u^2 \rangle = 1/2a^2$ [m^2/s^2]-square of thermal velocity, $\lambda_D = 2\pi/k_D = 2\pi\langle u^2\rangle/\omega_0$ [m]-Debye length.

We scale the independent and dependent variables as follows:

$$X = k_D x = 2\pi x/\lambda_D \ [\pi], \qquad T = \omega_0 t \ [\pi], \qquad K = k/k_D, \qquad \tau_o = 1/f_0,$$

$$\mathsf{K}(X,T) = (1/a)\mathsf{K}(x,t), \qquad \mathsf{R} = (1/a)\mathsf{R}(x,t).$$

Before commenting on the computer plots we would like to remind the reader that the amplitudes of all physical quantities are arbitrary, as in all linear theories.

Following [7], we may write

$$\mathsf{R}(k;t) \simeq -\omega_0 \sin(\omega_0(1 + 3k^2/4a_e^2\omega_0^2)t)\exp(-s_L(k)t), \qquad k \to 0, \tag{4.1}$$

where $s_L(k)$ is the Landau damping [10] and by virtue of the method of stationary phase, the asymptotic expansion takes the form

$$\mathsf{R}(x,t) \simeq -\omega_0(4\pi Dt)^{-1/2}\sin(\omega_0 t + \pi/4) \qquad \text{for} \quad t \to \infty \tag{4.2}$$

and $D = 3/4a_e^2\omega_0 = 3\langle u^2\rangle/2\omega_0$. We observe that the Landau damping has no influence on the asymptotic formula (4.2) since $s_L(k)$ and all its derivatives disappear as $k \to 0$ and, according to stationary phase method, it does not appear in Eq. (4.2), which is identical with that of undamped waves (3.12).

According to our numerical results, the effect of Landau damping is insignificant up to $K = 0.2$ but for $K = 0.25$ the damping rate reduces the amplitude of $\mathsf{R}(K,T)$ to approximately one half for each $50\tau_0$-interval, so that for $150\tau_0$, the amplitude is smaller a little less than 8 times. In the case of $K = 0.3$ the damping rate is drastically increased and the amplitude decreases 50, 70 and 90 times for the succesive intervals of $50\tau_0$, that is about $3{\cdot}10^5$ times for the whole $150\tau_0$ interval.

The properties of the damping phenomena of the resolvent F-transforms are summarized in Fig. 1. It refers to the behaviour of the resolvent as a function of K for fixed values of dimensionless T. We observe that in the vicinity of $K = 0.2$, a rapid increase of the damping rate starts. The distributions of zeros (nodes) of $\mathsf{R}(K,T)$ is in general agreement with the approximate formula (see Eq. (4.1)). The last feature should be emphasized as it also takes place for $\mathsf{R}(x,t)$, see formula (4.9). For comparison, the resolvent $\mathsf{R}(K,T)$ of the undamped dispersive wave, Eq. (3.9), is shown in Fig. 2.

Figures 3 and 4 refer to the behaviour of the Maxwellian resolvent $\mathsf{R}(X,T)$ versus time T for fixed values of dimensionless X. To comment on the diagrams we recall Eq. (3.15). According to the graphs of Figs. 3 and 4, we do not observe the wave fronts, which could be distinguished like in Fig. 5, where the $\mathsf{R}(X,T)$ of

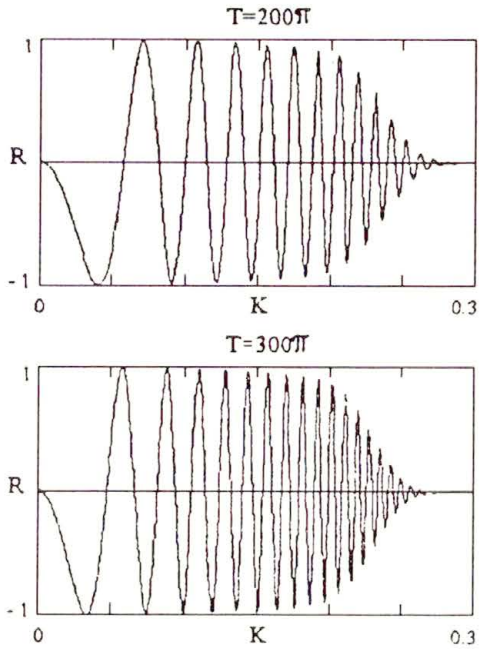

FIG. 1. Maxwellian plasma Fourier transforms $R(K,T)$ vs K for $T = 200\pi$, 300π.

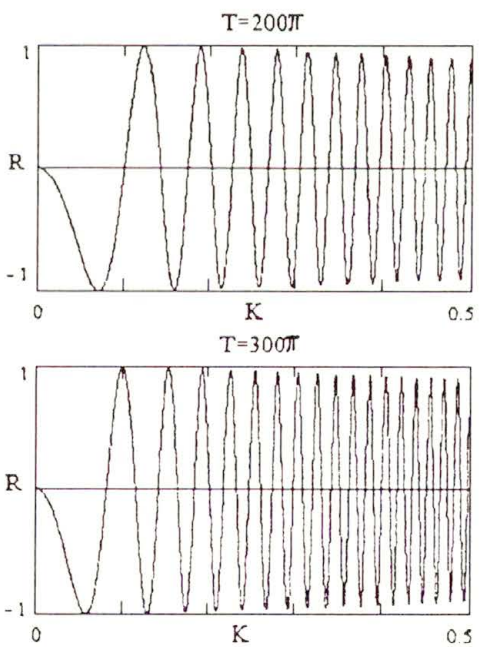

FIG. 2. Fourier transforms of Riemann's functions $R(K,T) = -(\sin(T(1 + K^2)))/(1 + K^2)^{1/2}$ vs K for $T = 200\pi$, and 300π.

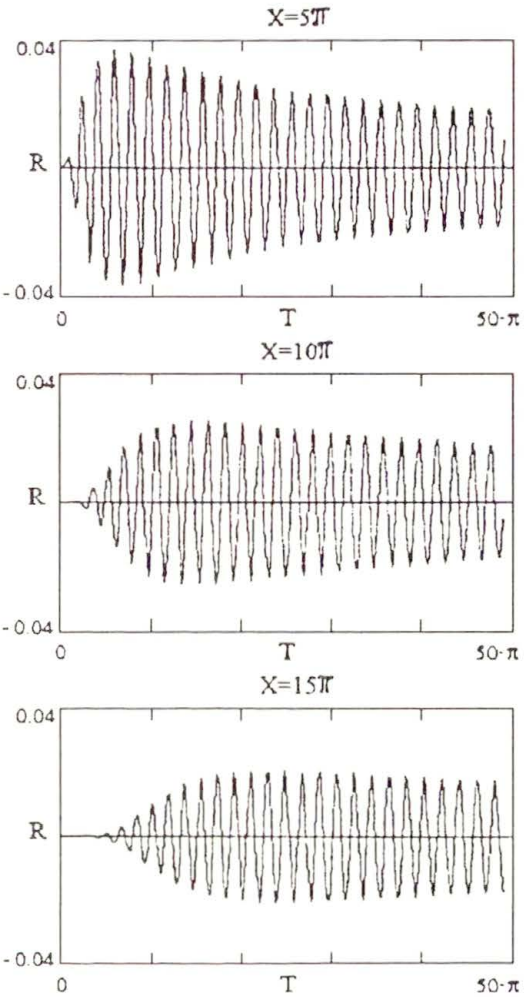

FIG. 3. Resolvent kernels of Maxwellian plasma $\mathrm{R}(X,T)$ vs T for $X = 5\pi$, 10π, and 15π.

"square" equilibrium is exhibited. However, there are two characteristic features of the Maxwellian resolvent profiles. The time period is slightly less than the electron plasma period τ_0 at the begining of time scale, but later on is equal to the period with computed accuracy. The second feature is that the profiles of amplitude envelopes behave according to the Gaussian distribution, that is like $A_x T^{-1/2} \exp(-B_x/T)$, where A_x and B_x are constant values for fixed values of X. These features are in agreement with the formula (3.15).

To discuss the remaining diagrams we need to use the formulae, which could explain the $\mathrm{R}(X,T)$ characteristics versus X for fixed values of T_n. One can note the striking resemblance between the $\mathrm{R}(K,T)$ and $\mathrm{R}(X,T)$ characteristics for fixed values of T_n.

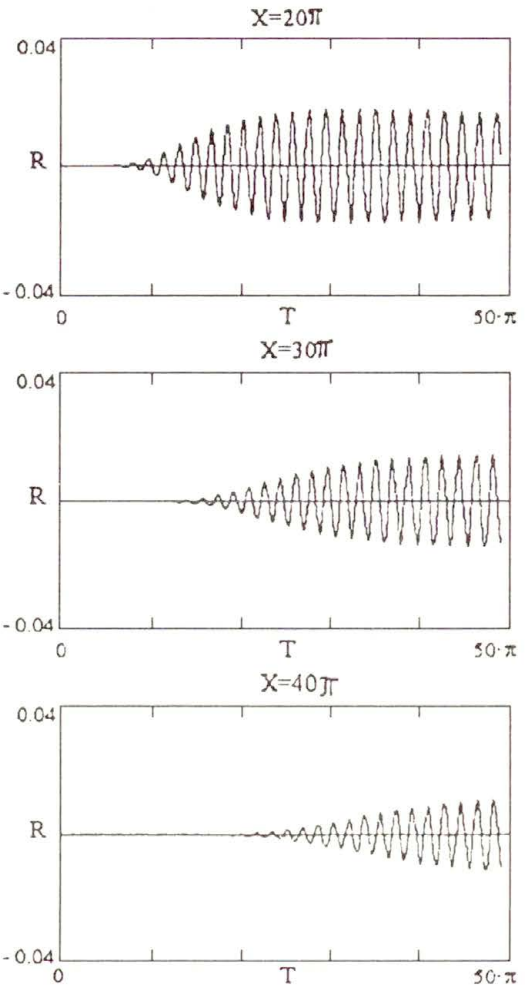

FIG. 4. Resolvent kernels of Maxwellian plasma $R(X,T)$ vs T for $X = 20\pi$, 30π, and 40π.

The Maxwellian kernel can be expanded in the following Taylor series

$$\mathsf{K}(x-\xi) = \mathsf{K}(x) + \xi\mathsf{K}'(x) + (\xi^2/2!)\mathsf{K}''(x) + \ldots = \sum_{l=0}^{\infty}(\xi^l/l!)\mathsf{K}^{(l)}(x). \tag{4.3}$$

We note, that

$$\mathsf{K}(x) = -\omega_0^2 a\pi^{-1/2} H_0(Z)\exp(-Z^2),$$
$$\mathsf{K}^{(l)}(x) = -\omega_0^2 a\pi^{-1/2} H_l(Z)\exp(-Z^2),$$

where $Z = ax/t$ and Hermite polynomials $H_l(Z)$ are determined by the formula

$$H_l(x) = (-1)^l e^{x^2}\frac{d^l}{dx^l}e^{-x^2}.$$

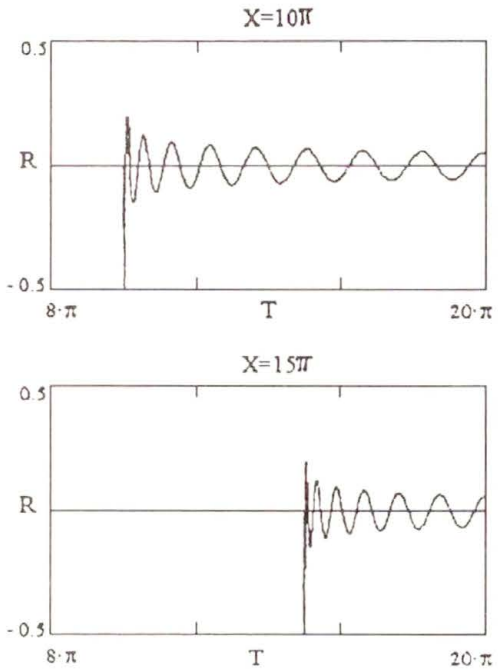

FIG. 5. Resolvent kernels for "square" velocity equilibrium; $\mathrm{R}(X,T) = -0.5\mathrm{J}_0((T^2 - X^2)^{1/2})$ vs T for $X = 10\pi$ and 15π.

Substituting (4.3) into Eq. (3.1), we have

$$\mathrm{R}(x,t) = -\omega_0^2 a\pi^{-1/2}\left[e^{-Z^2} + \sum_{n=0}^{\infty}\frac{1}{(2n)!}\int_0^t r_{2n}(t-t_1)\left(\frac{a}{t_1}\right)^{2n} \times H_{2n}(Z_1)e^{-Z_1^2}\,dt_1\right], \tag{4.4}$$

where

$$Z_1 = ax/t_1\,,$$

$$r_{2n}(t) = \int_{-\infty}^{\infty} x^{2n}\mathrm{R}(x,t)\,dx,$$

$$\int_{-\infty}^{\infty} x^m \mathrm{R}(x,t)\,dx = \int_{-\infty}^{\infty} x^m \mathrm{K}(x,t)\,dx = 0 \qquad \text{for odd } m.$$

Equations determining $r_{2n}(t)$ can be derived by multiplying Eq. (3.2) by x^{2n} and integrating it with respect to x. The first two solutions are

$$r_0(t) = -\omega_0 \sin(\omega_0 t), \qquad r_2(t) = -2\omega_0 D\left[\sin(\omega_0 t) - \omega_0 t\cos(\omega_0 t)\right].$$

The Fourier transform of Eq. (3.2) takes the form

$$\mathsf{R}(k;t) = \mathsf{K}(k,t) + \int_0^t \mathsf{K}(k,t-t_1)\mathsf{R}(k;t_1)\,dt_1\,, \tag{4.5}$$

where

$$\mathsf{K}(k;t) = -\omega_0^2 t \exp(-p^2t^2), \qquad p^2 = k^2/4a^2,$$

and proceeding like in the previous case, i.e substituting the Taylor series for $\mathsf{K}(k;t-t_1)$ into Eq. (4.5), we obtain

$$\mathsf{R}(k;t) = -\omega_0^2\left[te^{-p^2t^2} + \sum_{n=0}^{\infty}\frac{1}{(2n)!}\int_0^t r_{2n}(t-t_1)\left(\frac{a}{t_1}\right)t_1 H_{2n}(pt_1)e^{-p^2t_1^2}d_1\right]. \tag{4.6}$$

Equations (4.4) and (4.6) are symmetric and invariant with respect to the Fourier transform, due to the Hermite function properties. The following changes of variables lead from $\mathsf{R}(k;t)$ to $\mathsf{R}(x,t)$ and conversely,

$$\begin{aligned} te^{-p^2t^2}H_{2n}(pt) &\rightleftharpoons (a/\pi^{1/2})e^{-Z^2}H_{2n}(Z), \\ \frac{a}{\pi^{1/2}}e^{-Z^2} &\rightleftharpoons te^{-p^2t^2}. \end{aligned} \tag{4.7}$$

From relation (4.5) it is evident that $R(k,t)/p$ is a function of pt only for a fixed value of ω_0^2/p^2, and this property was also exhibited by the numerically calculated plots in [1]. The property of (4.7) will be exploited to derive an approximate formula for $\mathsf{R}(x,t)$ by use of an approximate expression for $\mathsf{R}(k;t)$. By virtue of the dispersion relation

$$\omega^2 \simeq \omega_0^2(1 + 6p^2/\omega_0^2 + 60p^4/\omega_0^4 + \ldots), \qquad p \to 0$$

and following the derivation of Eq. (4.1), we have

$$\mathsf{R}(k;t) \simeq \omega_0 e^{-s_L(k)t}\sin(\omega_0^2t^2 + 6p^2t^2 + 60p^4t^4/\omega_0^2t^2)^{1/2} \qquad \text{for} \quad p \to 0, \tag{4.8}$$

where $s_L(k)$ is a damping coefficient.

In view of the symmetry (4.7) we may expect the following approximate formula

$$\mathsf{R}(x,t) \simeq -(\omega_0 a/\pi^{1/2}t)e^{-\beta(x,t)}\sin(\omega_0 t(1 + 6X^2 + \ldots)^{1/2}) \qquad \text{for} \quad t \to \infty, \tag{4.9}$$

where $X = xa/\omega_0t^2$ and $\beta(x,t)$ is a damping rate. Analytical expression for $\beta(x,t)$ is not known.

Analyzing Figs. 6 and 7, we note that for $X = 0$ and fixed $T_n = 30\pi$, 50π, 100π, 200π and 300π, the amplitudes behave according to the asymptotic relaton

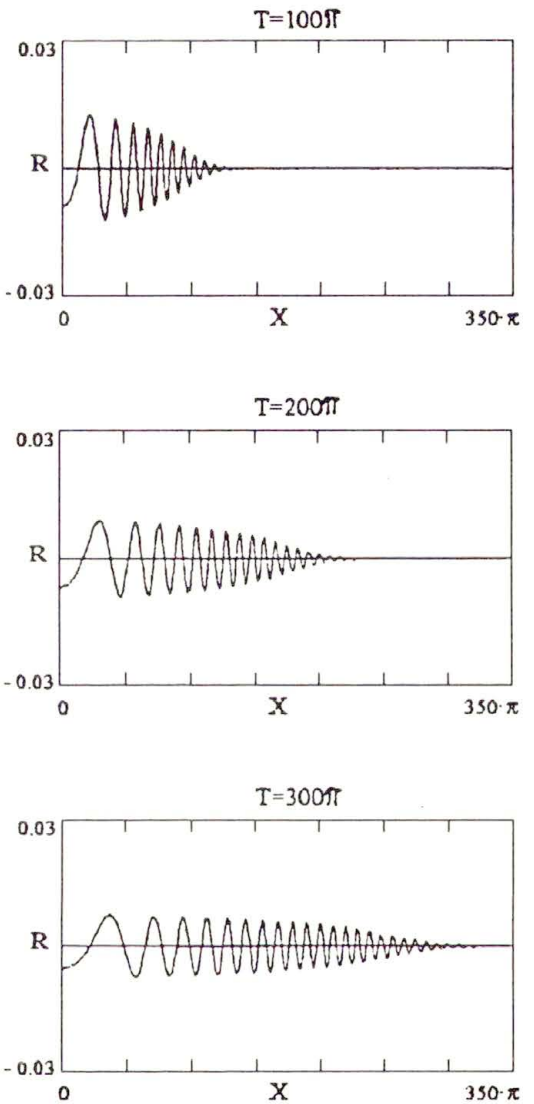

FIG. 6. Maxwellian plasma resolvent kernels $\mathrm{R}(X,T)$ vs X for $T = 100\pi$, 200π, and 300π.

(4.2), that is $\mathrm{R}_n \simeq CT_n^{-1/2}\sin(T_n + \pi/4)$ where C is a constant. We conclude that for $T_n \geq 30\pi$ and X small enough, the Maxwellian resolvent behaves qualitatively in accordance with the formula (4.9).

The characteristic feature of the curves in Figs. 6–8 is a distribution of resolvent zeros (nodes) for fixed time T and $x > 0$ according to (4.9). First of all we can not find such values of T that $\mathrm{R}(x,T)$ is zero for all x, $x \in (-\infty,\infty)$, as in the case of diffusive transitions of oscillations (see Eq. (3.14) and (3.15)), where $\mathrm{R}(x,\omega_0 t = m\pi) = 0$ for $x \in (-\infty,\infty)$.

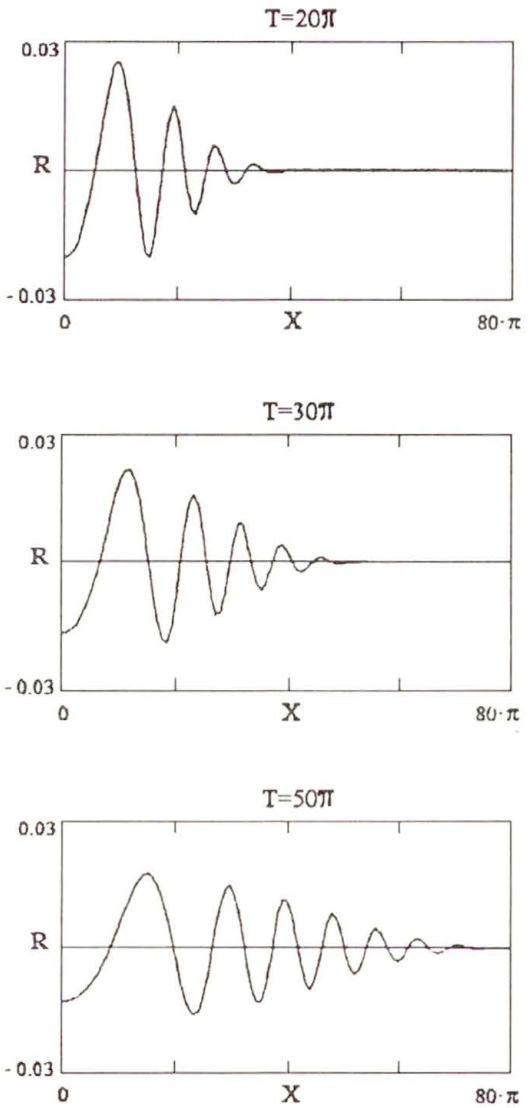

FIG. 7. Maxwellian plasma resolvent kernels $R(X,T)$ vs X for $T = 20\pi$, 30π, and 50π.

Also, a wave front is not marked contrary to the case of square equilibrium, see Fig. 9. The rate of spatial damping of the signal versus X is high for shorter times, i.e. $T_n = \pi$, 6π, $9\,1/6\pi$ and 20π, Figs. 7, 8. For $T_n = 50\pi$, 100π, 200π and 300π the rate of damping is nearly linear.

In the case of a dispersive wave, Eq. (3.10), the wave front propagates with velocity α but zeros are subject to dispersion and travel with the following velocities: $v_m = dx/dt = \alpha(1 - \kappa_m^2/\omega_0^2 t^2)^{-1/2}$, where $J_0(\kappa_m) = 0$ and for $(\kappa_m/\omega_0 t)^2 > 1$, $R(x,t) = 0$. In the case of Maxwellian plasmas, $v_m \simeq (m\pi/a)(6(1-\omega_0^2 t^2/m^2\pi^2))^{-1/2}$

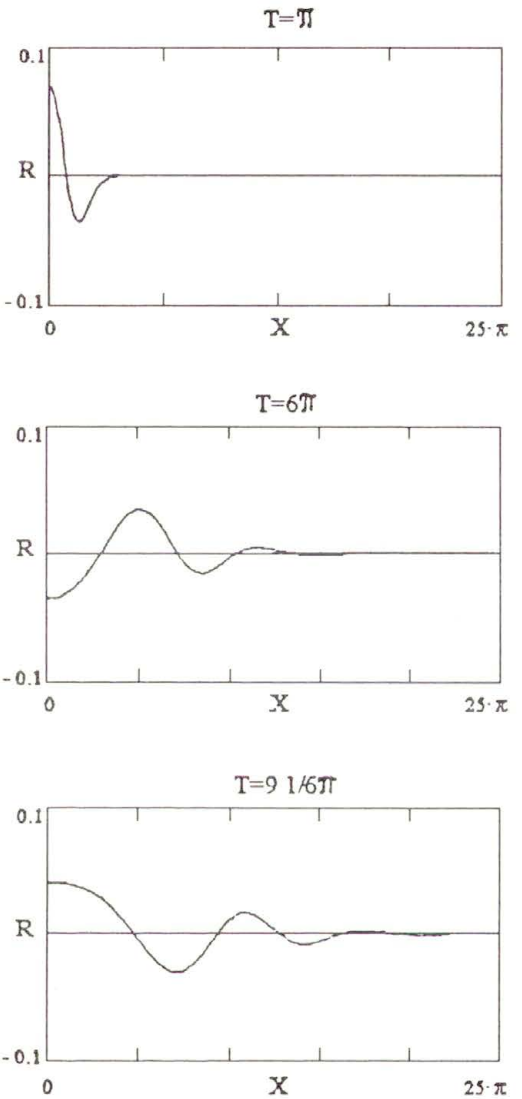

FIG. 8. Maxwellian plasma resolvent kernels $R(X, T)$ vs X for $T = \pi$, 6π, and $9\ 1/6\pi$.

according to Eq. (4.9), which is an asymptotic relation for $\omega_0 t/m\pi \gg 1$, hence v_m are purely imaginary.

By use of Eq. (4.9), we may write

$$\omega_0 t(1 + 6x^2a^2/\omega_0^2 t^4)^{1/2} \simeq \omega_0 t + 3x^2a^2/\omega_0 t^3.$$

If $6x^2a^2/\omega_0^2 t^4 \ll 1$ and denoting $X^2 = 6x^2a^2/t^2$, $T = \omega_0 t$, the equation

$$\sin(T + (1/2)X^2/T) = 0$$

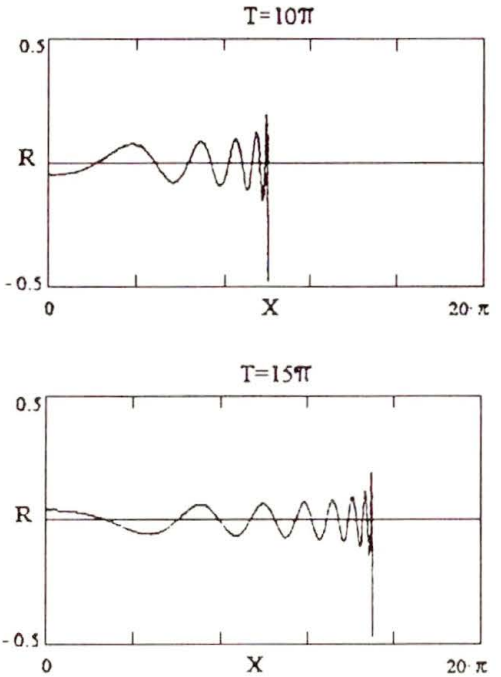

FIG. 9. Resolvent kernel for "square" velocity equilibrium; $\mathsf{R}(X,T) = -0.5\mathrm{J}_0((T^2 - X)^{1/2})$ vs X for $T = 10\pi$ and 15π.

must be satisfied. According to computer calculations, at least in the range $T_n = 100\pi \div 300\pi$, we have

$$X^2_{m,n} \simeq 2T_n d_m\,, \qquad d_m \simeq \pi + 3m\pi, \qquad m = 0,1,2...$$

hence, we may write

$$\frac{X^2_{m,n+1} - X^2_{m,n}}{T_{n+1} - T_n} \simeq 2d_m\,, \qquad X^2_{m,n}/X^2_{m,n+1} \simeq T_n/T_{n+1}\,. \tag{4.10}$$

We conclude, that the m-th zero (node) of the resolvent is moving along the X-axis in accordance with the law of diffusive transition. We note that the m-th zero is related to the m-th diffusive constant, $d_m = \pi + 3m\pi$.

Finally, we emphasize the fundamental difference between a diffusive transition of oscillations and wave propagation, both being based on our convolution equations, which uniquely transform the kernel $\mathsf{K}(x,t)$ into the respective resolvent $\mathsf{R}(x,t)$.

If we assume the solution in the form

$$\mathsf{R}(x,t) = -\omega_0 \varrho(x,t) sin(\omega_0 t),$$

where

$$\int_{-\infty}^{\infty} \varrho(x,t)\,dx = 1,$$

then Eq. (3.2) takes the form

$$\mathsf{F}_0(x,t) - t\varrho(x,t) = \omega_0 \int_0^t dt_1 (t-t_1)\sin(\omega_0 t_1) \times \left[\int_{-\infty}^{\infty} \varrho(x_1,t_1)\frac{\mathsf{F}_0(x-x_1,t-t_1)}{t-t_1}dx_1 - \varrho(x,t)\right], \tag{4.11}$$

where $\mathsf{K}(x,t) = -\omega_0^2 \mathsf{F}_0(x,t)$,

$$\sin(\omega_0 t) = \omega_0 t - \omega_0^2 \int_0^t (t-t_1)\sin(\omega_0 t_1)\,dt_1 .$$

If $\varrho(x,t) = (1/t)\mathsf{F}_0(x,t)$, then the resolvent equation implies the following Chapman-Kolmogoroff equation

$$\int_{-\infty}^{\infty} \varrho(x-x_1,t-t_1)\varrho(x_1,t_1)\,dx_1 = \varrho(x,t) \tag{4.12}$$

and

$$\int_{-\infty}^{\infty} x^2 \varrho(x,t)\,dx = 2Dt. \tag{4.13}$$

The equation (4.12) possesses a unique solution (see Eq. (3.15)). When the integral (4.13) does not exist (e.g. unlimited energy), then Eq. (4.12) can possess different solutions, (see Eq. (3.13) and (3.14)). The wave propagation can be derived by reduction of Eq. (3.2) to a wave equation, (see Eq. (3.11)). The case of Maxwellian equilibrium cannot be reduced neither to Chapman-Kolmogoroff equation or the wave equation.

However, as numerical calculations indicate, there is a set of values $(x_{m,n}; t_n)$ for which the resolvent $\mathsf{R}(x,t)$ comes to nodes and they travel along the x-axis according to the diffusive law, see Eq. (4.10). Moreover, on the basis of the Eq. (3.2), an approximate dispersion relation can be derived and an approximate wave equation can be regained, (see Eq. (3.11)).

5. Discussion and conclusions

In this article we have studied space-time responses of linearized Vlasov plasmas on the basis of multiple integral convolution equations. An initial-value problem for Vlasov–Poisson/Ampere equations can be reduced to the integral equation and the solution to the problem is expressed in terms of a forcing function $G(x,t)$ and its convolution with a resolvent kernel $R(x,t)$ (see Eq. (3.1)). The forcing function is responsible for the initial disturbance and the resolvent is responsible for an equilibrium velocity distribution, see Eq. (3.2). Resolvent kernel equations (3.2) are eligible for computer calculations.

We have presented three types of exact analytical solutions of the space-time resolvent equations. The solutions can be classified following the space-time behaviour. The first one is a dispersive wave solution (Riemann function) in the case of the simplified electron plasma equilibrium, called "square equilibrium" Then the resolvent equation (3.2) can be reduced to dispersion wave equation and the Bohm–Gross dispersion relation is satisfied. The second one is calculated for the Lorentz equilibrium of electron plasmas. We call this type of space-time behaviour "diffusive transition of oscillations" since the space-time amplitude of oscilations satisfies the Chapman–Kolmogoroff equation and there is no wave speed and no dispersion relation. On the ground of the two types of resolvent kernels, the solution to an initial-value problem of Vlasov–Poisson/Ampere equations can be determined if the respective forcing function is known. The last type of the exact solution of Eq. (3.2) is also a diffusive transition of oscillations with the amplitude being a Gaussian function (3.15). This example is not exactly applicable to linearized plasma equations since it has not been derived from any equilibrium, but it turns out that the resolvent approximates the Maxwellian plasma behaviour for fixed x and long time t according to (3.15) and due to the computer calculated results, Figs. 3 and 4. By use of the resolvent equation (3.2) one can easily prove the time-reversibility as well as the space-reflexivity for a given plasma kernel.

The main results of this paper concern the Maxwellian plasmas having the properties which can be summarized as follows. The nature of the plasma response is a compound of a diffusive transition, being essentially a plasma oscillation mode with the ω_0 - plasma frequency and the Gaussian type of amplitude profiles, and a damped dispersive wave mode. Differentiation of these two properties is not an easy task and we have not a ready conclusion but it seems that the Maxwellian plasma response exhibits mainly diffusive transition in space for fixed values of time in a long time range, and damped wave behaviour for fixed values of x with respect to time t. We note that the plasma response appears immediately in the whole space of x, and the zeros (nodes) travel according to (4.10) at least for long times. The step-density disturbance of electron Maxvellian plasmas appears to be the electric current forcing function, which is propotional to Maxwellian plasma kernel, hence the resolvent kernel is a plasma response to the step-density disturbance. It is noteworthy that the solitary plasma waves

can be excited experimentally by strong step-density disturbances in ion-electron plasmas.

By inspecting the series representing the resolvent and its Fourier transform, Eqs. (4.4) and (4.6), we found the symmetry property with respect to Fourier transforms. It can be used for constructing approximate formulae of $R(x,t)$ if the approximate expressions of their Fourier transforms are known, and vice versa.

Acknowledgment

The authors are grateful to Prof. H. ZORSKI for critical reading of the manuscript.

References

1. V.COLOMBO, G.G.M. COPPA and RAVETTO, *New approach to the problem of the propagation of electrostatic perturbations in Vlasov plasmas*, Phys. Fluids, **B 4**, 12, 3827–3837, 1992.
2. E.INFELD and G. ROWLANDS, *Nonlinear waves, solitons and chaos*, Cambridge University Press, Cambridge 1992.
3. A.J. TURSKI and B. ATAMANIUK, *Far field solutions of Vlasov–Maxwell equations and wave-particle interactions*, J. Tech. Phys., **30**, 2, 147–164, 1989.
4. A.J. TURSKI, *An integral equation of convolution type*, SIAM Review, **10**, 1, 108, 1968.
5. A.D. BAILEY, P.M. BELLAN and R.A. STERN, *Poincaré maps define topography of Vlasov distribution functions consistent with stochastic dynamics*, Phys. Plasmas, **2**, 8, 2963–2969, 1995.
6. A.J. TURSKI, *Diffusive transition of oscillations in unbounded longitudinal plasmas*, Il Nuovo Cimento, Serii X, **63B**, 115–131, 1969.
7. A.J. TURSKI, *Linear response theory of longitudinal plasma excitations*, Ann. der Physik, 7, Band 22, 3/4, 180–200, 1969.
8. A.J. TURSKI, *Transient and oscillating solutions of Boltzmann–Vlasov equations in linearized plasma*, Annals of Physics, **35**, 2, 240–249, 1965.
9. Z. MENG, R.M. THORNE and D. SUMMERS, *Ion-acoustic wave instability driven by drifting electrons in a generalized Lorentzian distribution*, J. Plasma Physics, **47**, 3, 445–464, 1992.
10. L. LANDAU, *On the vibrations of the electronic plasma*, J. Phys./USSR/, **10**, 1, 25–34, 1946.

POLISH ACADEMY OF SCIENCES
INSTITUTE OF FUNDAMENTAL TECHNOLOGICAL RESEARCH.

Received April 22, 1996.

Arch. Mech., 48, 6, pp. 1069–1088, Warszawa 1996

On double waves and wave-wave interaction in gasdynamics

Z. PERADZYŃSKI (WARSZAWA)

SPECIAL CLASSES of potential isentropic nonstationary flows in two space dimensions are considered. We demonstrate that locally these solutions can be understood as resulting from what we call *elastic* interaction (since no other waves are produced) of two Riemann waves (simple waves). It appears that this is a generic property of interactions of sound modes in gasdynamics. That is, two nonlinear (localised) sound waves propagating at any angle can cross each other without producing new waves – similarly as it happens in one space dimension.

1. Introduction

IN THIS PAPER we deal with certain classes of isentropic nonstationary flows of an ideal compressible fluid. Each of these classes depends on two arbitrary functions of one variable and may be obtained as a solution of a certain specialized system of two hyperbolic equations with two dependent and two independent variables. We call them hyperbolic double waves or, for short, double waves. It appears that they can be understood as resulting from the special type of interaction of two simple waves. This interaction can be called *elastic* since collision of two waves leads also to two waves, in contrast to the case of nonelastic interaction [18, 19]. This idea can be clearly explained in the case of one space dimension. One can take two localised perturbations in the form of two simple waves which are approaching each other. Then they begin to interact. Depending on the nature of the waves, different scenarios are possible:

1. In spite of nonlinear interaction, the waves can cross the region of interaction, the state of rest being there restored.

2. Due to nonlinear interaction, certain new disturbances are produced. This happens, for instance, when a sound wave is interacting with an entropy wave [18, 20].

In the Case 1 one can speak of elastic interaction. In a similar way, one can speak of elastic interaction in the case of waves crossing each other at a certain angle in many spatial dimensions. In this case one should restrict the considerations to the domain of determinacy of the solution. This will be explained later in Sec. 6.

Although this subject has a long history starting from Riemann (1858) [22, 5, 9, 23, 3, 4, 21, 12, 19, 20, 24, 6, 10, 11], it is still far from being exhausted. Like solitons, it contributes to the understanding of nonlinear phenomena. The most complete analysis of mathematical properties of such solutions, as well as the general theory of k-waves, is contained in [19]. A considerable part of this results can be found also in [20]. In this paper we present a simplified version of the theory, with application to nonstationary gasdynamics.

In Sec. 2 we define the Riemann (simple) waves and then the hyperbolic double waves for a general quasilinear system of the first order and derive the conditions of their existence. Section 3 contains the application of theory of Sec. 2 to the equations of nonstationary two-dimensional flows in gas-dynamics. We confined ourselves to the case of nonstationary two-dimensional flows, although, as it may be proved, a similar analysis can be made for three-dimensional flows. Having, however, a three-dimensional hodograph space (as there is for two-dimensional nonstationary or three-dimensional stationary flows) makes it possible to obtain a single equation i.e. Eq. (3.8) describing hodographs of double waves. In Secs. 4 and 5 specific classes of such hodographs and the corresponding double waves are considered. Then in Sec. 6 we discuss, in general, the interaction problem for sound modes in gasdynamics. We demonstrate there that for sufficiently small amplitudes (in order not to enter the elliptic region of Eq. (3.8) or Eq. (6.1), the waves are subjected to an elastic interaction described by double waves.

Similar considerations can be performed for stationary supersonic flows Also by using imaginary characteristic elements, one can generalize this procedure [19, 20] to the elliptic (or mixed) case of stationary supersonic (transonic) flows. Then one can prove that these generalized double waves can represent flows past three-dimensional profiles which are developable surfaces. This may be useful in searching for 3-D-developable airfoils, similarly as it was done in the two-dimensional case [1, 2, 8].

2. Simple and double waves

Let us consider a nonlinear system of PDE's

$$a_j^{s\nu}(u)\, u^j_{,x\nu} = 0, \qquad \nu = 1,\dots,n, \quad j = 1,\dots,l, \quad s = 1,\dots,m. \tag{2.1}$$

A solution $u(\cdot) : \Omega \to \mathbb{R}^l$, $\Omega \in \mathbb{R}^n$, of system (2.1) is of the simple wave-type if and only if the Jacobi matrix $du = (u^j{}_{,x^\nu})$ is of rank 1 in Ω.

Let us note that any $l \times n$ matrix of rank 1 can be represented as $\gamma \otimes \lambda = (\gamma^j \lambda_\nu)$, $j = 1,\dots,l$, $\nu = 1,\dots,n$. If $\gamma \otimes \lambda$ satisfies

$$a_j^{s\nu}(u)\, \gamma^j \lambda_\nu = 0, \tag{2.2}$$

then one speaks of the polarization vector $\gamma \in \mathbb{R}^l$ and the wave vector (or characteristic covector) $\lambda \in \mathbb{R}^n$. The matrix $\gamma \otimes \lambda$ satisfying (2.2) will be called the characteristic element at u. There are solutions of (2.1) associated with characteristic elements. These solutions, called simple waves (or Riemann waves), can be constructed by taking any parameterized C^1 curve $u = f(R)$, $R \in (a, b)$ in $\mathbb{R}^l$ and such that for every $R_0 \in (a, b)$, the tangent vector $\gamma := \dfrac{d}{dR} f_{|R=R_0}$ is a

polarization vector at $u_0 = f(R_0)$. Let $\lambda(R)$ be the field of the corresponding wave vectors defined over this curve, i.e.

$$a_j^{s\nu}(f(R))\gamma^j(R)\lambda_\nu(R) = 0, \qquad R \in (a, b).$$

Then one implicitly defines a class of local simple wave-type solutions

$$u = f(R), \qquad R = \varphi(\lambda_\nu x^\nu), \tag{2.3}$$

where $\varphi : \mathbb{R}^1 \to (a, b)$ is an arbitrary C^1 function. One can also easily verify that the equations

$$\lambda_\nu(R)(x^\nu - y^\nu(R)) = 0, \qquad u = f(R) \tag{2.4}$$

define a simple wave solution in some neighbourhood of the curve $x = y(R)$, which takes values $f(R)$ at this curve, provided $\lambda_\nu \dfrac{\partial y^\nu}{\partial R} \neq 0$. If $\lambda \wedge \lambda_{,R} \neq 0$, then the limiting case $u = f(R)$ and $\lambda_\nu(R)(x^\nu - \overset{0}{x}{}^\nu) = 0$ also defines a simple wave.

Similarly, any solution $u(\cdot) : \Omega \to \mathbb{R}^l$ is of a hyperbolic double wave-type if for every $x \in \Omega$, $du(x)$ is a sum of two characteristic elements

$$du = \underset{1}{\gamma} \otimes \overset{1}{\lambda} + \underset{2}{\gamma} \otimes \overset{2}{\lambda} \tag{2.5}$$

with linearly independent $\underset{1}{\gamma}, \underset{2}{\gamma}$ and $\overset{1}{\lambda}, \overset{2}{\lambda}$. Thus rank $du = 2$, and the range $u(\Omega)$ of $u(\cdot)$ is a two-dimensional surface in $\mathbb{R}^l$. The plane tangent to $u(\Omega)$ at $u(x)$ is spanned by $\underset{1}{\gamma}, \underset{2}{\gamma}$. As is known from differential geometry, given a two-dimensional surface with two independent vector fields $\underset{1}{\gamma}, \underset{2}{\gamma}$ defined on it, there exists a local system of coordinates on the surface, whose lines are tangent to $\underset{1}{\gamma}, \underset{2}{\gamma}$. In other words, there exists a local parameterization $u = f(R^1, R^2)$ of the surface, such that

$$\frac{\partial f}{\partial R^1} \sim \underset{1}{\gamma}, \qquad \frac{\partial f}{\partial R^2} \sim \underset{2}{\gamma}. \tag{2.6}$$

Therefore the double wave solution can be sought in the form $u = f(R^1(x), R^2(x))$. Inserting $u = f(R^1, R^2)$ into Eq. (2.5) one comes to the conclusion that the functions $R^1 = R^1(x)$, $R^2 = R^2(x)$ satisfy

$$dR^1 = \xi^1(x)\overset{1}{\lambda}(R^1, R^2), \qquad dR^2 = \xi^2(x)\overset{2}{\lambda}(R^1, R^2) \tag{2.7}$$

for some functions $\xi^1(x)$ and $\xi^2(x)$. Here $\overset{1}{\lambda}, \overset{2}{\lambda}$ are the wave vectors corresponding to the polarization vectors $\underset{1}{\gamma}, \underset{2}{\gamma}$, respectively.

The construction of double wave solutions is, however, much more involved than the one for simple waves. Since, in general, system (2.7) is overdetermined ($2n$ equations for four unknown functions R^1, R^2, ξ^1, ξ^2), it can have no solutions of rank 2. For this reason, not every two-dimensional surface parameterized according to (2.6) is in the range of a double wave solution. Additional restrictions which follow from the compatibility conditions of Eqs. (2.7) must be imposed. They require [15, 16, 20] the existence of functions $\alpha_2^1(R^1, R^2)$, $\alpha_1^2(R^1, R^2)$, $\beta_2^1(R^1, R^2)$, $\beta_1^2(R^1, R^2)$ such that

$$\overset{1}{\lambda}_{,R^2} = \alpha_2^1 \overset{2}{\lambda} + \beta_2^1 \overset{1}{\lambda}, \qquad \overset{2}{\lambda}_{,R^1} = \alpha_1^2 \overset{1}{\lambda} + \beta_1^2 \overset{2}{\lambda}. \tag{2.8}$$

The above conditions are equivalent to

$$\Delta_s^r := \overset{(r)}{\lambda} \wedge \overset{s}{\lambda} \wedge \overset{s}{\lambda}_{,R^r} = 0, \qquad r, s = 1, 2, \tag{2.9}$$

where $\wedge$ denotes an exterior product [7] and no summation over r is performed. If (2.8) is satisfied, then Eqs. (2.7) are compatible (involutive) and their general solution depends on two arbitrary functions of one variable [15, 16, 20]. In order to obtain a solution of Eqs. (2.7) several approaches may be applied. From the form of Eqs. (2.7) we see that the solution is constant over certain linear manifolds $\mathcal{M}_{\underset{0}{x}}$ of dimension $(n-2)$ (n is the dimension of the configuration space of $x^1, \ldots, x^n$ variables). $\mathcal{M}_{\underset{0}{x}}$ is given by the following equations for x

$$\begin{aligned} &\overset{1}{\lambda}_\nu \Big(f(R^1(\underset{0}{x}), R^2(\underset{0}{x})) \Big)(x^\nu - \underset{0}{x}^\nu) = 0, \\ &\overset{2}{\lambda}_\nu \Big(f(R^1(\underset{0}{x}), R^2(\underset{0}{x})) \Big)(x^\nu - \underset{0}{x}^\nu) = 0, \qquad \underset{0}{x} = (\underset{0}{x}^1, \ldots, \underset{0}{x}^n). \end{aligned}$$

Therefore, at the beginning of the solution we may confine our attention to a two-dimensional plane in the configuration space, which has the property of intersecting each $\mathcal{M}_{\underset{0}{x}}$ at only one point. Suppose that the plane x^1, x^2 has this property. In such a case system (2.7) may be restricted to the plane x^1, x^2, to obtain

$$R^1_{,xs} = \xi^1 \overset{1}{\lambda}_s, \qquad R^2_{,xs} = \xi^2 \overset{2}{\lambda}_s, \qquad s = 1, 2. \tag{2.10}$$

Eliminating the variables ξ^1, ξ^2 we reduce Eq. (2.10) to the following hyperbolic system

$$C_1^s(R^1, R^2) R^1_{,xs} = 0, \qquad C_2^s(R^1, R^2) R^2_{,xs} = 0, \qquad s = 1, 2, \tag{2.11}$$

where $C_1 = (\overset{2}{\lambda}_2, -\overset{2}{\lambda}_1)$, $C_2 = (\overset{1}{\lambda}_2, -\overset{1}{\lambda}_1)$ are "tangent characteristic vectors" for system (2.11). This system can be treated by the method of characteristics.

Another possibility is to apply the hodograph transformation which converts Eq. (2.11) into a linear system. Indeed, multiplying Eqs. (2.10) by $\partial x^s/\partial R^2$ and by $\partial x^s/\partial R^1$ respectively, we obtain a linear homogeneous system in R^1, R^2

$$\overset{1}{\lambda}_s(f(R^1, R^2))\frac{\partial x^s}{\partial R^2} = 0, \qquad \overset{2}{\lambda}_s(f(R^1, R^2))\frac{\partial x^s}{\partial R^1} = 0,$$

which is equivalent to the previous one for nondegenerate solutions (rank $\|R^\alpha_{,s}\| = 2$).

Another approach can be also applied in which system (2.7) is also reduced to a linear hyperbolic system. This approach may sometimes be useful. Assuming that $\alpha_2^1(R^1, R^2)$, $\alpha_1^2(R^1, R^2)$, $\beta_2^1(R^1, R^2)$, $\beta_1^2(R^1, R^2)$ are the coefficients appearing in conditions (2.8), we have

THEOREM 1. *If ψ^1, ψ^2 is a solution of the linear equations*

$$\psi^1{}_{,R^2} = \alpha_2^1\psi^2 + \beta_2^1\psi^1, \qquad \psi^2{}_{,R^1} = \alpha_1^2\psi^1 + \beta_1^2\psi^2, \tag{2.12}$$

then the implicit formulae

$$\psi^1(R^1, R^2) = \overset{1}{\lambda}_\nu(R^1, R^2)x^\nu, \qquad \psi^2(R^1, R^2) = \overset{2}{\lambda}_\nu(R^1, R^2)x^\nu, \tag{2.13}$$

define a solution of Eqs. (2.1) *in some neighbourhood of* $(\overset{0}{x}, \overset{0}{R}{}^1, \overset{0}{R}{}^2)$ *provided that* $(\psi^1 - \overset{1}{\lambda}_\nu\overset{0}{x}{}^\nu)_{,R^1} \neq 0$ *and* $(\psi^2 - \overset{2}{\lambda}_\nu\overset{0}{x}{}^\nu)_{,R^2} \neq 0$ *at* $(\overset{0}{x}, \overset{0}{R}{}^1, \overset{0}{R}{}^2)$ *satisfying* (2.13).

Indeed, by differentiating the implicit formulae (2.13) we see that the gradient of R^1, R^2 is proportional to $\overset{1}{\lambda}(R^1, R^2)$, $\overset{2}{\lambda}(R^1, R^2)$, respectively.

Formulae (2.13) constitute an interesting generalization of a similar formula (Eq. (2.3)) for simple waves. Let us note that Eqs. (2.13) have always the trivial solution $\psi_1 \equiv \psi_2 \equiv 0$ which by Eqs. (2.13) defines a certain double wave (generalization of formula (2.4)). Theorem 1 can be generalized in an obvious way for k-waves by replacing indices 1 and 2 with $\alpha, \beta = 1, \ldots, k$, $\alpha \neq \beta$. Then the general solution depends on k-functions of one variable, e.g. defining the problem of waves entering the interaction (the formulation of the theorem in [10, 11] is erroneous).

In principle one can start from two independent characteristic elements in Eq. (2.5) expressed as some functions of u. Then the Frobenius theorem tells us that for any given point u_0, there exists a two-dimensional surface passing through u_0 and tangent at each of its points to the vector fields $\underset{1}{\gamma}$, $\underset{2}{\gamma}$ if and only if

$$\left[\underset{1}{\gamma}, \underset{2}{\gamma}\right] \in \mathrm{Lin}\{\underset{1}{\gamma}, \underset{2}{\gamma}\},$$

where $[X,Y] = X^i \frac{\partial}{\partial u^i} Y - Y^i \frac{\partial}{\partial u^i} X$ is the commutator of the vector fields X, Y and $\mathrm{Lin}\{X,Y\}$ denotes the linear combination of X, Y. In such a case differentiation with respect to R^1, R^2 in Eqs. (2.8) must be replaced by differentiation along $\underset{1}{\gamma}$, $\underset{2}{\gamma}$, e.g. $\frac{\partial}{\partial R^2} \overset{1}{\lambda} \to \underset{2}{\gamma}^i \frac{\partial}{\partial u^i} \overset{1}{\lambda}$.

Now we will demonstrate that the solution of Eq. (2.5) *can be interpreted locally as resulting from the interaction of two localised Riemann waves, in the sense that one wave is propagating across the other. By "localised" we mean here that the first derivative of* φ *in* (2.3) *is localised.*

The level sets $R^1(x) = \text{const}$ and $R^2 = \text{const}$ can be thought of as constant phase surfaces of the first and second wave, respectively. Since they are solutions of the Pfaff forms $\overset{1}{\lambda}_\nu dx^\nu = 0$ and $\overset{2}{\lambda}_\nu dx^\nu = 0$ respectively, they are orthogonal to their wave vectors, $\overset{1}{\lambda}$ or $\overset{2}{\lambda}$. For an unperturbed Riemann wave such a surface is a hyperplane. In general, however, the mutual interaction expressed in the nonlinearity of system (2.5) leads to local changes of the wave vectors. For brevity, in the following we confine our attention to the two-dimensional case, when the level sets of R^1 and R^2 define two families of curves which are characteristic curves of Eq. (2.5). In case of three dimensions t, x^1, x^2 one can think of the picture at any constant t.

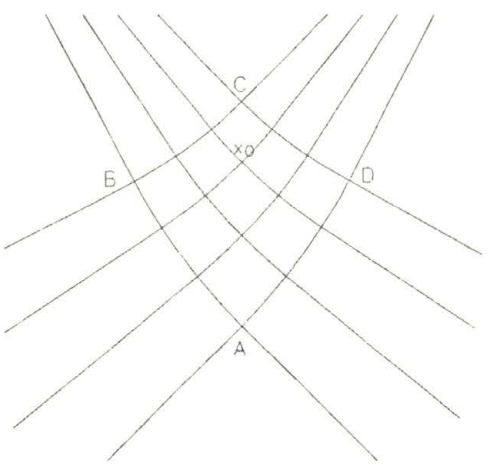

FIG. 1.

Now, suppose a solution of Eq. (2.5) of rank 2 is given in a region Ω containing a point x_0. Consider a neighbourhood of the point x_0 bounded by a curvilinear quadrangle A, B, C, D (Fig. 1), the sides of which are characteristic curves (i.e. these curves are perpendicular to $\overset{1}{\lambda}$ and $\overset{2}{\lambda}$, respectively). By what we call the circumvention procedure, we construct a new solution which takes the same values as the former one in the quadrangle (including its sides). Outside it we extend the solution in the following way: first we prolong any characteristics contained in

$ABCD$ by a straight half-line keeping the direction of the characteristic (Fig. 2). On this line we define the solution u to be a constant equal to the value it takes at the point where the line crosses the side of the quadrangle.

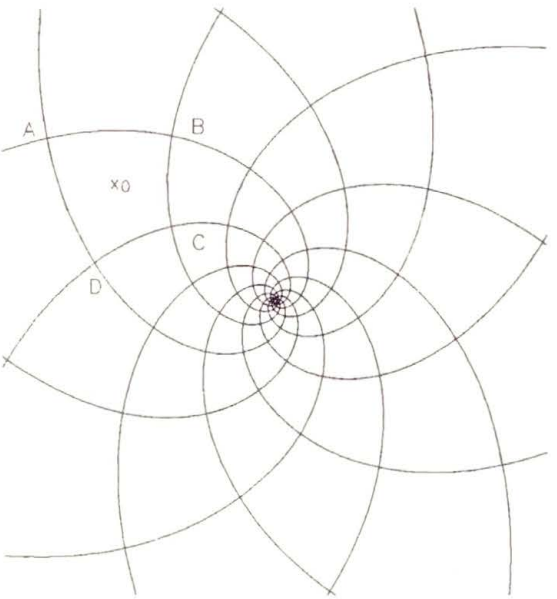

FIG. 2.

In the remaining domains which are the interiors of the four angles with the vertices A, B, C, D we put u equal to $u(A)$, $u(B)$, $u(C)$, $u(D)$, respectively. This procedure defines, in a certain neighbourhood of the quadrangle, a Lipschitz continuous mapping which is also differentiable in this neighbourhood, perhaps with the exception of characteristic curves passing through any of the points A, B, C, D. In this way weak discontinuity of a solution may occur. This mapping is the new solution of Eq. (2.5) which represents two interacting localized Riemann waves. The interior of the quadrangle is a domain of interaction, and outside it, by construction, the mapping is either a constant or is constant on the lines orthogonal to the respective wave vector λ, thus assuring that it is a Riemann wave-type solution.

3. The hodograph problem

We will consider equations of plane nonstationary isentropic flows [5, 13]

$$
\begin{aligned}
&(\partial_t + \mathbf{u}\cdot\nabla)a + \frac{\kappa-1}{2}a\,\operatorname{div}\mathbf{u} = 0,\\
&(\partial_t + \mathbf{u}\cdot\nabla)\mathbf{u} + \frac{2}{\kappa-1}a\nabla a = 0,
\end{aligned}
\tag{3.1}
$$

where $\mathbf{u} = (u^1, u^2)$, $\nabla = (\partial_x, \partial_y)$, a is the sound speed, $a^2 = dp/d\varrho$ and κ is the isentropy exponent, $1 < \kappa < 3$. The number of equations is equal to three, as is the number of unknown functions a, u^1, u^2 or the number of independent variables t, x^1, x^2.

According to Eq. (2.2), the characteristic directions are

$$\begin{aligned} &1) \quad \gamma = \left(\frac{\kappa-1}{2},\ e^1,\ e^2\right) \longrightarrow \lambda = (\langle \mathbf{u}|\gamma\rangle\rangle,\ -e^1,\ -e^2), \\ &2) \quad \gamma = (0,\ e^1,\ e^2) \qquad\quad \longrightarrow \lambda = (u^1e^2 - u^2e^1,\ -e^2,\ e^1), \end{aligned} \tag{3.2}$$

where $\langle \mathbf{u}|\gamma\rangle = [2/(\kappa-1)]a\gamma^0 + u^1\gamma^1 + u^2\gamma^2$ and $e = (e^1, e^2)$ is a two-dimensional unit vector [17]. Similarly to three-dimensional flows [17], the first type of simple elements generates potential flows (sound modes) and this case will be considered here. Note that the characteristic vector λ for the potential elements can be represented as a linear function of γ

$$\lambda = \mathbb{P}\gamma,$$

where

$$\mathbb{P} = \begin{vmatrix} \dfrac{2}{\kappa-1}, & u^1, & u^2 \\ 0, & -1, & 0 \\ 0, & 0, & -1 \end{vmatrix}.$$

Let us denote $f_{,\gamma} := \gamma^j \dfrac{\partial}{\partial u^j} f$, for simplicity. The exterior product of three vectors in three-dimensional space t, x^1, x^2 may be identified with the determinant, so that

$$\Delta^s_r := \overset{s}{\lambda} \wedge \overset{r}{\lambda} \wedge \overset{s}{\lambda}_{,\gamma} = \left[\overset{s}{\lambda} \mid \overset{r}{\lambda} \mid \overset{s}{\lambda}_{,\gamma}\right] = \left[\mathbb{P}\gamma \mid \mathbb{P}\gamma \mid \mathbb{P}_{,\gamma}\gamma\right],$$

where $[\alpha \mid \beta \mid \gamma] = \det \|\alpha, \beta, \gamma\|$.

By a well-known transformation property of determinants $[\mathbb{P}\alpha \mid \mathbb{P}\beta \mid \mathbb{P}\gamma] = \det \mathbb{P}[\alpha, \beta, \gamma]$, we can write the conditions of involutions (2.9) $\Delta^s_r = 0$ as follows

$$\Delta^s_r = \langle \gamma \mid \gamma \rangle \cdot \left[\gamma \mid \gamma \mid q\right] + \frac{2}{\kappa-1} a \left[\gamma \mid \gamma \mid \gamma_{,\gamma}\right] = 0, \qquad q = (1,0,0),$$

or

$$\Delta^r_s = (\gamma \times \gamma) \cdot (q\langle \gamma \mid \gamma \rangle + \frac{2}{\kappa-1} a\gamma_{,\gamma}) = 0, \tag{3.3}$$

where the dot denotes the scalar product.

Suppose that the hodograph surface which will be denoted by G^2 is described by a C^1-function $F(a, u^1, u^2) = 0$, with a nonvanishing gradient. The gradient $\nabla_u F = (F_a, F_{u^1}, F_{u^2})$ is orthogonal to the surface G^2 and therefore it must be proportional to the vector product $\underset{1}{\gamma} \times \underset{2}{\gamma}$ of vectors $\underset{1}{\gamma}, \underset{2}{\gamma}$ which are tangent to G^2. Using this fact, we substitute $\nabla_u F$ for $\underset{1}{\gamma} \times \underset{2}{\gamma}$ in Eq. (3.3) to obtain

$$\Delta_r^{'s} = \langle \underset{s}{\gamma} \mid \underset{r}{\gamma} \rangle F_{,a} + \frac{2}{\kappa - 1} a F_{,u^j} (\underset{s}{\gamma}{}^j_{,\underset{r}{\gamma}}) = 0, \quad s \neq r, \quad a = u^0, \quad j = 0, 1, 2. \tag{3.4}$$

On the other hand, differentiation of a self-evident relation $F_{,u^j} \underset{r}{\gamma}{}^j = 0$ with respect to u^i and multiplication by $\underset{r}{\gamma}{}^i$ yields

$$F_{,u^j} (\underset{s}{\gamma}{}^j_{,\underset{r}{\gamma}}) = -F_{,u^i u^j} \underset{s}{\gamma}{}^i \underset{r}{\gamma}{}^j,$$

which allows us to transform Eq. (3.4) to the following symmetric form

$$\Delta_r^{'s} = \langle \underset{s}{\gamma} \mid \underset{r}{\gamma} \rangle F_{,a} - \frac{2}{\kappa - 1} a F_{,u^i u^j} \underset{s}{\gamma}{}^j \underset{r}{\gamma}{}^j.$$

Therefore, the set of conditions (3.4) is reduced to the following one

$$\langle \underset{1}{\gamma} \mid \underset{2}{\gamma} \rangle F_{,a} - \frac{2}{\kappa - 1} a F_{,u^j u^i} \underset{1}{\gamma}{}^j \underset{2}{\gamma}{}^i = 0. \tag{3.5}$$

In accordance with 1) of (3.2) we can assume

$$\underset{s}{\gamma} = \left(\frac{\kappa - 1}{2}, \cos \varphi_s, \sin \varphi_s \right).$$

Then we have $\langle \underset{1}{\gamma} \mid \underset{2}{\gamma} \rangle = (\kappa - 1)/2 + \cos 2\delta$, where $\delta = \varphi_1 - \varphi_2$ and the vectors $\underset{1}{\gamma}$, $\underset{2}{\gamma}$ can be obtained from the relations

$$F_a \gamma^0 + F_{u^1} \gamma^1 + F_{u^2} \gamma^2 = 0. \tag{3.6}$$

Further on, $\cos 2\delta$ may be expressed by the derivatives of F to obtain

$$\cos^2 \delta = \frac{F_a^2}{F_{u^1}^2 + F_{u^2}^2} \left(\frac{\kappa - 1}{2} \right)^2 \tag{3.7}$$

from which it follows that in order to have a real δ, we must satisfy the following inequality

$$F_a^2 < \left(\frac{2}{\kappa - 1} \right)^2 \left(F_{u^1}^2 + F_{u^2}^2 \right).$$

Introducing $\tilde{a} = [2/(\kappa - 1)]a$ in Eq. (3.5) and expressing $F_{u^i u^j}\gamma^i\gamma^j$ in terms of derivatives of F, we arrive at the following, rather complicated, equation which must be satisfied on surface G^2

$$(3.8)\qquad \left(\frac{\kappa-3}{2}+\frac{2F_{\tilde{a}}^2}{F_u^2+F_v^2}\right)\frac{2F_{\tilde{a}}}{\kappa-1} - \tilde{a}\left(F_{\tilde{a}\tilde{a}}+\frac{1}{2}(F_{uu}-F_{vv})\frac{F_u^2-F_v^2}{F_u^2+F_v^2}+2F_uF_v\frac{F_{uv}}{F_u^2+F_v^2} + \frac{1}{2}\frac{F_{uu}+F_{vv}}{F_u^2+F_v^2}\left(2F_{\tilde{a}}^2-F_u^2-F_v^2\right) + \frac{2F_{\tilde{a}}}{F_u^2+F_v^2}\left(F_{\tilde{a}u}+F_{\tilde{a}v}F_v\right)\right)=0,$$

where u, v denote u^1, u^2.

By specialization $F \equiv \varphi(\tilde{a}) - f(u,v)$ we may remove the terms involving the derivatives $F_{\tilde{a}u}$ and $F_{\tilde{a}v}$. This form of F can be assumed without much loss of generality. As follows from the Sard theorem [14], such a representation of F can cease to hold only on a set of measure zero. A particular case $F \equiv \psi(\tilde{a}) - \frac{1}{2}(u^2+v^2)$, leads to rotational hodograph surfaces, described by ordinary differential equations

$$(3.9)\qquad \left(\frac{\kappa-3}{2}+\frac{\psi'^2}{\psi}\right)\frac{2\psi'}{\kappa-1} - \tilde{a}\left(\psi''-\frac{\psi'^2}{\psi}+1\right)=0.$$

Here "$'$" denotes differentiation with respect to $\tilde{a}$. The solution of Eqs. (3.9) depends on two arbitrary constants both of which have a physical meaning, i.e. they cannot be retransformed by Galilean transformation. Therefore both constants determine the shape of the rotational surface. It may be checked that the functions

$$\text{a)}\quad \psi(\tilde{a}) \equiv \frac{1}{4}\tilde{a}^2, \qquad \text{and} \qquad \text{b)}\quad \psi(\tilde{a}) \equiv -\frac{\kappa-1}{4}\tilde{a}^2 + c$$

are the particular solutions of Eqs. (3.9). Both solutions lead to hodographs which are the quadratic surfaces:

a. $\frac{1}{2}\tilde{a}^2 - u^2 - v^2 = 0$ – the hodograph is a cone; its equation in variables a, u, v takes the form $\left(\frac{a\sqrt{2}}{\kappa-1}\right)^2 - u^2 - v^2 = 0$. From relation (3.7) we have $\cos^2\delta = 1/2$; we can put $\delta = \pi/4$ since other cases provide nothing new.

b. $\frac{2}{\kappa-1}a^2 + u^2 + v^2 = c$ – describes a family of ellipsoids and physically expresses Bernoulli's law. Therefore, solutions associated with such hodographs are the well known two-dimensional stationary hypersonic flows (if $u^2+v^2 > c^2$).

4. Flows with constant Mach number

We direct our attention to the conical hodograph surface (Case a). The curves tangent to $\underset{1}{\gamma}$ and $\underset{2}{\gamma}$ are spirals and their projections on the (u, v)-plane are logarithmic spirals. In the parametrical form with parameters φ, ϱ, the cone may be represented by the following expressions

$$a = \frac{\kappa - 1}{\sqrt{2}}\varrho, \qquad u = \varrho\cos\varphi, \qquad v = \varrho\sin\varphi. \tag{4.1}$$

The mentioned spirals on the cone are given by Eqs. (4.1) with an additional relation between ϱ and φ

$$\varrho = e^{\cot\delta(\varphi+2R^2)}, \tag{4.2}$$

with constant R^2 on the curves of the first family; or

$$\varrho = e^{-\cot\delta(\varphi-2R^1)} \tag{4.3}$$

with constant R^1 on the spirals of the second family.

By eliminating ϱ and φ from relations (4.2) and (4.3) we may take R^1, R^2 as the coordinates. Thus, remembering that $\cot\delta = 1$, ϱ, φ become functions of R^1, R^2

$$\varrho = e^{-(R^1+R^2)}, \qquad \varphi = R^1 - R^2. \tag{4.4}$$

Since $\underset{s}{\gamma} \simeq \dfrac{\partial}{\partial R^s}(a, u, v)$ then, utilizing Eqs. (4.1), (4.4) and (3.2), we arrive at the characteristic elements ($\underset{1}{\gamma}$ corresponds to $-$ and $\underset{2}{\gamma}$ to $+$)

$$\begin{aligned}
\underset{1}{\gamma}, \underset{2}{\gamma} &= \left(\frac{\kappa-1}{2},\ \cos\left(\varphi \mp \frac{\pi}{4}\right),\ \sin\left(\varphi \mp \frac{\pi}{4}\right)\right),\\
\overset{1}{\lambda}, \overset{2}{\lambda} &= \left(\frac{\kappa}{\sqrt{2}}\varrho,\ -\cos\left(\varphi \mp \frac{\pi}{4}\right),\ -\sin\left(\varphi \mp \frac{\pi}{4}\right)\right)
\end{aligned}$$

and the vector $\sigma \sim \overset{1}{\lambda} \times \overset{2}{\lambda}$. As we know from Sec. 1, the solution is constant along the directions σ orthogonal to $\overset{1}{\lambda}$, $\overset{2}{\lambda}$. Thus $\sigma = \overset{1}{\lambda} \times \overset{2}{\lambda} = (1, \kappa\varrho\cos\varphi, \kappa\varrho\sin\varphi) = (1, \kappa u, \kappa v)$. By using this property, the Pfaff equations (3.8) which in this case take the form

$$\begin{aligned}
dR^1 &= \xi^1\left(\frac{\kappa}{\sqrt{2}}\varrho\,dt - \cos\left(\varphi - \frac{\pi}{4}\right)dx^1 - \sin\left(\varphi - \frac{\pi}{4}\right)dx^2\right),\\
dR^2 &= \xi^2\left(\frac{\kappa}{\sqrt{2}}\varrho\,dt - \cos\left(\varphi + \frac{\pi}{4}\right)dx^1 - \sin\left(\varphi + \frac{\pi}{4}\right)dx^2\right)
\end{aligned} \tag{4.5}$$

can be restricted to the plane $t = \text{const}$. Then their solution $R_0^1(x^1, x^2)$, $R_0^2(x^1, x^2)$ may be extended to a certain neighborhood of the plane $t = \text{const}$ in such a way that this extended solution is constant along the straight lines defined in each point $(0, x^1, x^2)$ by the vector $\sigma(R^1(x^1, x^2), R^2(x^1, x^2))$. Let us note that σ is never parallel to the (x^1, x^2)-plane. Putting $dt = 0$ and eliminating ξ^1, ξ^2 from Eqs. (4.5) we arrive at an equivalent hyperbolic system

$$R^1_{0,x^1} = R^1_{0,x^2} \cot\left(R_0^1 - R_0^2 - \frac{\pi}{4}\right), \qquad R^2_{0,x^1} = R^2_{0,x^2} \cot\left(R_0^1 - R_0^2 + \frac{\pi}{4}\right), \tag{4.6}$$

which is treatable by the method of characteristics. In the case of nondegenerate solutions of Eqs. (4.6) one can also apply the hodograph transformation which, by exchanging the role of dependent and independent variables, leads to the following linear system

$$\begin{aligned} x^1_{,R^2} \cos\left(R^1 - R^2 - \frac{\pi}{4}\right) + x^2_{,R^2} \sin\left(R^1 - R^2 - \frac{\pi}{4}\right) &= 0, \\ x^2_{,R^1} \cos\left(R^1 - R^2 + \frac{\pi}{4}\right) + x^2_{,R^1} \sin\left(R^1 - R^2 + \frac{\pi}{4}\right) &= 0. \end{aligned} \tag{4.7}$$

Equations (4.5) may be also reduced to the telegraphic equation by introducing new variables ψ^1, ψ^2 according to Theorem 1. Then from (2.12) one obtains an equivalent form of Eqs. (4.5)

$$\psi^1_{,R^2} - \psi^2 = 0, \qquad \psi^2_{,R^1} - \psi^1 = 0. \tag{4.8}$$

Elimination of one of the unknown functions, say ψ^2, reduces Eqs. (4.7) to the telegraphic equation

$$\psi^1_{,R^1R^2} - \psi^1 = 0.$$

The solution is then determined by

$$\begin{pmatrix} \psi^1 \\ \psi^2 \end{pmatrix} = \begin{pmatrix} \cos\left(R^1 - R^2 - \frac{\pi}{4}\right), & \sin\left(R^1 - R^2 - \frac{\pi}{4}\right) \\ \cos\left(R^1 - R^2 + \frac{\pi}{4}\right), & \sin\left(R^1 - R^2 + \frac{\pi}{4}\right) \end{pmatrix} \begin{pmatrix} x^1 \\ x^2 \end{pmatrix} - \frac{\kappa}{\sqrt{2}} \varrho t \begin{pmatrix} 1 \\ 1 \end{pmatrix} \tag{4.9}$$

and by Eq. (4.4) in a parametric form, R^1, R^2 are the parameters. Let us note that the considered solutions describe nonstationary flows with the constant Mach number $M = (u^2 + v^2)^{1/2}/a = \sqrt{2}/(\kappa - 1)$.

The matrix in (4.9), call it $S(\varphi - \pi/4)$, is an orthogonal matrix of the clockwise rotation by the angle $R^1 - R^2 - \pi/4 = \varphi - \pi/4$. The coordinates (x^1, x^2) can be easily expressed as

$$(x^1, x^2)^T = S\left(\varphi - \frac{\pi}{4}\right)(\psi^1, \psi^2)^T + \frac{\kappa}{2}\varrho t S(\varphi)(1,0)^T,$$

where T denotes the matrix transposition. In the trivial case $\psi^1 \equiv \psi^2 \equiv 0$ which obviously satisfies (4.8), we arrive at

$$\mathbf{u} = \frac{\sqrt{2}}{\kappa}\frac{\mathbf{x}}{t}. \tag{4.10}$$

Then according to (4.1) $a = (\kappa - 1)/\kappa|\mathbf{x}/t|$. In Fig. 1 the projection on u^1, u^2 plane of the curves $R^1 = \text{const}$ and $R^2 = \text{const}$, respectively, defined by Eq. (4.4) are shown. By Eq. (4.10), up to the scaling factor $\sqrt{2}/\kappa$, they are also characteristic curves on $\mathbf{x}/t$-plane.

As it was pointed out in Sec. 1, every double wave can be locally interpreted as resulting from the interaction of two localised simple waves. In this way, a somewhat trivial solution defined by Eq. (4.4) may give rise to interesting interactions of simple waves. Inside the quadrangle $ABCD$ (Fig. 2) on the $(x^1/t, x^2/t)$ plane, the solution is defined by (4.10). Outside it we have simple waves (or constant states in the corners A, B, C, D). The sides of the quadrangle are lines defined by

$$\frac{\mathbf{x}}{t} = \frac{\kappa}{\sqrt{2}} e^{R^1 + R^2}\left\{\cos(R^1 - R^2),\ \sin(R^1 - R^2)\right\},$$

where R^1 (respectively R^2) take appropriate constant values. The straight lines emanating from the quadrangle are the lines of constant phase of the corresponding simple waves. In accordance with Sec. 1 these waves are defined analytically by Eq. (2.4).

5. Cylindrical hodograph

Now we may ask whether the hodographs which are cylindrical surfaces exist. The case $F = F(u, v)$ is an immediate generalization of one-dimensional non-stationary flows for which the hodograph is $v \equiv 0$. Of course, by adjusting the system of coordinates we may at least locally restrict our attention to functions F of the following form $F(u, v) \equiv u - \psi(v)$ (a consequence of implicit function theorem) which, substituted into equation (3.8) yields

$$-\frac{1}{2}\psi''\frac{1 - \psi'^2}{1 + \psi'^2} + \frac{1}{2}\psi'' = 0.$$

This may be split into two alternative conditions

$$\psi'' = 0, \qquad \text{or} \qquad \frac{1-\psi'^2}{1+\psi'^2} = 1.$$

In both cases we obtain nothing more than linear functions (hence defined globally) which by an appropriate Galilean transformation can be transformed into a one-dimensional case $v = 0$.

Thus, in addition to the planes described by the above linear functions, there are no hodographs of the form $F(u, v) = 0$.

We shall see, however, that there are other hodographs generated by a curve moving along the constant direction in the space of a, u, v – each cylindrical surface is generated by an appropriate curve moving in a constant direction. As an example, consider the hodograph given by the relation $u - \psi(\tilde{a}) = 0$. Substituting it to Eq. (3.8) we obtain the following ordinary differential equation

$$\frac{2}{\kappa-1}\left(\frac{\kappa-3}{2} + 2\psi'^2\right)\psi' - \tilde{a}\psi'' = 0 \tag{5.1}$$

with separable variables. Hence we have

$$\frac{d\psi'}{\left(\frac{\kappa-3}{2} + 2\psi'^2\right)\psi'} = \frac{2}{\kappa-1}\frac{d\tilde{a}}{\tilde{a}}, \tag{5.2}$$

which may be integrated to yield for $1 < \kappa < 3$

$$\psi(\tilde{a}) = \pm\frac{\sqrt{3-\kappa}}{2}\int\left(1 - C\tilde{a}^{2(3-\kappa)/(\kappa-1)}\right)^{-1/2} d\tilde{a} + C_1, \tag{5.3}$$

where C, C_1 are arbitrary constants. This solution depends on two arbitrary constants but one of them, C_1, may be retransformed by the Galilean transformation.

As follows from a closer analysis, constant C can also be retransformed to obtain one of the three values $C = -1,\ 0,\ 1$. This can be achieved by using the following transformation $(a, u) \to (\mu a, \mu u)$, $(t, x) \to (\beta t, \mu\beta x)$ which transforms solutions of Eqs. (3.1) into other solutions, μ and β are arbitrary nonzero constants. The case $C = 0$ leads to the plane hodograph of noninteracting waves which were found in [17]. These represent a certain interesting feature of the gasdynamic system: nonlinear waves can be subjected to a linear interference. Therefore we may restrict ourselves to the cases $C = \pm 1$. Equation (3.4), Case 1, leads to the following expressions

$$\underset{1}{\gamma} = \left(1,\ \psi'(\tilde{a}),\ \sqrt{1-\psi'^2(\tilde{a})}\right), \qquad \underset{2}{\gamma} = \left(1,\ \psi'(\tilde{a}),\ -\sqrt{1-\psi'^2(\tilde{a})}\right)$$

for the polarization vectors in the hodograph space of $(\tilde{a}, u, v)$ variables.

Calculating the characteristic vectors $\overset{1}{\lambda}, \overset{2}{\lambda}$ corresponding to $\underset{1}{\gamma}, \underset{2}{\gamma}$ respectively, we have (+ for $\overset{1}{\lambda}$ and − for $\overset{2}{\lambda}$)

$$\overset{1}{\lambda}, \overset{2}{\lambda} = \left(\frac{\kappa-1}{2}\tilde{a} + \psi'(\tilde{a})\psi(\tilde{a}) \pm v\sqrt{1-\psi'^2(\tilde{a})},\ -\psi'(\tilde{a}),\ \pm(-1)\sqrt{1-\psi'(\tilde{a})}\right),$$

and the direction $\boldsymbol{\sigma} = \overset{1}{\lambda} \times \overset{2}{\lambda}$ on which the solution must be constant

$$\boldsymbol{\sigma} = \left(1,\ \frac{\kappa-1}{2\psi'}\tilde{a} + u,\ v\right).$$

In the case $\kappa = 2$ integration in formula (5.3) may be done explicitly and we obtain

$$\psi(\tilde{a}) = \frac{1}{2}\int \frac{d\tilde{a}}{\sqrt{1+C\tilde{a}^2}} = \pm \begin{cases} \frac{1}{2}\operatorname{arsh}\tilde{a} & \text{if} \quad C = 1, \\ -\frac{1}{2}\operatorname{arsin}\tilde{a} & \text{if} \quad C = -1. \end{cases}$$

The hodograph surfaces may be given by relations

(5.4) 1) $\tilde{a} - \sinh 2u = 0$, 2) $\tilde{a} - \sin 2u = 0$.

Taking advantage of the fact that the operator

$$\sigma^0\frac{\partial}{\partial t} + \sigma^1\frac{\partial}{\partial x^1} + \sigma^2\frac{\partial}{\partial x^2} \qquad \left(= \frac{\partial}{\partial t} + \mathbf{u}\cdot\nabla + \frac{\kappa-1}{2\psi'(\tilde{a})}\tilde{a}\frac{\partial}{\partial x^1}\right)$$

vanishes on the solutions considered, one can replace $\partial_t + \mathbf{u}\cdot\nabla$ in Eqs. (3.1) by $-(\kappa-1)(2\psi'(\tilde{a}))^{-1}\tilde{a}\partial/\partial x^1$. Expressing then $\tilde{a}$ in terms of u according to Eq. (5.3) (e.g. $\tilde{a} = \sinh 2u$ or $\tilde{a} = \sin 2u$, for $\kappa = 2$), one immediately obtains two equations defining double waves in terms of the original variables u, v

$$\begin{aligned} \left(\tilde{a}_u^2 - 1\right) u_{x^1} - v_{x^2} &= 0, \\ v_{x^1} - u_{x^2} &= 0. \end{aligned}$$

Their solutions define double waves taken at some constant t, therefore they must be extended over the space t, x^1, x^2 in such a way that they are constant along the directions of $\boldsymbol{\sigma}(u, v)$. This illustrates another procedure of obtaining the equations defining double waves, probably the fastest since no additional variables R^1, R^2 are required. In the Case 1 of (5.4) this system is hyperbolic for any value of u, whereas in the Case 2 it changes its type on lines $u = \pm\pi/6$, (i.e. $\cos 4u = -1/2$). For $\cos 4u < -1/2$ it becomes elliptic. One can demonstrate, however, that its solutions are still solutions of the basic system (3.1) [19, 20]. To conclude, let us also note that the most general cylindrical surface can be locally represented by $u - \psi(\tilde{a} - \alpha v) = 0$, α is a constant. This leads, however, to a more complicated equation than Eq. (5.1).

6. A general remark on the problem of wave-wave interaction

By substitution $F = \tilde{a} - \psi(u, v)$, Eq. (3.8) may be transformed to the following form

$$\frac{2}{\kappa - 1}\left[\frac{\kappa - 1}{2}\left(\psi_u^2 + \psi_v^2\right) + 2\right] - \psi\left\{\left(\psi_v^2 - 1\right)\psi_{uu} + \left(\psi_u^2 - 1\right)\psi_{vv} - 2\psi_u\psi_v\psi_{uv}\right\} = 0. \tag{6.1}$$

This specialization excludes the case when $F = F(u, v)$ but, as we know from previous consideration, only one-dimensional nonstationary flows are of this form. Equation (6.1) is of the second order and its characteristics $(u(s), v(s))$ are given by

$$(\psi_u^2 - 1)u'^2 + (\psi_v^2 - 1)v'^2 + 2\psi_u\psi_v u' v' = 0. \tag{6.2}$$

However, as follows from Eq. (3.2), any C^1 curve $(\tilde{a}(s), u(s), v(s))$ is a range of an irrotational simple wave if its tangent vector $(\tilde{a}, u', v')$ is a polarization vector, i.e. if it satisfies

$$(\tilde{a}')^2 - u'^2 - v'^2 = 0. \tag{6.3}$$

Suppose that this curve lies on the surface $\tilde{a} - \psi(u, v) = 0$. Differentiating this relation with respect to s we have $a' = \psi_u u' + \psi_v v'$. When applied to Eq. (6.3) it converts it into Eq. (6.2). Thus, characteristic lines of Eq. (6.1) are also projections of characteristics of Eq. (3.8) on the (u, v) plane. However, according to our considerations in Sec. 2, the characteristics of Eq. (3.8) are the images of simple waves. As can be seen from (6.2), Eq. (6.1) becomes elliptic if $\psi_u^2 + \psi_v^2 < 1$.

Let us now consider the initial condition for the flow equations (3.1) which is defined in a circle on the (x, y) plane for $t = 0$, and which represents two localized simple waves approaching each other, separated by a constant state $U_0 = (a_0, u_0, v_0)$ (Fig. 3). If the amplitudes and their derivatives are not too large, then, in the "conical" region of t, x^1, x^2, where the solution is uniquely determined, the solution exists and it represents two simple waves crossing each other for some larger t (similarly as in Fig. 2).

In order to demonstrate this, let us notice that the image (the set of values) of the initial conditions consists of two pieces of characteristic curves Γ_1, Γ_2 in the hodograph space passing through point U_0 (Fig. 4). Let us now take Γ_1, Γ_2 as the Darboux problem for Eq. (6.1). The value of ψ is then given on two intersecting characteristics of Eq. (6.1). Let Γ_1, Γ_2 be given in a parametrical form

$$\Gamma_1 = \left(\tilde{a} = \alpha_0(s),\ u = \alpha_1(s),\ v = \alpha_2(s)\right), \qquad b_1 \leq s \leq b_2,$$

$$\Gamma_2 = \left(\tilde{a} = \beta_0(\tau),\ u = \beta_1(\tau),\ v = \beta_2(\tau)\right), \qquad c_1 \leq \tau \leq c_2.$$

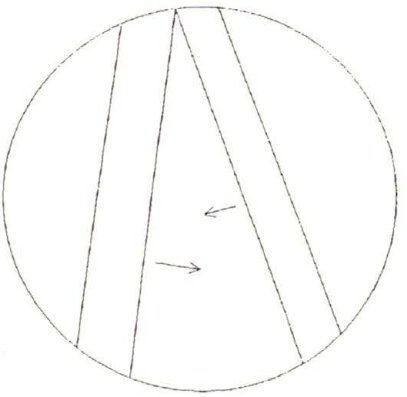

FIG. 3.

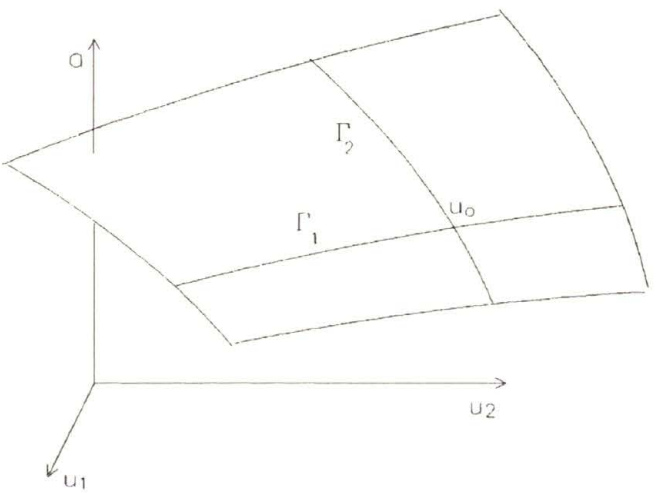

FIG. 4.

Then the projection $\tilde{\Gamma}_1 = (\alpha_1(s),\ \alpha_2(s))$, $\tilde{\Gamma}_2 = (\beta_1(\tau),\ \beta_2(\tau))$ are the characteristics of Eq. (6.1) and we may set

$$\psi_{|\tilde{\Gamma}_1} = \alpha_0(s), \qquad \psi_{|\tilde{\Gamma}_2} = \beta_0(\tau).$$

Let us also assume that $\alpha_0(s)$, $\beta_0(\tau) > 0$, otherwise we would have a singularity in Eq. (6.1). Indeed, $a^2 = dp/d\varrho$, $a = 0$ corresponds to the vacuum.

In conclusion, we state the following theorem

THEOREM 2. *Let Γ_1, Γ_2 be two characteristic curves of class C^2 in the hodograph space passing through the point $U_0 = (a_0, u_0, v_0)$. If $a_0 > 0$, then*

1) *there exists a unique solution of the above Darboux problem provided that Γ_1, Γ_2 are of sufficiently small length and have a curvature small enough*;

2) *the surface* $\tilde{a} = \psi(u, v)$ *representing the solution is covered by two families of characteristic curves in the hodograph space, and its boundary consists of pieces of characteristic curves passing through the end points of* Γ_1 *and* Γ_2, *thus forming a curvilinear quadrangle* (Fig. 3).

The proof can be obtained by representing the solution of the linearized problem in the form of a double integral along the characteristics. Then, using successive approximations and the Banach contraction principle one can prove the convergence. Let us note, that we work in the region of hyperbolicity of Eq. (6.1), since there are two characteristics Γ_1, Γ_2 at U_0 and this must be true in some neighborhood of the Darboux data.

We do not present the details of the proof since the proof for a general case of interacting waves can be found in [20].

Suppose now, that the considered solution $a = \psi(u, v)$ of Eq. (6.1), representing the surface as shown in Fig. 3, is given. At this moment one can assume a new system of coordinates on the surface, whose lines are the two families of characteristic curves from which the surface is "weaved". Vectors tangent to these lines are the polarization vector-fields and thus λ^1, λ^2 can be determined according to (3.1) and expressed in terms of R^1, R^2. Having λ^1, λ^2, the equations for $R^1(t, x, y)$, $R^2(t, x, y)$ can be solved by assuming for $R^1(0, x, y)$, $R^2(0, x, y)$ the profiles of the waves specified by the initial conditions.

If the amplitudes of the waves are large, the solution of Eq. (6.1) can enter the ellipticity region (e.g. Case 2 in Sec. 5). Similarly, if the profiles of initial waves are too steep, the solution can develop the singularities (gradient catastrophe) before the interaction is fully developed.

The form of Eq. (6.1) suggests the possibility of a geometric interpretation. The term

$$(\psi_v^2 - 1)\psi_{uu} + (\psi_u^2 - 1)\psi_{vv} - 2\psi_u\psi_v\psi_{uv}$$

in Eq. (6.1) is proportional to the mean curvature of the surface $\tilde{a} = \psi(u, v)$ when the surface is considered as embedded in the hodograph space endowed with the Minkowskian metric $(1, -1, -1)$. But this is the form (6.3) defining the polarization vectors. One can also verify that the first term in Eq. (6.1) vanishes when computed for the surface representing the range of two noninteracting waves [7]. This also suggests that the first term in Eq. (6.1) measures in some way the strength of interaction. This line of reasoning which appears to be also useful in the proof of existence, was developed in [19, 20].

Equation (6.1) was obtained also in [21], where the authors were searching for solutions with degenerate hodograph. They did not relate these solutions to interacting waves. It seems that Yanenko was also aware (private conversation) of the connection between Eq. (6.1) and the curvature of the hodograph surface. This justifies to call Eq. (6.1) the Yanenko equation.

In conclusion, we should emphasize, however, that the property of elastic interaction that irrotational modes exhibit when subjected to a nonlinear interaction,

is rather exceptional. If one of these two interacting waves were the shear wave or the entropic wave [18], then the picture would be more complicated due to the production of new waves (e.g. reflected waves) in the process of interaction. For this reason, in such cases as represented by the two potential modes considered here, we propose to speak of an elastic interaction.

The first (unpublished) version of this paper, which constituted a part of the authors' Ph. D. Thesis, was submitted for publication in 1972 under the title: "Some problems of double waves in gas dynamics". The present version contains several improvements.

The paper was supported by grant KBN No. PB 20480-90-1.

References

1. F. BAUER, R. GARABEDIAN and D. KORN, *Supercritical wing sections*, Lectures Notes in Economics and Mathematical Systems – 66, Springer Verlag, New York 1972.
2. F. BAUER, R. GARABEDIAN, D. KORN and A. JAMESON, *Supercritical wing sections II*, Lectures Notes in Economics and Mathematical Systems – 108, Springer Verlag, New York 1978.
3. M. BURNAT, *Hyperbolic double waves*, Bull. Acad. Polon. Sci., Série Sci. Techn., **16**, 1, 867, 1968.
4. M. BURNAT, *The method of Riemann invariants for multidimensional nonelliptic system*, Bull. Acad. Polon. Sci., Série Sci. Techn., **17**, 97, 1019, 1969.
5. R. CAOURANT and K.O. FRIEDRICHS, *Supersonic flow and shock waves*, Interscience Publishers, New York 1948.
6. L. DINU, *Some remarks concerning the Riemann invariance. Burnat – Peradzyński and Martin approaches*, Rev. Roumaine de Math. Pures et Appl., **35**, 203, 1990.
7. H. FLANDERS, *Differential forms with applications to the physical sciences*, Academic Press, New York 1963.
8. R. GARABEDIAN and D. KORN, *Numerical design of transonic airfoils. Numerical solution of partial differential equations* – II, Academic Press, New York 1971.
9. J.H. GIESE, *Compressible flow with degenerate hodographs*, Quarterly Appl. Math., **9**, 237, 1951.
10. A.M. GRUNDLAND and P.J. VASSILIOU, *On the solvability of the Cauchy problem for Riemann double-waves by the Monge–Darboux method*, Analysis, **11**, 221, 1991.
11. A.M. GRUNDLAND and R. ŻELAZNY, *Simple waves in quasilinear hyperbolic systems*. Part I and II., J. Math. Phys., **24**, 1983.
12. P. KUCHARCZYK, Z. PERADZYŃSKI and E. ZAWISTOWSKA, *Unsteady multi-dimensional isentropic flow described by linear Riemann invariants*, Arch. Mech., **25**, 319–350, 1973.
13. R. VON MISES, *Mathematical theory of compressible fluid flow*, Academic Press, New York 1958.
14. L. NIRENBERG, *Lectures on nonlinear functional analysis* [in Russian], Seria Matematika, Mir, Moskva 1977.
15. Z. PERADZYŃSKI, *Nonlinear plane k-waves and Riemann invariants*, Bull. Acad. Polon. Sci., Série Sci. Techn., **19**, 9, 59–66, 1971.
16. Z. PERADZYŃSKI, *Riemann invariants for the nonplanar k-waves*, Bull. Acad. Polon. Sci., Série Sci. Techn., **19**, 10, 59–74, 1971.
17. Z. PERADZYŃSKI, *On certain classes of exact solutions for gasdynamics equations*, Arch. Mech., **24**, 287–303, 1972.
18. Z. PERADZYŃSKI, *Asymptotic decay of solutions of hyperbolic system into simple waves*, Bull. Acad. Polon. Sci., Série Sci. Techn., **26**, 12, 513–519, 1078.
19. Z. PERADZYŃSKI, *Geometry of nonlinear interaction in partial differential equations* [in Polish], IFTR Reports, Warszawa 1981.

20. Z. PERADZYŃSKI, *Geometry of Riemann waves*, [in:] Advances in Nonlinear Waves, L. DEBNATH [Ed.], Pitman, 244–285, 1985.

21. YU. YA. POGODIN, V.A. SUTCHKOV and N.N. YANENKO, *Equations of wave propagation in dynamics of gases* [in Russian], DAN SSSR, **119**, 3, 443, 1958.

22. G.B. RIEMANN, *Über die Fortpflanzung ebener Luftwellen von endlicher Schwingungsweite*, Abhandl. Ges. Wiss., Göttingen Math.–Physik., Kl. 8, 43, 1958/59.

23. B.L. ROZHDESTVENSKI and N.N. YANENKO, *Systems of quasi-linear equations and their applications to dynamics of gases* [in Russian], Nauka, Moskva 1968.

24. A.F. SIDOROV, V.P. CHAPEEV and N.N. YANENKO, *The method of differential constraints and its application in gas-dynamics* [in Russian], Nauka, Moskva 1984.

POLISH ACADEMY OF SCIENCES
INSTITUTE OF FUNDAMENTAL TECHNOLOGICAL RESEARCH.

Received May 17, 1996.

Arch. Mech., 48, 6, pp. 1089–1100, Warszawa 1996

An approach to gauge potentials in the non-Abelian $ISO(3)$-gauge model of defects in solids

C. MALYSHEV (ST.-PETERSBURG)

A METHOD is proposed to reduce the Cartan structure equations and the Bianchi identities of the non-Abelian $ISO(3)$-gauge model of defects in solids to the appropriate relations of the theory of disclinations considered as the Abelian $i\tilde{s}o(3)$-gauge model. As the result, the possibility arises to identify the $ISO(3)$-gauge potentials in terms of the defect loop densities.

1. Introduction

IN THE REFS. [1, 2] it has been shown that both the field equations and the continuity equations of the theory of disclinations [3] can be rewritten in the form inherent to Abelian gauge models. The Lie algebra $i\tilde{s}o(3)$ of the group $ISO(3) = T(3) \otimes SO(3)$ ($\otimes$ – semi-direct product of groups) of 3D rigid body motions can be considered as additive Abelian group (as a vector space $\mathbb{R}^6$, in fact) and it plays the role of non-compact gauge group in the picture revealed in [1, 2]. In Refs. [1, 2] the possibility is suggested to apply a special exterior calculus where the role of exterior differential is played by the SCHAEFER'S differential [4]. Once the additive action of $i\tilde{s}o(3)$ is non-homogeneous (i.e. coordinate-dependent) under the Schaefer's differential, both the disclination and dislocation densities appear as components of the $i\tilde{s}o(3)$-valued gauge field strength. Eventually, the field equations of the defect theory [3] acquire the form of Cartan structure equation, while the continuity equations – of Bianchi identity of a certain Abelian gauge model.

On the other hand, the idea is widely known (cf. [5, 6]) to use $ISO(3)$ to formulate a geometrically nonlinear dynamical theory of defects in solids as a classical model of Yang-Mills type (that is $ISO(3)$ is attempted to be gauged as internal symmetry in [5, 6]). The algebra $i\tilde{s}o(3)$ plays an important role in [5, 6] thus rising the question: is it possible to reduce certain relations of this general model so that the corresponding ones of the theory [3] will appear just in the $i\tilde{s}o(3)$-representation found in [1, 2]? Such reduction would deserve consideration because, linear as it is, the approach [3] (R. deWit emphasizes that the linear assumption promotes complete analytical computations) provides a reliable scheme for a number of calculations concerning both the isolated defects and their distributions (see [7, 8] and numerous refs. therein).

The question proposed has been asked at the end of [1], and the present paper will point out a possible strategy to answer it. That is, a way to map the geometric relations of the $ISO(3)$-gauge model to the appropriate relations of [3]

is presented below. Namely, it is proposed to reduce by linearization the $ISO(3)$ Cartan equations to the "Cartan equation" (i.e. to the field equations written in the $\mathfrak{iso}(3)$-representation) of the theory [3]. The same is true for the Bianchi identities. Provided a correspondence between the gauge transformation groups is accounted for, a special restriction arises for the $\mathfrak{iso}(3)$-gauge parameters. It is demonstrated that this restriction is fulfilled by a finite loop defect. As the result, the correspondence established allows for a "mechanical" interpretation for the $ISO(3)$-fields. Though a different one has been proposed in [5, 6], we hope to argue the naturalness of that suggested here.

The paper is organized as follows. Section 2 reminds briefly [1, 2] to specify the meaning of the $\mathfrak{iso}(3)$-gauge fields. Section 3 contains both the Cartan structure equations and the Bianchi identities of the $ISO(3)$-gauge model and the truncation prescription for them. Section 4 concerns the mapping between the two sets of relations. Discussion in the Sec. 5 completes the paper.

We establish the following conventions. Our consideration is time-independent and all indices run from 1 to 3, the repeated ones imply summation. The Lie algebra $\mathfrak{so}(3)$ consists of real skew matrices of third order and the matrix elements of its three generators l_a coincide with the permutation symbol components. Therefore we shall represent $\lambda = \lambda_a l_a \in \mathfrak{so}(3)$ as 3-vectors $\boldsymbol{\lambda}$ and matrix action of λ as vector multiplication. For elements of $\mathfrak{iso}(3)$ two notations are equivalent: $\begin{pmatrix} \boldsymbol{\lambda} \\ \boldsymbol{\eta} \end{pmatrix}$ (by R. VON MISES [9]) and $\boldsymbol{\eta} \dot{+} \boldsymbol{\lambda}$ (semi-direct sum), where $\boldsymbol{\eta} \in \mathfrak{t}(3)$ and $\boldsymbol{\lambda} \in \mathfrak{so}(3)$. For shortness $G \equiv ISO(3)$ and $\mathfrak{g} \equiv \mathfrak{iso}(3)$.

2. The theory of disclinations as the Abelian $\mathfrak{iso}(3)$-gauge model

In this section we sketch some basic relations obtained in [1, 2]. Let M be a flat three-dimensional manifold and T^*M be a cotangent bundle over M. The objects we need here are sections

$$\omega^{(n)} \in \Omega^n(M) \equiv C^\infty(M, \mathfrak{g} \otimes \wedge^n(T^*M)) \tag{2.1}$$

of sheaves [10] of smooth differential n-forms taking their values in $\mathfrak{g}$. In (2.1) $\wedge^n(T^*M)$ means exterior product of n copies of T^*M (n does not exceed 3, clearly). According to the "6-vector" structure of $\mathfrak{g}$, we shall put $\omega^{(n)}$ (2.1) as $\overset{(n)}{\boldsymbol{\eta}} \dot{+} \overset{(n)}{\boldsymbol{\lambda}}$, where both the vectors are referred to a frame $\{\mathbf{e}_a\}$ in a covering U. That is to say that as the frame $\{\mathbf{e}_a\}$ is transformed, the vectors $\boldsymbol{\eta}$ and $\boldsymbol{\lambda}$ are transformed too.

Apart from the standard exterior differential d, there exists a homeomorphism d^{Sh} on $\Omega^n(M)$ such that n is increased by one:

$$d^{Sh} : \Omega^n(M) \to \Omega^{n+1}(M). \tag{2.2}$$

The corresponding operator is known as the Schaefer's differential [4] and with respect to $\{\mathbf{e}_a\}$ it takes the form:

$$d^{Sh}\overset{(n)}{\omega} = \begin{pmatrix} d\overset{(n)}{\boldsymbol{\lambda}} \\ d\overset{(n)}{\boldsymbol{\eta}} + d\mathbf{x} \overset{\times}{\wedge} \overset{(n)}{\boldsymbol{\lambda}} \end{pmatrix}, \tag{2.3}$$

where $\overset{\times}{\wedge}$ implies that the differential forms are multiplied externally while their coefficients as 3-vectors. It can be verified that d^{Sh} (2.3) is nilpotent, i.e. $d^{Sh} \circ d^{Sh} = 0$ [4, 1]. The definition (2.3) gives us the corresponding partial differentiation operator $P_a \equiv \partial_a^{Sh}$ which is one of the two generators of $\mathfrak{g}$. The second one $M_a \equiv (\mathbf{x} \times \boldsymbol{\partial})_a^{Sh}$ has been found in [1, 2] so that P_a and M_a fulfil together the fundamental brackets which display $\mathfrak{g}$ as a semi-direct sum of $\mathfrak{t}(3)$ and $\mathfrak{so}(3)$.

Using the definitions (2.1) – (2.3) one gets the following relations in the theory of disclinations [3]. Let us consider $\mathcal{A}^{Sh} \in \Omega^1(M)$

$$\mathcal{A}^{Sh} = \boldsymbol{\gamma} \oplus \boldsymbol{\zeta}, \tag{2.4}$$

and $\mathcal{F}^{Sh} \in \Omega^2(M)$ in the form

$$\mathcal{F}^{Sh} \equiv \boldsymbol{\mathcal{F}}_m \oplus \boldsymbol{\mathcal{F}}_v = d^{Sh}\mathcal{A}^{Sh}, \tag{2.5}$$

that is

$$\begin{aligned} \boldsymbol{\mathcal{F}}_v &= d\boldsymbol{\zeta}, \\ \boldsymbol{\mathcal{F}}_m &= d\boldsymbol{\gamma} + \boldsymbol{\zeta} \overset{\times}{\wedge} d\mathbf{x}. \end{aligned} \tag{2.6}$$

Defining duals to the coefficients of $\boldsymbol{\mathcal{F}}_v$ and $\boldsymbol{\mathcal{F}}_m$ by

$$\theta_{qp} = \frac{1}{2}\epsilon^{qab}(\mathcal{F}_v)_{ab}^{p}, \qquad \alpha_{qp} = \frac{1}{2}\epsilon^{qab}(\mathcal{F}_m)_{ab}^{p}, \tag{2.7}$$

one has (2.6) written in components:

$$\begin{aligned} \theta_{qp} &= \epsilon^{qab}\partial_a\zeta_{bp}, \\ \alpha_{qp} &= \epsilon^{qab}(\partial_a\gamma_{bp} + \epsilon^{bpc}\zeta_{ac}). \end{aligned} \tag{2.8}$$

The formulas (2.8) are nothing but the fundamental relationships between disclination and dislocation densities θ_{qp}, α_{qp} and disclination and dislocation loop densities ζ_{bp}, γ_{bp} just in the sense of [3]. In other words, the coefficients of $\mathcal{A}^{Sh}$ (2.4) can be viewed as the defect loop densities, once the L.H.S. of (2.5) is considered as the motor of the defect densities. Note that we call Eqs. (2.8) the field equations to distinguish them from the Eqs. (2.10) below.

Let us also introduce the vector-valued 1-form φ by the equation

$$\zeta = \varphi - \frac{1}{2} d(\mathbf{e}_c \times \boldsymbol{\gamma}_c), \tag{2.9}$$

where $\boldsymbol{\gamma}_c$ are the coefficients of $\boldsymbol{\gamma}$ (2.4) and $\{\mathbf{e}_c\}$ is the frame. Then (2.8) reads:

$$\begin{aligned} \theta_{qp} &= \epsilon^{qab} \partial_a \varphi_{bp}, \\ \alpha_{qp} &= \epsilon^{qab} (\partial_a \gamma_{(bp)} + \epsilon^{bpc} \varphi_{ac}), \end{aligned} \tag{2.10}$$

where $\gamma_{(bp)}$ implies symmetrization $(1/2)(\gamma_{bp} + \gamma_{pb})$. It seems that the reasons to write (2.9) are independent from the matter considered here, i.e. they have nothing to do with the algebra and gauging at hands below and therefore [3] contains more information about them. Once we introduce $-e^P_{bp}$ instead of $\gamma_{(bp)}$ and $-\kappa^P_{bp}$ instead of φ_{bp}, (2.10) express the defect densities through the basic plastic fields of strain (e^P_{bp}) and bend-twist (κ^P_{bp}) [3]. Recall that in order to extend the theory of dislocations so that both translations and rotations would be no longer integrable, R. deWit has proposed to postulate basic plastic fields of strain and bend-twist instead of plastic distortion (which does not exist with disclinations) to describe static distributions of defects.

By nilpotency of d^{Sh} it is seen that integrability for the Eq. (2.5) is expressed by

$$d^{Sh} \mathcal{F}^{Sh} = 0, \tag{2.11}$$

or

$$\begin{aligned} d\boldsymbol{\mathcal{F}}_v &= 0, \\ d\boldsymbol{\mathcal{F}}_m - \boldsymbol{\mathcal{F}}_v \overset{\times}{\wedge} d\mathbf{x} &= 0. \end{aligned} \tag{2.12}$$

It is straightforward to verify that the Eqs. (2.12) imply the standard continuity equations for α_{qp}, θ_{qp} provided (2.7) holds [1, 2]. Though (2.4)–(2.6), (2.11), (2.12) has already appeared in [1, 2], their interpretation is more transparent here. The Eqs. (2.9), (2.10) are useful connecting [1] and [3].

To conclude the section, the 2-form $\mathcal{F}^{Sh}$ (2.5) (gauge field strength) is invariant under the shift

$$\mathcal{A}^{Sh} \to \mathcal{A}^{Sh} - \delta \mathcal{A}^{Sh}, \qquad \delta \mathcal{A}^{Sh} = d^{Sh} \omega^{(0)} \tag{2.13}$$

for any $\omega^{(0)} \in \Omega^0(M)$. Therefore it is seen that the Eqs. (2.5) ("Cartan structure equation"), (2.11) ("Bianchi identity") and (2.13) (gauge transformation group) display us the theory of disclinations [3] as the Abelian gauge model with the additive gauge group $\mathfrak{g} \approx \mathbb{R}^6$ [1, 2].

3. Cartan structure equations and Bianchi identities of the $ISO(3)$-gauge model

Now let us have a look at the geometric relations in affine gauge models, i.e. in the models using principal fiber bundles of affine frames as geometric background. To this end we shall follow [11] (see also [12]) but more rigorous details on bundles of affine and linear frames can be found in [13, 14].

Let us start with the bundles $\mathbb{A}(M)$ of affine frames and $\mathbb{L}(M)$ of linear frames over an arbitrary manifold M. Our gauge group is G. We shall denote by ε the homeomorphism of $\mathbb{L}(M)$ to $\mathbb{A}(M)$ induced by the injection $\mathbb{L}(M) \to \boldsymbol{\mathcal{O}} \otimes \mathbb{L}(M) \subset \mathbb{A}(M)$ ($\boldsymbol{\mathcal{O}}$ is a "zero" vector). Let $\tilde{\mathbf{A}}$ be a generalized affine connection 1-form on $\mathbb{A}(M)$. The conjugated homeomorphism (pullback) ε^* maps it in a $\mathfrak{g}$-valued 1-form on $\mathbb{L}(M)$ which is split as follows:

$$\varepsilon^* \tilde{\mathbf{A}} = \boldsymbol{\phi} \oplus \mathbf{A}, \tag{3.1}$$

where $\mathbf{A}$ and $\boldsymbol{\phi}$ are $\mathbb{R}^3$-valued differential 1-forms on $\mathbb{L}(M)$. The corresponding affine curvature 2-form on $\mathbb{A}(M)$ is $\tilde{\mathbf{F}}$ and it also is split into the translation and linear parts $\boldsymbol{\Phi}$ and $\mathbf{F}$:

$$\varepsilon^* \tilde{\mathbf{F}} = \boldsymbol{\Phi} \oplus \mathbf{F}. \tag{3.2}$$

The 1-form $\mathbf{A}$ can be referred to as a linear connection on M, while $\mathbf{F}$ as its curvature 2-form (both are $\mathfrak{so}(3)$-valued, in fact). The couple of structure equations holds for the objects in the R.H.S. of (3.1), (3.2):

$$\begin{aligned} d\mathbf{A} + (1/2)\,\mathbf{A} \overset{\times}{\wedge} \mathbf{A} &= \mathbf{F}, \\ d\boldsymbol{\phi} + \mathbf{A} \overset{\times}{\wedge} \boldsymbol{\phi} &= \boldsymbol{\Phi}, \end{aligned} \tag{3.3}$$

where $\overset{\times}{\wedge}$ is defined in the Sec. 2.

It is well known that the translation part $\boldsymbol{\Phi}$ of the affine curvature $\tilde{\mathbf{F}}$ is transformed non-homogeneously under the infinitesimal affine gauge transformation

$$\begin{aligned} \mathbf{A} &\to \mathbf{A} - \mathbf{A} \times \boldsymbol{\lambda} - d\boldsymbol{\lambda}, \\ \boldsymbol{\phi} &\to \boldsymbol{\phi} + \boldsymbol{\lambda} \times \boldsymbol{\phi} - \mathbf{A} \times \boldsymbol{\eta} - d\boldsymbol{\eta}, \end{aligned} \tag{3.4}$$

where $\boldsymbol{\eta} \oplus \boldsymbol{\lambda} \in \Omega^0$ are the group parameters, and therefore it is impossible to consider it as the torsion of the linear connection $\mathbf{A}$ (3.1) though the Eq. $(3.3)_2$ looks properly [14]. In order to "extract" from $\boldsymbol{\Phi}$ the contribution which is transformed under (3.4) appropriately, let us define the vector-valued zero-form $\boldsymbol{\chi}$ ("affine Higgs" field, following [11]) which is a local cross-section of an associated vector bundle and its gauge transformation is

$$\boldsymbol{\chi} \to \boldsymbol{\chi} + \boldsymbol{\lambda} \times \boldsymbol{\chi} + \boldsymbol{\eta}.$$

Then

$$\vartheta = \Phi + \mathbf{F} \times \chi \tag{3.5}$$

is transformed as required:

$$\vartheta \to \vartheta + \lambda \times \vartheta .$$

Namely ϑ (3.5) can be referred to as the torsion 2-form of the linear connection $\mathbf{A}$, while $\mathbf{F}$ is its curvature [11, 14]. Now the Eq. (3.5) may be rewritten as the corresponding Cartan structure equation

$$d\mathcal{B} + \mathbf{A} \overset{\times}{\wedge} \mathcal{B} = \vartheta , \tag{3.6}$$

where $\mathcal{B} = \phi + d\chi + \mathbf{A} \times \chi$ can be thought as a canonical ("soldering") 1-form [11, 12, 14–16]. Therefore $(3.3)_1$ and (3.6) give us the couple of Cartan structure equations where all the ingredients are transformed appropriately. The corresponding Bianchi identities appear straightforwardly:

$$\begin{aligned} d\mathbf{F} &= \mathbf{F} \overset{\times}{\wedge} \mathbf{A}, \\ d\vartheta &= \mathbf{F} \overset{\times}{\wedge} \mathcal{B} - \mathbf{A} \overset{\times}{\wedge} \vartheta . \end{aligned} \tag{3.7}$$

As to the matter at hands, the picture suggested in [5, 6] seems to be geometrically very close to affine gauge models with the group G because the fundamental Eqs. (3.3), (3.6), (3.7) have been extensively used there. The basic "fields" $\mathbf{A}$, ϕ, χ have been supplied in [5, 6] with space and time dependence (i.e. dim M is four) to be considered as dynamical variables describing media with continuously distributed defects. As it might be understood from [12] (the Chapter 3), whenever affine gauge models are concerned, the "affine Higgs" field (χ in our context) gets an appropriate problem-motivated interpretation. In the monograph [6] considerable attention has been paid to motivate χ in the framework of the dynamical model of defects. Loosely speaking one can say that χ has been put there as a field of current configurations $\chi = \mathbf{x} + \mathbf{u}(\mathbf{x}, t)$, so that $\mathbf{u}(\mathbf{x}, t)$ implies a displacement corresponding to point $\mathbf{x}$ in a reference configuration at time t.

The truncated version of $(3.3)_1$, (3.6), (3.7) we are interested in relies drastically on the decomposition $\chi = \mathbf{x} + \mathbf{u}$, and can easily be obtained. To this end let us consider $\mathbf{u}$, functions parametrizing the differential forms $\mathbf{A}$, ϕ, and their derivatives to be small so that all their products can be neglected. It means, for instance, that (3.4) are simply shifts by exact 1-forms $d\lambda$ and $d\eta$. Linearizing the L.H.S. of Eqs. (3.3) one obtains for $\mathbf{F}$ $(3.3)_1$ and ϑ (3.5):

$$\begin{aligned} d\mathbf{A} &= \mathbf{F}, \\ d\phi + d\mathbf{A} \times \mathbf{x} &= \vartheta . \end{aligned} \tag{3.8}$$

Further, simplifying analogously the R.H.S. of (3.7) one can see that the resulting equations

$$d\mathbf{F} = 0, \qquad d\boldsymbol{\vartheta} = \mathbf{F} \overset{\times}{\wedge} d\mathbf{x}, \tag{3.9}$$

are the integrability conditions for (3.8). It has to be noticed that the prescription alleged to drop out the products would imply in fact not spacially global but rather local (being valid, say, only for certain regions) weakness of some concrete field configurations which display a chosen geometry by means of the set of Eqs. (3.3), (3.6), (3.7).

4. The mapping

At last let us establish the correspondence between the Eqs. (2.6), (2.12) of the $i\mathfrak{so}(3)$-model and the Eqs. $(3.3)_1$, (3.6), (3.7) of the $ISO(3)$-gauge model of defects in solids. For as it has already been stressed, we shall do it by comparing the first group of equations with the truncated ones (3.8), (3.9).

It is indeed seen that (2.6) and (3.8) being written as

$$d^{Sh}\begin{pmatrix}\mathbf{A}\\ \boldsymbol{\phi} + \mathbf{A}\times\mathbf{x}\end{pmatrix} = \begin{pmatrix}\mathbf{F}\\ \boldsymbol{\vartheta}\end{pmatrix} \tag{4.1}$$

look similar and lead us to the following basic identification: the connection 1-form $\mathbf{A}$ would be the 1-form of disclination loop densities $\boldsymbol{\zeta}$ while the 1-form $\mathbf{A}\times\mathbf{x}+\boldsymbol{\phi}$ would be the 1-form of dislocation loop densities $\boldsymbol{\gamma}$. Once this interpretation is accepted, it becomes natural to say that the curvature and the torsion 2-forms $\mathbf{F}$ and $\boldsymbol{\vartheta}$ in the R.H.S. of (3.8) acquire the sense of $\mathcal{F}_v$ and $\mathcal{F}_m$, accordingly, i.e. of the disclination and dislocation densities 2-forms. It has to be reminded that the idea to identify dislocation density as a differential geometric torsion is not new at all [17]. Finally, the continuity equations (2.12) and (3.9) are fairly identical upon the identifications proposed. However, the correspondence of the gauge transformations requires some attention. Besides, the fact that the continuity equations for α_{pq}, θ_{pq} result from the linearized Bianchi identities, has been discussed also in [18] but in the framework of a metric-torsion gauge approach to the continuum defects.

In view of (3.4) the gauge variation of $\boldsymbol{\phi} + \mathbf{A}\times\mathbf{x} \oplus \mathbf{A}$ reads:

$$\delta\begin{pmatrix}\mathbf{A}\\ \boldsymbol{\phi} + \mathbf{A}\times\mathbf{x}\end{pmatrix} = \begin{pmatrix}d\boldsymbol{\lambda}\\ d\boldsymbol{\eta} + d\boldsymbol{\lambda}\times\mathbf{x}\end{pmatrix}, \tag{4.2}$$

where the R.H.S. is not a d^{Sh}-differential as in (2.13):

$$\delta\mathcal{A}^{Sh} = d^{Sh}\begin{pmatrix}\boldsymbol{\omega}\\ \mathbf{u}\end{pmatrix} = \begin{pmatrix}d\boldsymbol{\omega}\\ d\mathbf{u} - \boldsymbol{\omega}\times d\mathbf{x}\end{pmatrix}. \tag{4.3}$$

However, in both the cases $\vartheta \oplus \mathbf{F}$ (4.1) and $\mathcal{F}^{Sh}$ (2.5) are d^{Sh}-differentials invariant under the variations (4.2) and (4.3), respectively. The case here is simple: the relation

$$d(d\mathbf{v} \times \mathbf{x}) = -d\mathbf{v} \overset{\times}{\wedge} d\mathbf{x} = d(-\mathbf{v} \times d\mathbf{x}) \tag{4.4}$$

holds for any 3-vector $\mathbf{v}$ and it is why $\mathcal{F}^{Sh}$ and $\vartheta \oplus \mathbf{F}$ are both invariant.

The transformation parameters $\boldsymbol{\lambda}$ and $\boldsymbol{\eta}$ are small independent 3-vector functions in the $ISO(3)$ approach. Let us put the R.H.S. of (4.2) as a complete d^{Sh}-differential:

$$\begin{pmatrix} d\boldsymbol{\lambda} \\ d(\boldsymbol{\eta} + \boldsymbol{\lambda} \times \mathbf{x}) - \boldsymbol{\lambda} \times d\mathbf{x} \end{pmatrix}. \tag{4.5}$$

After this it is suggestive to state that $\boldsymbol{\lambda}$ (4.5) would correspond to $\boldsymbol{\omega}$ (4.3) and $\boldsymbol{\eta} + \boldsymbol{\lambda} \times \mathbf{x}$ (4.5) to $\mathbf{u}$ (4.3). This observation means that the gauge parameters in (4.3) have not to be considered as independent to get one-to-one correspondence (at the linearized level) with the $ISO(3)$-gauge geometry. Precisely, $\boldsymbol{\omega}$ as rotation becomes related to the displacement $\mathbf{u}$ by $\frac{1}{2}\partial \times \mathbf{u}$ at constant $\boldsymbol{\lambda}$, $\boldsymbol{\eta}$. In this way, the Eqs. $(3.3)_1$, (3.6) and (3.7) supplied with the gauge transformation rules indeed result in the $\mathfrak{iso}(3)$-represented relations of the theory of disclinations under the truncation prescribed.

In order to argue the correspondence presented, it is worth to find concrete non-trivial gauge transformation in the theory [3] which fulfils the restriction found, thus confirming its meaning. Fortunately, such example is given by an isolated defect loop

$$\begin{aligned} \boldsymbol{\zeta}_k &= \delta_k(S)\,\boldsymbol{\Omega}, \\ \boldsymbol{\gamma}_k &= \delta_k(S)\,(\mathbf{b} + \boldsymbol{\Omega} \times \mathbf{x}), \end{aligned} \tag{4.6}$$

where $\boldsymbol{\Omega}$ and $\mathbf{b}$ are the Frank and the Burgers vectors, and $\delta_k(S)$ is the singular function concentrated on the surface S [19, 3]. Here S is an open surface (so-called jump surface) which is bounded by closed defect line $L = \partial S$. It is easily seen that (4.6) respects our basic identification if we put $\mathbf{A}_k = \delta_k(S)\boldsymbol{\Omega}$ and $\boldsymbol{\phi}_k = \delta_k(S)\mathbf{b}$.

Let us define another open surface $\tilde{S}$ which is also bounded by L but oriented with respect to L oppositely to S so that $S \cup \tilde{S}$ is a closed smooth surface enclosing the volume V. Further, the variation (4.3) with the parameters

$$\begin{aligned} \boldsymbol{\omega} &= \delta(V)\,\boldsymbol{\Omega}, \\ \mathbf{u} &= \delta(V)\,(\mathbf{b} + \boldsymbol{\Omega} \times \mathbf{x}) \end{aligned} \tag{4.7}$$

acts on (4.6) as follows:

$$\begin{aligned} &\boldsymbol{\zeta}_k \to \boldsymbol{\zeta}_k + \partial_k\,(\delta(V))\,\boldsymbol{\Omega}\,, \\ &\boldsymbol{\gamma}_k \to \boldsymbol{\gamma}_k + \partial_k\,[\delta(V)\,(\mathbf{b} + \boldsymbol{\Omega} \times \mathbf{x})] - \delta(V)\boldsymbol{\Omega} \times \mathbf{e}_k \\ &\qquad\qquad = \boldsymbol{\gamma}_k + \partial_k\,(\delta(V))\,(\mathbf{b} + \boldsymbol{\Omega} \times \mathbf{x}). \end{aligned} \tag{4.8}$$

Taking into account

$$\partial_k(\delta(V)) = -\delta_k(S \cup \tilde{S})$$

and the formal equation

$$\delta_k(S) - \delta_k(S \cup \tilde{S}) = -\delta_k(\tilde{S}) = \delta_k(-\tilde{S})$$

($-\tilde{S}$ and $\tilde{S}$ are of opposite orientation), again one obtains from (4.8) the loop (4.6) with the jump surface $-\tilde{S}$. Therefore, the transformation given by (4.3), (4.7) is nothing but an orientation-preserving change of non-physical jump surface of the defect loop. Besides, the R.H.S. of (4.8) looks like the R.H.S. of (4.2) thus confirming the coincidence of the two sets of relations. For (4.6) the continuity equations (2.12) are satisfied too and so, the solution found indeed behaves properly. The defect loop (4.6) serves in [3] as the source which allows to obtain, for instance, the complete set of relations characterizing straight dislocation and disclination in an isotropic infinite body.

Before concluding the section let us try to make the correspondence found more transparent. Indeed, the defect loop definition (4.6) turns out to be a complete d^{Sh}-differential if one admits the surface S to be closed:

$$\begin{pmatrix} \zeta \\ \gamma \end{pmatrix} = -\begin{pmatrix} d\boldsymbol{\nu} \\ d\boldsymbol{\mu} + d\boldsymbol{\nu} \times \mathbf{x} \end{pmatrix} = -d^{Sh}\begin{pmatrix} \boldsymbol{\nu} \\ \boldsymbol{\mu} + \boldsymbol{\nu} \times \mathbf{x} \end{pmatrix}, \tag{4.9}$$

where $\boldsymbol{\nu} = \delta(W)\,\boldsymbol{\Omega}$, $\boldsymbol{\mu} = \delta(W)\,\mathbf{b}$, and W is volume inside S. This is because the components $\partial_k S$ become the derivatives $-\partial_k(\delta(W))$ for closed S. One simply has to replace $d\boldsymbol{\nu}$ and $d\boldsymbol{\mu}$ by certain 1-forms $\mathbf{A}$ and ϕ which are not exact, to break the d^{Sh}-exactness of $\gamma \oplus \zeta$ (4.9) and to obtain (4.6). It is just the way how the definition (4.6) appears for unclosed surface bounded by defect line. From a more general point of view, the Eqs. (4.6), (4.7) and (4.9) are particular manifestations of the sequence of homeomorphisms (2.2) being considered for elements $\mathcal{P}^{(n)} \in \Omega^n(M)$ of the following form:

$$\mathcal{P}^{(n)} = \begin{pmatrix} \boldsymbol{\nu} \\ \boldsymbol{\mu} + \boldsymbol{\nu} \times \mathbf{x} \end{pmatrix} \xrightarrow{d^{Sh}} \begin{pmatrix} d\boldsymbol{\nu} \\ d\boldsymbol{\mu} + d\boldsymbol{\nu} \times \mathbf{x} \end{pmatrix}, \tag{4.10}$$

where $\boldsymbol{\nu}$ and $\boldsymbol{\mu}$ imply now vector-valued n-forms. This special choice of $\mathcal{P}^{(n)}$ ensures that they are motors under coordinate shift $\mathbf{x} \to \mathbf{x} + \mathbf{y}$. Now it is seen that (4.9) gives the action of d^{Sh} on $\mathcal{P}^{(0)}$ being a rigid body displacement of inclusion W in motor representation. The coefficients (4.6) correspond to the defect loop 1-form $\mathcal{P}^{(1)}$ which is not d^{Sh}-exact. Differentiating $\mathcal{P}^{(1)}$ (4.6) one obtains the defect densities 2-form $\mathcal{P}^{(2)}$ (compare with (2.5), (2.6)) where the density components $\boldsymbol{\nu}_{kl} = \epsilon_{klm}\,\delta_m(L)\,\boldsymbol{\Omega}$, $\boldsymbol{\mu}_{kl} = \epsilon_{klm}\,\delta_m(L)\,\mathbf{b}$ are singular on the line L (see [19, 3] about $\delta_m(L)$). Moreover, one can see that gauge variations $\delta\mathcal{P}^{(1)}$ preserving any d^{Sh}-exact defect density $\mathcal{P}^{(2)}$ are not of the general form (2.13), (4.3) but rather of the form (4.2).

Realizing the differential complex (4.10) to contain all the relevant gauge-geometric information concerning [3], it is straightforward to try to relate it to the $ISO(3)$ geometric relations which would generalize the Abelian ones. As it has been stressed, the underlying algebra $\mathfrak{iso}(3)$ is of importance here. From (3.8) and (4.10) at $n = 1$ it is especially easy to understand the above key identification: after truncation in the structure equations $(3.3)_1$, (3.5), the gauge potentials $\mathbf{A}$ and $\boldsymbol{\phi}$ coincide with the corresponding elements of the defect loop densities 1-form $\mathcal{P}^{(1)}$ and the R.H.S. of (3.8) acquires the sense of motor of the defect densities. The Bianchi identities do not impose extra restrictions and are fairly identical. Therefore the reduction proposed both points out natural interpretation for the $ISO(3)$-gauge fields and shows definitely that the reduced gauge transformation can be combined as that corresponding to (4.10).

5. Discussion

We have described the reduction of the Cartan structure equations and the Bianchi identities of the $ISO(3)$-gauge model of defects in solids to the field equations and the continuity equations of the theory of disclinations being considered as the Abelian $\mathfrak{iso}(3)$-gauge model. It is the basis for both the cases underlying Lie algebra $\mathfrak{iso}(3)$ which prompts the idea to do this reduction by linearizing the non-Abelian geometric relations. Requiring additionally that the gauge parameters (rotations and translations) of the $\mathfrak{iso}(3)$-model are not independent, it is possible to display a certain correspondence between the two sets of relations.

Special example in the Sec. 4 fulfils the restriction found for the gauge parameters thus seemingly testifying on behalf of the chosen strategy. Besides, it is known that point-like sources are forbidden for non-compact Abelian gauge group, i.e. only sourceless strings might appear as solutions to the corresponding equations. So it is attractive to encounter the densities of the defect loops (closed strings) in our investigation. It is hopeful that such loop solutions should find generalization in non-Abelian situation.

The way proposed to identify the $ISO(3)$-gauge fields differs from that in [5, 6], and it is worth to pay some more attention to this fact. It is crucial that the pair of equations analogous to the Eqs. (2.12) has been written in [5, 6] as

$$\begin{aligned} d\boldsymbol{\Omega} &= 0, \\ d\mathbf{D} - \boldsymbol{\Omega} &= 0, \end{aligned} \tag{5.1}$$

(time is fixed) so that $\mathbf{D}$ and $\boldsymbol{\Omega}$ $(5.1)_2$ are the vector-valued differential forms corresponding to $\mathcal{F}_m$ and $\mathcal{F}_v \overset{\times}{\wedge} d\mathbf{x}$ $(2.12)_2$, accordingly. Because the disclination density $\boldsymbol{\Omega}$ has been referred to as a 3-form in [5, 6], the Eq. $(5.1)_1$ holds identically for the three-dimensionality of d, though it looks like integrability condition for $(5.1)_2$.

After this the following key identification has been made in [5, 6] to pass to the non-Abelian case: the kinematic equation

$$d\mathbf{B} + \mathbf{K} = \mathbf{D}$$

(it is reminiscent of $(2.6)_2$ in our notation, see also $(2.10)_2$ and the comment after that), where **B** is distortion 1-form and **K** is bend-twist 2-form, would correspond to the Cartan equation (3.6) itself (not to its linearization $(3.8)_2$ as we do) so that $\boldsymbol{\mathcal{B}}$, $\mathbf{A} \overset{\times}{\wedge} \boldsymbol{\mathcal{B}}$, and $\boldsymbol{\vartheta}$ would be **B**, **K**, and **D**, respectively. It is for these reasons that the Bianchi equation $(3.7)_2$ has been considered as the generalization of $(5.1)_2$ so that just the 3-form $\mathbf{F} \overset{\times}{\wedge} \boldsymbol{\mathcal{B}} - \mathbf{A} \overset{\times}{\wedge} \boldsymbol{\vartheta}$ acquires the sense of the source $\boldsymbol{\Omega}$ in the nonlinear situation. Obviously, such generalized "disclinations" will be also sourceless.

Conversely, in our approach both the disclination and dislocation densities are the vector and moment parts of the $\mathfrak{iso}(3)$-valued 2-form $\mathcal{F}^{Sh}$ which appears owing to the use of d^{Sh}. Therefore both the couples of the $ISO(3)$ Cartan structure equations and Bianchi identities after linearization are also considered as vector and moment parts of certain $\mathfrak{iso}(3)$-valued equations. Further, the 1-form $\mathbf{A} \times \mathbf{x} + \boldsymbol{\phi}$ (up to exact contribution it is just the reduced "soldering" 1-form) is identified here as the dislocation loop densities 1-form while in [5, 6] it is a distortion 1-form. The linear connection 1-form **A** corresponds here to the disclination loop densities 1-form.

The distinctive suggestion of the given approach is that that the curvature 2-form $\mathbf{F}$ $(3.3)_1$ should be treated as a generalization of the disclination density $\boldsymbol{\mathcal{F}}_v$. For the truncated case it is "almost" as $d\mathbf{A} \overset{\times}{\wedge} d\mathbf{x}$ which arises from $\boldsymbol{\Omega} = \mathbf{F} \overset{\times}{\wedge} \boldsymbol{\mathcal{B}} - \mathbf{A} \overset{\times}{\wedge} \boldsymbol{\vartheta}$ [5, 6] (see [1]), but the general situation is different because $d\mathbf{F}$ is not zero by $(3.7)_1$ and therefore nonlinearity of the $ISO(3)$ model can result in sources for "disclinations". Besides, the way how the group of the $ISO(3)$-gauge transformations includes that of the disclination theory is also different in [5, 6], i.e. it is not in the sense of one-to-one correspondence as in the Sec. 4.

To conclude, the given approach seems to show that the way adopted in [5, 6] to connect the affine gauge model with the classical defect model is not the only one possible. The main disagreement between the two viewpoints is clear. The present treatment proposes that only after reduction (e.g. asymptotically), the non-Abelian $ISO(3)$ relations could be identified in the framework of the theory of disclinations [3], whereas in [5, 6] the idea is that the form of the appropriate equations of the defect theory remains externally unchanged but their ingredients become complicated for $ISO(3)$. But surely the decisive conclusion would be drawn only by explicit $ISO(3)$ stringy solutions which allow simple loops, like that found above as a limiting case. Besides, having in mind a successive descent from affine frames to orthogonal ones [11, 13], it would be interesting to make contact with [17, 18, 20] where similar problems have been treated in a metric approach. Anyway, further considerations seem to be needed.

Acknowledgment

The author is grateful to Professors F.W. HEHL and A.E. ROMANOV for reading the manuscript.

References

1. C. MALYSHEV, *Underlying algebraic and gauge structures of the theory of disclinations*, Arch. Mech., **45**, 1, 93–105, 1993.
2. K.L. MALYSHEV, *Gauge group and gauge transformation in the continual theory of defects*, J. Math. Sci., **71**, 1, 2281–2287, 1994.
3. R. DE WIT, *Theory of disclinations. II. Continuous and discrete disclinations in anisotropic elasticity*, J. Res. Nat. Bur. Stand. US, **77A**, 1, 49–100, 1973; *Theory of disclinations. III. Continuous and discrete disclination in isotropic elasticity*, J. Res. Nat. Bur. Stand. US, **77A**, 3, 359–368, 1973; *Theory of disclinations. IV. Straight disclinations*, J. Res. Nat. Bur. Stand. US, **77A** 5, 607–658, 1973.
4. H. SCHAEFER, *Analyse der Motorfelder im Cosserat-kontinuum*, ZAMM, **47**, 5, 319–328, 1967.
5. A. KADIČ and D.G.B. EDELEN, *A gauge theory of dislocations and disclinations*, Lect. Notes Phys., Springer-Verlag, Berlin, **174**, 1983.
6. D.G.B. EDELEN and D.C. LAGOUDAS, *Gauge theory and defects in solids*, North-Holland Publ. Co, Amsterdam 1988.
7. A.E. ROMANOV and V.I. VLADIMIROV, *Disclinations in crystalline solids* [in:] Dislocations in Solids, vol. **9**, F.R.N. NABARRO [Ed.], North-Holland Elsevier, Amsterdam 1992, 191–402.
8. A.E. ROMANOV, *Screened disclinations in solids*, Mater. Sci. Engng., **164A**, 53–68, 1993.
9. R. VON MISES, *Motorrechnung, ein neues Hilfsmittel der Mechanik*, ZAMM, **4**, 2, 155–181, 1924.
10. F.W. WARNER, *Foundations of differential manifolds and Lie groups*, Springer-Verlag, New York 1983.
11. E.W. MIELKE, *Geometrodynamics of gauge fields – on the geometry of Yang-Mills and gravitational gauge theories*, Akademie-Verlag, Berlin 1987.
12. F.W. HEHL, J.D. MCCREA, E.W. MIELKE and Y. NE'EMAN, *Metric-affine gauge theory of gravity: field equations, Noether identities, world spinors, and breaking of dilaton invariance*, Phys. Rep., **258**, 1&2, 1–171, 1995.
13. A. LICHNEROWICZ, *Theorie globale des connexions et des groupes d'holonomie*, Edizioni Cremonese, Roma 1955.
14. S. KOBAYASHI and K. NOMIZU, *Foundations of differential geometry, V.I*, Interscience Publishers, New York 1963.
15. A. TRAUTMAN, *The geometry of gauge fields*, Czech. J. Phys., **29B**, 1, 107–116, 1979.
16. L.K. NORRIS, R.O. FULP and W.R. DAVIS, *Underlying fibre bundle structure of A(4) gauge theories*, Phys. Lett., **79A**, 4, 278–282, 1980.
17. E. KRÖNER, *Continuum theory of defects* [in:] Physique des Défauts (Les Houches, Session XXXV, 1980), R. BALIAN *et al.* [Eds.], North-Holland Publ. Co, Amsterdam 1981, 215–316.
18. A. VERÇIN, *Metric-torsion gauge theory of continuum line defects*, Int. J. Theor. Phys., **29**, 1, 7–21, 1990.
19. I.A. KUNIN, *The fields of arbitrarily distributed dislocations and force dipoles in elastically anisotropic infinite medium*, [in Russian], J. Appl. Mech. Techn. Phys., 5, 76–83, 1965.
20. H. KLEINERT, *Double gauge theory of stresses and defects*, Phys. Lett., **97A**, 1&2, 51–54, 1983.

RUSSIAN ACADEMY OF SCIENCES
ST.-PETERSBURG BRANCH OF STEKLOV MATHEMATICAL INSTITUTE, ST.-PETERSBURG, RUSSIA.

Received May 20, 1996.

Arch. Mech., 48, 6, pp. 1101–1113, Warszawa 1996

Necking in steady-state drawing of polymer fibres

S. ZAHORSKI (WARSZAWA)

THE CONCEPT of non-uniform extensional motions of materially non-uniform simple locally isotropic solids is used to discuss some general properties of fibre drawing processes. In the approach presented, axial and radial temperature and structure variations can be taken into account as some kind of non-uniformity. For steady cold-drawing processes various necking conditions are considered in general and particular cases. The effects of particular force components, i.e. inertial and rheological, are discussed in greater detail for S-shaped velocity profiles.

1. Introduction

DRAWING IS THE OPERATION which changes the textile characteristics of man-made fibres, improving, in particular, initially low tenacity, high irreversible deformation, low moduli, etc. It consists of irreversible elongation in the solid state from 20 to 20000 % of the original length. Such a process with coexistent undrawn and drawn parts, exhibiting the necking phenomenon, is often called the "cold drawing" although it may be realized at pretty high temperatures of baths or heaters. The most exhaustive information on drawing of polymer fibres can be found in the monograph by ZIABICKI [1].

From the rheological point of view, drawing of a long filament can be considered as a non-uniform and frequently non-isothermal quasi-elongational motion. As compared to melt-spinning processes, a relevant analysis is much more difficult since usually for deformed solids the dissipation energy cannot be neglected, leading to an additional increase of temperature. Also the nonlinear viscoelastic behaviour of solid polymers is an essential factor of the process considered, and neither Newtonian nor linearly elastic approximations can be applied at all.

In the present paper we use our previous concept of non-uniform extensional motions (NUEM) of materially non-uniform simple locally isotropic solids [2] to discuss some general properties of fibre-drawing processes without applying any particular models. This approach enables taking into account temperature and structure variations along and across the filament, replaced by some kind of spatial non-uniformity. The corresponding constitutive equations used for description of steady quasi-elongational motions involve the stretch ratios (axial velocities) as well as their derivatives in the direction of the axis (axial velocity gradients). An explicit dependence of material properties on the radial and axial coordinates can also be introduced. To satisfy the boundry conditions in stresses at the free surface of a filament, the assumptions very similar to those made in the case of flows with dominating extension (FDE) may be used like in [3, 4].

In Sec. 2 we discuss the drawing process as a steady non-uniform quasi-elongational motion, using the constitutive equations of a materially non-uniform simple locally isotropic solid. Next Sec. 3 is entirely devoted to various necking conditions expressed either in velocities or stresses. In Sec. 4 the effect of rheological force on the conventional stresses along the filament is discussed in greater detail. Last Sec. 5 summarizes our previous results in the form of several conclusions.

2. Drawing as a steady non-uniform motion of materially non-uniform solids

In the paper [2] it was proved that a steady non-uniform drawing process can be described by the following stress-components difference, resulting from the more general constitutive equations of materially non-uniform simple solids:

$$T^{33} - T^{11} = \sigma(V, V'; r, z) = \sigma_1(\lambda, \lambda'; r, z) = \sigma_2(\varepsilon, \dot{\varepsilon}, r, z), \tag{2.1}$$

where $V(z)$ is the axial velocity under a quasi-elongational approximation and the primes denote the corresponding derivatives with respect to the axial coordinate z (Fig. 1). The stretch ratio λ, the strain ε and their derivatives are defined as follows:

$$\lambda = \frac{V(z)}{V_0}, \qquad \frac{\lambda'}{\lambda} = \frac{V'}{V}, \tag{2.2}$$

$$\varepsilon = \ln \lambda, \qquad \dot{\varepsilon} = \frac{\lambda'}{\lambda} V = V', \tag{2.3}$$

where the dot denotes the corresponding time-rate and V_0 – the feeding velocity (at the first pair of godets, Fig. 1). Denoting by V_L the take-up velocity, we can

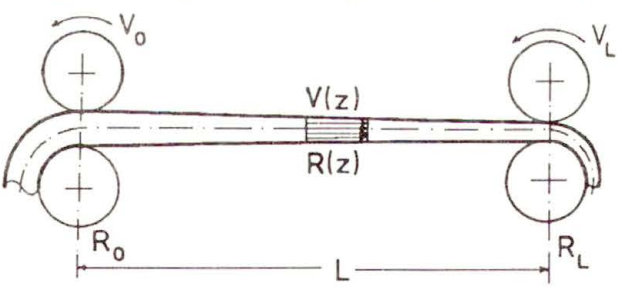

FIG. 1. Scheme of drawing process.

define the draw ratio $\mathfrak{R}$ (see Ref. [1]) as

$$\mathfrak{R} = V_L/V_0, \tag{2.4}$$

and the conventional or normal stress (related to the original cross-section) as

$$\sigma^0 = \sigma/\lambda, \tag{2.5}$$

if the process is steady-state, the mass flow rate remains constant, i.e.

$$W = \varrho\pi R^2 V = \varrho\pi R_0^2 V_0 = \varrho\pi R_L^2 V_L = \text{const.} \tag{2.6}$$

We should emphasize that Eqs. (2.1) or (2.5) can describe many types of non-linear visco-elastic behaviour, in particular, that shown for the polystyrene [5] in Fig. 2. The rate- and temperature-dependent stress-strain characteristics with stress overshoot before yielding usually lead to the necking phenomenon (see Ref. [1]).

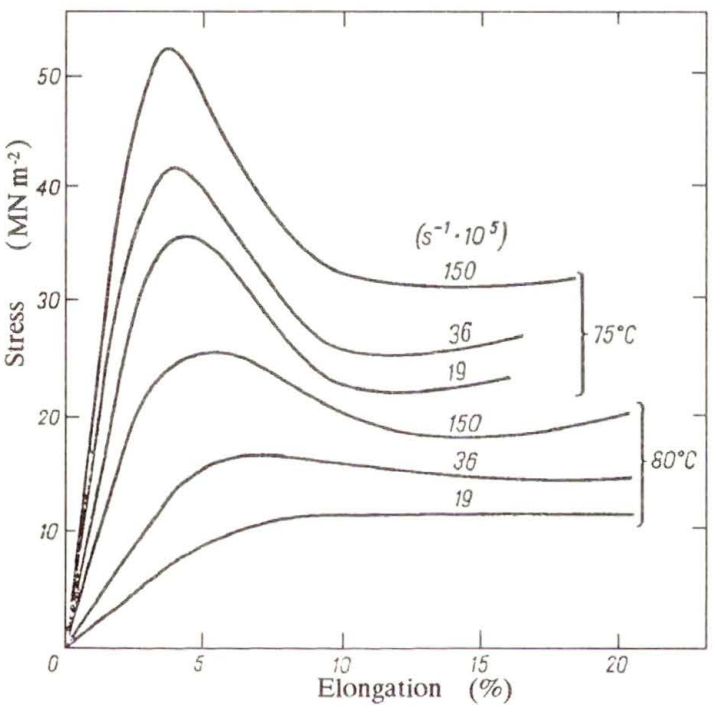

FIG. 2. Deformation characteristics for polystyrene samples after [5]. Temperatures and deformation rates indicated.

The balance of forces acting in a drawn filament can be written as follows (see Refs. [1] and [6]):

$$F(z) = F_{\text{ext}}(z) = F_{\text{rh}}(z) + F_{\text{in}}(z) + F_{\text{ad}}(z) + F_{\text{st}}(z) - F_{\text{gr}}(z), \tag{2.7}$$

where the subscripts rh, in, ad, st and gr denote rheological, inertial, air-drag, surface-tension and gravitational components, respectively.

Moreover, introducing a simplifying model assumption that (see Ref. [4])

$$\sigma^0 = \gamma(V, V'; z)\varphi(r), \tag{2.8}$$

where the function $\varphi(r)$ describes the radial dependence on r, the same for all z, we arrive at

$$F(z) = \gamma\lambda \int_0^R 2\pi r\varphi(r)\,dr = \gamma\lambda\pi\Phi, \tag{2.9}$$

where

$$\Phi = \int_0^R 2r\varphi(r)\,dr, \qquad \Phi = R^2 \quad \text{for} \quad \varphi(r) \equiv 1. \tag{2.10}$$

If, in particular, we apply the parabolic approximation according to the first term in KASE'S [7] expansion:

$$\varphi(r) = 1 + ar^2, \qquad a > 0, \tag{2.11}$$

we obtain

$$\Phi = R^2\left(1 + \frac{1}{2}aR^2\right). \tag{2.12}$$

Differentiating with respect to z the relation for λ resulting from Eq. (2.9), and taking into account Eqs. (2.2), (2.3), and that

$$\gamma = \frac{F}{\pi R_0^2}, \qquad \frac{\gamma'}{\gamma} = \frac{F'}{F}, \qquad \frac{\lambda'}{\lambda} = -2\frac{R'}{R}, \tag{2.13}$$

we can calculate the first and second derivatives of the radius R with respect to z in the following forms:

$$R' = -\frac{\varrho\pi V' R^3}{2W}\,\frac{\left(1 + \frac{1}{2}aR^2\right)^2}{(1 + aR^2)}, \tag{2.14}$$

and

$$R'' = -\frac{\varrho\pi R^3}{2W}\,\frac{\left(1 + \frac{1}{2}aR^2\right)^2}{(1 + aR^2)}\left[V'' - \frac{3}{2}\,\frac{V'^2}{V}\,\frac{\left(1 + \frac{1}{2}aR^2\right)^2}{(1 + aR^2)} + \frac{aR^2V'^2}{V}\,\frac{\left(1 + \frac{1}{2}aR^2\right)^2}{(1 + aR^2)^2} - \frac{aR^2V'^2}{V}\,\frac{\left(1 + \frac{1}{2}aR^2\right)}{(1 + aR^2)}\right], \tag{2.15}$$

respectively.

3. Necking conditions expressed in velocities or stresses

If we assume that the necessary condition of necking, characteristic for cold-drawing processes, is connected with a change of sign of the corresponding curvature (see Refs. [8] and [9]), we may use the following condition:

$$R'' \leq 0, \tag{3.1}$$

where negative values describe convex parts of the filament profile, and the equality defines an inflexion point. The above condition, after taking into account Eq. (2.15), leads to

$$V''V \geq \frac{3}{2}V'^2 D, \tag{3.2}$$

where

$$D = \frac{\left(1 + \frac{1}{2}aR^2\right)^2}{(1 + aR^2)}\left[1 + \frac{1}{3}\frac{(aR^2)^2}{(1 + aR^2)\left(1 + \frac{1}{2}aR^2\right)}\right] \tag{3.3}$$

denotes the function which is identically equal to 1, if there is no radial variation of properties. In this particular case the necessary condition of necking simplifies to the form:

$$V''V \geq \frac{3}{2}V'^2, \tag{3.4}$$

which is exclusively of kinematic character, independently of the form of the constitutive equations considered! (1)

It is noteworthy that for fluids ZIABICKI [10] attempted to establish a "necking intensity" of the kinematic character, but the introduced quantity was not related to any necking condition (see Refs. [8] and [11]).

The solution of the differential equation resulting from Eq. (3.4):

$$f = \overline{V}''\overline{V} - \frac{3}{2}\overline{V}'^2 = 0, \tag{3.5}$$

with the following boundary conditions: $\overline{V}(0) = V_0$ and $\overline{V}(L) = V_L$, amounts to

$$\overline{V} = V_0 \frac{1}{(1 - \bar{c}z)^2}, \tag{3.6}$$

(1) It can be shown that the above inequality is also valid for fluids.

where the overbars in Eq. (3.5) emphasize the solution corresponding to the equality in Eq. (3.4), and

$$\bar{c}L = 1 - \sqrt{\frac{V_0}{V_L}} = 1 - \frac{1}{\sqrt{\Re}}. \tag{3.7}$$

The above solution is schematically shown by a solid line in Fig. 3. For such a velocity distribution the curvature of the filament profile is always equal to zero. This means that the dependence of the radius $R(z)$ on z is linear.

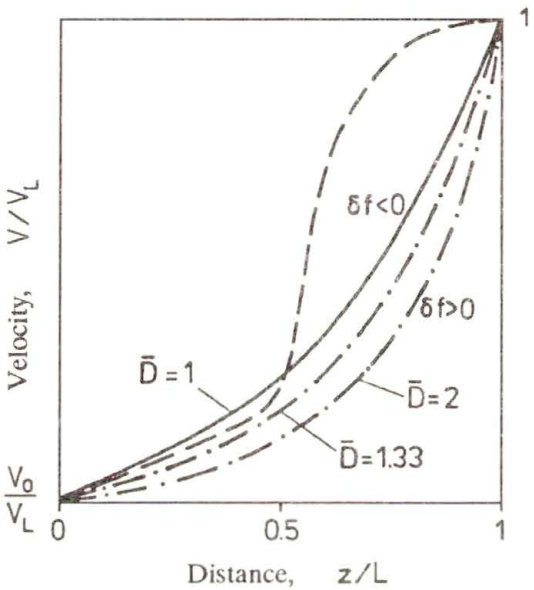

FIG. 3. Velocity profile along the filament. Solid-line – the profile for vanishing curvature; broken-line – the S-shaped profile characteristic for necking; dotted lines – the profiles for vanishing curvatures in the case of radial variations of material properties.

In more general cases, when $D \neq 1$, introducing the notion of mean value $\overline{D}$ of the function D along the length L (the parameter a is a constant and the radius R does not vary so much), we obtain the simplified differential equation:

$$f_1 = \overline{V}''\overline{V} - \frac{3}{2}\overline{V}'^2\overline{D} = 0, \tag{3.8}$$

the solution of which amounts to

$$\overline{V} = V_0 \frac{1}{(1 - \bar{c}_1 z)^n}, \tag{3.9}$$

where

$$\bar{c}_1 L = 1 - \left(\frac{V_0}{V_L}\right)^{1/n} = 1 - \frac{1}{(\Re)^{1/n}}, \qquad n = \frac{2}{3\overline{D} - 2}. \tag{3.10}$$

The corresponding curves for $\overline{D} = 1.33$ and $\overline{D} = 2$ are also shown by dotted lines in Fig. 3. Thus, we may conclude that any radial variation of the conventional stresses lowers the graphs describing solutions for zero curvatures.

3.1. S-shaped velocity profiles required for the existence of necking

It is commonly accepted that the existence of necking during cold-drawing processes is connected with the type of stress-strain curves shown in Fig. 3, leading to the well-known instability conditions (see Ref. [1]). A similar result can be inferred on the basis of our further considerations.

Since the differential expression f described by Eq. (3.5) is continuous at the profile (3.6) in the sense of proximity of the 2-nd order, we can prove that the variation:

$$\delta f = \overline{V}\delta V'' - 3\overline{V}'\delta V' + \overline{V}''\delta V, \tag{3.11}$$

where the quantities V, V' and V'' are defined in the Appendix, changes its sign depending on the values of the small parameter m (see the Appendix) viz.

$$\begin{aligned} &\delta f > 0 \quad \text{if} \quad m < 0, \\ &\delta f = 0 \quad \text{if} \quad m = 0, \\ &\delta f < 0 \quad \text{if} \quad m > 0. \end{aligned} \tag{3.12}$$

Thus, any S-shaped velocity profile starting at $z = 0$ slightly below the curve described by Eq. (3.6) leads to negative values of the curvature R''. The inflexion point $V'' = 0$ on the velocity profile may be situated either below or above the curve (3.6). In the case of $\overline{D} \neq 1$, the region in which negative values of R'' can be expected is seriously diminished and the curves corresponding to $R'' = 0$ for $\overline{D} \neq 1$ always lie below the curve (3.6).

It should be noted, however, that S-shaped velocity profiles leading to two inflexion points on the filament profile are possible either below or above the curve described by Eq. (3.6). Then the filament curvatures take positive, negative and again positive values corresponding to the "bottle-like" shape of the drawn fibre.

As an illustration, consider the following velocity profile (S-shaped for particular $g(z)$)

$$V = V_0 \exp\left\{ \ln \frac{V_L}{V_0} \frac{\int_0^z g(z)\,dz}{\int_0^L g(z)\,dz} \right\}, \tag{3.13}$$

satisfying automatically the relevant boundary conditions. The condition (3.4) leads to

$$g' \geq \frac{1}{2} \ln \frac{V_L}{V_0} \frac{1}{\int_0^L g(z)\,dz} g^2. \tag{3.14}$$

In the case of exponential viscosity function, used for the description of Newtonian behaviour (see Ref. [9]), i.e. for $g = \exp(-Az)$, we obtain e.g. $A = -0.64$ if $V_L/V_0 = 4$, and the velocity profile corresponding to Eq. (3.13) at $z = 0$ is tangent to the curve (3.6).

In a more general case of $\overline{D} \neq 1$, negative curvatures R'' are possible only for

$$z \leq -\frac{1}{A} \ln \left\{ \frac{1}{\ln \frac{V_L}{V_0} \left(\frac{3}{2}\overline{D} - 1 \right)} [\exp(-AL) - 1] \right\}, \tag{3.15}$$

i.e. for negative values the parameter A or positive viscosity gradients.

3.2. Purely inertial and isothermal cases

If only rheological and inertial terms occurring in the force balance (2.7) are retained and F_0 denotes the rheological force F_{rh} at $z = 0$, we obtain

$$F(z) = F_0 + W(V(z) - V_0), \qquad W = \varrho \pi R_0^2 V_0 \tag{3.16}$$

or

$$\gamma(z) = \varrho V_0 \left[\frac{F_0}{W} - V_0 + V(z) \right]. \tag{3.17}$$

On the basis of the inequality (3.4), we arrive at

$$\gamma'' \left[\gamma - \varrho V_0 \left(\frac{F_0}{W} - V_0 \right) \right] \geq \frac{3}{2} \gamma'^2. \tag{3.18}$$

The solution of the differential equation resulting from the equality in Eq. (3.18) amounts to

$$\gamma = 6V_0 K + \frac{1}{(c_0 - c_1 z)^2}, \qquad K = \frac{\varrho}{6} \left(\frac{F_0}{W} - V_0 \right), \tag{3.19}$$

where

$$c_0 = \frac{1}{(\gamma_0 - 6V_0 K)^{1/2}}, \qquad c_1 L = \frac{1}{(\gamma_0 - 6V_0 K)^{1/2}} - \frac{1}{(\gamma_L - 6V_0 L)^{1/2}}; \tag{3.20}$$

γ_0 and γ_L denote the conventional stresses at the exit and take-up end, respectively.

The graphs illustrating the functions (3.19) are very similar to those shown in Fig. 3. Our previous remarks concerning S-shaped velocity profiles remain valid in the case considered.

In a purely inertial case, if also $a = 0$, Eq. (2.15) can be replaced by

$$
\begin{aligned}
(3.21)\qquad R''\left[1-\frac{6V_0}{\gamma R^2}(KR^2+M)\right] = -\frac{3V_0}{\gamma R}\left\{\left(\frac{\gamma'}{\gamma}+\frac{R'}{R}\right)\right. \\
\left.\times\left[(KR^2+M)\frac{\gamma'}{\gamma}+2(KR^2+2M)\frac{R'}{R}\right]\right. \\
\left.-2KRR'\frac{\gamma'}{\gamma}-(KR^2+M)\left(\frac{\gamma''}{\gamma}-\frac{\gamma'^2}{\gamma^2}\right)-4KR'^2+2(KR^2+2M)\frac{R'^2}{R}\right\},
\end{aligned}
$$

where $M = W/6\pi$.

If we assume, moreover, that in an isothermal case the appropriate constitutive equations can be approximated by the following power-law equations:

$$
(3.22)\qquad \gamma = \gamma_0\lambda^n, \qquad n > 0,
$$

where γ_0 does not depend on z, Eq. (3.21) takes the simplified form:

$$
(3.23)\qquad R''\left[\frac{\varrho V^2}{\lambda\gamma}-n\right] = \frac{12V_0}{\gamma R}\left\{(n-1)KR'^2+(n-1)(n-2)M\frac{R'^2}{R^2}\right\}.
$$

An inspection of the above equality shows that the necking condition (3.1) can be satisfied only for n belonging to the open domain $(0, 1)$. This is the case, in particular, for

$$
(3.24)\qquad
\begin{aligned}
&n = 2/5 \quad \text{if} \quad \frac{3}{2}V_L \le \frac{F_0}{W} - V_0 \le 4V_0, \\
&n = 1/2 \quad \text{if} \quad V_L \le \frac{F_0}{W} - V_0 \le 3V_0, \\
&n = 3/5 \quad \text{if} \quad \frac{2}{3}V_L \le \frac{F_0}{W} - V_0 \le \frac{7}{3}V_0.
\end{aligned}
$$

If $n = 1$, we have $R'' = 0$, what means that for a linear dependence of the conventional stress γ on λ, the radius of filament varies also linearly.

It is noteworthy that the conditions (3.24) can be satisfied for small inertia region defined as follows (see Ref. [7]):

$$
(3.25)\qquad \frac{KR_0^2}{M} \ge \Re, \qquad \text{or} \qquad \frac{F_0}{W} \ge V_0 + V_L.
$$

4. Temperature-dependent rheological force

If we assume that the only force acting in the filament is the rheological force $F_{rh} = F_{ext}$, we conclude that such a force has to be constant with respect to z. On the other hand, if only thermal effects are considered, the dependence $\gamma(V)$ may be an increasing or decreasing function of V like in Fig. 4. In particular, for the processes close to adiabatic ones, the plot of the conventional stress γ versus the velocity V (or the draw-ratio $\Re$) may be a decreasing function because of dissipative effects (see Ref. [1]).

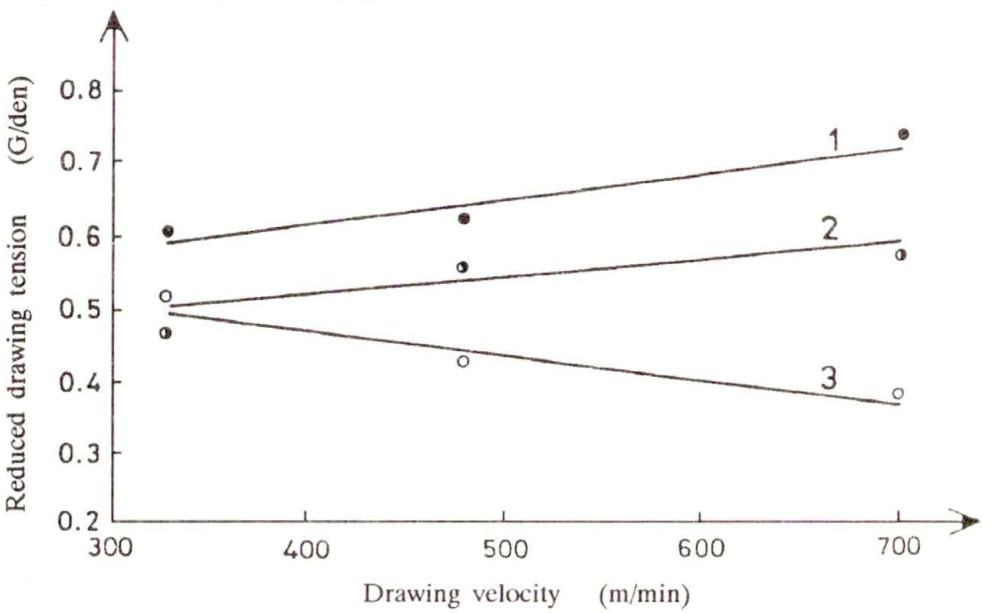

FIG. 4. Reduced drawing tension vs. drawing velocity from [1]. 1, nylon-6, temperature 80° C; 2, nylon-6, temperature 20° C; 3, polyethylene tetraphtalate, temperature 80° C.

Since *a priori* we know very little on how the function $\gamma(V)$ as well as the profile $V(z)$ look like, we assume, for simplicity, that the conventional stress can formally be described by

$$\gamma = \gamma_0(V^n/V_0^n) = \exp\left[n \ln(V_L/V_0) \frac{\int_0^z g(z)\,dz}{\int_0^L g(z)\,dz}\right], \tag{4.1}$$

with $g = \exp(-Az)$, in particular. Such an approach enables taking into account any increasing ($n > 0$) or decreasing ($n < 0$) functions $\gamma(V)$ as well as an S-shaped character of the velocity profile $V(z)$. A linear dependence $\gamma(V)$, like that shown in Fig. 4, corresponds to $n = 1$.

The velocity profile in the form of Eq. (3.13), introduced into the condition (3.4) or the more general Eq. (3.2), proves that the necking phenomenon is possible for

$$z \leq -\frac{1}{A} \ln \left\{ \frac{1}{n} \frac{1}{\ln \frac{V_L}{V_0} \left(\frac{3}{2} \overline{D} - 1 \right)} \left[\exp(-AL) - 1 \right] \right\}, \tag{4.2}$$

where $\overline{D}$ denotes the mean value of the parameter defined in Eq. (3.3).

It results from Eq. (4.2) that for $n > 0$ positive values of z can be obtained for any $A > 0$ and some $A < 0$. In other words, the above result means that necking is possible in the concave and for the S-shaped velocity profiles only for increasing functions $\gamma(V)$.

5. Final conclusions

On the basis of our previous considerations we may formulate the following conclusions:

1. The concept of non-uniform extensional motions (NUEM) of materially non-uniform simple locally isotropic solids is useful to discuss effectively the case of steady drawing of polymer fibres and to investigate some properties of general character, without assuming any particular constitutive equations.

2. The necessary condition of necking, characteristic for cold-drawing processes, can be formulated in terms of purely kinematic quantities: the velocities and their first and second derivatives with respect to the axial coordinate.

3. The necking phenomenon for an S-shaped velocity profile is possible, in principle, if its initial part is situated slightly below the concave velocity profiles obtained for the case of zero curvatures of the filament profile.

4. The existence of radial variation (Kase's type) of the conventional stress changes the regions in which negative curvatures of the filament profiles are possible for S-shaped velocity profiles.

5. The previous remarks do not exclude the cases in which two inflexion points on the filament profile are possible leading to the "bottle-like" shape of the drawn fibre.

6. In the cases of purely inertial and isothermal effects, necking is possible for small inertia regions.

7. In the case in which the only force is the temperature-dependent rheological force, the necking phenomenon can be observed for increasing as well as decreasing (caused by energy dissipation effects) dependence of the conventional stress on the velocity of drawing. For S-shaped velocity profiles necking may appear only if the conventional stresses increase with the velocity.

Appendix

A differential expression $f = f(V(z))$, involving derivatives of V at most of the k-th order, is continuous at the function $\overline{V} = \overline{V}(z)$ in the sense of proximity of the k-th order, if for any small positive ε there exists such a positive δ that

$$|f(V) - f(\overline{V})| < \varepsilon, \tag{A.1}$$

at

$$\begin{aligned} |V(z) - \overline{V}(z)| &< \delta, \\ |V'(z) - \overline{V}'(z)| &< \delta, \\ |V^{(k)}(z) - \overline{V}^{(k)}(z)| &< \delta. \end{aligned} \tag{A.2}$$

To prove that the differential expression f in Eq. (3.5) is continuous at $\overline{V}$ defined by Eqs. (3.6), (3.7) in the sense of proximity of the 2-nd order, it is sufficient to take the following functions:

$$\begin{aligned} V &= V_0 \frac{1}{(1 - cz)^{2+m}}, \qquad V' = V_0 \frac{c(2 + m)}{(1 - cz)^{3+m}}, \\ V'' &= V_0 \frac{c^2(2 + m)(3 + m)}{(1 - cz)^{4+m}}, \end{aligned} \tag{A.3}$$

where m is a small parameter (positive or negative) and

$$cL = 1 - \left(\frac{V_0}{V_L}\right)^{1/2} \left(\frac{V_0}{V_L}\right)^{-m/4}, \tag{A.4}$$

and pass to the corresponding limits for m tending to zero.

References

1. A. ZIABICKI, *Fundamentals of fibre formation. The science of fibre spinning and drawing*, Wiley, London 1976.
2. S. ZAHORSKI, *Non-uniform extensional motions of materially non-uniform simple solids*, Arch. Mech., **48**, 747–751, 1996.
3. S. ZAHORSKI, *Viscoelastic flows with dominating extensions: application to squeezing flows*, Arch. Mech., **38**, 191–207, 1986.
4. S. ZAHORSKI, *An alternative approach to non-isothermal melt spinning with axial and radial viscosity distributions*, J. Non-Newtonian Fluid Mech., **36**, 71–83, 1990.
5. P.B. BOWDEN and S. RAHA, *The formulation of microshear bounds in polystyrene and polymethylmetacrylate*, Phil. Mag., **22**, 463–482, 1970.
6. C.J.S. PETRIE, *Elongational flows*, Pitman, London 1979.
7. S. KASE, *Studies on melt spinning. III. Velocity field within the thread*, J. Appl. Polymer Sci., **18**, 3267–3278, 1974.

8. A. ZIABICKI and JIANJUN TIAN, *"Necking" in high-speed spinning revisited*, J. Non-Newtoinian Fluid Mech., **47**, 57–75, 1993.
9. S. ZAHORSKI, *Necking in non-isothermal high-speed spinning with radial viscosity variation*, J. Non- Newtonian Fluid Mech., **50**, 65–77, 1993.
10. A. ZIABICKI, *The mechanisms of "neck-like" deformation in high-speed melt spinning. 1. Rheological and dynamic factors*, J. Non-Newtonian Fluid Mech., **30**, 141–155, 1988.
11. A. ZIABICKI, *Fundamental scientific problems*, [in:] High-speed fiber spinning, A. ZIABICKI and H. KAWAI [Eds.], Interscience, New York 1985.

POLISH ACADEMY OF SCIENCES
INSTITUTE OF FUNDAMENTAL TECHNOLOGICAL RESEARCH

Received July 5, 1996.

Centre International des Sciences Macaniques

International Centre for Mechanical Sciences

Programme 1997

Modern Methods of Analytical Mechanics and their Applications Coordinators: V. Rumyantsev (Moscow), A.V. Karapetyan (Moscow)	June 16 – 20
Uncertainty in Engineering: Probability, Convexity and Fuzziness Coordinator: I. Elishakoff (Boca Raton, Florida)	June 23 – 27
Lifetime Assessment at High Temperatures Coordinators: J. Ginsztler (Budapest), P. Skelton (London)	June 30 – July 4
Recent Advances in Boundary Layer Theory Coordinator: A. Kluwick (Vienna)	July 7 – 11
Contact Problems Coordinators: P.D. Panagiotopoulos (Thessaloniki), P. Wriggers (Darmstadt)	July 14 – 18
Free Surface Flow Coordinators: H.C. Kuhlmann (Bremen), H.J. Rath (Bremen)	Sept. 1 – 5
High-Cycle Metal Fatigue in the Context of Mechanical Design Coordinators: K. Dang Van (Palaiseau), I.V. Papadopoulous (Ispra)	Sept. 8 – 12
Behaviour of Granular Materials Coordinator: B. Cambou (Lyon)	Sept. 22 – 26
Localization and Fracture Phenomena in Inelastic Solids Coordinator: P. Perzyna (Warsaw)	Sept. 29 – Oct. 3
Fracture Mechanics in Structural Concrete Coordinator: B.L. Karihaloo (Aalborg)	October 6 – 10
Modern Optical Flow Measurement Coordinator: G.E.A. Meier (Göttingen)	October 13 – 17

Additional and more detailed information will be available on

http://www.uniud.it/cism/homepage.htm

I-33100 Udine (Italy), Palazzo del Torso, Piazza Garibaldi, 18
e-mail: CISM@HYDRUS.CC.UNIUD.IT / Tel.: +39 (432) / 294989-508251 / Fax 501523